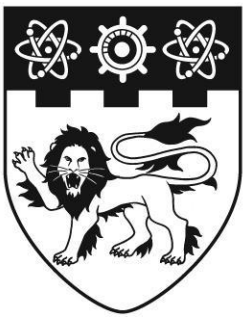

NANYANG TECHNOLOGICAL UNIVERSITY

ASYMMETRIC SYNTHESIS OF *N*-BENZYL-5-METHYLHYDROXY-PIPERIDONE

AND

MODULAR SYNTHESIS OF C1-SUBSTITUENT TETRAHYDROISOQUINOLINES (THIQ) AND C_2-SYMMETRIC BISISOQUINOLINES (C_2-BIQ) AND THEIR CATALYTIC APPLICATION IN THE ENANTIOSELECTIVE HENRY REACTION

KHONG DUC THINH

SCHOOL OF CHEMICAL AND BIOMEDICAL ENGINEERING

2015

Asymmetric Catalysis

KHONG DUC THINH

2015

ASYMMETRIC SYNTHESIS OF *N*-BENZYL-5-METHYLHYDROXY-PIPERIDONE

AND

MODULAR SYNTHESIS OF C1-SUBSTITUENT TETRAHYDROISOQUINOLINES (THIQ) AND C_2-SYMMETRIC BISISOQUINOLINES (C_2-BIQ) AND THEIR CATALYTIC APPLICATION IN THE ENANTIOSELECTIVE HENRY REACTION

KHONG DUC THINH

SCHOOL OF CHEMICAL AND BIOMEDICAL ENGINEERING

A thesis submitted to the Nanyang Technological University partial fulfillment of the requirement for the degree of

Doctor of Philosophy

2015

Acknowledgements

First of all, I would like to express my deepest gratitude to my superviosr, Associate Professor Zaher Judeh, for his patient guidance and encouragement during the course of my research. I could not have completed this thesis without absorbing his enthusiasm and persistence for chemistry.

Thanks to the members of Prof. Zaher's group: Dr. Gao Qi, Dr. Panda, Dr.Yao Qiongji, Dr. A. Manjuvani for valuable advice and suggestion on my research work. I also want to show my appreciation to the intern students: Florian, Liu Jiawei, Kris, Illya, Aaron, Cynthia and Ayuni for their constant supports on my research work.

Many thanks to Dr. Ong Teng Teng, Dr. Wang Xiu Juan, Jacqueline, Jessica, Nay Yee, Anderson and Rachel for technical support.I am very grateful to Dr. Sudipta Chaterjee, Dr. Lim Chia Juan, Surabhi and Varsha for their great patience in reviewing and proofreading my thesis.

I would like to thank the School of Chemical and Biomedical Engineering of Nanyang Technological University for scholarship support.

And last but never the least; I owe deepest gratitude to my family especially my parents, and my wife. They have always encouraged me to persist in my research goals, and have provided wholehearted support.

Abstract

The core objective of this thesis is to develop effective strategies for the asymmetric synthesis of *N*-benzyl-5-methoxypiperidone, a common building block embedded in many biologically active compounds such as cytisine, vareniciline, paroxetine, tacamonine, and deplaincheine. Two main approaches were investigated: (1) chiral auxiliary, and (2) asymmetric catalysis. Both approaches successfully gave the enantiopure *N*-benzyl-5-methylhydroxy.

With (*S*)-4-benzyloxazolidinone as the chiral auxiliary, asymmetric synthesis of (*R*)-*N*-benzyl-5-methylhydroxy-piperidone was achieved in six steps in 20% overall yield. The key step in this synthesis involved the diastereoselective aldol reaction of (*S*)-methyl 5-(4-benzyl-2-oxooxazolidin-3-yl)-5-oxopentanoate with 1,3,5-trioxane. The major diastereomeric aldol adduct was subjected to hydrolysis, amidation, chiral auxiliary removal and intramolecular cyclization to give the required enantiopure (*R*)-*N*-benzyl-5-methylhydroxy-piperidone..

Asymmetric catalysis through desymmetrization of 1,3-diols as precursor to *N*-benzyl-5-methoxy-piperidone, using chiral metal-ligand catalysts and lipases was investigated. Desymmetrization using Trost catalyst on our 1,3-diols only offered up 47% *ee* and 51% yield of monobenzoate product. On the hand, desymmetrization using lipase AK on our 1,3-diols provided up to 92% *ee* and 93% yield of (*R*)-monoacetate after optimization. In addition, we also found that desymmetrization of 1,3-diacetate gave the opposite enantiomer (*S*)-monoacetate in 95% *ee* and 41% yield. Therefore, in this approach, access to two enantiomers of *N*-benzyl-5-methoxy-piperidone was achieved in 70-80% yield in two steps after desymmetrization. The two asymmetric synthetic

approaches provided a significant improvement in the overall yield of *N*-benzyl-5-methoxy-piperidone product. While the chiral auxiliary approach offererd enantiopure product in up to 20% yield afet six step, synthetic method using lipase provided up to 45% overall yield afeter six steps, which are higher comparing to Gallagher's enzymatic resolution approach (approximately 15% yield after five steps). In addition, opposite enantiomeric product can also be conveniently obtained using the same type of lipase.

Another objective of this work was to develop an effective modular synthesis of C1-substituent tetrahydroisoquinoline amino alcohols (THIQ) and C_2-symmetric bisisoquinoline amino alcohols (C_2-BIQ). The synthesis only comprised of two steps: H_2SO_4-catalyzed *N*-acyl Pictet Spengler reaction between (*S*)-4-benzyloxazolidinone and aldehyde substrates, followed by hydrolysis under alkali condition. The reactions proceeded smoothly under easy conditions and the products were obtained in high yields and purities. This synthetic approach provides modular, convergent methodology for the synthesis novel THIQ. To the best of our knowledge, this is the first diastereoselective approach towards the synthesis tetrahydroisoquinoline amino alcohol with tunable substituent group at C1. Application of these THIQs and C_2-BIQs as chiral ligands in the Cu(II)-catalyzed asymmetric Henry reaction was also investigated. An optimal catalytic system of $Cu(OAc)_2.H_2O$-NNO THIQ (10 mol%) was found to promote the asymmetric Henry reaction between aromatic aldehydes and nitromethane to give the β-nitroalcohol products in up to 96% yield and up to 80% *ee*.

List of abbreviations

Å	Angstrong
Ac	Acetyl
acac	Acetylacetonate
Ac_2O	Acetic anhydride
AcOH	Acetic acid
Ar	Aryl
BIQ	Biisoquinoline
Bn	Benzyl
n-BuLi	*n*-Butyllithium
br	Broad (in NMR spectroscopy)
Bz	Benzoyl
BzCl	Benzoyl chloride
°C	Degree Celsius
^{13}C NMR	Carbon Nuclear Magnetic Resonance
Cy	Cyclohexyl
cm^{-1}	Wavenumber
δ	Chemical shift in parts per million downfield from tetramethylsilane
d	Day; doublet (in NMR spectroscopy)
DEPT	Distortionless Enhancement by Polarization Transfer
DMAP	*N*,*N*-Dimethylaminopyridine
DMF	*N*,*N*-Dimethylformamide
dd	Doublet of doublet

Et	Ethyl
Et_3N	Triethylamine
EtOH	Ethanol
EtOAc	Ethyl acetate
ESI-MS	Electrospray Ionization Mass Spectroscopy
equiv.	equivalent
FT-IR	Fourier Transformed Infrared Spectroscopy
g	Gram
h	Hour
Hz	Hertz
^{1}H NMR	Proton Nuclear Magnetic Resonance
J	Coupling constant (in NMR spectroscopy)
m	Multiplet (in NMR spectroscopy)
m/z	Mass/ charge
min	Minute
mmol	Milimole
Me	Methyl
MeOH	Methanol
ppm	parts per million
Ph	Phenyl
PhMe	Toluene
n-Pr	*n*-Propyl
i-Pr	*i*-Propyl
i-PrOH	Isopropanol
R_f	Retention factor

rt	Room temperature
t	Triplet (in NMR spectroscopy)
t-Bu	*tert*-Butyl
TBDMSCl	*tert*-Butyl-dimethylsilyl chloride
TMSCl	Trimethylsilyl chloride
TLC	Thin layer chromatography
THF	Tetrahydrofuran
THIQ	Tetrahydroisoquinoline

Contents

Acknowledgements i

Abstract ii

List of abbreviations iv

Chapter I: Introduction 1

1. Chirality and stereochemistry in organic synthesis 1

1.1 Chiral resolution 2

1.2 Asymmetric synthesis 3

2. Racemic and asymmetric synthesis of *N*-benzyl-5-methoxy-piperidone 1 .. 4

3. (-)-Cytisine **2** 10

4. Research objectives and significance 11

5. Research methodologies 13

Chapter II: Asymmetric synthesis of piperidone 1 using oxazolidinone chiral auxiliary 16

1. Introduction 16

2. Research methodology 19

3. Diastereoselective aldol reaction of oxazolidinone **57** with 1,3,5-trioxane **58** 21

3.1 Synthesis of starting materials: carboxylic acid **42**, oxazolidinone **46** and oxazolidinone **57** 21

3.2 Diastereoselective aldol reaction between oxazolidinone **57** and 1,3,5-trioxane **58** 25

4. Diastereoselective aldol reaction between oxazolidinone 80 and 1,3,5-trioxane **58**.....31

5. Conclusion.....41

Chapter III: Asymmetric synthesis of piperidone 1 *via* desymmetrization of 1,3-diols using metal-chiral ligand approach.....43

1. Introduction.....43

1.1 Lewis acids catalyzed acylation of alcohols.....43

2. Research methodology.....51

3. Synthesis of 1,3-diol 43.....52

4. Synthesis of the chiral ligands for the enantioselective desymmetrization reactions.....55

4.1 Synthesis of Trost ligand **111**, **151**-**154**.....55

4.2 Synthesis of zinc-sulfonamide catalyst **120**.....59

5. Screening of Lewis acids for acetylation of 1,3-diol **43**.....60

6. Screening of complexes of $Yb(OTf)_3$ with chiral ligands for enantioselective acetylation of 1,3-diol **43**.....64

7. Desymmetrization of 1,3-diol **43** *via* enantioselective acylation using Trost, sulfonamide and PyBOX ligands.....67

8. Desymmetrization of 1,3-diol **169** via enantioselective acylation using Trost, sulfonamide and PyBOX ligands.....70

9. Optimization of the desymmetrization of 1,3-diol **169** *via* enantioselective benzoylation using Trost ligand **111** based on method A.....72

9.1 Effects of catalyst loadings.....72

9.3 Effects of temperature and solvents.....77

10. Conclusion.....78

Chapter IV: Asymmetric synthesis of piperidone 1 *via* desymmetrization of 1,3-diols and their diacetate using enzymatic approach 80

1. Introduction 80

2. Research methodology 83

3. Enantioselective acetylation of 1,3-diol **43** 84

3.1 Screening of enantioselective acetylation of 1,3-diol **43** with different lipases 84

3.2 Effects of organic solvent 86

4. Enantioselective hydrolysis of diacetate **168** 92

4.1 Synthesis of diaceate **168** 92

4.2 Opimization of enantioselective hydrolysis of diacetate **168** 92

5. Enantioselective acylation of 1,3-diol **169** 100

6. Synthesis of piperidone 1 105

7. Conclusion.....106

Chapter V: Synthesis of chiral C1-functionalized tetrahydroisoquinoline and C_2-bi-tetrahydroisoquinolines and application in asymmetric Henry reactions. 107

1. Introduction 107

2. Diastereoselective synthesis of chiral THIQs and C_2-BIQs.....111

2.1 Optimization of *N*-acyl Pictet Spengler reaction between oxazolidinone 46 and benzladehyde **191a** 111

2.2 Diastereoselective synthesis of C_2-BIQs 122

3. Application of THIQs and C_2-BIQs ligands in asymmetric Henry reaction. 129

3.1 Screening of asymmetric Henry using different $Cu(OAc)_2.H_2O$ complexes with THIQ and C_2-BIQ ligands 131

3.2 Effects of enantioselective Henry reaction by *N*-methylation of THIQs and C_2-BIQs 136

4. Conclusion 152

Chapter VI: Future Works 153

1. Enzymatic desymmetrization of 1,3-diols using lipases immobilized on magnetic nanoparticles 153

2. Further application of THIQs as chiral ligand and chiral catalyst in asymmetric reactions. 154

Chapter VII: Experimental procedures 156

Chapter II 158

Chapter III 170

Chapter IV 189

Chapter V 192

References 274

Chapter I: Introduction

1. Chirality and stereochemistry in organic synthesis

In chemistry, a molecule is considered chiral when it is not superimposable with its mirror image, and thus the molecules are not configurationally identical in three dimensional configurations (Figure 1). Mirror-image molecules (e.g. A and B) share identical physical (except the optical rotation) and chemical properties under normal condition. However, those properties become significantly different under a chiral environment such as in living systems. Chiral molecules are widespread in nature.[1] Examples of chiral molecules are amino acids, carbohydrates, nucleotides which are the basic building blocks of enzymes, proteins, DNAs, etc that play vital roles in the living systems.[2]

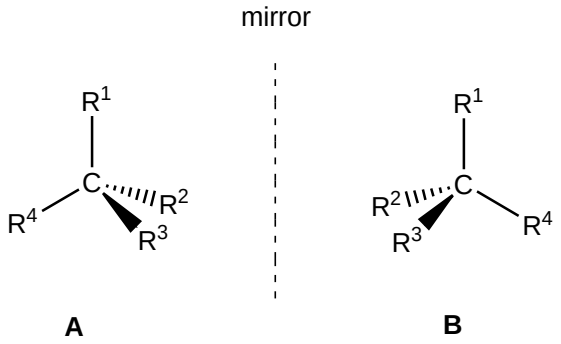

Figure 1: Chiral molecule A and its mirror-image B

Chiral drug molecules are traditionally synthesized and administered as mixture of two mirror-image stereoisomers known as racemates.[3] However, generally only one stereoisomer can fit the binding pocket of the receptor efficiently and hence trigger the desired therapeutic response, while the other stereoisomer would be either inactive, or induce weaker therapeutic response or even lead to severe side effects.[3] An infamous example of using racemic drugs is the (±)-

thalidomide which was traditionally used to treat morning sickness in pregnant women. It was later discovered that (*R*)-thalidomide is effective against nausea, but the (*S*)-thalidomide caused fetal damage.[4] Therefore, using the correct mirror-image stereoisomer (or enantiomer) of a chiral drug to achieve only the optimal beneficial effects has become more critical than ever. It has been shown that the two enantiomers may differ drastically in terms of bioavailability, rate of metabolism, metabolites, excretion, potency, toxicity and selectivity for receptors, transporters, and/or enzymes.[3a] In addition, advantages of using single enantiomer (enantiopure) drug can also result in simpler and more selective pharmacodynamics and pharmacokinetic profile with improved the therapeutic indices.[5]

With the increasing importance of chiral molecules, particularly in the pharmaceutical and biological sciences, progress in the synthesis of enantiopure molecules has seen a tremendous growth since mid-20th century.[6] Chiral synthesis provides an economic and more accessible protocol towards desired chiral products. There are two basic strategies for the preparation of enantiopure compounds: (1) chiral resolution and (2) asymmetric synthesis.[7]

1.1 Chiral resolution

Chiral resolution refers to the techniques in which a racemic mixture is separated into its enantiomers. Since the two enantiomers have similar physical and chemical properties in an achiral environment, it is impossible to separate them using conventional separation techniques used for achiral mixtures such as flash chromatography or recrystallization. However, due to their distinct physical properties in a chiral environment, we can effectively separate the two

enantiomers using different methods. Three basic chiral resolution methods are commonly employed, namely: (i) chiral column chromatography,[8] (ii) diastereoselective recrystallization[9] and (iii) kinetic resolution.[10] Unfortunately, chiral resolution gives only a maximum yield of 50% of the desired enantiomer.

1.2 Asymmetric synthesis

Asymmetric or enantioselective synthesis refers to the strategy of the formation of a single enantiomer from the reaction of prochiral or chiral starting material. A common approach to achieve enantioselective induction is *via* an additional asymmetric factor such as chiral starting material, chiral solvent, chiral reagent, chiral catalyst or chiral auxiliary.[11] The involvement of those chiral factors causes the formation of diastereomeric transition states with different energy barriers. The transition state with lower energy forms one enantiomer predominantly over the other. Therefore, a large energy barrier between those two transition states will result in a large difference between the formations of two enantiomeric products. Enantiomeric excess (*ee*) is a parameter to measure the effectiveness of enantioselective induction which is defined as the absolute difference between the mole fractions of the two enantiomers (Equation 1). The two main approaches for asymmetric synthesis are the chiral auxiliary and the chiral catalysts.

$$ee\ (100\%) = \frac{R - S}{R + S} \times 100$$

where R and S are the respective mole fractions of each enantiomer

Equation 1: Determination of enantiomeric excess (*ee*)

In comparison, asymmetric synthesis has many advantages over chiral resolution. One major advantage is that asymmetric synthesis, theoretically, allows the preparation of single enantiomer in up to 100% yield, while chiral resolution only results in up to a maximum of 50% yield of the desired enantiomer.

2. Racemic and asymmetric synthesis of *N*-benzyl-5-methoxy-piperidone 1

Chiral piperidones and chiral piperidines are abundant in nature and are embedded in many biologically active compounds.[12] Our group is particularly interested in the asymmetric synthesis of the chiral *N*-benzyl-5-methoxy-piperidone **1** (Scheme 1), which is the common building block of many biologically active natural and synthetic alkaloids such as cytisine **2**,[13] varenicline **3**,[14] paroxetine **5**,[15] deplancheine **7**,[15] tacamonine **8**[15].

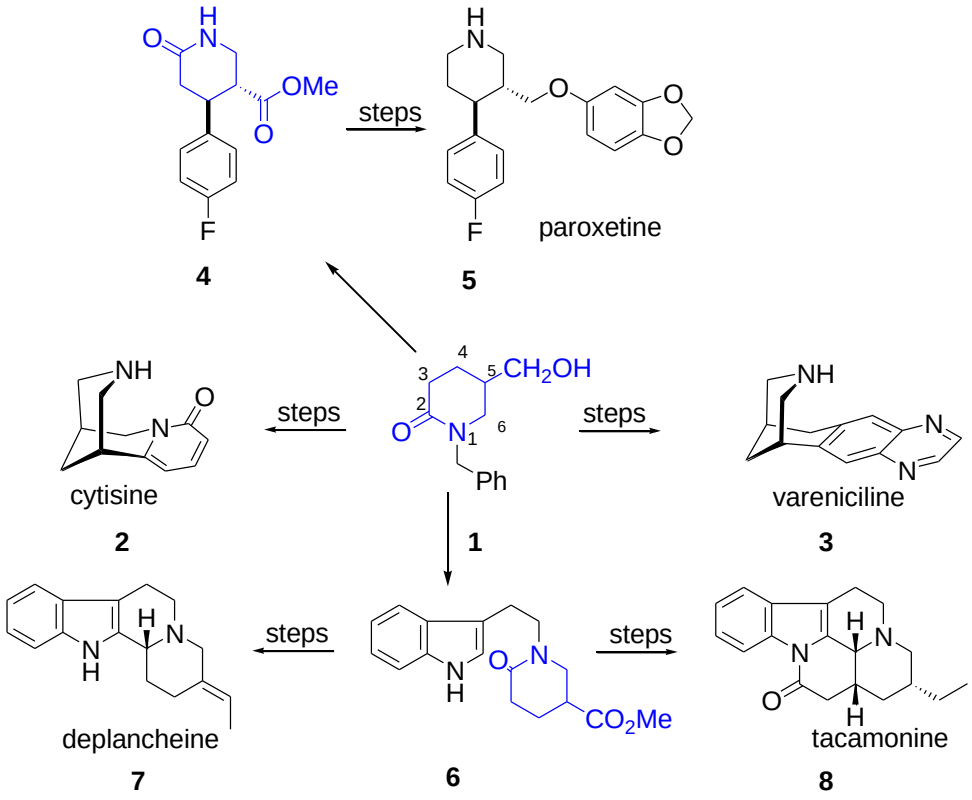

Scheme 1: Piperidone 1 as a chiral building block for biologically active compounds

Only a few approaches towards the synthesis of racemic and enantiopure piperidone **1** have been reported in the literature. Samarat *et. al*[16] reported that Michael addition and cyclization between dimethyl-2-methylenepentanedioate **10** and benzylamine **11** gave racemic ester *rac*-**9** in 82% yield. Racemic piperidone *rac*-**1** was obtained by the reduction of racemic ester *rac*-**9** using $LiAlH_4$ or $LiBH_4$ in 71-89% yield (Scheme 2).[13, 17]

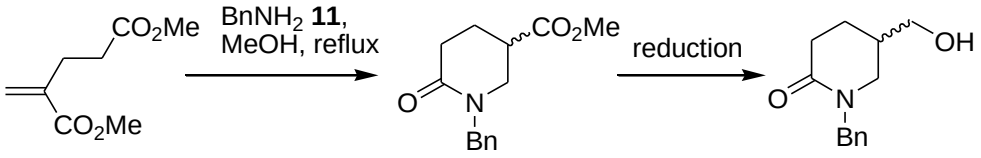

10 *rac*-**9** *rac*-**1**

Scheme 2: Racemic synthesis of piperidone 1 from dimethyl 2-methylenepentanedioate 10 and benzylamine 11[16]

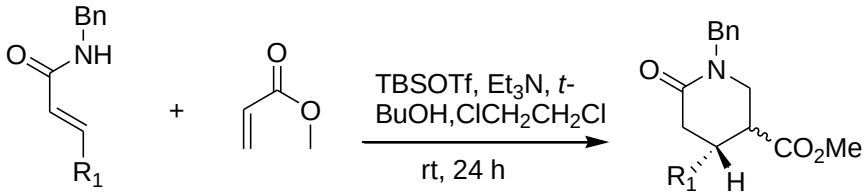

12 **13** **14**

	R^1		Yield (%)
12a	4-MeOPh	**14a**	52
12b	4-F-Ph	**14b**	59
12c	H	**9**	0
12d	$(CH_2)_2OTBS$	**14d**	66

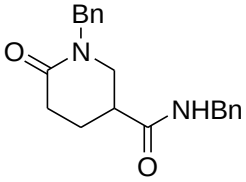

14c

Scheme 3: Synthesis of substituted piperidones 14 by double Michael addition from acrylamide 12 and methyl acrylate 13[15]

On the other hand, Takasu *et. al*[15] reported a general strategy for the synthesis of a series substituted piperidone analogues based on double Michael addition between α,β-unsaturated amides **12** and methyl acrylate **13** (Scheme 3). The reactions worked well with 3-substituted acrylamides **12a**, **12b** and **12d** to give the corresponding piperidones **14a**, **14b** and **14d** in 50-66% yield in nearly 1:1 *cis*-*trans* ratio. However, reaction of *N*-benzylacrylamide **12c**, which should give the expected ester *rac*-**9**, was unsuccessful and only the homodimer **14c** from cyclization of **12c** was obtained in ~70% yield.[15]

Asymmetric synthesis of piperidone (*R*)-**1** through kinetic resolution of its ester precursor *rac*-**9** was reported by Gallagher *et. al* in the total synthesis of *rac*-cytisine **2** (Scheme 4).[18] The synthesis of racemic ester *rac*-**9** was achieved in 53% yield after two steps from aza-annulation reaction[19] of benzylamine **11**, acryloyl chloride **15**, and methyl propiolate **16** to give *N*-heterocyclic product **17**, followed by hydrogenation using Pd/C as the catalyst. Subsequently, the racemic ester *rac*-**9** was subjected to kinetic resolution using *α*-chymotrypsin[20] to afford the enantiopure (*R*)-**9** in 42% yield and >98% *ee* followed by $LiAlH_4$ reduction to give the corresponding piperidone (*R*)-**1** in 16% overall yield.[18]

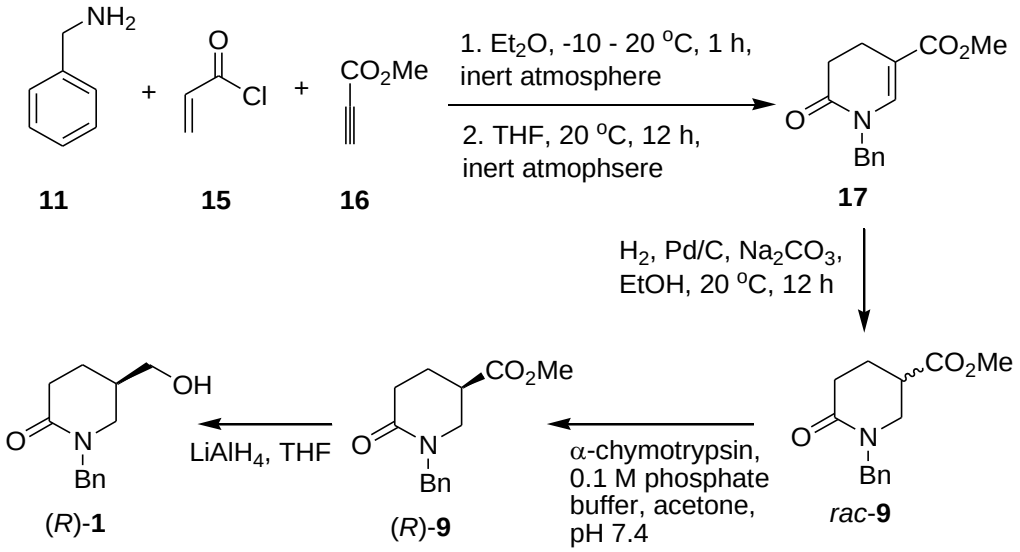

Scheme 4: Synthesis of racemic ester *rac*-9 and its enzymatic resolution to ester (*R*)-9 and piperidone (*R*)-1

On the other hand, enantioselective synthesis of piperidone (*S*)-**18**, a structurally similar compound to piperidone **1**, was reported by Kim *et. al*[21] (Scheme 5). In this synthesis, the enantioselectivity was introduced to piperidone **18** by the asymmetric monoalkylation of malonamide ester **19** with bromoalkene **20** catalyzed by chiral phase transfer catalyst **21**[22] (1 mol%). The monoalkylated product **22**, which was obtained in 95% yield and 95% *ee*, was converted to piperidone (*S*)-**18** after seven steps in 35% overall yield.

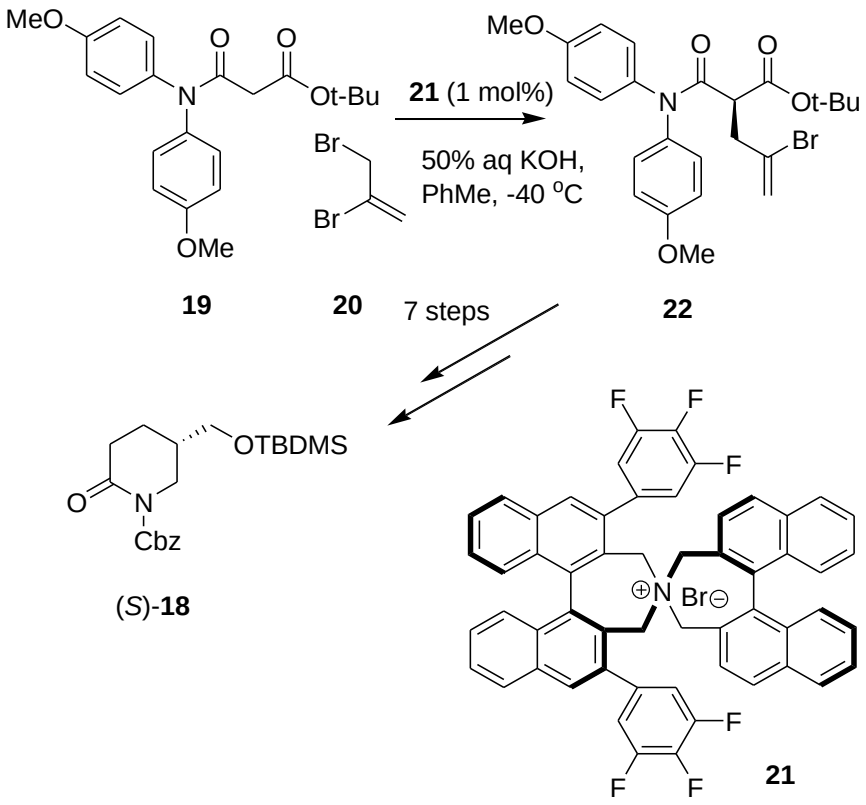

Scheme 5: Synthesis of piperidone (*S*)-18 using asymmetric phase-transfer catalytic monoalkylation of malonamide ester 19 with bromoalkene 20[21]

The first enantioselective synthesis of piperidone (*S*)-**1** was reported by Maruoka *et. al* (Scheme 6).[23] The enantioselectivity was induced through asymmetric conjugate addition of aldehyde **23** to methylenemalonate **24** using the axially chiral aminodiol **25** as the organocatalyst. The resulting chiral adduct **26** underwent intramolecular cyclization in TFA/ PhMe to afford the *O*-benzylated piperidone (*S*)-**27**, which was subsequently *O*-debenzylated *via* Pd/C-catalyzed hydrogenation in AcOH to give the corresponding piperidone (*S*)-**1** in 88% *ee*. This strategy was also employed in the total synthesis of pelitrexol, a potent angiogenesis inhibitor.[24]

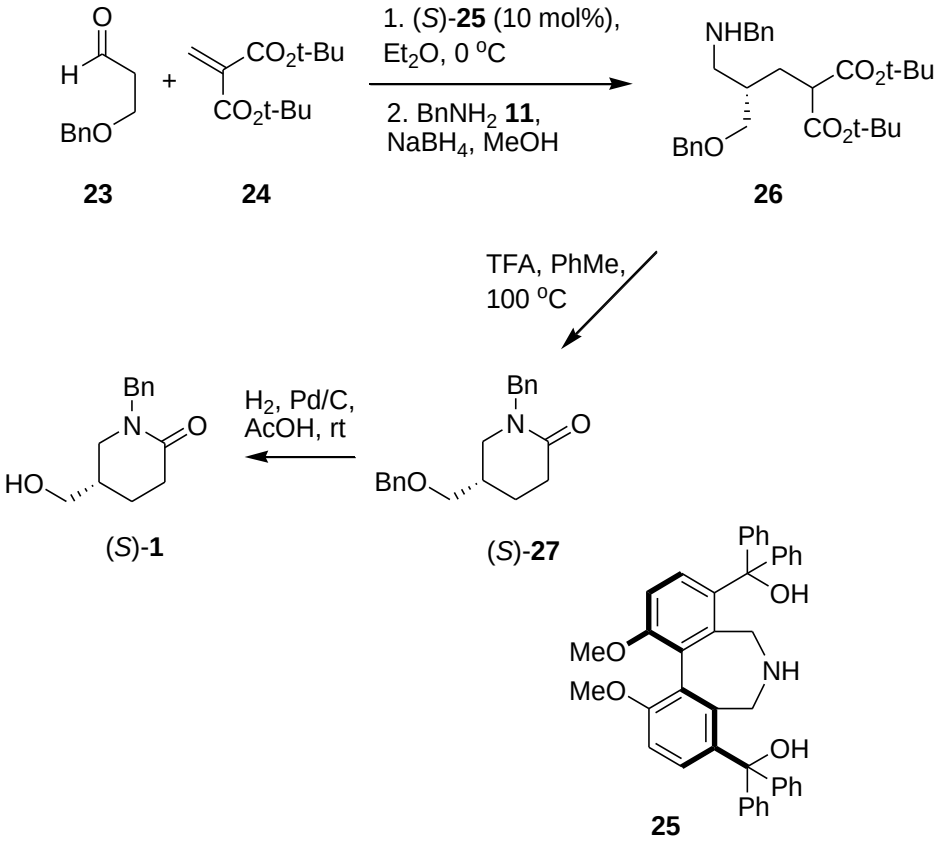

Scheme 6: Synthesis of piperidone (*S*)-1 from enantioselective conjugate addition of aldehyde 23 to methylenemalonate 24

Though these reported strategies provided impressive enantioselectivity for the final product, their major limitation comes from the low availability and the complexity of the starting materials and the chiral catalysts. While Gallagher's approach required much simpler starting materials, the kinetic resolution method only offered up to 50% theoretical yield of the enantiopure product. In addition, access to the other enantiomeric product may not be feasible due to the availability of the chiral catalysts to give the opposite enantiomer. Therefore, it can be seen that approaches for the enantioselective synthesis of piperidone **1** are still limited. Therefore, novel strategies for the convenient, affordable, and enantioselective synthesis of both enantiomers of piperidone **1** are highly desirable. The availability of piperidone **1** as a single enantiomer would provide a convergent approach to the synthesis of many valuable

products (Scheme 1). As an example, the next section briefly describes the biological activity and total synthesis of (-)-cytisine **2** as an important compound affecting different cognitive processes in human.

3. (-)-Cytisine 2

(-)-Cytisine **2** is a tricyclic quinolizidine alkaloid extracted from the seeds of *Cytisus laburnum* and other plants in *Leguminosae* family.[25] Early studies on (-)-cytisine **2** in the 19th century revealed its cathartic and diuretic utility[26]. However, recent discoveries on its biological activities towards the central nervous system once again raised the interest of the scientific community.[27] As a partial agonist to β2-containing nicotinic acetylcholine receptor (nAChRs),[28] cytisine can also affect different cognitive processes in human.[29]

In the development of a novel treatment for nicotine addiction, (-)-cytisine **2** was one of Pfizer's target as a lead compound.[30] Besides, there is accumulating evidence that nicotinic receptor densities are being affected in many central nervous system pathologies[31] such as Parkinson's[32] and Alzheimer's disease.[33] For this reason, ligand or agonist of these receptors have traditionally been targeted as potential therapeutic agents in the treatment of epilepsy, neurodegenerative and psychiatric disorders, such as Alzheimer's[34] Parkinson's diseases,[35] schizophrenia,[36] anxiety and depression.[37]

Developments in the total synthesis of cytisine have attracted special interest from various research groups and have been reviewed extensively.[27e, 38] Scheme 7 shows various synthetic routes towards racemic and enantiopure cytisine **2**. The routes are categorized based on the core intermediate used in the

synthesis. Among these routes, three main commonly encountered intermediates are tetrahydroquinolizinones **28**[39] and **29**,[40] piperidines **30**,[41] **31**[42] and **32**;[43] and piperidones **33**.[18, 44] Methods to induce stereoselectivity in cytisine include chiral pool synthesis,[42] enzymatic resolution[18] and enzymatic desymmetrization.[43]

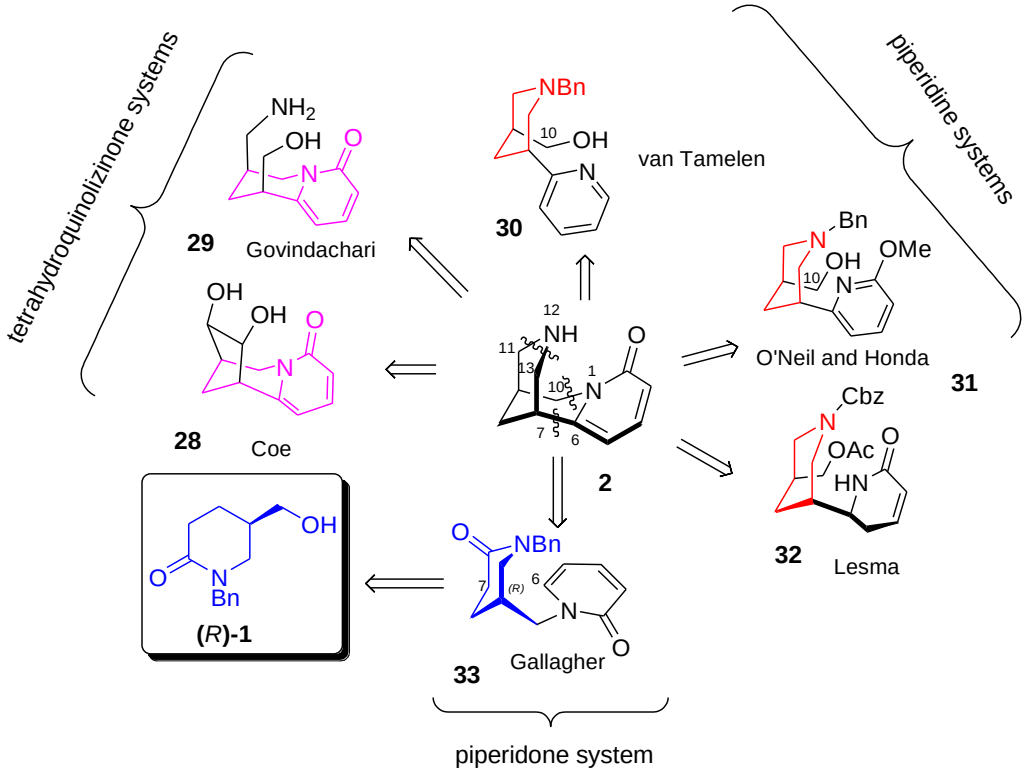

Scheme 7: Reported syntheses of racemic and enantiopure cytisine 2

4. Research objectives and significance

The main objective of this research project is to develop convenient and efficient strategies, which use only readily available and simple starting materials, for the asymmetric synthesis of piperidone **1** in excellent enantioselectivity and yield.

An effective asymmetric synthesis of piperidone **1** would provide the enatiopure precursor for various cytisine's analogues **36** (Scheme 8) with substituents at C7 and C8. This would enrich the library of cytisine analogues and offer a deeper understanding of the relationship between cytisine structure and its pharmacological properties (structure-activity-relationship).

As mentioned previously, the availability of enantiopure chiral piperidone **1** would lead to a convergent entry to many biologically important compounds such as cytisine **2**,[13] varenicline **3**,[14] paroxetine **5**,[15] deplancheine **7**,[15] tacamonine **8**[15] (Scheme 1). As mentioned in section 2, cytisine **2** is a key member of the lupin alkaloids[25c] and interest in this molecule (and its derivatives) stems from its partial agonist activity to α4β2 nAChRs.[45] As such, they are potential therapeutic agents for various central nervous system pathologies[31] such as Parkinson's[32] and Alzheimer's disease.[33] In another example, enantiomerically pure (−)-paroxetine hydrochloride **5** [Paxil®, Seroxat®] is a selective serotonin reuptake inhibitor used for the treatment of depression, panic disorder, and posttraumatic stress disorder.

In addition, we also perceive that piperidone **1** could have a much broader application as the precursor to highly functionalized piperidones **35** and piperidines **37** through 1,4-addition reactions of **34** (Scheme 8).[46]

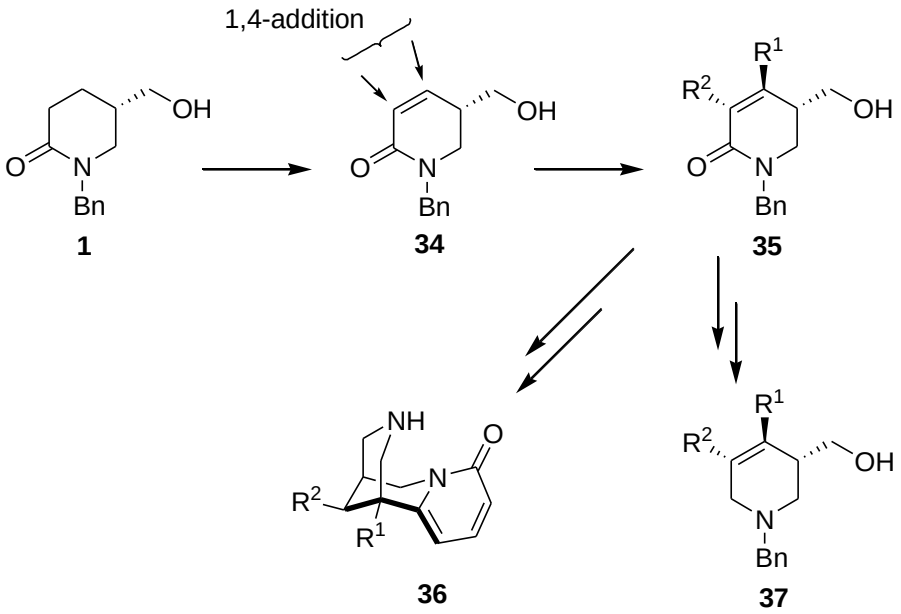

Scheme 8: Further applications of piperidone 1

5. Research methodologies

Disconnection of N1-C6 or N1-C2 bond of piperidone **1** results in chiral acyclic **38** and **39**, respectively. Acyclic **38** and **39** can easily be converted to each other. Therefore, we focused on approach involved the disconnection of N1-C6 bond since the acyclic precursor **38** can be conveniently cyclized to piperidone **1** by intramolecular amide alkylation. The critical step in this synthesis is the introduction of chirality at C5 of **38**.

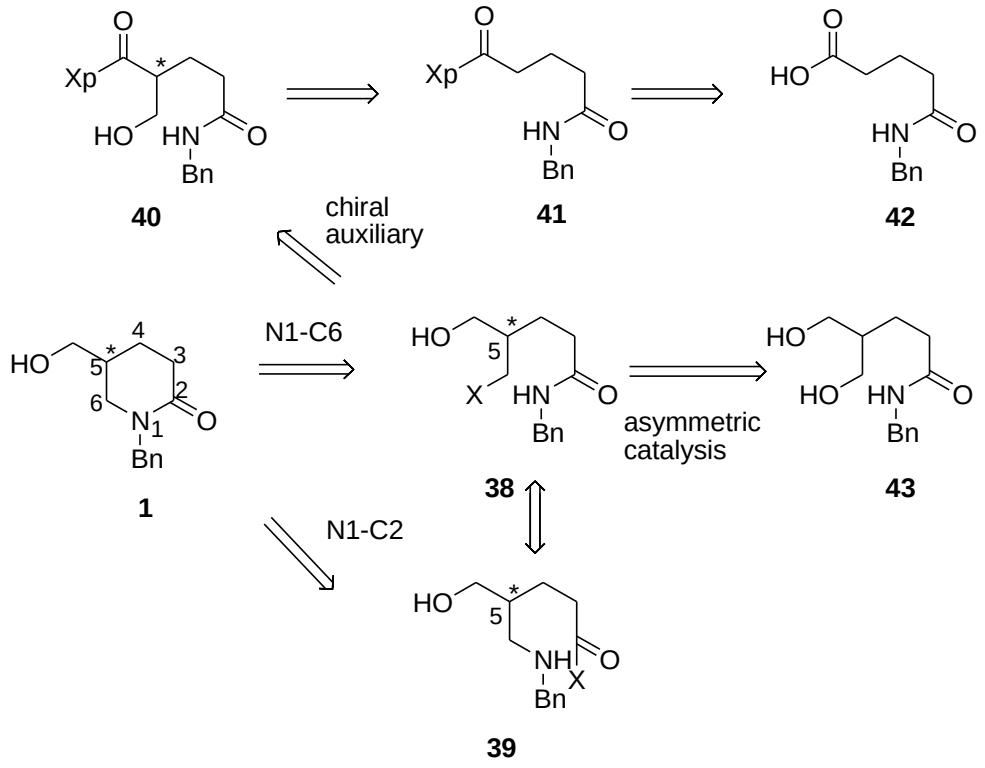

Scheme 9: Retrosynthetic analysis of piperidone 1

In this project, we will focus on two approaches: (i) asymmetric synthesis using chiral auxiliary; and (ii) asymmetric catalysis using chiral ligands and enzymes. In the chiral auxiliary approach, a chiral auxiliary (Xp) will be temporarily attached to carboxylic acid **42** through the coupling reaction to give chiral starting material **41**. Reactions at the α-carbon of compound **41** will proceed in a diastereoselective fashion under the influence of the chiral auxiliary Xp moiety. After the desired chiral center at the α-carbon has been formed, the chiral auxiliary will be cleaved from **40** to give acyclic product **38** which can be cyclized to the piperidone **1** through intramolecular amide alkylation. It can be seen that through this approach, stereoselectivity of **38** can be controlled by using the right configuration of the chiral auxiliaries, which are normally commerically available in both enantiomeric forms. Chapter II is devoted for the chiral auxiliary approach.

In asymmetric catalysis approach, we will focus on the desymmetrization of 1,3-diol **43** by catalytic enantioselective acylation (through acetylation and benzoylation). Desymmetrization is a reaction in which one of two enantiotopic groups of a prochiral or *meso* starting material is enantioselectively transformed to give a desymmetrized/ asymmetrized product.[47] Desymmetrization is a powerful, versatile and atom-economical method for the synthesis of enantiopure compounds from a prochiral source. Desymmetrization of 1,3-diol **43** through enantioselective acylation should furnish acyclic product **38** which can then be cyclized to piperidone **1** by intramolecular amide alkylation. Catalytic desymmetrization can be achieved by either using chiral metal complex systems or lipases. In the former approach, access to the two enantiomeric products can be achieved by switching the chirality of the ligands. In the latter approach, based on the unique property of lipases which can perform selective catalytic acylation/deacylation of the diol/ diester substrates, the resulting two enantiomeric products can also be conveniently obtained.[48]Two main types of catalysis will be explored: metal-based catalysis (Chapter III) and enzymatic catalysis (Chapter IV).

Chapter II: Asymmetric synthesis of piperidone 1 using oxazolidinone chiral auxiliary

1. Introduction

Chiral auxiliaries have been widely applied for many asymmetric reactions such as enolate, Michael and nucleophilic additions to C=X bonds (X= C, N), cycloadditions, rearrangements, *ortho*-lithiations, radical reactions and reductions.[49] Criteria to determine an effective chiral auxiliary include the convenience to install and to cleave from the compound of interest, strong predisposition for stereoselective processes and commercial availability.[11] A large number of chiral auxiliaries have been reported in the literature for different applications with variable effectiveness. Examples of commonly used chiral auxiliaries are shown in figure 2.[50] While majority of these chiral auxiliaries are derived from α-amino acids[51] such as *L*-proline derivatives **44** and **45**, *L*-phenylalanine derivative **46**, others are derived from natural molecules such as chiral pseudoephenamine **47**,[52] camphor derivatives **48**,[53] carbohydrate derivatives **49**[54] and *trans*-2-phenylcyclohexanol **50**.[55]

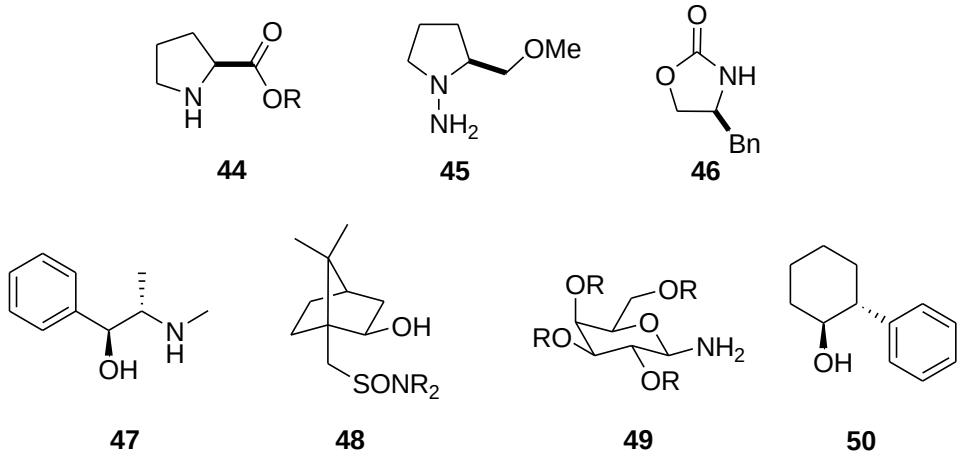

44 **45** **46** **47** **48** **49** **50**

Figure 2: Selected examples of widely used chiral auxiliaries

Perhaps the most commonly used chiral auxiliaries for asymmetric aldol reactions is Evans' chiral auxiliary, oxazolidinone **46**[56] which can easily be coupled with a non-chiral carboxylic acid **51** or an acyl chloride **52** to form oxazolidinone **53** *via N*-acylation (Scheme 10). The presence of 1,3-dicarbonyl group in **53** allows a rigid chelation with oxophilic Lewis acids such as LiN(*i*-Pr)$_2$,[56c, 57] Bu_2BOTf,[56b, 57] $Sn(OTf)_2$,[58] $TiCl_4$,[58-59] $MgCl_2$[60] and $MgBr_2.OEt_2$[60] to form metal enolate intermediate **54** (Ti is shown as an example in Scheme 10). With the presence of the bulky benzyl group, the resulting metal enolate preferentially react with the electrophile from the less hindered face. Regarding asymmetric aldol reactions, *syn* and *anti* aldol selectivity can be controlled by appropriate selection of the chelating metals. For example, while chiral titanium- and boron-enolates promote the *syn*-diastereoselective aldol reactions,[61] magnesium derived enolates provide the aldol adduct with excellent *anti*-diastereoselectivities (Scheme 10).[60]

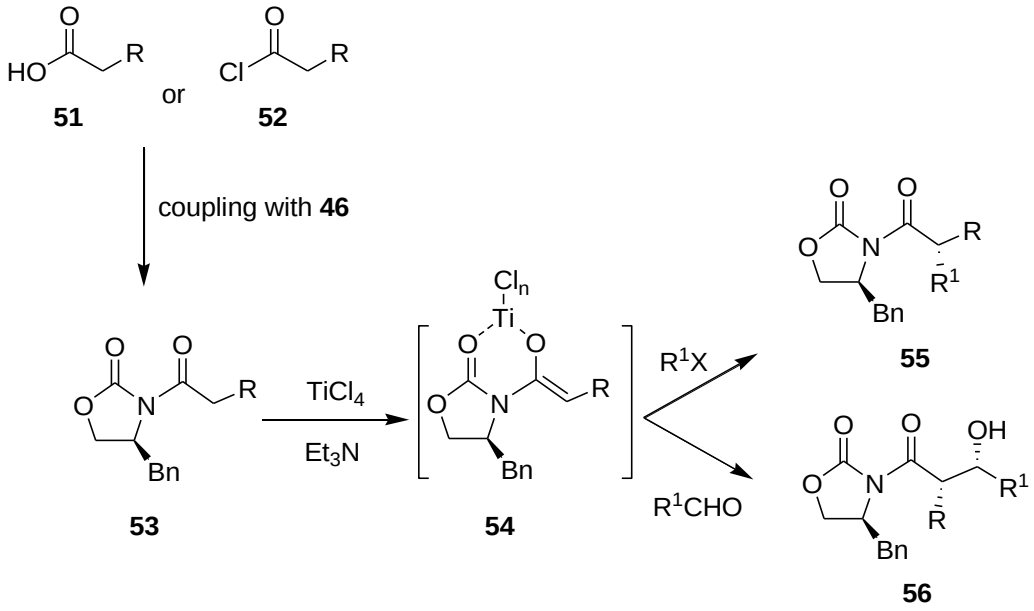

Scheme 10: Diastereoselective aldol reaction using the chiral auxiliary

In general, while the research and development of asymmetric catalysis has progressed significantly, in many cases where asymmetric synthesis might not be effective, chiral auxiliaries often represent alternative viable approach.[49b] After the removal of chiral auxiliary, the chiral product is usually obtained in very high enantiomeric purity. However, the major drawback in this approach is the two additional steps of attachment and removal of the chiral auxiliary.

In this chapter, the asymmetric synthesis of chiral piperidone **1** using chiral auxiliary approach is discussed.

2. Research methodology

Based on our retrosynthetic analysis of piperidone **1** (Scheme 9, chapter I and shown again below), the planned synthetic route for asymmetric synthesis of piperdione 1 using chiral auxiliary is elaborated in scheme 11. The key step in this route involves the formation of a new chiral center by the addition of a hydroxymethyl group $–CH_2OH$ at C5 through asymmetric aldol reaction of chiral starting material **41** with a $–CH_2OH$ source.

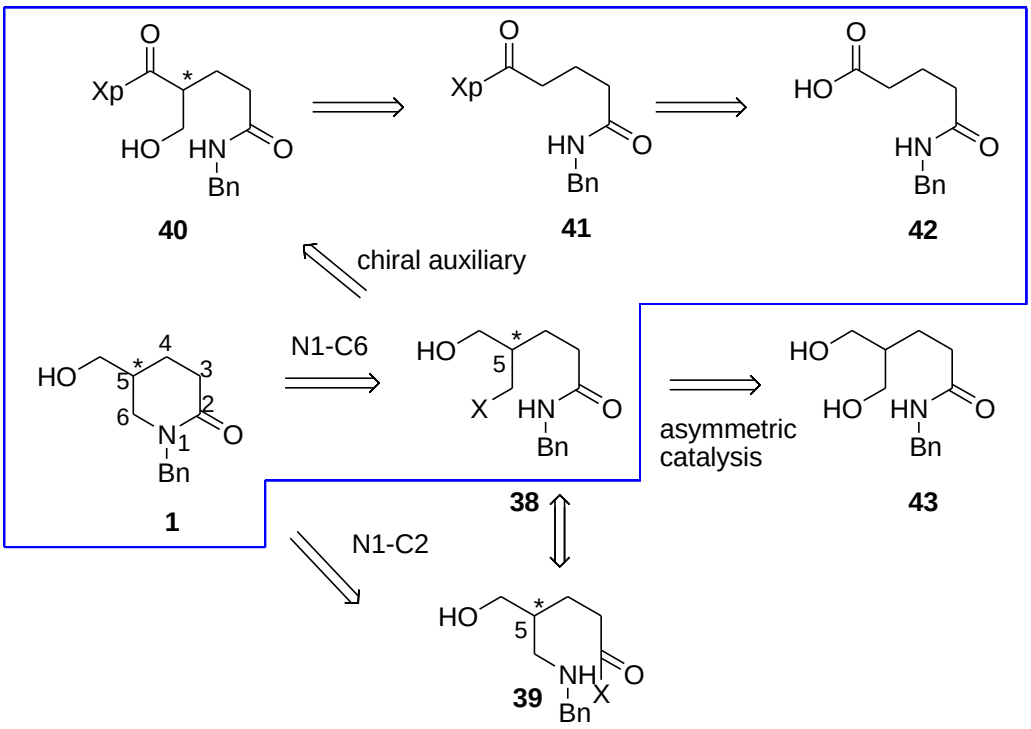

Scheme 9: Retrosynthetic analysis of chiral piperidone 1 (chiral auxiliary approach is highlighted)

The synthetic plan (Scheme 11) begins with coupling of the carboxylic acid **42** with the oxazolidinone **46** to give oxazolidinone **57**. This chiral oxazolidinone **57** is expected to undergo diastereoslective aldol reaction with 1,3,5-trioxane **58**

using $TiCl_4$/ Et_3N[59a] as the enolizing agent to give the aldol adduct **59** as the major diastereomer. The structure of the chiral auxiliary should cause the space around the prochiral carbon C5 to become highly asymmetric so that it can attack 1,3,5-trioxane **58** (which depolymerize to formaldehyde under acidic condition) preferentially at one side to give a highly diastereoselective aldol adduct **59**. Cyclization of aldol adduct **59** to piperidone **60** can be achieved by first converting the other hydroxyl group to a better leaving group followed by intramolecular amide alkylation.[62] The oxazolidinone auxiliary can then be removed by reductive cleavage[63] to afford the enantiopure piperidone (*R*)-**1** as the expected product.

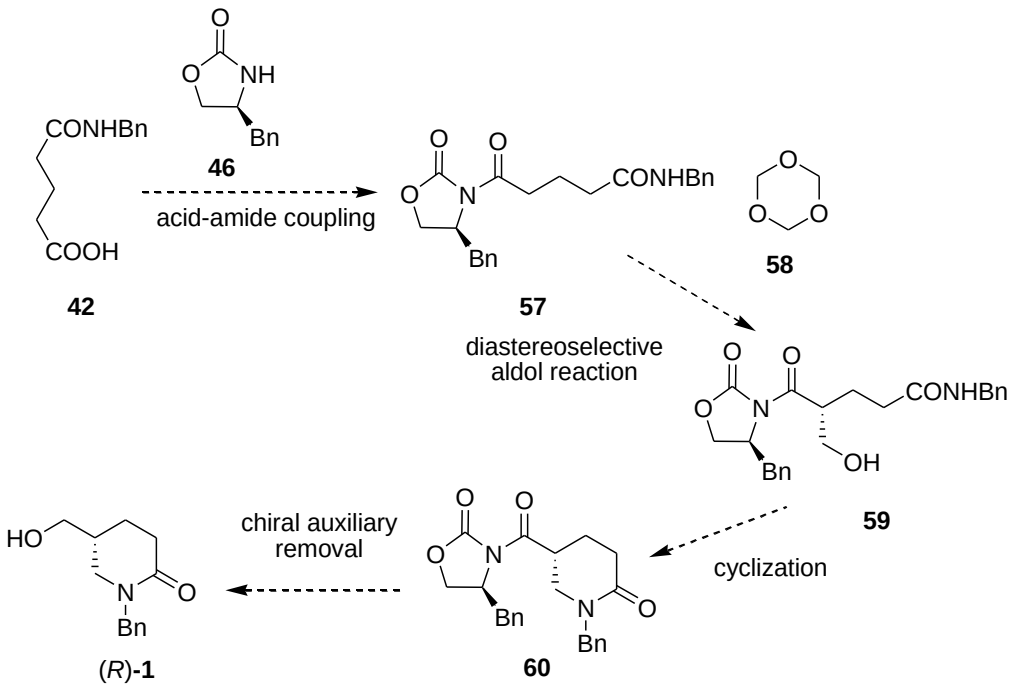

Scheme 11: Proposed synthesis of piperidone (*R*)-1 using oxazolidinone auxiliary approach

3. Diastereoselective aldol reaction of oxazolidinone 57 with 1,3,5-trioxane 58

3.1 Synthesis of starting materials: carboxylic acid 42, oxazolidinone 46 and oxazolidinone 57

Carboxylic acid **42** was prepared according to scheme 12. Glutaric acid **61** underwent cyclization in the presence of AcCl[64] to give glutaric anhydride **62** in 95% yield as white crystal. The ^{1}H NMR and ^{13}C NMR of glutaric anhydride **62** was in agreement with the literature values.[64-65] In the next step, ring opening of glutaric anhydride **62** with benzylamine **11** following the published protocol provided the corresponding carboxylic acid **42** in 90% as white solid after crystallization from water.[66]

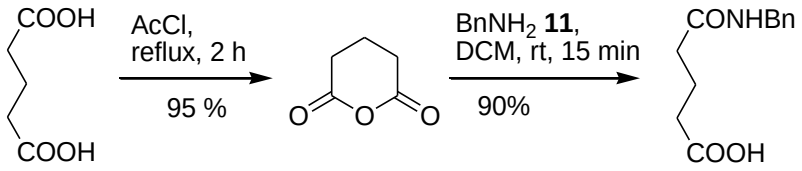

61 **62** **42**

Scheme 12: Preparation of carboxylic acid 42

Oxazolidinone **46** was also prepared according to scheme 13 following literature protocols. The synthesis started with the esterification of *L*-phenylalanine **63** using $SOCl_2$ in MeOH to give *L*-phenylalanine ester **64**, immediately followed by reduction of using $NaBH_4$[67] to give the corresponding *L*-phenylalaninol **65** in 92% yield as the white solid in one-pot.[68] Cyclization of *L*-phenylalaninol **65** with triphosgene **66** in CH_2Cl_2 afforded the required oxazolidinone **46** in 80% yield as white solid after purification by column chromatography (EtOAc: hexane, 1: 1 v/v).[69]

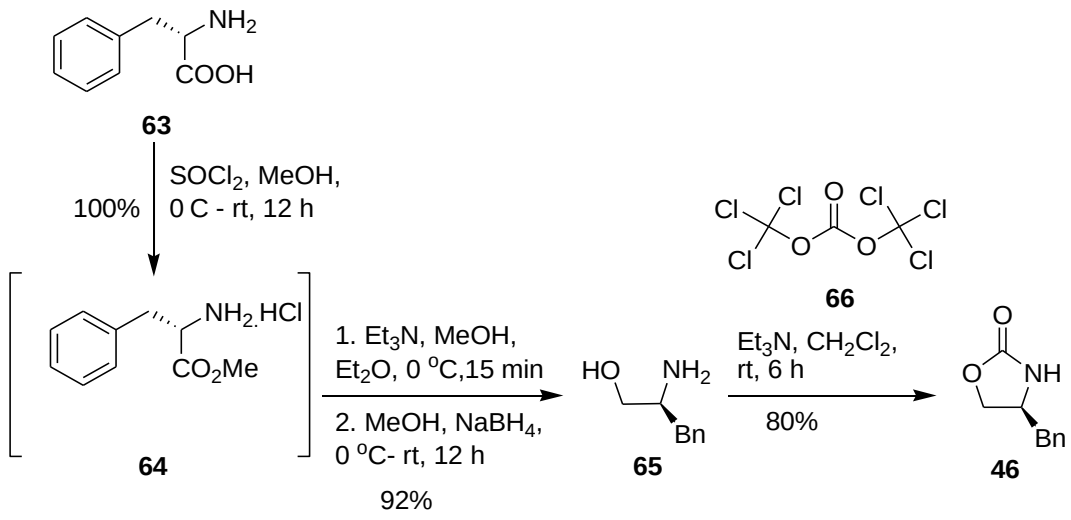

Scheme 13: Synthesis of oxazolidinone 46

With the availability of carboxylic acid **42** and oxazolidinone **46**, we proceeded for coupling reaction of those two compounds to give oxazolidinone **57**. Steglich reaction using DCC/ DMAP[70] was unsuccessful. TLC and ^{1}H NMR analysis of the crude reaction product showed unchanged starting materials **42** and **46** even after 48 h (Scheme 14).

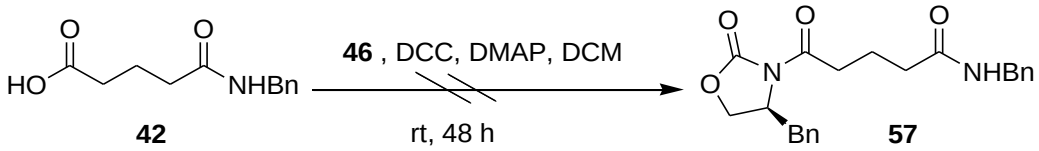

Scheme 14: Unsuccessful Steglich reaction between carboxylic acid 42 and oxazolidinone 46

In order to enhance the electrophilicity of the carboxylic acid group of **42**, the compound was converted to the corresponding acid chloride by treatment with oxalyl chloride/ DMF[71] and was added directly to a suspension of activated oxazolidinone **46** at 0 °C in CH_2Cl_2 (Scheme 15). TLC analysis of the reaction products showed the complete conversion of carboxylic acid **42** and revealed the formation of a new spot and another one corresponding to oxazolidinone **46**.

The new spot was identified by ^{1}H NMR and ^{13}C NMR analysis to be cyclic imide **67.**[72]

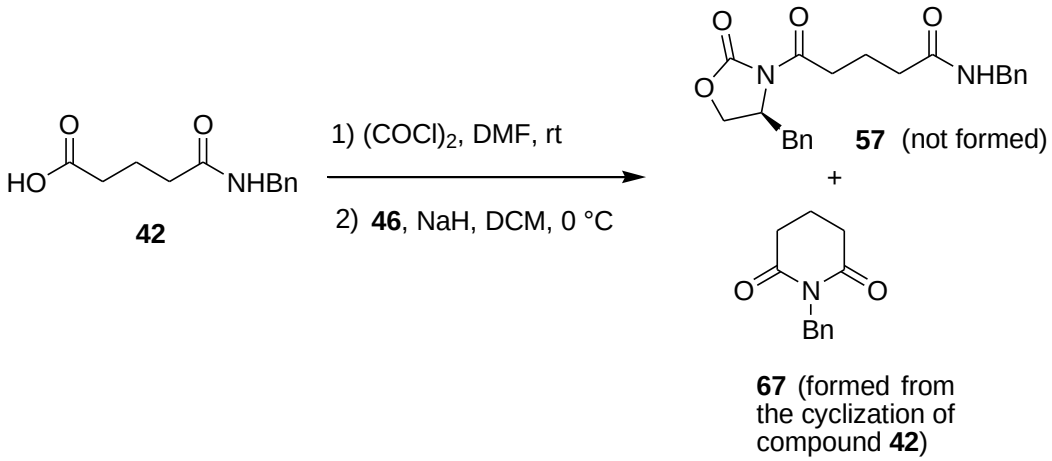

Scheme 15: Coupling of amide carboxylic acid 42 and oxazolidinone 46 using oxalyl chloride/ DMF approach

The formation of cyclic imide **67** can be explained by the deprotonation of the amide group of *in situ* acid chloride **68**, followed by intramolecular nucleophilic *N*-attack to the electrophilic carbonyl group of the acid chloride of **68** (Scheme 16).

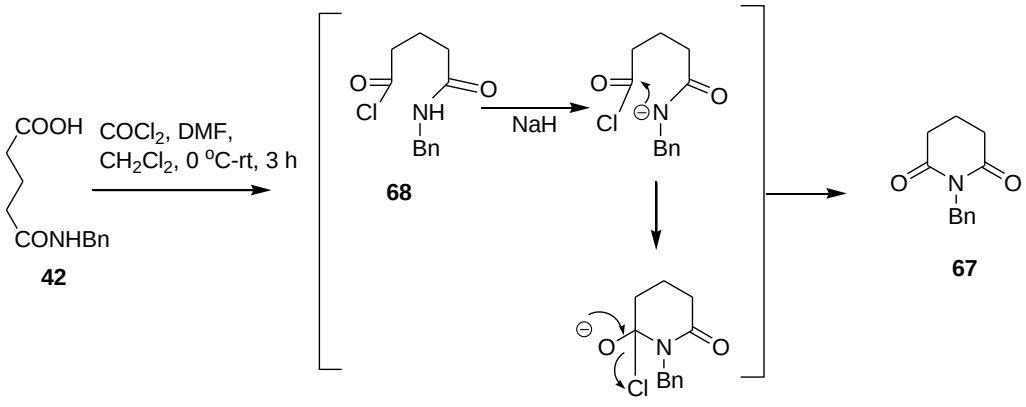

Scheme 16: Mechanism of formation of cyclic imide 67

In another attempt to obtain oxazolidinone **57**, carboxylic acid **42** was converted to pivalic anhydride by treatment with pivaloyl chloride[73] in THF at

-50 °C (Scheme 17). The resulting *in situ* anhydride was then added to a suspension of pre-formed lithiated oxazolidinone **46** in anhydrous THF at the same temperature. TLC analysis of the crude reaction product indicated the consumption of carboxylic acid **42** without the formation of cyclic imide **67**. Purification of the reaction mixture by column chromatography (EtOAc:hexane, 1:1 v/v, R_f value of ~ 0.5) provided a viscous colorless oil in 82% yield. The viscous oil slowly solidified to a white solid at room temperature, mp: 81-83 °C. FT-IR analysis of the compound revealed three peaks at 1790 cm^{-1}, 1699 cm^{-1} and 1643 cm^{-1} corresponding to the absorption bands of the C=O of the oxazolidinone group and two amide groups. The high resolution ESI-MS showed a molecular ion *m/z* value of 403.1628 corresponding to $(M+Na)^+$ thus supporting the molecular formula $C_{22}H_{24}N_2O_4$ of chiral oxazolidinone **57** (*m/z* calcd for $C_{22}H_{24}N_2O_4Na$ $(M+Na)^+$: 403.1634). Its ^1H NMR spectrum showed 10 aromatic protons at δ 7.18-7.37 which indicated the presence of two phenyl rings corresponding to the oxazolidinone and *N*-benzylamide phenyls. The characteristic protons of the oxazolidinone moiety were found at δ 2.75 (dd, *J*=13.5, 9.75 Hz, 1H), δ 3.28 (dd, *J*=13.5, 9.75 Hz, 1H), δ 4.13-4.23 (m, 2H), and δ 4.61-4.69 (m, 1H).[69] The aliphatic protons from the carboxylic acid moiety were also found at δ 2.03-2.12 (m, 2H), δ 2.31-2.36 (t, *J*= 7.2 Hz, 2H), 2.97-3.03 (m, 2H).[66] ^{13}C NMR of the compound showed a carbon signal at δ 153.5 which corresponded to the C=O carbon of the oxazolidinone moiety and the two carbon signals at δ 172.0 and δ 172.6 corresponded to the two C=O carbons of the amide moieties. Optical rotation measurement gave a value of $[\alpha]_D^{23} = +50$ (*c*, 1.0, CH_2Cl_2). Based on the above data, the product was assigned structure **57**.

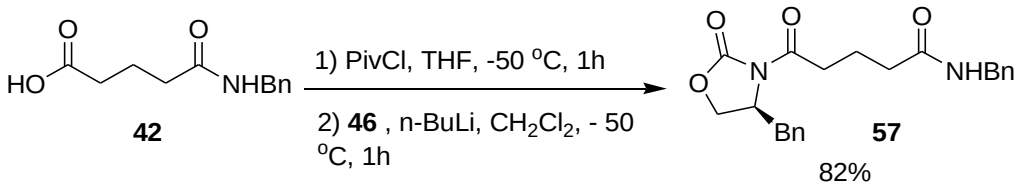

Scheme 17: Synthesis of oxazolidinone 57 using PivCl/ *n*-BuLi approach

With the availability of chiral oxazolidinone **57** in hand, diastereoselective aldol reaction with 1,3,5-trioxane **58** was then examined.

3.2 Diastereoselective aldol reaction between oxazolidinone 57 and 1,3,5-trioxane 58

The diastereoselective aldol reaction was performed according to the established procedure.[59a] The reaction involved drop-wise addition of $TiCl_4$ (1.1 equiv.) to a solution of oxazolidinone **57** in dry CH_2Cl_2 at 0 °C (Scheme 20). A suspension of yellow precipitates was formed immediately and then turned to dark red solution after subsequent treatment with Et_3N (1.1 equiv.). This observation was in agreement with the literature procedure, indicating the successful formation of the titanium-enolate complex.[59a] However, the characteristic dark red color of the solution gradually faded away and the mixture deposited dark-brown precipitated in the reaction flask. Nevertheless, a solution of 1,3,5-trioxane **58** (1.2 equiv.) in dry CH_2Cl_2 was added to the reaction mixture followed by addition of $TiCl_4$ (1.1 equiv.) at 0 °C. TLC analysis of the crude reaction product indicated the presence of two new spots besides the starting material chiral oxazolidinone **57**. Purification of the crude product by column chromatography (EtOAc: hexane, 1: 2 v/v) provided oxazolidinone **46** (23% yield) (which has the similar R_f value as that of chiral oxazolidinone **57**), cyclic imide **67** (91% yield), and an unknown product as

white crystal **69** (52% yield) (The identification of the structure of **69** will be discussed below). Unfortunately, the expected aldol adduct product **59** was not detected.

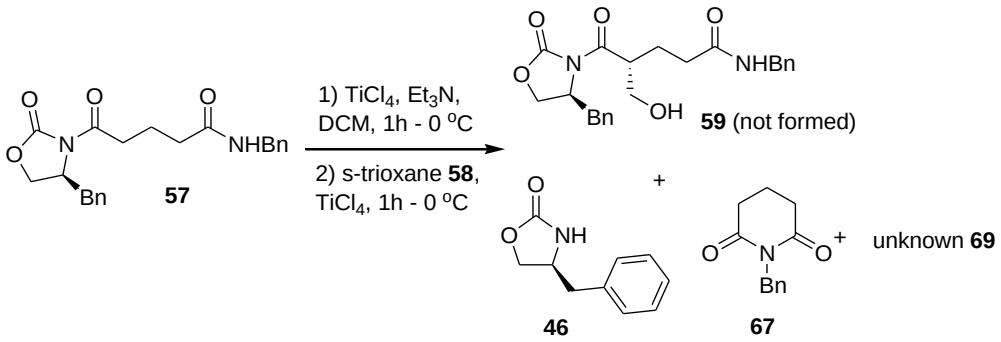

Scheme 18: Reaction of oxazolidinone 57 with 1,3,5-trioxane 58 using $TiCl_4$/ Et_3N

To investigate the mechanism of the formation of cyclic imide **67** in scheme 18, the $TiCl_4$-catalyzed reaction was repeated using only oxazolidione **57** with Et_3N in CH_2Cl_2. As the reaction progressed, the dark violet reaction mixture gradually turned brown with brown solid depositing inside the flask. TLC analysis of the crude reaction mixture indicated the formation of oxazolidinone **46** as well as cyclic imide **65**, which were confirmed by NMR analysis. In addition, compound **69** was not detected in this reaction. This indicated that the decomposition of starting material **57** happened before the addition of 1,3,5-trioxane **58** and probably that 1,3,5-trioxane **58** was involved in the formation of product **69**. A mechanism for the cleavage of the starting material chiral oxazolidinone **57** to form oxazolidinone **46** and cyclic imide **67** is proposed in scheme 19.

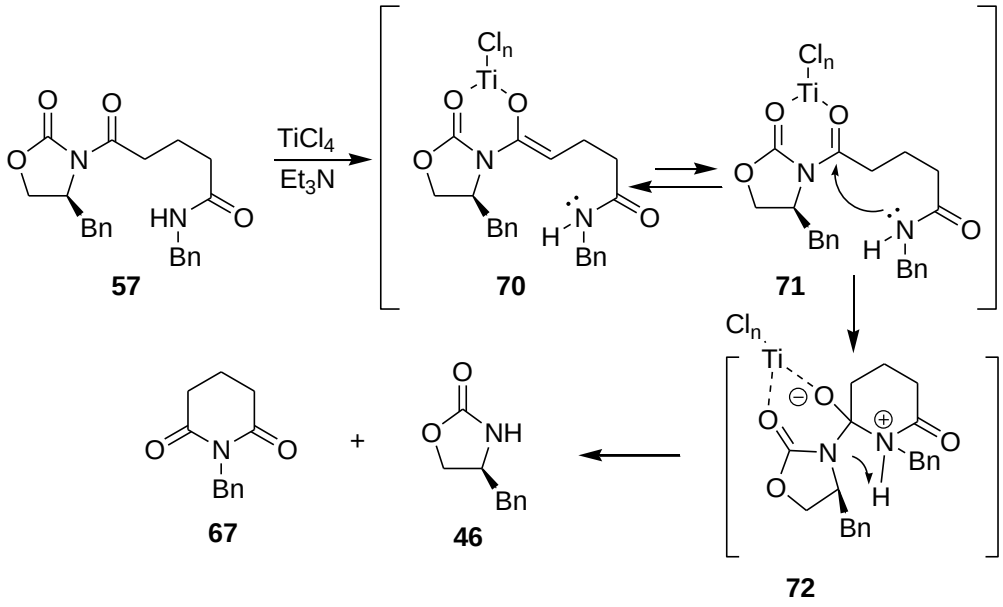

Scheme 19: Proposed mechanism for cleavage of oxazolidinone 57 to form oxazolidinone 46 and cyclic imide 67

Coordination of chiral oxazolidinone **57** with $TiCl_4/Et_3N$ resulted in titanium enolates **70** and **71**. The intramolecular nucleophilic attack of the lone pair electrons of the amide nitrogen to the electrophilic α-carbon of **71** resulted in two stable molecules oxazolidinone **46** and cyclic imide **67**.

Based on the sequence of the experiments above, it can be seen that the compound **69**, mp 134-136 °C , only formed after the addition of 1,3,5-trioxane **58**. Therefore, product **69** may be derived from the reaction of either oxazolidinone **46** or cyclic imide **67**. To resolve this, two separate reactions were carried out in which both oxazolidinone **46** and cyclic imide **67** were reacted separately with 1,3,5-trioxane **58** in the presence of $TiCl_4$ in CH_2Cl_2 (Scheme 20). The results showed that while the latter did not give product **69**, the former provided product **69** in almost quantitative yield.

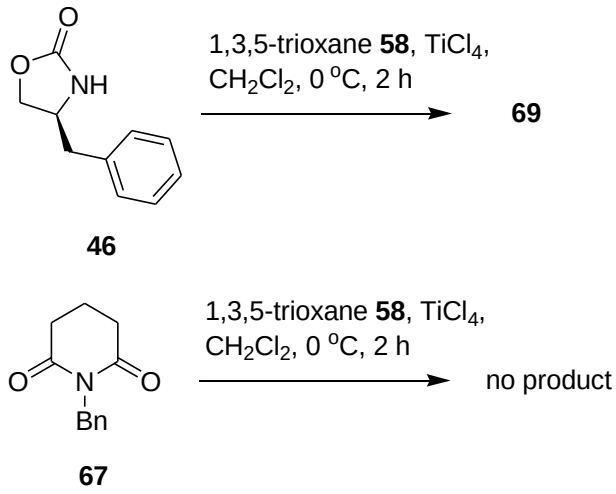

Scheme 20: Reactions of oxazolidinone 46 and cyclic imide 67 and with 1,3,5-trioxane 58 using $TiCl_4$ in CH_2Cl_2

FT-IR spectrum of the product **69** indicated a sharp peak at 1750 cm^{-1} which corresponded to the absorption band of C=O bond. Nominal ESI-mass spectrum showed a molecular ion *m/z* value of 190.09 corresponding to $(M+H)^+$ and supporting the molecular formula $C_{11}H_{11}NO_2$ (*m/z* calcd for $C_{11}H_{12}NO_2$ $(M+H)^+$: 190.09). Its ^1H NMR spectrum showed only four aromatic protons at δ 7.13-7.27 (m, 4H) which indicated involvement of the phenyl ring in the cyclization. In comparison with the ^1H NMR of oxazolidinone **46**, two new doublets were observed in compound **69** at δ 4.37 (d, *J*= 16.7 Hz, 1H) and δ 4.82 (d, *J*= 16.7 Hz, 1H) which corresponded to the diastereotopic protons of the new $–CH_2–$ methylene bridge. The ^{13}C NMR spectrum showed a carbon signal at δ 157.3 indicating the presence of C=O carbon. In addition, six different carbon signals at δ 126.4, δ 126.8, δ 127.0, δ 129.4, δ 131.4, and δ 131.6 confirmed the asymmetry of the phenyl ring due to cyclization. Spectroscopic data of compound **67** was further confirmed by comparison with the literature data.[74] Therefore, the product was assigned the structure **69** as a tricyclic oxazolidinone (Scheme 21).

Two syntheses of the tricyclic oxazolidinone **69** were previously reported in the literature (Scheme 21). One was achieved through acylation of tetrahydroisoquinoline **73** with diethyl carbonate **74**[74a] while the other approach was the cyclocondensation between oxazolidinone **46** and paraformaldehyde **75** *via* TMSOTf catalyzed *N*-acyl Pictet-Spengler reaction.[74b] In our case, the tricyclic oxazolidinone **69** was synthesized by $TiCl_4$-catalyzed *N*-acyl Pictet Spengler reaction between oxazolidinone **46** and 1,3,5-trioxane **58** in quantitative yield.

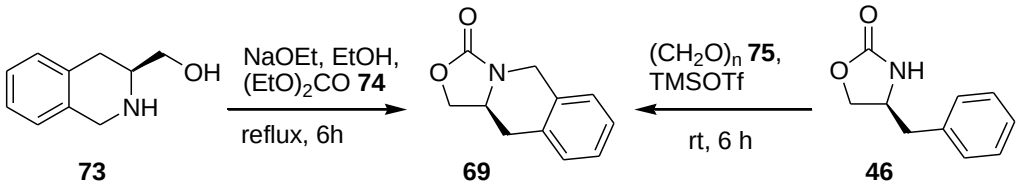

Scheme 21: Synthesis of tricyclic oxazolidinone 69

In the presence of $TiCl_4$ as a strong Lewis acid, oxazolidinone **46** condensed with 1,3,5-trioxane **58** (which was converted to HCHO under acidic condition) to give α-hydroxy amide **76** which quickly converted to *N*-acyliminium intermediate **77** in the presence of $TiCl_4$ (Scheme 22).[75] Intramolecular nucleophilic attack from the phenyl moiety to the *N*-acyliminum species of **77**, give the tricyclic oxazolidinone **69**.

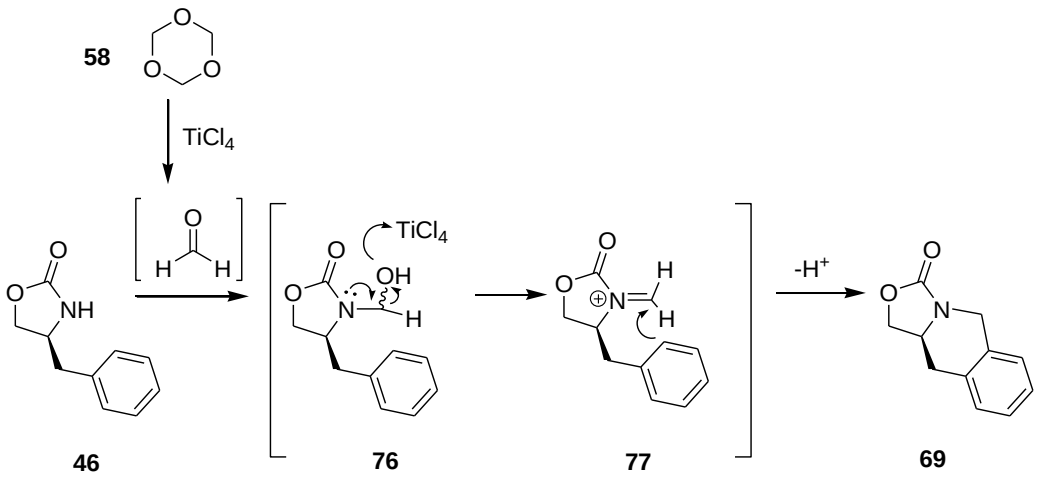

Scheme 22: Mechanism of the formation of tricyclic oxazolidinone 69

We envisioned the potential of this reaction since the tricyclic oxazolidinone **69** can easily be converted to tetrahydroisoquinoline (THIQ) amino alcohol **73** under mild conditions in quantitative yield. It can be envisaged that by using different aldehydes (RCHO), different substituents (R) can be introduced at C1 position of THIQ **79** (Scheme 23). THIQs are intermediates in isoquinoline alkaloid synthesis[74b, 76] as well as chiral ligands and catalysts for asymmetric reactions.[77] Discussion of the stereoselective synthesis of THIQ amino alcohols based on *N*-Pictet-Spengler reaction and its application in asymmetric catalysis will be presented in chapter V.

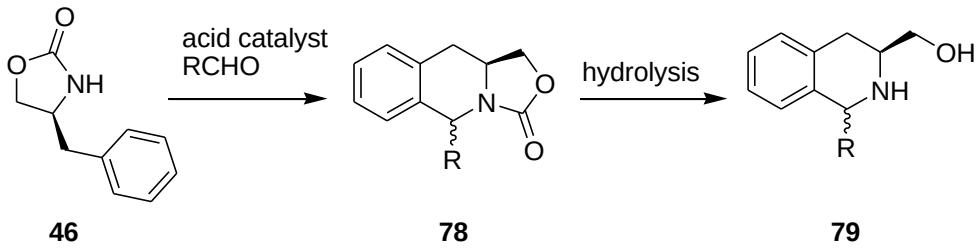

Scheme 23: Diastereoselective synthesis of THIQ amino alcohol 79

From scheme 18 and scheme 19, it can be concluded that the unsuccessful aldol reaction between chiral oxazolidinone **57** and 1,3,5-trioxane **58** is due to the feasible reaction between the amide nitrogen and the electrophilic α-carbonyl group under the reaction condition employed. In an attempt to overcome this problem, the reaction was carried out at -50 °C and also at -78 °C. However, the decomposition of oxazolidinone **57** still happened within a short reaction time. In a separate experiment, LDA[56c] was used as the enolizing agent but no positive results were obtained. Recognizing the incompatibility within oxazolidinone **57**, we decided to replace the amide group of **57** with a relatively less reactive methyl ester by preparing oxazolidinone **80** (Scheme 24).[59a]

4. Diastereoselective aldol reaction between oxazolidinone 80 and 1,3,5-trioxane 58

The overall synthetic route for the synthesis of chiral piperidone **1** using chiral oxazolidinone **80** was revised following the same methodology described in scheme 11 and is depicted in scheme 24.

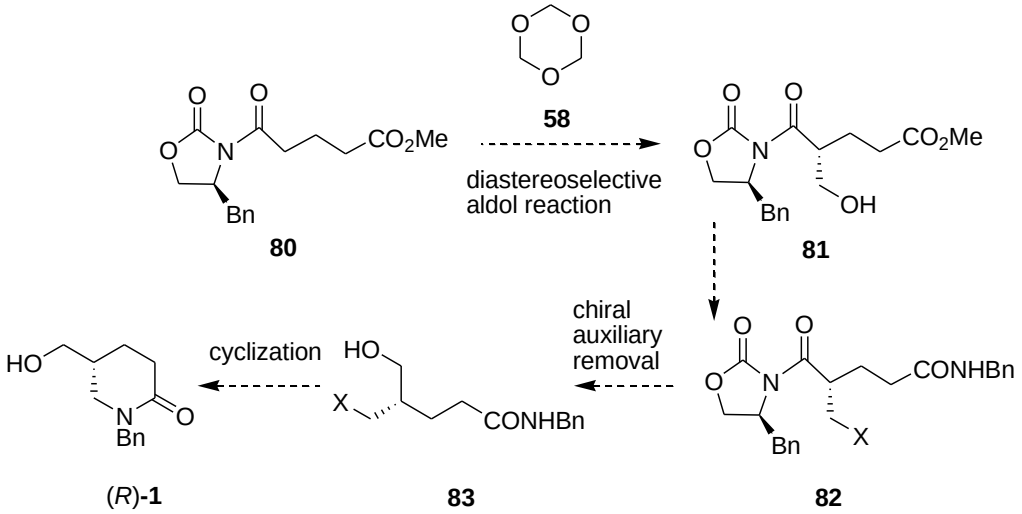

Scheme 24: Revised asymmetric synthetic route for piperidone (*R*)-1 using oxazolidinone 80

In the revised synthetic plan, we expected the diastereoselective aldol reaction of chiral oxazolidinone **80** with 1,3,5-trioxane **58** will give the aldol adduct **81** as the major product. Conversions of the methyl ester of compound **81** to amide and conversion of its hydroxyl group to a better leaving group (X), gives compound **82**. Cleavage of the chiral auxiliary of compound **82** should give acylic product **83** which can then be cyclized to the required chiral piperidone (*R*)-**1**.

In contrast to oxazolidinone **57**, synthesis of oxazolidinone **80** was achieved easily (Scheme 25) by *N*-acylation of oxazolidione **46** with the commercially available mono-methyl glutarate **84**. Three different approaches were examined including Steglich esterification (method A) and acyl transfer from pivalic anhydride to lithiated oxazoldinone **46** using *n*-BuLi (method B) or LiCl (method C). All of these methods provided oxazoldinone **80** as white solid, mp: 71 °C, with comparable yields (76%, 82% and 87% yield, respectively). However, method C is the most effective due to its operational simplicity, facile

work up and purification. The structure of chiral oxazolidinone **80** was confirmed by comparing the ^{1}H NMR and ^{13}C NMR with the literature values.[59b, 78]

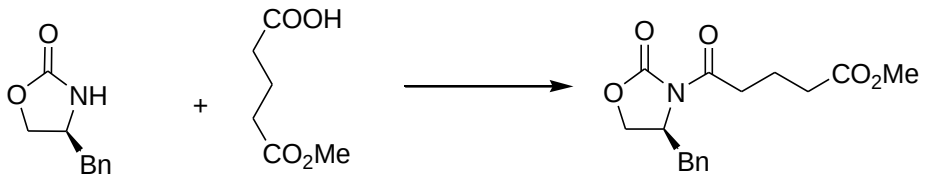

46 **84** **80**

Reagents and conditions:
Method A: DCC, DMAP, DCM, rt, 12 h (76%)
Method B: PivCl, TEA, THF, -50 - 0 ^{o}C, 1 h, then **46**, BuLi, -50 - 0 ^{o}C, 1 h (82%)
Method C: PivCl, TEA, THF, -25 ^{o}C, 1 h, then **46** LiCl, 0 ^{o}C, 12 h (87%)

Scheme 25: Synthesis of oxazolidinone 80

Reactions of titanium enolate of **80** have been reported by Evans using electrophiles such as acryloyl nitrile and *N*-(chloromethyl)benzamide with excellent diastereoselectivity.[59a] Similarly, we carried out the diastereoselective aldol reaction by gradual addition of $TiCl_4$ (1.1 equiv.) followed by Et_3N (1.2 equiv.) into a solution of oxazolidinone **80** in dry CH_2Cl_2 at 0 °C. A characteristic dark-red solution was obtained. A solution of 1,3,5-trioxane **58** (1.2 equiv.) in CH_2Cl_2 was then added to the reaction followed by the more $TiCl_4$ (1.1 equiv.) (Scheme 26). TLC analysis of the reaction mixture showed, in addition to the starting material oxazolidinone **80,** two new major spots with R_f values lower than that of the starting material oxazolidinone **80**.

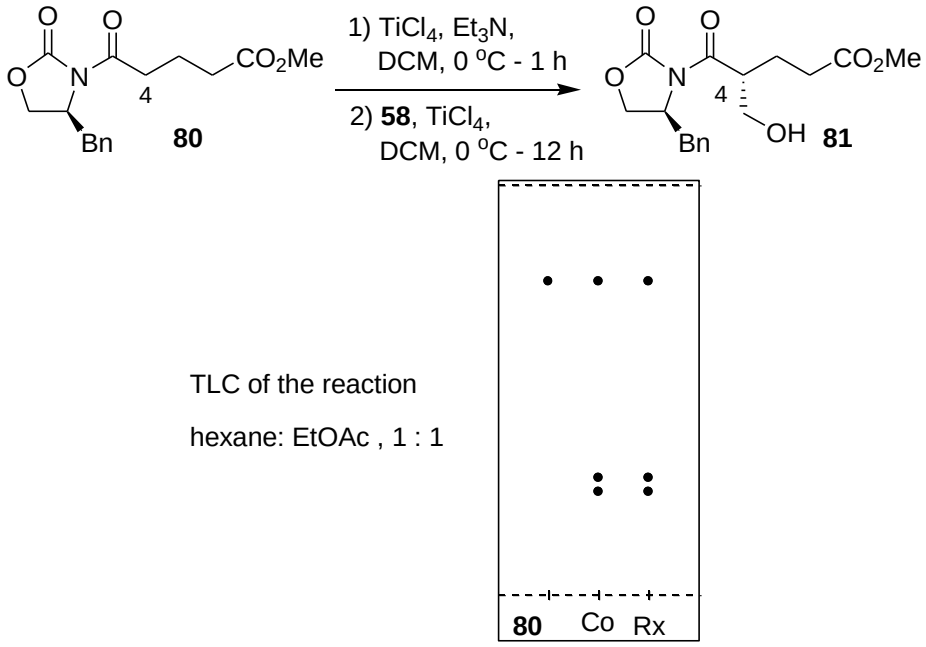

Scheme 26: Diastereselective aldol reaction between oxazolidinone 80 and 1,3,5-trioxane 58

The reaction mixture was quenched with NH_4Cl and saturated $NaHCO_3$ aqueous solutions and extracted with CH_2Cl_2 and evaporated under reduced pressure. The crude reaction mixture was purified by column chromatography (EtOAc: hexane, 2: 3 v/v) and gave three fractions. The first fraction contained the starting oxazolidinone **80** recovered in 20% yield, the middle fraction in 63% yield as a gummy solid and the lower fraction in 9% yield as viscous gum.

FT-IR spectrum of the middle fraction showed three sharp peaks at 1786 cm^{-1}, 1743 cm^{-1} and 1704 cm^{-1} that corresponded to the absorption bands of C=O bonds assigned to the carbonyls of the oxazolidinone, methyl ester and amide moieties, respectively. The high resolution ESI-MS showed a molecular ion *m/z* value of 358.1328 corresponding to $(M+Na)^+$ and supporting the molecular formula $C_{17}H_{21}NO_6$ of aldol adduct **81** (m/z calcd for $C_{17}H_{21}NO_6Na$ $(M+Na)^+$: 358.1267). In comparison with the ^1H NMR spectrum of the starting material

oxazolidinone **80**, the ^{1}H NMR spectrum of the middle fraction showed one less proton signals at C4 (which was at δ 2.93-3.11 (m, 2H) in the starting material oxazolidinone **80**), indicating that the reaction was took place at C4. The two diastereotopic protons of the newly formed hydroxymethyl group were observed at δ 3.75-3.80 (m, 1H) and δ 4.00-4.10 (m, 1H) overlapping with the multiplet of the proton signals from the oxazolidinone moiety. The proton signal at the tertiary C4 was found at δ 3.62-3.67 (m, 1H).[79] The ^{13}C NMR spectra of the middle fraction, showed a new carbon signal at δ 68.4 which corresponded to the –*C*H_2OH carbon.[79] Based on these results, the middle fraction was assigned structure **81** (Figure 3). The aldol adduct **81** gave optical rotation of $[\alpha]_D^{21} = +113$ (c, 0.43, $CHCl_3$). The positive optical rotation value suggested a *R* configuration at the newly created chiral center which is in accordance with other products from similar reactions.[79-80]

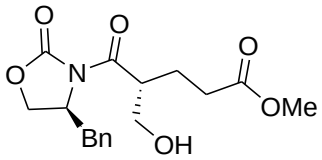

81

Figure 3: Aldol adduct 81

FT-IR spectrum of the bottom fraction showed three peaks at 1782 cm^{-1}, 1764 cm^{-1} and 1700 cm^{-1} that corresponded to the absorption bands of three C=O of the oxazolidinone, ester and amide moieties, respectively. The absorption band of the C=O of the ester moiety moved to a higher frequency at 1764 cm^{-1} (in comparison to 1743 cm^{-1} of aldol adduct **81**). This probably indicated the presence of a cyclic ester product. The high resolution ESI-MS showed a molecular ion *m/z* value of 326.1063 corresponding to $(M+Na)^+$ and supporting

the molecular formula $C_{16}H_{17}NO_5$ (m/z calcd for $C_{16}H_{17}NO_5Na$ $(M+Na)^+$: 326.1004). ^1H NMR of this compound show no proton signal corresponding to the methyl ester group (which was observed at δ 3.58 (s, 3H) in aldol adduct **81**). In addition, the significant splitting of the diastereotopic aliphatic protons also hinted the presence of a cyclic structure. ^{13}C NMR showed three carbon signals at δ 153.1, δ 170.9 and δ 171.9 corresponding to C=O carbonyls from the oxazolidinone, ester and amide moieties. The carbon signal corresponding to the ester methyl group was also absent. Furthermore, intramolecular transeterification of the aldol adduct **80** in benzene with catalytic amount of *p*-toulenesulfonic acid (PTSA) (Scheme 27)[78b] provided the same product as judged from the NMR analysis. Based on the above data, the lower fraction was assigned structure **85**. Lactone **85** gave optical rotation of $[\alpha]_D^{21}$ = +157 (*c*, 0.6, $CHCl_3$). Since this lactone **85** was derived from aldol adduct **81**, an absolute configuration of *R* was assigned to its new chiral center.

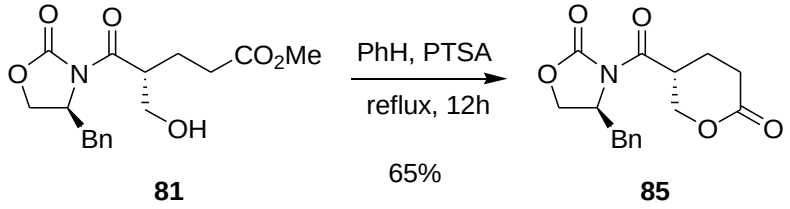

Scheme 27: Intramolecular transesterification of aldol adduct 81 to lactone 85

In addition, we also observed a slow, continuous conversion of a pure sample of aldol adduct **81** to lactone **85** while standing at room temperature. It can be explained from the intramolecular nucleophilic attack of the hydroxyl group on the electrophilic carbonyl of the ester favored by the formation of stable six-membered ring resulted in formation of the product **85**. However, we observe

that the formation of lactone **85** is not the real issue as the mixture of aldol adduct **81** and lactone **85** can be converted to the same bromocarboxylic acid product **86** following a slightly revised synthetic plan described in scheme 28.

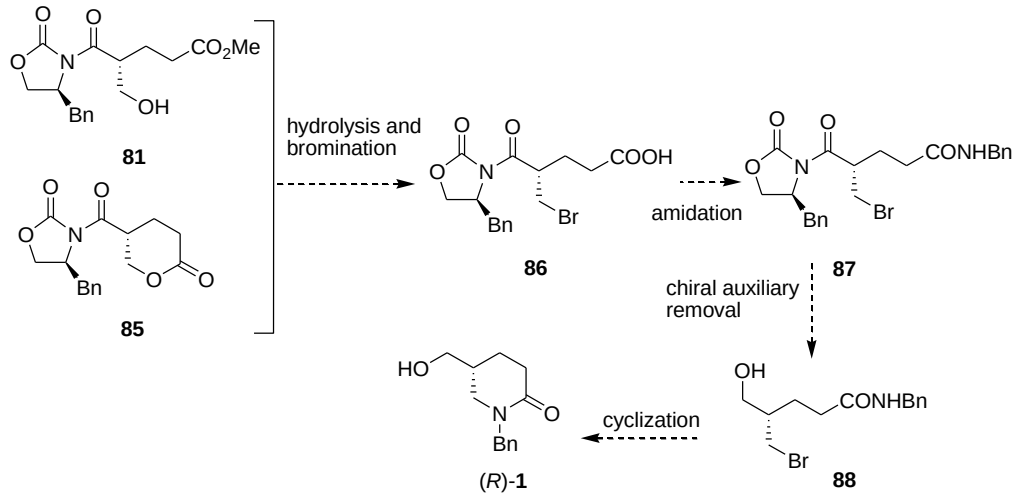

Scheme 28: Revised synthetic plan for asymmetric synthesis of piperidone (*R*)-1

Therefore, in the next step, a mixture of aldol adduct **81** and lactone **85** was treated with HBr/ AcOH[81] and bromocarboxylic acid **86** was obtained as a light brown viscous oil in 85% yield (Scheme 29). FT-IR of this product showed three peaks at 1782 cm^{-1}, 1764 cm^{-1} and 1700 cm^{-1} that corresponded to the absorption bands of three C=O bonds from oxazolidinone, ester and amide moieties, respectively. The high resolution ESI-MS showed a molecular ion *m/z* value of 406.0294 corresponding to $(M+Na)^+$ and supporting the molecular formula $C_{16}H_{18}BrNO_5$ of bromocarboxylic acid **86** (m/z calcd for $C_{16}H_{18}BrNO_5Na$ $(M+Na)^+$: 406.0266). ^1H NMR spectrum of the product showed the absence of the proton signals from the methyl ester group at δ 3.58 (s, 3H). The proton signals corresponding to $-CH_2Br$ protons were found at δ 3.58-3.73 (m, 2H) which were in accordance with similar bromo compounds.[82] ^{13}C NMR spectrum showed the carbon signals of the carboxylic acid –*C*OOH

carbon at δ 172.5 and the carbon of –*C*H_2Br at δ 32.3. Based on the above data, the compound was assigned structure **86**. Bromocarboxylic acid **86** gave optical rotation of $[\alpha]_D^{21}$= +25.6 (*c*, 0.6, $CHCl_3$).

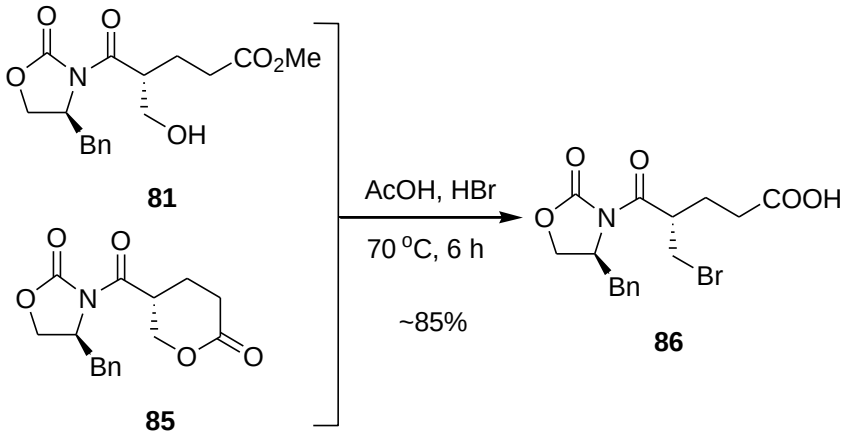

Scheme 29: Hydrolysis and bromination of a mixture of 81 and 85

In the next step, acid-amine coupling reaction between bromocarboxylic acid **86** and benzylamine **11** using oxalyl chloride/ DMAP provided the bromo-*N*-benzylamide product **87** (Scheme 28). Though this compound was easily purified by column chromatography, it was relatively unstable and decomposed into several unidentified compounds. Though the reason for such decomposition was not clearly investigated, its extent can be minimized by quickly cleaving its chiral oxazolidinone moiety (Scheme 30).

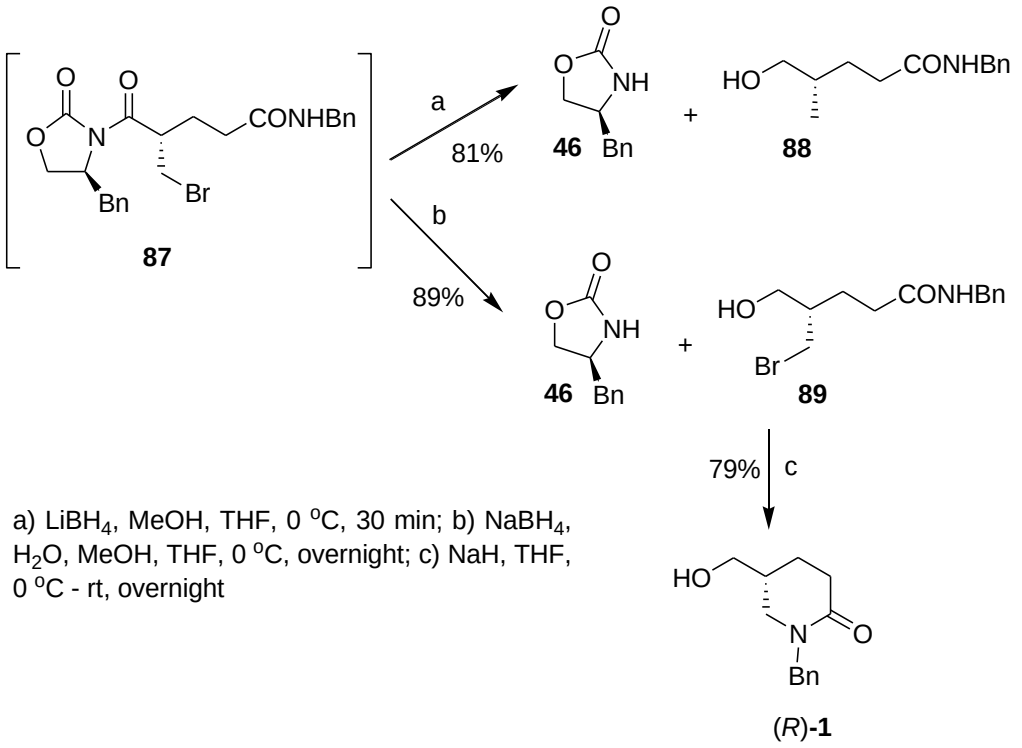

Scheme 30: Synthesis of piperidone (*R*)-1 from the crude bromo-*N*-benzylamide product 87

However, reductive cleavage of the oxazolidinone moiety from the crude bromo-*N*-benzylamide product **87** by $LiBH_4$[83] provided oxazoldinone **46** and debrominated acylic product **88** as a colorless oil in 81% yield (Scheme 30). FT-IR spectrum of the oil showed a sharp peak at 1649 cm^{-1} indicating the presence of the C=O of the amide moiety. High resolution ESI-mass spectrum showed a molecular ion *m/z* value of 244.1388 corresponding to $(M+Na)^+$ and 222.1578 corresponding to $(M+H)^+$ and supporting the molecular formula $C_{13}H_{19}NO_2$ of debrominated acylic product **88** (m/z calcd for $C_{13}H_{19}NO_2Na$ $(M+Na)^+$: 244.1313 and $C_{13}H_{20}NO_2$ $(M+H)^+$: 222.1494). The ^1H NMR spectrum of the oil showed the absence of characteristic protons from the chiral auxiliary moiety as well as the $–CH_2Br$. On the other hand, a doublet corresponding to the protons of a methyl group was observed at δ 0.89 (d, *J*= 6.6 Hz, 3H). The ^{13}C NMR also showed a carbon signal at δ 172.7

corresponding to the C=O carbon of *N*-benzylamide moiety. The carbon signals for -CH_3 and –CH_2OH were found at δ 15.6 and δ 66.0, respectively. Based on the above data, the compound was assigned structure **88** (Figure 4). Debrominated compound **88** gave optical rotation of $\alpha_D^{23} = -5$ (c, 0.14, CH_2Cl_2).

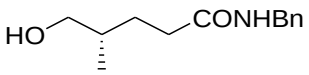

88

Figure 4: Acyclic product 88

To avoid debromination using $LiBH_4$, reduction of crude bromo-*N*-benzylamide product **87** with $NaBH_4$[84] was examined (Scheme 30) which gave a colorless oil in 89% yield. FT-IR spectrum of the oil showed a sharp peak at 1650 cm^{-1} indicating the presence of the C=O of the amide moiety. The high resolution ESI-mass spectrum showed a molecular ion *m/z* value of 301.1310 corresponding to $(M+2H)^{2+}$ and supporting the molecular formula $C_{13}H_{18}BrNO_2$ of bromo acyclic product **89** (m/z calcd for $C_{16}H_{18}BrNO_5Na$ $(M+2H)^{2+}$: 301.0677). The ^{1}H NMR spectrum showed the absence of the characteristic protons of oxazolidinone moiety. The protons corresponding to the benzyl group were found at δ 4.44 (d, *J*= 5.7 Hz, 2H) and δ 7.26-7.38 (m, 5H). The proton signal corresponding to –CH_2OH and –CH_2Br were found at δ 3.60-3.70 (m, 2H) and 3.49-3.51 (m, 2H), respectively. The ^{13}C NMR spectrum showed a carbon signal at δ 172.6 corresponding to the C=O bond of the amide moiety. The carbon signals for –CH_2OH and –CH_2Br were also found at δ 62.8 and δ 35.6, respectively. Optical rotation measurement of product **89** gave

$\alpha_D^{21} = -9$ (c, 0.23, CH_2Cl_2). Based on the above data, the compound was assigned structure **89** (Figure 5).

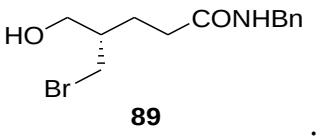

89

Figure 5: Acyclic product 89

In the final step (Scheme 30), cyclization of the bromo acyclic product **89** through intramolecular amide alkylation using NaH in THF provided the required chiral piperidone **1** in 79% yield after column chromatography purification (EtOAc: hexane, 1: 1 v/v). The ^{1}H and ^{13}C NMR spectroscopic data of chiral piperidone **1** matched with the literature values.[13, 17-18] It showed an optical rotation of $\alpha_D^{22} = +43.6$ (c, 1.0, CH_2Cl_2) thus confirming the *R* configuration of the piperidone (*R*)-**1** (Figure 6)**.**[18, 85]

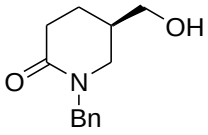

(*R*)-**1**

Figure 6: Piperidone (*R*)-1

5. Conclusion

The asymmetric synthesis of piperidone **1** using the chiral auxiliary approach was examined. The key step in this strategy involved the diastereoselective aldol reaction between oxazolidinone **57** or **80** and 1,3,5-trioxane **58** using $TiCl_4$/ Et_3N as the enolizing agents.

The diastereoselective aldol reaction between oxazolidinone **57** and 1,3,5-trioxane **58** using $TiCl_4$/ Et_3N in CH_2Cl_2 led to the decomposition to oxazolidinone **46** (23% yield), cyclic imide **67** (91% yield) and a tricyclic oxazolidinone **69** (52% yield).

However, the diastereoselective aldol reaction between oxazolidinone **80** and 1,3,5-trioxane **58** using $TiCl_4$/ Et_3N in CH_2Cl_2 gave a mixture of the desired aldol adduct **81** as the main product and lactone **85** as a side product. Treatment of this product mixture with HBr/ AcOH, followed by acid-amine coupling reaction with benzylamine **11**, chiral auxiliary cleavage with $NaBH_4$ and intramolecular amide alkylation afforded the enantiopure chiral piperidone (*R*)-**1** in approximately 20% overall yield after six steps starting from methyl ester glutaric acid **84**.

The presented approach provides the opportunity to access both enantiomers (*R*)- and (*S*)-piperidone **1** by using either the (*R*)- or (*S*)-oxazolidione **46**, both of which are commercially available. However, this approach requires stoichiometric amount of the chiral auxiliary, making it unattractive for large scale synthesis. Though it is theoretically possible to recover the chiral auxiliary during the cleavage step, the overall recovery yield was approximately 50% (calculated from the attachment step to removal step).

Chapter III: Asymmetric synthesis of piperidone 1 *via* desymmetrization of 1,3-diols using metal-chiral ligand approach

1. Introduction

1.1 Lewis acids catalyzed acylation of alcohols

Acylation of alcohols are widely catalyzed by acids and bases.[86] Large number of Lewis acids have been reported as effective esterification catalysts for a wide range of acyl donors including acyl halides, acyl anhydrides, carboxylic acids and esters (Scheme 31). Examples of such Lewis acids include metal halides such as $ZnCl_2$,[87] $BF_3.OEt_2$,[88] $CoCl_2$,[89] $AlCl_3$,[90] $FeCl_3$,[91] $TiCl_4/AgClO_4$,[92] $MgBr_2/NR_3$,[93] $RuCl_3$,[94] $InCl_3$,[95] transition metal triflates such as $Cu(OTf)_2$,[96] $In(OTf)_3$,[97] $Bi(OTf)_3$,[98] $Sn(OTf)_2$,[99] $Zn(OTf)_2$[100] and rare earth metal triflates such as $Sc(OTf)_3$,[101] $Sc(OTf)_3$/DMAP[102] and $Yb(OTf)_3$.[103]

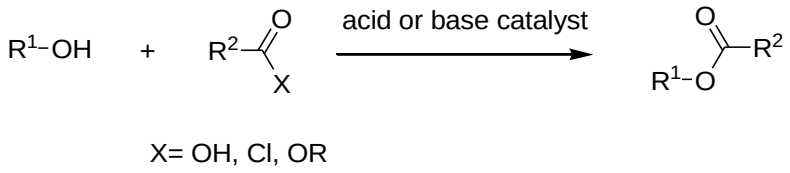

Scheme 31: Acylation of alcohol substrates

While routes for acylation of monoalcohols have been very well established, the high activity of Lewis acids often leads to multiple acylation when more than one hydroxyl group is present in the substrate. Effective and controlled monoacylation of diols have been reported to a lesser extent in comparison to monoalcohols. For example, Clarke *et. al*[104] reported the effective use of lanthanide chloride as catalyst in mono acylation of *meso*-1,2-,[103c] 1,3- and 1,4-diols[105] with good to excellent yields (Scheme 32)

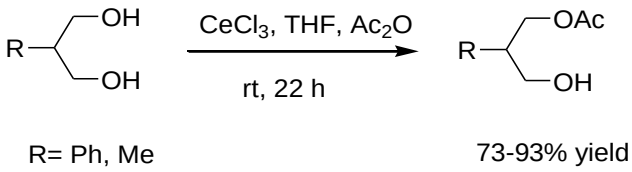

Scheme 32: Selective monoacetylation of 1,3-diol using $CeCl_3$

Complexation between chiral ligands and metal Lewis acids creates a chiral catalysts that has the potential to induce chirality during the monoacylation reaction.[106] However, application of chiral Lewis acid catalysis for asymmetric acylation of diols is still limited.[107]

The Ti-TADDOL catalyst **100** was the first example of a chiral Lewis acid catalyst to show kinetic resolution by de-esterification of racemic α-arylpropionic(2-pyridinethiol) (±)-**103** to give compounds **104** and **105** (Scheme 33a). However, the reaction only resulted in modest yield and low selectivity.[108] Chandrasekhar[109] found that kinetic resolution of racemic alcohol **106** using Ta-TADDOLate catalyst **101** gave products **107** and **108** in good yields and up to 40% *ee* (Scheme 33b). On the other hand, Seebach[110] found that desymmetrization of anhydride **109** using Ti-TADDOLate **102** gave the mono ester product **110** in up to 96% *ee* (Scheme 33c). However, harsh reaction conditions and long reaction times (24 days) were the main drawbacks of this approach.

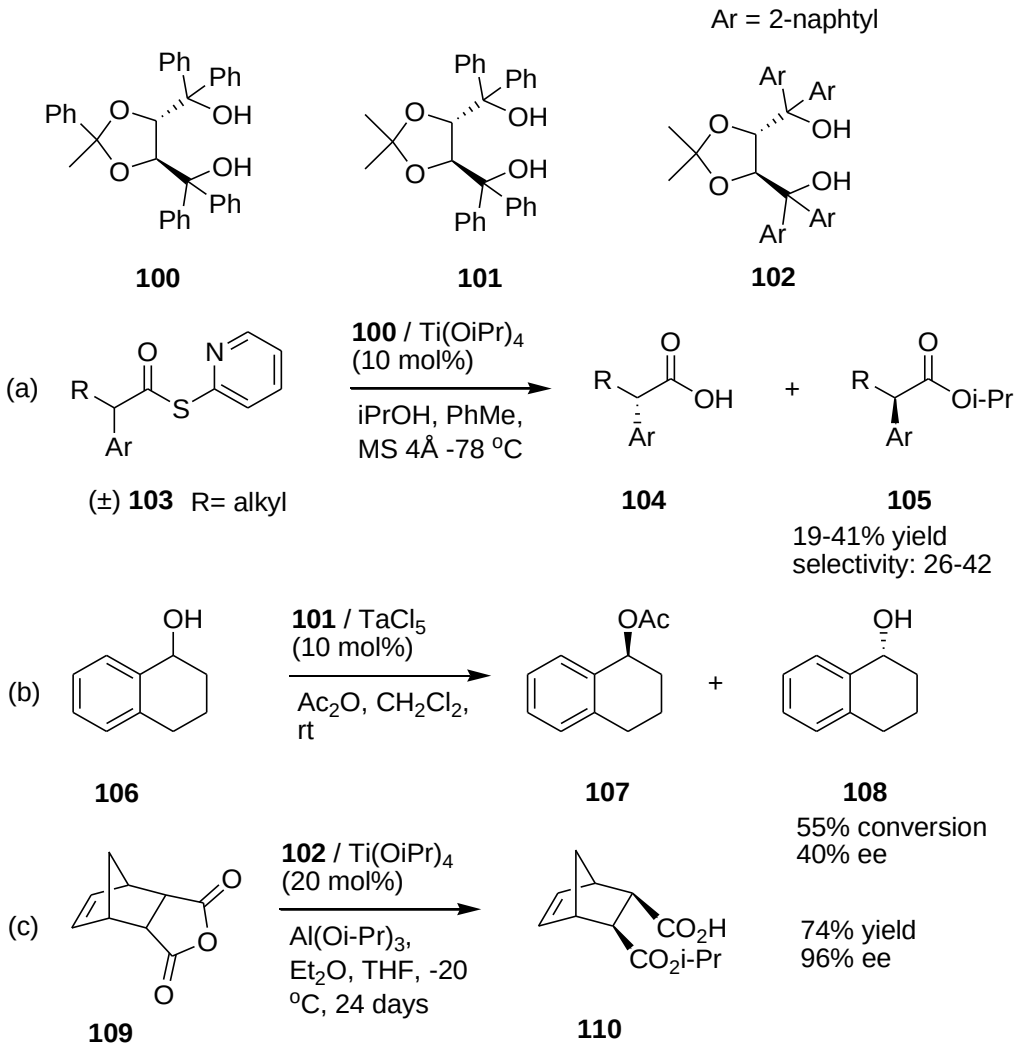

Scheme 33: Enantioselective acylation catalyzed by Ti (or Ta)-TADDOL 100-103

The first application of metal-based catalysis for enantioselective benzoylation of 1,3-diol substrates was reported by Trost's group in 2003.[111] Initially designed for asymmetric aldol reaction,[112] the Trost catalyst **112** obtained *in situ* from the reaction between Trost ligand **111** (1 equiv.) and Et_2Zn (2 equiv.) proved to be an effective catalyst for desymmetrization of different 1,3-diol substrates(Scheme 34).[111, 113]

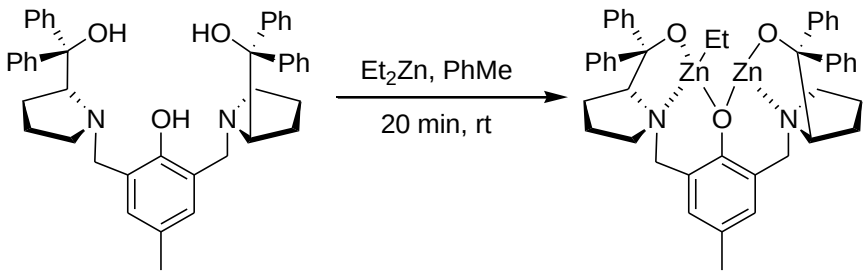

111 **112**

Scheme 34: Synthesis of Trost catalyst 112 from Trost ligand 111

A wide range of 2-alkyl- and 2-aryl-1,3-diols **113** were benzoylated catalytically using the Trost catalyst **112** to give the monobenzoate products **114** in good yield and up to 93% *ee* (Scheme 35).

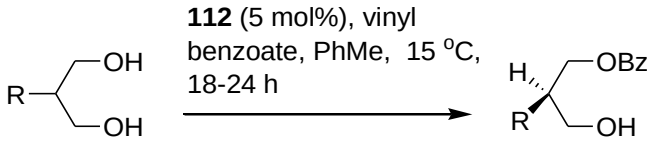

113 **114**

Scheme 35: Enantioselective benzoylation of 2-alkyl- and 2-aryl-1,3-diols 113 using Trost catalyst 112

A detailed study was carried out to further optimize the enantioselectivity of benzoylation by Trost catalyst by examining several reaction parameters such as temperature, solvent, substrate concentration, acylating agent and catalyst loading.[113] The study revealed a minimal impact of those parameters on the enantioselectivity of the product. However, while aliphatic and aromatic 1,3-diols such as **113** provided excellent results in terms of yield and enantioselectivity, the presence of functional groups on the side chain severely diminished the enantioselectivity.[113] For example, 2-*O*-substituted-1,3-diol

115 and **116** provided the respective monobenzoate products **117** and **118** in 40% and 60% *ee*, respectively (Scheme 36).

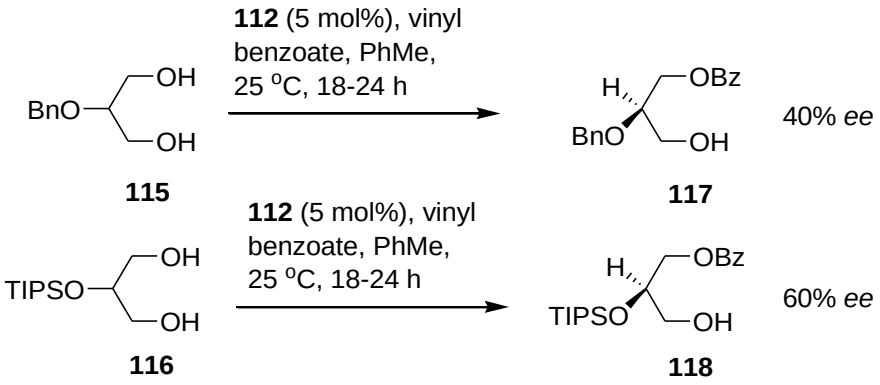

Scheme 36: Enantioselective benzoylation of 1,3-diol 115-116 using Trost catalyst 112

On the other hand, Nagao[114] developed another chiral catalyst system based on zinc-sulfonamide catalyst **120** for the enantioselective acetylation of 1,3-diol **121** (Scheme 37). The zinc-sulfonamide catalyst **120**, prepared by complexation between sulfonamide **119** (1 equiv.) and Et_2Zn (0.55 equiv.), promoted the enantioselective acetylation of 1,3-diols **121** which have a *N*-functional group at C2 to give monoacetate **122** in good yield and in up to 88% *ee*. Desymmetrization of these diols with Trost catalyst **120** was unsuccessful.

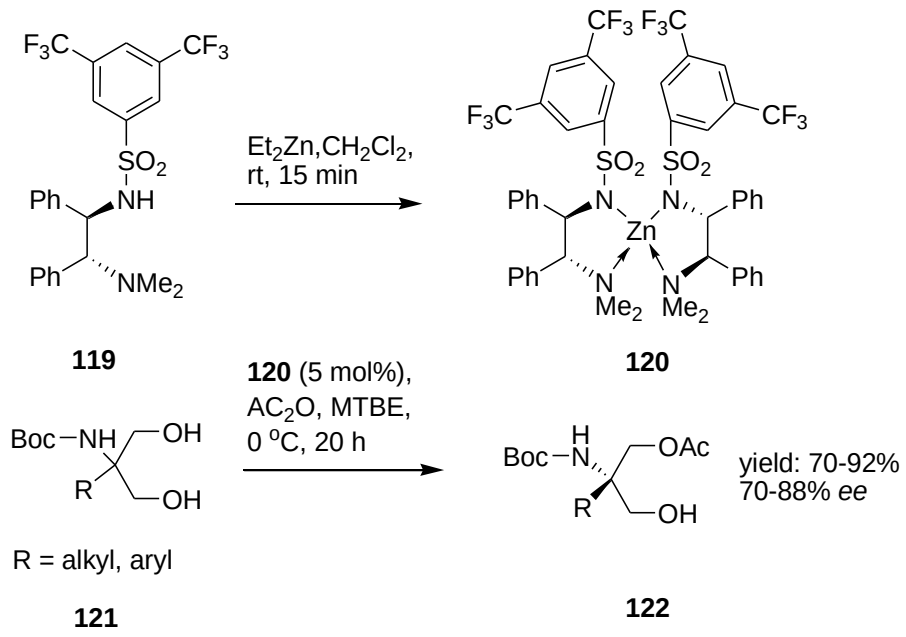

Scheme 37: Enantioselective acetylation of 1,3-diol 121 using zinc-sulfonamide catalyst 120

In an independent study, Matsumura[115] developed organotin **123** for kinetic benzoylation of racemic diol **124**. It gave good yield and up to 84% *ee* of monobenzoate product **125** (Scheme 38a). However, the chiral catalyst organotin **123** was not amenable for structural modifications, thus limiting its potential application for desymmetrization of different diol substrates. Subsequently, chiral $CuCl_2$-BOX **126**[116] was developed by the same group and was demonstrated to catalyze the kinetic benzoylation of *trans*-benzoin **127** to give the monobenzoate **128** in 48% yield and 99% *ee* (Scheme 38b).

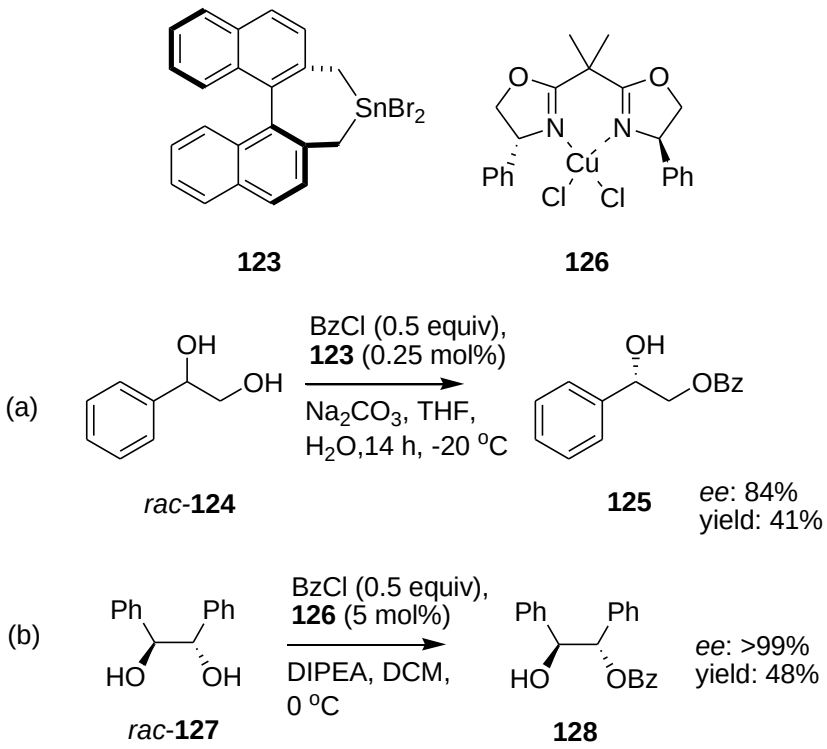

Scheme 38: Kinetic benzoylation of 1,2-diols using chiral organotin 123 and $CuCl_2$-BOX 126 catalysts

Recently, Kang *et. al*[117] expanded the scope of $CuCl_2$-BOX **129**[117b, c] and $CuCl_2$-PyBOX **130**[117a] catalyst systems established above for enantioseleective benzoylation of various 1,3-diols **131** with different functional group at C2 (Scheme 39). After optimization, monobenzoate products **132** can be obtained with enantioselectivity up to 99% *ee*. It was observed that the *ee* was strongly dependent on various factors including structural variation on the chiral ligands, presence of functional groups X (X = OH, NHCbz, alkyl) on the diol substrates and to a lesser extent on the type of solvent and temperature.

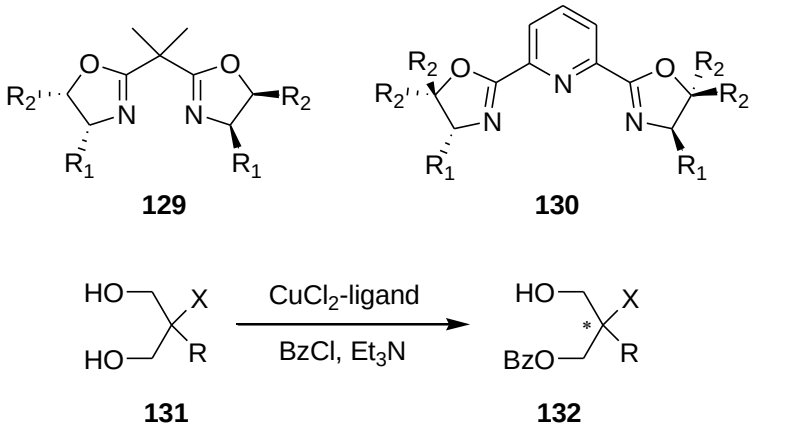

Scheme 39: Enantioselective benzoylation of 1,3-diols 131 using $CuCl_2$-BOX 129 and $CuCl_2$-PyBOX 130 catalysts

In summary, the enantioselectivity in asymmetric acetylation or benzoylation is mostly dependent on the nature of the catalytic system, the diol substrate as well as the acylating agents. Reactions involving acyl halides or acyl anhydrides generally proceeded under kinetic control to prevent over-acylation and racemization. In addition, a stoichiometric amount of non-nucleophilic base such as Et_3N would also be required to neutralize the HCl by-product. On the other hand, vinyl acylate, under activated state through coordination with chiral catalysts, can react readily with the diol substrates. The by-product in this case is vinyl alcohol which would immediately isomerize to acetaldehyde, thus driving the equilibrium of the desymmetrization forward. While the methods mentioned above offer fascinating results, they worked for limited types of 1,3-diol substrates. So far, no general catalytic system has been established to be effective for a wide range of prochiral 1,3-diol substrates. It should be noted that asymmetric desymmetrization of these compounds is particularly challenging due to the remote distance between the prochiral center and the enantiotopic hydroxyl groups.

2. Research methodology

Based on our retrosynthetic analysis of chiral piperidone **1** (Scheme 9, chapter I and shown below), the planned synthetic route for asymmetric synthesis of piperidone **1** using asymmetric catalysis is elaborated in scheme 40.

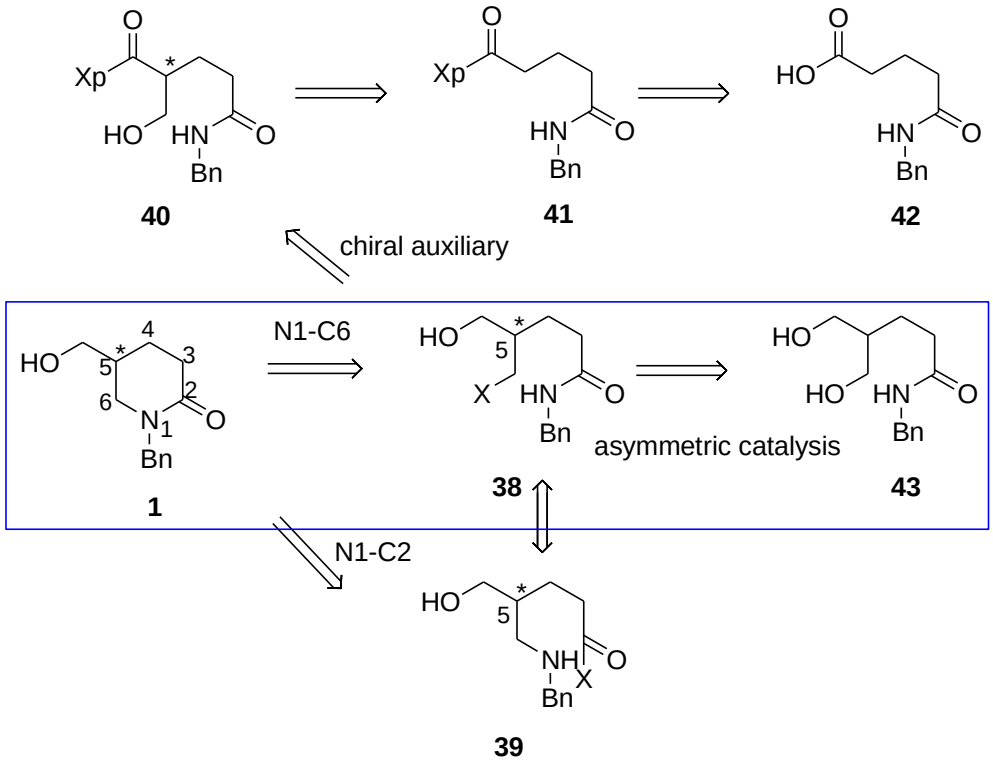

Scheme 9: Retrosynthetic analysis of piperidone 1 (asymmetric catalysis route is highlighted)

The key step in this approach is the desymmetrization of 1,3-diol **43** *via* enantioselective acetylation or enantioselective benzoylation to give the monoacetate or monobenzoate products **133a-b** in enantioenriched form (Scheme 40). Cyclization of **133a-b** can be achieved by substituting the hydroxyl group with a better leaving group, followed by intramolecular amide alkylation to give the expected chiral piperidone **1**.

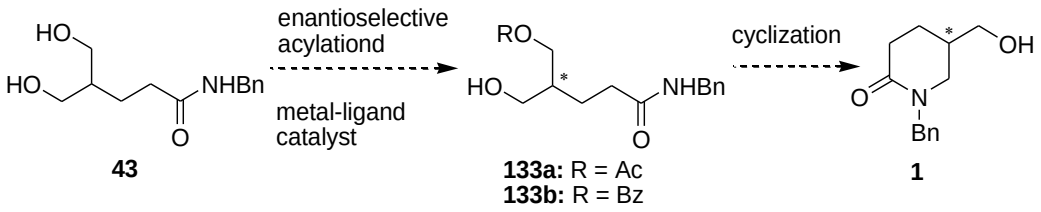

Scheme 40: Strategy for asymmetric synthesis of piperidone 1 *via* asymmetric catalysis

In this chapter, we will feature our approach for the synthesis of 1,3-diol **43** and desymmetrization through enantioselective acylation (using acetylation and benzoylation) of 1,3-diol **43** to **133a-b**. For the purpose of desymmetrization, we will also discuss the synthesis of some Trost and Nagao ligands and their structural modifications.

3. Synthesis of 1,3-diol 43

The synthesis of 1,3-diol **43** was achieved as shown in scheme 41. Michael addition reaction of dimethyl malonate **135** to *tert*-butyl acrylate **134** and dimethyl malonate **135**[118] gave the triester **136** as a colorless oil in 91% yield. The ^{1}H and ^{13}C NMR spectroscopic data of triester **136** were in agreement with the literature values.[118-119] In the next step, chemoselective hydrolysis of the *tert*-butyl ester group of triester **136** using trifluoroacetic acid (TFA)[119a] afforded carboxylic acid **137** in 95% yield as colorless oil. The ^{1}H and ^{13}C NMR spectroscopic data of carboxylic acid **137** were in agreement with the literature values.[119a, 120]

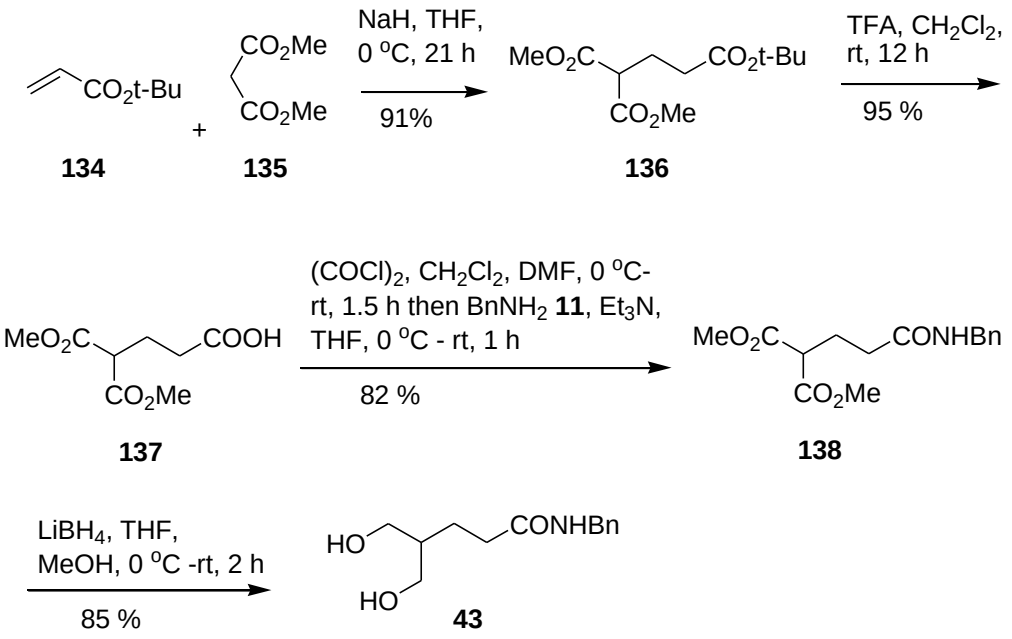

Scheme 41: Synthesis 1,3-diol 43

Subsequently, coupling of carboxylic acid **137** with benzylamine **11** using $(COCl)_2$/ DMF method[121] gave a colorless viscous oil in 82% yield as the main product after purification by column chromatography (EtOAc: hexane, 1: 2 v/v, R_f = 0.3). The FT-IR spectrum of the oil revealed two peaks at 1741 cm^{-1} and 1661 cm^{-1} that corresponded to the absorption bands of the C=O bonds of the methyl ester and *N*-benzylamide moieties, respectively. The high resolution ESI-MS showed a molecular ion *m/z* value of 316.1175 corresponding to $(M+Na)^+$ and supporting the molecular formula $C_{15}H_{19}NO_5$ (*m/z* calcd for $C_{15}H_{19}NO_2Na$ $(M+Na)^+$: 316.1161). The ^1H NMR spectrum showed five aromatic protons at δ 7.28-7.38 and a doublet at δ 4.44 (d, *J*= 15 Hz, 2H) that indicated the presence of the benzyl group. A singlet with six protons at δ 3.75 (s, 6H) accounted for the presence of the two methyl ester groups. In addition, the ^{13}C NMR indicated two carbon signals at δ 169.6 and δ 171.5 that corresponded to two C=O carbons of the ester and amide moieties. Aliphatic carbon signals were also found at δ 24.5 and δ 33.3 that corresponded to the two

secondary carbons and at δ 50.5 that corresponded to tertiary carbon. Based on these data, the compound was assigned structure **138** (Figure 7).

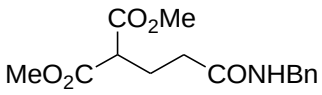

138

Figure 7: Amide 138

In the next step, chemoselective reduction of the two methyl ester groups of amide **138** using $LiBH_4$[122] in MeOH-THF proceeded smoothly and provided a crude viscous oil. Recrystallization of the oil from EtOAc gave white solid in 85% yield. The FT-IR spectrum of the solid showed absorption band at 1646 cm^{-1} corresponding to amide C=O. No ester C=O was observed in the FT-IR spectrum indicating successful reduction. The high resolution ESI-MS showed a molecular ion *m/z* value of 260.1261 corresponding to $(M+Na)^+$ and supporting the molecular formula $C_{13}H_{19}NO_3$ (*m/z* calcd for $C_{13}H_{19}NO_3Na$ $(M+Na)^+$: 260.1263). The ^1H NMR in methanol-d_4 confirmed the disappearance of the proton signals from the methyl ester groups while the proton signals corresponding to the benzyl group still remained intact. In addition, the presence of a new doublet at δ 3.53 (d, *J*=5.1 Hz, 4H) accounted for the two newly formed -C*H*$_2$OH groups. The ^{13}C NMR spectrum indicated a carbon signal at δ 177.6 corresponding to the amide carbonyl carbon-*C*ONHBn. The carbon signal of –*C*H_2OH was found at δ 64.8 and was also confirmed from DEPT135 analysis. Thus, the compound was assigned structure **43** (Figure 8).

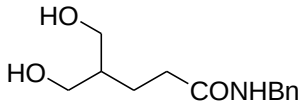

43

Figure 8: 1,3-Diol 43

In conclusion, the 1,3-diol **43** has been synthesized in 61% overall yield in four steps.

4. Synthesis of the chiral ligands for the enantioselective desymmetrization reactions

4.1 Synthesis of Trost ligand 111, 151-154

Synthesis of Trost ligand **111** from dibromide **139** and α,α'-diphenyl prolinol **140** was achieved based on the reported procedure (Scheme 42).[111-112]

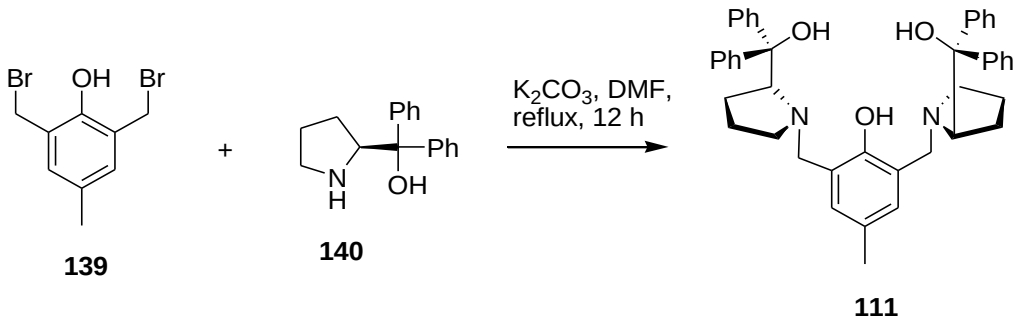

139 **140** **111**

Scheme 42: Synthesis of Trost ligand 111

Synthesis of dibromide **139** was achieved according to scheme 43.[111] Reaction of *p*-cresol **141** with formaldehyde **142** afforded phenol **143** in 89% yield.[123] Selective bromination[124] of phenol **143** at the hydroxymethyl moieties using HBr/AcOH gave the required dibromide **139** in 77% yield. The spectroscopic data of dibromide **139** was in accordance with the literature values.[111]

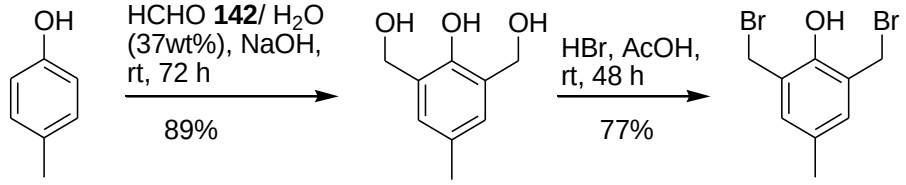

141 **143** **139**

Scheme 43: Synthesis of dibromide 139

The syntheses of α,α'-diphenylprolinol **140**,[125] and its diaryl derivatives α,α'-di(4-biphenyl)prolinol **144**,[126] α,α'-dinaphthylprolinol **145**,[127] α,α'-di(3-methylphenyl)prolinol **146**[128] and α,α'-di(3-methoxyphenyl)prolinol **147**[128] were accomplished according to the literature procedures (Scheme 42). The syntheses started with the protection of the amine group of *L*-proline **148** with ethyl chloroformate **149**[129] to give *L*-proline diacetate **150** in 78% yield as colorless oil.[129] At this stage, structural modifications of the aryl groups were carried out by treating *L*-proline diacetate **150** with different arylmagnesium bromides such as phenylmagnesium bromide, 4-biphenylmagnesium bromide, 2-naphthylmagnesium bromide, 3-methylphenylmagnesium bromide and 3-methoxyphenylmagnesium bromide, respectively. The resulting crude products were subjected to amine deprotection in refluxed KOH-MeOH mixture[130] to give the corresponding α,α'-diaryl prolinol **140**, **144-147** in 50-60% yield after column chromatography (EtOAc:hexane, 1:2 v/v). The spectroscopic data of these diaryl prolinols were in agreement with the literature values.[125-128]

Next, α,α'-diaryl prolinols **140**, **144-147** were coupled with dibromide **139**[126a] to give the corresponding Trost ligand **48,** in 70-85% yield (Scheme 44). The spectroscopic data of ligand **48** and its derivatives **89-92** matched with the literature data, thus confirming the structures of these ligands.[111-112, 128, 131]

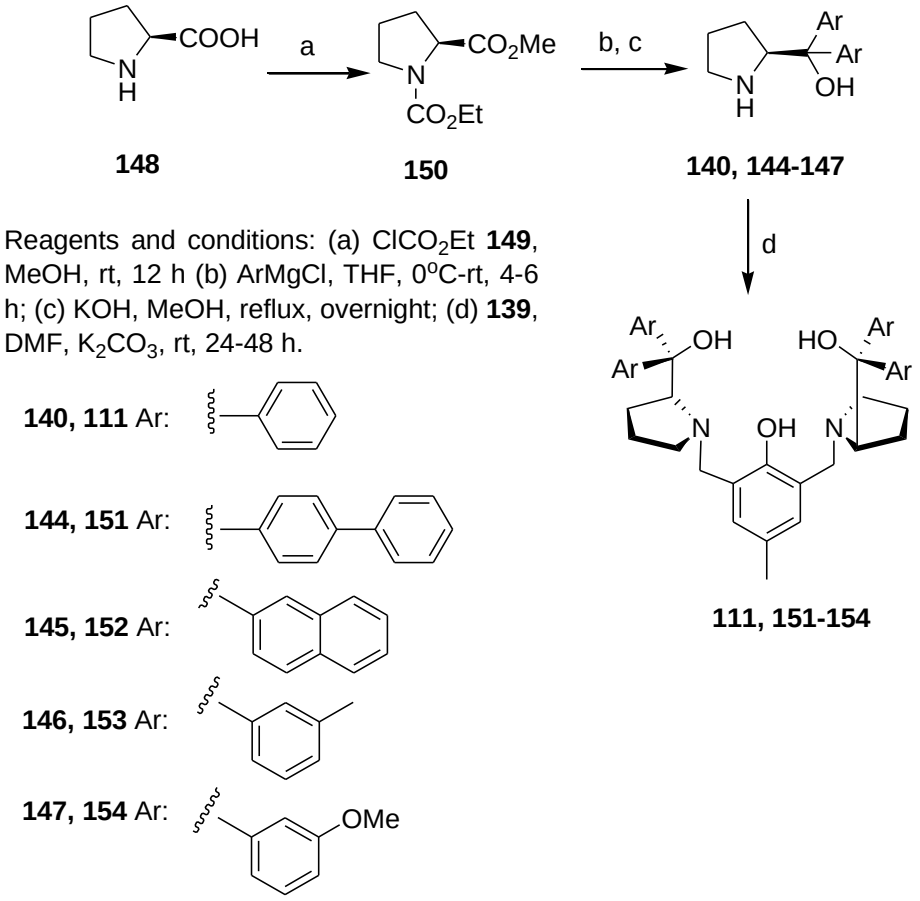

Scheme 44: Synthesis of Trost ligands 111, 151-154

Changing the nature of the linking group between the two prolinol moieties is expected to affect the complexation and potentially show a profound effect on the overall catalytic activity. For example, replacement of the phenol linker with a pyridine linker would change the nature of the donating group from being weakly acidic donating group to basic amine donating group.

Therefore, we made structural modifications on dibromide **139** linker. We synthesized dibromide **155** (Scheme 45) using the same approach described in scheme 41 (the spectroscopic data of dibromide **155** was in agreement with the literature values[132]) and coupled it with α,α'-diphenylprolinol **140** in refluxing K_2CO_3/DMF[126a] to obtain Trost ligand **158**[131] in 73% yield (Scheme 46).

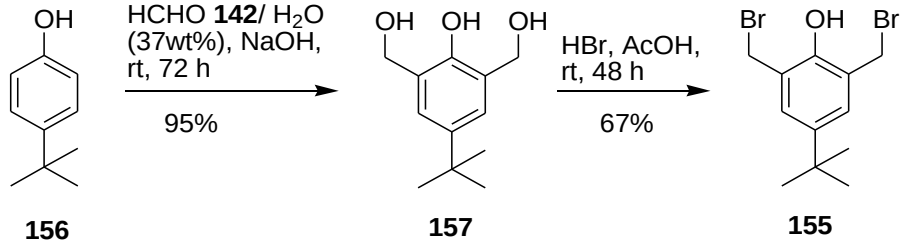

Scheme 45: Synthesis of dibromide 155

Likewise, coupling reactions between the commercially available dibromide **159** and α,α'-diphenylprolinol **140** provided the Trost ligand **160**[133] in 79% yield (Scheme 46). The spectroscopic data of Trost ligands **158** and **160** were in agreement with the literature data.[131, 133]

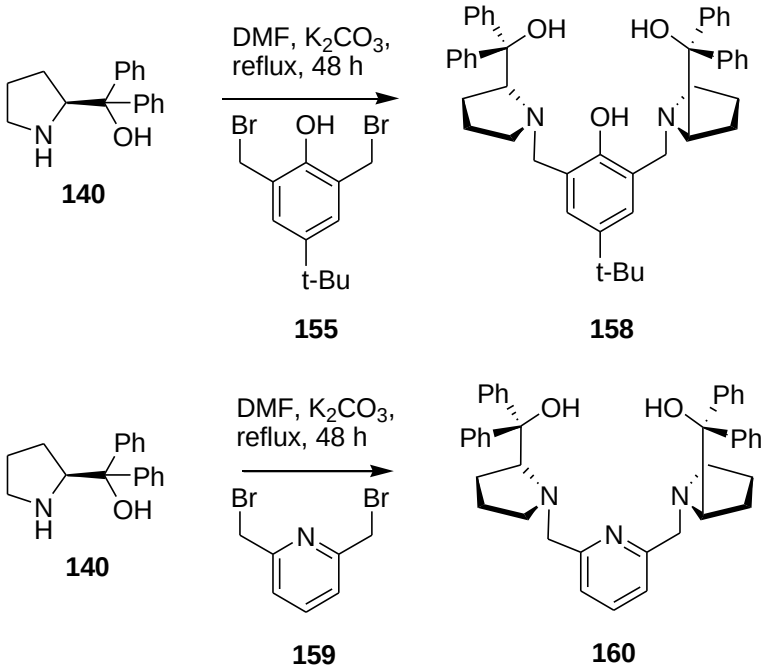

Scheme 46: Synthesis of Trost ligands 158 and 160

In conclusion, it can be seen that the modular nature of this synthetic approach allows for facile structural modifications at the aryl moieties of the prolinol substrate **140** and the dibromide linker **139**. By introducing different substituent groups on the phenyl rings of prolinol moieties**,** stereoelectronic effects of the

aryl groups on the enantioselectivity may be obtained.[126a] Changing the nature of the linkage can also have profound effect on the enantioselectivity.

4.2 Synthesis of zinc-sulfonamide catalyst 120

Synthesis of chiral sulfonamide **119** and its zinc-sulfonamide catalyst **120** were achieved following the reported procedure (Scheme 47).[114] Chiral diamine **161** underwent one-pot mono-sulfonylation with 3,5-bis(trifluoromethyl)benzenesulfonyl chloride **162** followed by double *N*-methylation of the terminal amine group with MeI. After work up and purification by column chromatography (EtOAc: hexane; 1: 2 v/v), chiral sulfonamide **119** was obtained as white crystals in 63% yield. ^{1}H and ^{13}C NMR data of this compound matched the literature values.[114] Treatment of chiral sulfonamide **119** with Et_2Zn in $CHCl_3$ provided zinc-sulfonamide catalyst **120** as white solid in quantitative yield.[114]

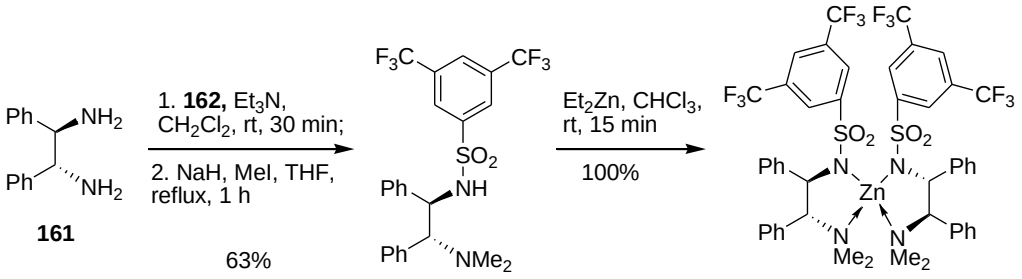

Scheme 47: Synthesis of chiral sulfonamide 119 and zic-sulfonamide catalyst 120

With the availability of Trost ligands **111**, **151-154**, **158**, **160 (**Scheme 44, 46), zinc-sulfonamide catalyst **120** (Scheme 47) and other commercially available "privilege" ligands including TADDOL **102**, pyBOX **163-164**, (-)-sparteine

165, Salen **166**, and BINOL **167** (Figure 9), we proceeded to investigate the feasibility of chiral desymmetrization of 1,3-diol **21**.

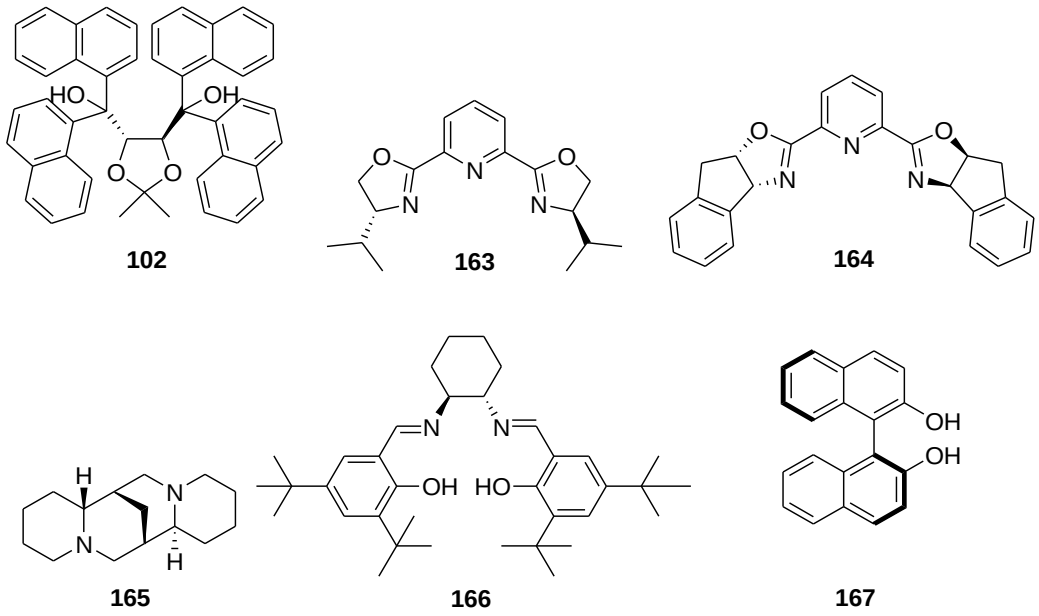

Figure 9: Commercially available chiral ligands to be used for desymmetrization of 1,3-diol 43

Before examining the asymmetric desymmetrization of 1,3-diol 43, we decided to examine the most suitable Lewis acid to be used.

5. Screening of Lewis acids for acetylation of 1,3-diol 43

For our purpose, different Lewis acids including metal triflates and metal chlorides were screened for acetylation of 1,3-diol **43** using Ac_2O as the acylating agent (Table 1).[107] A typical acetylation experiment involved using 0.5 mmol of 1,3-diol **43** (1.0 equiv.), Lewis acid (10 mol%) and Ac_2O (5.0 equiv.) in CH_2Cl_2 at room temperature (Table 1). The reaction was monitored by TLC and worked up after consumption of 1,3-diol **43**. TLC analysis of these reactions showed two new spots above the starting material 1,3-diol **43** (using pure EtOAc as the eluent). The crude reaction mixture was purified by column

chromatography (EtOAc: hexane, 4: 1) to give two fractions corresponding to the two new spots observed in the TLC.

The FT-IR spectrum of the top fraction (R_f= 0.8, pure EtOAc as the eluent) showed two peaks at 1741 cm^{-1} and 1655 cm^{-1} that corresponded to the absorption of the C=O bonds of the ester and amide moieties, respectively. The high resolution ESI-MS showed a molecular ion *m/z* value of 344.1481 corresponding to $(M+Na)^+$ and supporting the molecular formula $C_{17}H_{23}NO_5$ (*m/z* calcd for $C_{17}H_{23}NO_5Na$ (M+Na)+: 344.1474). In comparison with the ^1H NMR spectrum of the starting material 1,3-diol **43**, the ^1H NMR spectrum of the top fraction showed a new singlet at δ 2.04 (s, 6H) which indicated the presence of two acetyl moieties in the product. The ^{13}C NMR showed the carbon signals corresponding to the methyl carbon and carbonyl carbon of the acetyl moiety at δ 21.0 and δ 171.2 respectively. Therefore, the top fraction was assigned structure **168** (Figure 10).

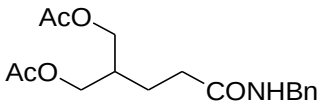

168

Figure 10: Diacetate 168

The FT-IR spectrum of the bottom fraction (R_f= 0.4, pure EtOAc as the eluent) showed two peaks at 1737 cm^{-1} and 1659 cm^{-1} that corresponded to the absorption of two C=O bonds of the ester and amide moieties, respectively. The high resolution ESI-MS of this bottom fraction showed a molecular ion *m/z* value of 302.1373 corresponding to $(M+Na)^+$ and supporting the molecular formula $C_{15}H_{21}NO_4$ (m/z calcd for $C_{15}H_{21}NO_4Na$ $(M+Na)^+$: 302.1368). In

comparison with the ^{1}H NMR spectrum of starting material 1,3-diol **43**, ^{1}H NMR spectrum of the bottom fraction showed a new singlet at δ 1.96 (s, 3H) which indicated the presence of one acetyl moiety in the product. The ^{13}C NMR spectrum showed the carbon signals corresponding to the methyl carbon and carbonyl carbon of the acetyl moiety at δ 20.9 and δ 171.6 respectively. Therefore, the bottom fraction was assigned the structure **133a** (Figure 11).

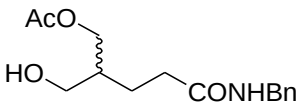

***rac*-133a**

Figure 11: Racemic monoacetate 133a

The results in table 1 showed that $Yb(OTf)_3$ is the most active Lewis acid since it gave the diacetate **168** in 70% yield in the shortest reaction time of 3 h (Table 1, entry 1). $Bi(OTf)_3$ is very chemoselective for monoacetylation of diol **21** and gave 71% yield of the monoacetate **133a** after 5 h (Table 1, entry 5). Similarly, $Cu(OTf)_2$ gave the monoacetate **133a** in 72% yield along with trace amount of the diacetate **168** (3%) after 6 h (Table 1, entries 9). Other triflates including $Ga(OTf)_3$, $In(OTf)_3$, $Zn(OTf)_2$ were less effective (Table 1, entries 6-8). In particular, while $Ga(OTf)_3$ provided the monoacetate **133a** in 57% yield after more than 12 h, $In(OTf)_3$ and $Zn(OTf)_2$ were even less effective and gave around 75% yield of the monoacetate **133a** after 20 h. Interestingly, while $FeCl_3$ provided 58% yield of the monoacetate **133a** after 18 h (Table 1, entry 12), $CuCl_2$, $ZnCl_2$ and $CoCl_2$ gave only traces of the product (Table 1, entries 10, 11 and 13, respectively).

Table 1: Screening of different metal Lewis acid for acetylation of 1,3-diol 43[a]

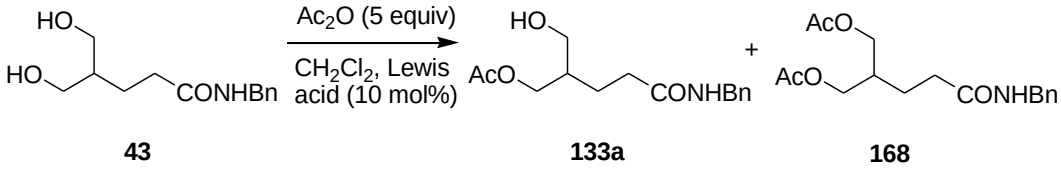

43 **133a** **168**

Entry	Lewis acid	Time (h)	**133a**[b] Yield (%)	**168**[b] Yield (%)
1	$Yb(OTf)_3$	3	29	70
2	$Yb(OTf)_3$	1.5	79	4
3	$Yb(OTf)_3$ (5 mol%)	4	84	6
4	$Yb(OTf)_3$ (1 mol%)	9	92	3
5	$Bi(OTf)_3$	5	71	15
6	$Ga(OTf)_3$	20	57	9
7	$In(OTf)_3$	20	75	15
8	$Zn(OTf)_2$	18	78	12
9	$Cu(OTf)_2$	6	72	3
10	$CuCl_2$	24	trace	0
11	$ZnCl_2$	24	trace	0
12	$FeCl_3$	18	58	17
13	$CoCl_2$	24	trace	0

[a]: All the reactions started with 0.5 mmol of 1,3-diol **43** (1.0 equiv.), Lewis acid (10 mol%) and Ac_2O (5.0 equiv.) in CH_2Cl_2 at room temperature.
[b]: Isolated yield

We then attempted to shift the chemoselectivity of $Yb(OTf)_3$ (Table 1, entry 1) to the monoacetate **133a** product since it is the most active Lewis acid. Gladly, reduction in the reaction time from 3 to 1.5 h basically reversed the selectivity

and gave the monoacetate **133a** in 79% yields on the account of the diacetate **168** which was obtained in just 4% yield (Table 1, entry 2). Furthermore, when we decreased the amount of $Yb(OTf)_3$ from 10 mol% to 5 mol% then to 1 mol%, the selectivity and yield significantly improved and monoacetate **133a** was obtained in 84% and 92%, respectively (Table 1, entries 3-4).

In conclusion, we found that $Yb(OTf)_3$ is the most suitable Lewis acid catalyst for the selective monoacylation of 1,3-diol **43**. Next, complexes of $Yb(OTf)_3$ with chiral ligands including Trost ligands **111** and **160** (Scheme 46), TADDOL **102**, PyBOX **163** and **164**, (-)-sparteine **165**, salen **166**, BINOL **167** (Figure 5) will be examined for the enantioselective acetylation of 1,3-diol **43**.

6. Screening of complexes of $Yb(OTf)_3$ with chiral ligands for enantioselective acetylation of 1,3-diol 43

Chiral $Yb(OTf)_3$ complexes have been characterized and utilized successfully in many enantioselective C-C bond forming reactions.[134] For example, $Yb(OTf)_3$/ BINOL/ bulky amine systems developed by Kobayashi,[135] have been used as chiral Lewis acids in Diels-Alder reactions,[135-136] ring opening of *meso* epoxide,[137] as well as 1,3-dipolar addition.[138] The $Yb(OTf)_3$/ PyBOX ligands have also been used effectively for 1,3-dipolar cycloaddition,[139] hetero-Diels-Alder reaction[140] and glyoxylate ene reaction.[141] Due to the lanthanide contraction effect, the atomic radii decrease as the atomic mass increases. Yb^{3+} is the second smallest lanthanide anion and thus has the second strongest Lewis acidic activity in the lanthanide group.[142] Therefore, as hard acid, Yb^{3+} preferentially chelates with hard ligands such as *O*- and *N*-donor ligands.[142]

Complexes of $Yb(OTf)_3$ with chiral *N*-, *O*-donor and *N*,*O*-donor ligands, including TADDOL **102**, Trost ligand **111** (Scheme 40) and **160** (Scheme 44), PyBOX **163** and **164**, (-)-sparteine **165**, salen **166**, BINOL **167** (Figure 3) were screened for the enantioselective acetylation of 1,3-diol **21**. The chiral complexes were prepared *in situ* by mixing a 1:1 molar ratio of $Yb(OTf)_3$ with the respective ligand in CH_2Cl_2 (to make a 5 mol% solution) for 1 h at room temperature. The reaction was performed by addition of 1,3-diol **43** and Ac_2O to the above catalyst solution (Table 2).

Table 2: Screening of complexes of $Yb(OTf)_3$/chiral ligands for enantioselective acetylation of 1,3-diol 43[a]

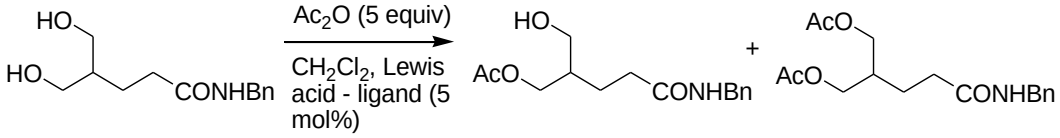

43 **133a** **168**

Entry	Ligand	Time (h)	**133**[b] Yield (%)	ee[c] (%)	**168**[b]
1	**102**	1.5	85	0	3
2	**111**	168	trace	-	-
3	**160**	168	trace	-	-
4	**163**	5	60	0	-
5	**164**	4	80	0	-
6	**165**	5	65	0	-
7	**166**	4	83	0	-
8	**167**	1.5	81	0	5

[a]: All the reactions started with 0.5 mmol of 1,3-diol **43** (1.0 equiv.), Lewis acid-ligand (3.0 mol%) and Ac_2O (5.0 equiv.) in CH_2Cl_2 at room temperature.

[b]: Isolated yield
[b]: *ee* was determined by HPLC, Chiralpak AD-H (hexane: *i*-PrOH, 95: 5 v/v), 0.9 ml/ min, 254 nm, t_1: 46.3 min, t_2: 49.8 min

The following observations can be deduced from table 2:

1. Ligands **102**, **163-167** gave the monoacetate **133a** in yields ranging from 60-85% (Table 2, entries 1, 4-8). The presence of starting material 1,3-diol **43** was still detected in TLC.
2. The yield of diacetate **168** was negligible in all cases.
3. The pentadentate Trost's ligand **111** and **160** severely retarded the reactions as only trace amount of the desired product could be obtained even after one week reaction time (Table 2, entries 2-3).
4. In all cases, no enantioselectivity was detected. Only racemic products were obtained according to chiral HPLC analysis.
5. The presence of chiral ligands significantly enhanced the reaction rate since the reaction can be completed in 1.5 h in comparison to 4 h (Table 2, entries 1 and 8 *vs* Table 1, entry 3).
6. Selectivity between monoacetate **133a** and diacetate **168** was significantly enhanced in the presence of the ligands, especially in the case of TADDOL **102** and BINOL **167**.
7. The reactivity of these $Yb(OTf)_3$/ chiral ligands were highly dependent on the temperature. In particular, reactions at 0 ^oC were very sluggish.

Combinations of other metal triflates $Bi(OTf)_3$, $Cu(OTf)_2$ and $Zn(OTf)_2$ with chiral ligands **102, 111, 160**, and **163-167** under similar reaction conditions described in table 2 gave similar outcomes to $Yb(OTf)_3$ *albeit* with lower yields and longer reaction times. The reason why no induction took place in these

reactions may be attributed to the formation of TfOH and acyl triflate that may be the actual catalysts in metal triflate-catalyzed acylation.[143] No investigations were carried out to ascertain this.

Since no enantioselective induction was observed in the acetylation of 1,3-diol **43** with Yb(OTf)3/ chiral ligand **102, 111, 160**, and **163-167**. Trost,[111, 113] Nagao,[114] and Kang[117a] procedures were then examined for better results.

7. Desymmetrization of 1,3-diol 43 *via* enantioselective acylation using Trost, sulfonamide and PyBOX ligands

Trost catalyst **112** (Scheme 34), zinc-sulfonamide catalyst **120** (Scheme 37), and $CuCl_2$-PyBOX **130** (Scheme 39) were screened for the enantioselective acylation of 1,3-diol **43**. While PyBOX **163** and **164** are commercially available, Trost ligand **111** and chiral sulfonamide **119** were synthesized as mentioned in section 3 of this Chapter.

Different desymmetrization methods A, B and C were screening using 1,3-diol **43** in an attempt to establish the best conditions (Table 3). Unfortunately, the insolubility of 1,3-diol **43** in CH_2Cl_2, PhMe or MTBE made the reactions very sluggish. Catalytic method A[111, 113] (Table 3, entries 1-2) and C[117a] (Table 3, entries 4-5) gave no products. On the other hand, method B[114] which utilized zinc-sulfonamide catalyst **120** afforded very modest yield of monoacetate **133a** in racemic form (Table 3, entry 3).

Table 3: Enantioselective acylation of 1,3-diol 43 under different reaction conditions

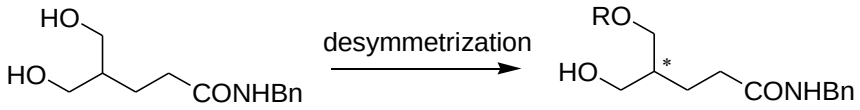

43 **133a** R: Ac
133b R: Bz

Method A: **111** (10 mol%), Et_2Zn (20 mol%), vinyl benzoate (5.0 equiv), rt, 24 h
Method B: **119** (10 mol%), Et_2Zn (5 mol%), Ac_2O (1.5 equiv), 0 ^oC, 12 h
Method C: **163** or **164** (10 mol%), $CuCl_2$ (10 mol%), BzCl (1.5 equiv), Et_3N (1.1 equiv), -78 ^oC, 6 h

Entry	Method	Solvent	Time	Product	Yield[a] (%d)	*ee*[b] (%)
1	A	PhMe	48	**133b**	-	-
2	A	THF	20	**133b**	trace	-
3	B	MTBE	48	**133a**	23	0
4	C (**163**)	CH_2Cl_2	48	**133b**	-	-
5	C (**164**)	CH_2Cl_2	48	**133b**	-	-

[a]: Isolated yields
[b]: *ee* was determined by HPLC, Chiralpak AD-H (hexane: *i*-PrOH, 95: 5), 0.9 ml/ min, 254 nm, t_1: 46.3 min, t_2: 49.8 min

To overcome the insolubility issue of 1,3-diol **43**, we made structural modification by converting its *N*-benzylamide group to an ester group and thus synthesized 1,3-diol **169** (Scheme 48).

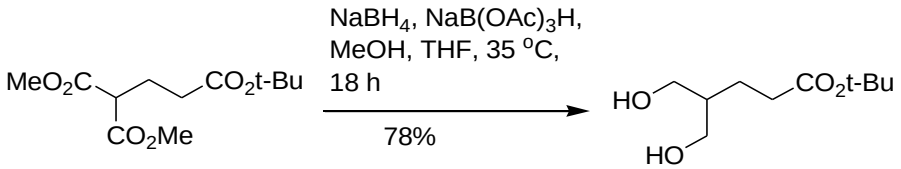

136 **169**

Scheme 48: Synthesis of 1,3-diol 169

Selective reduction of the two methyl ester groups of triester **136** (Scheme 39) was achieved using $NaBH_4$ in the presence of catalytic amount of $NaB(OAc)_3H$.[144] After purification using column chromatography using pure EtOAc as eluent (R_f = 0.3), the product was obtained as colorless viscous oil in 78% yield. The FT-IR spectrum of the oil showed a sharp peak at 1731 cm^{-1} which corresponded to the absorption of C=O bond of the ester moiety. High resolution ESI-MS of the oil showed a molecular ion *m/z* value of 227.1261 corresponding to $(M+Na)^+$and supporting the molecular formula $C_{10}H_{20}O_4$ (m/z calcd for $C_{10}H_{20}O_4Na$ (M+Na)+: 227.1259). In comparison to the ^1H NMR spectrum of its starting material triester **136**, the ^1H NMR spectrum of the oil showed the disappearance of the singlet corresponding to the methyl protons of two acetyl moieties. Meanwhile, the proton signal corresponding to the tert-butyl group was found at δ 1.45 (s, 9H), indicating the selective reduction of methyl ester groups. In addition, the ^{13}C NMR showed the carbon signals of the *tert*-butyloxy moiety at δ 28.1, δ 80.8 and δ 173.7 (for the C=O carbon). The carbon signal for HOCH_2- was found at δ 65.2. These results confirmed the formation and the structure of 1,3-diol **169**.

Next, desymmetrization of 1,3-diol **169** *via* asymmetric acylation using Trost,[111, 113] Nagao,[114] and Kang[117a] protocols were investigated.

8. Desymmetrization of 1,3-diol 169 via enantioselective acylation using Trost, sulfonamide and PyBOX ligands.

Preliminary screening results of the asymmetric acylation of 1,3-diol **169** are summarized in table 4. Contrary to the case of 1,3-diol **43**, method A using Trost ligand **111** afforded the monobenzoate product **170b** in 33% yield as an oil and in 28% *ee* (Table 4, entry 1) after purification by column chromatography (EtOAc: hexane, 1: 3 v/v). However, method B provided poor yield of the racemic monobenzoate product **170b** while method C failed to offer any products (Table 4, entries 2-4, respectively).

Table 4: Enantioselective acylation of 1,3-diol 169 under different reaction conditions

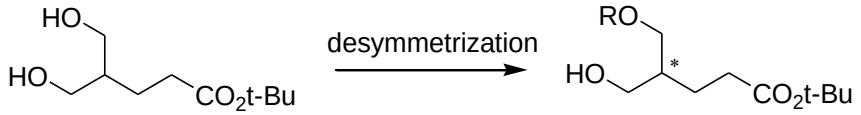

169 **170a** R: Ac
170b R: Bz

Method A: **111** (10 mol%), Et_2Zn (20 mol%), vinyl benzoate (5.0 equiv), rt, 24 h
Method B: **119** (10 mol%), Et_2Zn (5 mol%), Ac_2O (1.5 equiv), 0 ^oC, 12 h
Method C: **163** or **164** (10 mol%), $CuCl_2$ (10 mol%), BzCl (1.5 equiv), Et_3N (1.1 equiv), -78 ^oC, 6 h

Entry	Method	Solvent	Time	Product	Yield[a]	*ee*[b](%)
1	A	PhMe	20	**170b**	33	28[b]
2	B	MTBE	48	**170a**	15	0
3	C (**163**)	CH_2Cl_2	48	**170b**	-	-
4	C (**164**)	CH_2Cl_2	48	**170b**	-	-

[a]: Isolated yield
[b]: Determined by HPLC, Chiralcel OD-H (hexane: *i*-PrOH, 90: 10), 1.0 ml/ min, 254 nm, t1: 21.6 min, t2: 29.8 min.

The monobenzoate **170b** was fully characterized by FT-IR, high resolution ESI-MS, ^{1}H and ^{13}C NMR. The FT-IR spectrum of **170b** showed a sharp peak at 1725 cm^{-1} which indicated the absorption band of C=O bond of ester moiety. High resolution ESI-MS of the compound showed a molecular ion *m/z* value of 331.1522 corresponding to $(M+Na)^{+}$ and supporting the molecular formula $C_{17}H_{24}O_5$ (*m/z* calcd for $C_{17}H_{24}O_5Na$ (M+Na)+: 331.1521). In comparison with the 1H NMR of its starting material 1,3-diol **169** the ^{1}H NMR spectrum of the product **170b** showed five aromatic protons at δ 7.35-7.98 indicating the presence of only one phenyl moiety in the compound. The singlet at δ 1.38 which integrated for nine protons confirmed the presence of the *tert*-butyloxy moiety. The ^{13}C NMR showed the typical aromatic carbon signals at δ 128.4, δ 129.6, δ 130.0, and δ 133.1. In addition, carbon signals corresponding to two C=O of the ester moieties were found at δ 167.0 and δ 173.1. Those results confirmed the formation and the structure of monobenzoate **170b**.

Since only 1,3-diol **169** provided promising results with Trost ligand **111**, optimizations by examining the effects of catalyst loading, structural modification of the ligand, solvent and temperature were carried out in an attempt to obtain better yield and enantioselectivity.

9. Optimization of the desymmetrization of 1,3-diol 169 *via* enantioselective benzoylation using Trost ligand 111 based on method A

9.1 Effects of catalyst loadings

Table 5: Enantioselective benzoylation of 1,3-diol 169 at different loading of Trost catalyst 112[a]

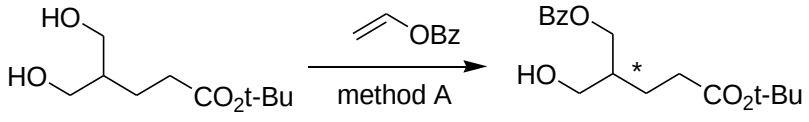

169 **170b**

Entry	Loading (mol%)	Yield[b] (%)	*ee*[c] (%)
1	5	26	25
2	10	33	28
3	20	35	36
4	50	41	51
5	100	51	74

[a]:All the reactions were performed using 0.5 mmol of 1,3-diol **169** in the solution containing a given loading of *in situ* Trost catalyst **112** in PhMe(prepared from Trost ligand **111** and Et_2Zn in 1:2 molar ratio) with vinyl benzoate (5.0 equiv.) in dry PhMe under inert atmosphere at room temperature (25 °C) in 24 h.
[b]: Isolated yield
[c]: Determined by HPLC, Chiralcel OD-H (hexane: *i*-PrOH, 90: 10), 1.0 ml/ min, 254 nm, t1: 21.6 min, t2: 29.8 min.

The effect of Trost catalyst **112** (Scheme 32) loading on the desymmetrization reaction was examined first using 5-100% loading (Table 5). An increase in the enantioselectivity and yield of monobenzoate **170b** was observed with gradual increase in the catalyst loading (Table 5, entries 1-5). In particular, the *ee* was highest at 74% when 100 mol% of the catalyst (Table 5, entry 5) was used and

it decreased to 51% *ee* at 50 mol% catalyst loading (Table 5, entry 4). However, when the catalyst loading was below 50 mol%, the *ee* was significantly reduced to below 35% (Table 5, entries 1-3). The yield of the monobenzoate **170b** increased as the catalyst loading increased and ranged from a low of 26% (5 mol% loading) to moderate 51% (100% mol loading) after 24 h. In addition, we observed that as the reaction time increased, the enantioselectivity of the monobenzoate **105** gradually diminish suggesting *in situ* racemization.

Stoichiometric catalytic loading is usually not desirable in asymmetric reactions due to many disadvantages including atom economy and costs. Subsequently, the effect of structural modification of Trost ligand on enantioselectivity was examined.

9.2 Effects of structural modifications of Trost ligands

For this purpose, we synthesized Trost ligands **151-154**, **158** and **160** as described before in section 2 (Figure 12). Using a catalyst loading of 10 mol%, the effects of different Trost ligands **151-154**, **158** and **160** were examined for enantioselective benzoylation of 1,3-diol **169** and the results compared to the Trost ligand **111** (Table 6).

Better enantioselectivities were obtained with increasing bulkiness of the diaryl groups in the prolinol moieties probably due to their influence on the steric demand of the chiral space (Table 6, entries 1-5). Ligand **151**, with the highest steric demand, afforded the highest *ee* of 39% and gave 43% yield after 4 days (Table 6, entry 2). When *o*-methoxy group was incorporated in the aryl moiety as in ligand **154** (Table 6, entry 5), the ligand offered similar result to that of ligand **151**. Influence of the nature of the metal-chiral ligand linkage was also

examined. Ligand **158** which has a *tert*-butyl group at the phenol linker (instead of the methyl group as in ligand **111**) gave monobenzoate **170b** in just 9% *ee* (Table 6, entry 6). Unfortunately, dinuclear zinc complex of **160** was unsuccessful in catalyzing the benzoylation of 1,3-diol **169** (Table 6, entries 7).

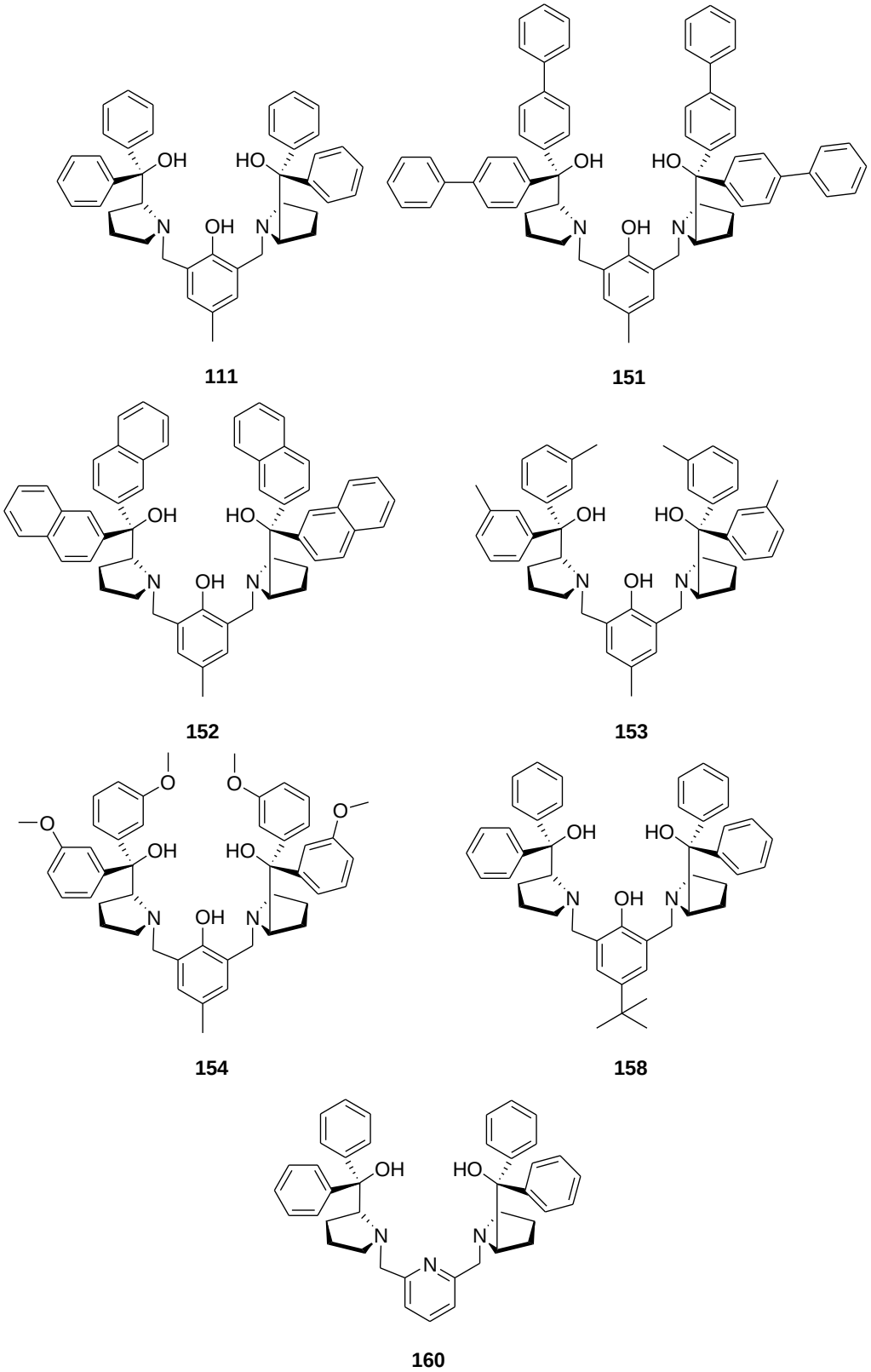

Figure 12: Structural modifications of Trost ligands

Table 6: Desymmetrization of 1,3-diol 169 with different Trost ligands 111, 151-154, 158 and 160[a]

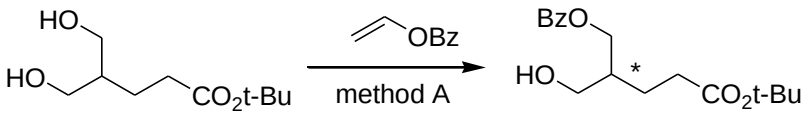

169 **170b**

Entry	Ligand	Loading (mol%)	Yield[b] (%)	*ee*[c] (%)
1	**111**	10	33	28
2	**151**	10	20	36
3	**152**	10	43	39
4	**153**	10	19	31
5	**154**	10	36	38
6	**158**	10	12	9
7	**160**	10	-	-

[a]:All the reactions were performed using 0.5 mmol of 1,3-diol **169** in the solution containing a 10 mol% of *in situ* Trost catalyst in PhMe (prepared from a given Trost ligand and Et_2Zn in 1:2 molar ratio) with vinyl benzoate (5 equiv.) in dry PhMe under inert atmosphere at room temperature (25 °C) in 24 h.
[b]: Isolated yield
[c]: Determined by HPLC, Chiralcel OD-H (hexane: *i*-PrOH, 90: 10), 1.0 ml/ min, 254 nm, t1: 21.6 min, t2: 29.8 min.

Though the enantioselectivity obtained from **151** and **154** were similar, ligand **154** was used for further optimizations due to its facile separation from the monobenzoate **170b** and the Trost ligand **154**. In the next step, the effects of temperature and solvents were investigated using ligand **154**.

9.3 Effects of temperature and solvents

The effects of temperature and solvents on the desymmetrization of 1,3-diol **169** are summarized in table 7. Reaction at 0 °C (Table 7, entry 1) proved to be sluggish and the monobenzoate **170b** was obtained in trace amount. However, though increasing the reaction temperature to 50 °C improved the yield, the *ee* was drastically decreased from 38% to 11% (Table 7, entry 2). Therefore, after several experiments, room temperature or 25 °C was thought to be the optimal temperature.

Table 7: Enantioselective benzoylation of 1,3-diol 169 at different temperature and solvents[a]

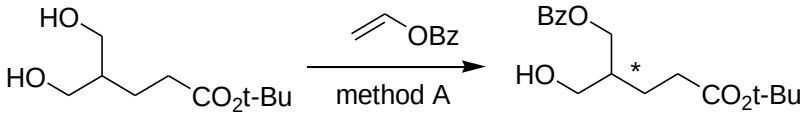

169 **170b**

Entry	Solvent	Temp. (°C)	Time (h)	Yield[c] (%)	*ee*[d] (%)
1	PhMe	0	192	trace	n.d
2	PhMe	50	96	50	11
3	THF	rt[b]	192	39	28
4	Et_2O	rt	192	38	47
5	CH_2Cl_2	rt	192	39	44
6	$CHCl_3$	rt	192	20	41
7	MeCN	rt	192	15	14

[a]:All the reactions were performed using 0.5 mmol of 1,3-diol **169** in the solution containing a 10 mol% of *in situ* Trost catalyst in PhMe (prepared from given Trost ligand **154** and Et_2Zn in 1:2 molar ratio) with vinyl benzoate (5 equiv.) in given solvent under inert atmosphere at given temperature.

[b]: 25 °C
[c]: Isolated yield
[d]: Determined by HPLC, Chiralcel OD-H (hexane: *i*-PrOH, 90: 10), 1.0 ml/ min, 254 nm, t1: 21.6 min, t2: 29.8 min.

The effects of different solvents were then examined. Coordinating solvents such as THF and Et_2O showed contrasting results. While Et_2O gave 47% *ee*, THF gave only 28% ee (Table 7, entries 3-4). On the other hand, non-coordinating, chlorinated solvents like CH_2Cl_2 (Table 7, entry 5) and $CHCl_3$ (Table 7, entry 6) provided slightly better *ee* compared to the nonpolar hydrocarbon solvent such as toluene or polar solvent such as MeCN which only gave 14% *ee* (Table 7, entry 7).

It can be seen that though Trost catalysts provided the most positive result in the enantioselective benzoylation of 1,3-diol **169**, the level of enantioselectivity was not satisfactory. The electron withdrawing group on the side chain of 1,3-diols **43** and **169** may have decreased the nucleophilicity of the hydroxyl groups which probably resulted in weakened coordination of these 1,3-diols to the acidic zinc species in the catalysts. This may have led to reduction in the propensity to undergo benzoylation reactions.

10. Conclusion

We have synthesized several chiral ligands and applied them for the desymmetrization of 1,3-diol **43** and 1,3-diol **169** *via* the enantioselective acylation using several metal-based chiral catalysts.[111, 113-114, 117] Selective monoacetylation of 1,3-diol **43** can be effectively accomplished using $Yb(OTf)_3$. However, incorporation of chiral ligands to $Yb(OTf)_3$ significantly enhanced the acylation rate but with no enantioselectivity.

Desymmetrization *via* enantioselective benzoylation of 1,3-diol **43** and 1,3-diol **169** using Trost catalysts were also investigated. The results showed that the Trost catalyst derived from Trost ligand **154** and Et_2Zn complex was most successful in desymmetrization of 1,3-diol **169** to give monobenzoate **170b** in up to 50% yield and up to 47% *ee* after extensive optimization.

Chapter IV: Asymmetric synthesis of piperidone 1 *via* desymmetrization of 1,3-diols and their diacetate using enzymatic approach

1. Introduction

Organic reactions catalyzed by enzymes have been widely employed in the laboratory[48, 145] and at industrial scale.[146] Advantages of using enzymes as biocatalysts in asymmetric reactions compared to those catalyzed by chemical catalysts include high chemoselectivity, regioselectivity and stereoselectivity.[146] Reactions catalyzed by enzymes normally happen under mild conditions and thus avoiding many potential side reactions including racemization, isomerization, epimerization and rearrangement.[146] Enzymatic reactions are also considered to be environmentally friendly as they usually proceed without the use of toxic solvents. Nevertheless, a major disadvantage of enzymes is the difficulty to access the other enantiomer since enzyme extracted from nature only has one enantiomeric form.[147]

It was commonly believed that enzymatic reactions were only applicable in aqueous media where enzymes retain their configuration and activity.[148] In fact, denaturation of enzymes occurred in aqueous-organic mixtures.[149] However, studies over the past decades demonstrated that not only enzymes can work in organic solvents containing little or no water, but they exhibit many useful and unique catalytic properties which is not observed in traditional aqueous media.[150] For example, in organic solvents, lipases can catalyze the transesterification reactions with various nucleophiles including alcohols, amines and thiols; a process which is completely reversed in aqueous media.[145a] Therefore, the compatibility of enzyme in organic solvents allows a

much wider application of enzyme as biocatalysts for many unconventional enzymatic reactions. The use of enzymes, especially lipases, in enantioselective acetylation of *meso* and prochiral diols have been reviewed extensively.[145a] The two enantiomeric acetylated products can be obtained using the same lipase through acetylating a diol such as 1,3-diol **171** to obtained **173** or deacetylating a diacetate such as 1,3-diacetate **172** to obtain ent-**173** (Scheme 49).[151]

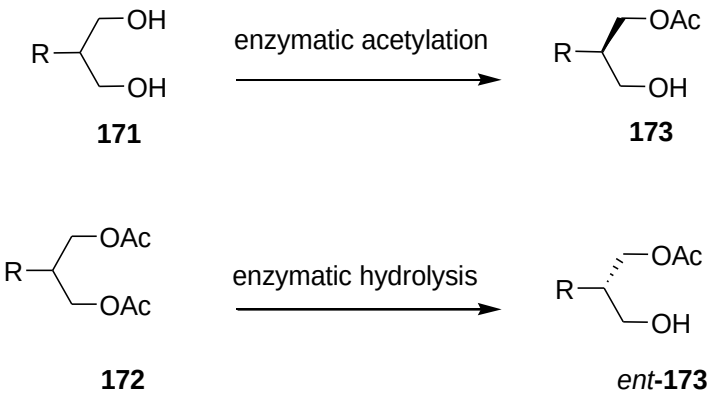

Scheme 49: Desymmetrization of 1,3-diol and 1,3-diacetate

Based on the literature review, enzymatic acetylation of analogues of our 1,3-diol **43** (Scheme 41, chapter III) and 1,3-diol **169** (Scheme 48, chapter III) have been investigated. Takabe[152] investigated the enantioselective acetylation of different 1,3-diols such as **174** and **175** (analogues to 1,3-diol **43**) using lipase PS (from *Burkholderia cepacia*) (Scheme 50). Along with the high enantioselectivity obtained at optimal conditions *albeit* in fairly low yield; the stereospecificity showed a strong dependence to the *C*2-substituent of the 1,3-diol structure. In particular, a slight modification in the amide group could lead to a complete stereochemical inversion in the product (Scheme 50).

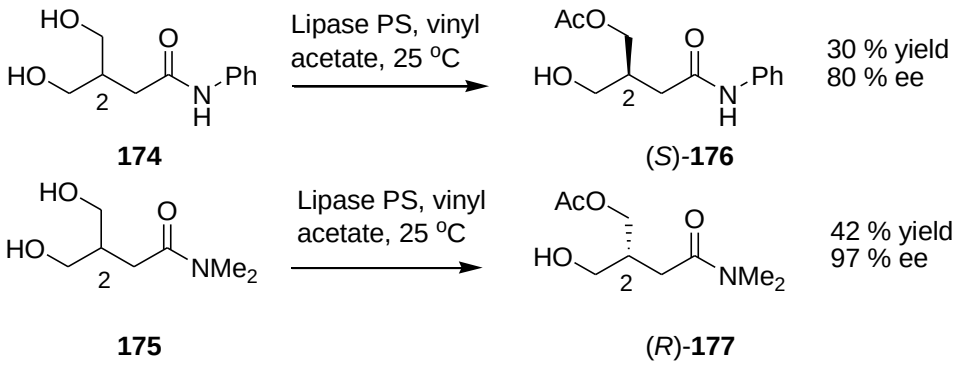

174 (*S*)-**176**

175 (*R*)-**177**

Scheme 50: Enantioselective acetylation of 1,3-diol 174, 175 using lipase PS[152]

Banfi and Guanti[153] showed that both enantiomers of the same monoacetate **180** can be obtained in excellent yield and up to 98% *ee* by enantioselective acetylation of 1,3-diol **178** (analogues to 1,3-diol **169**) and enantioselective hydrolysis of its corresponding diacetate **179** (Scheme 51).

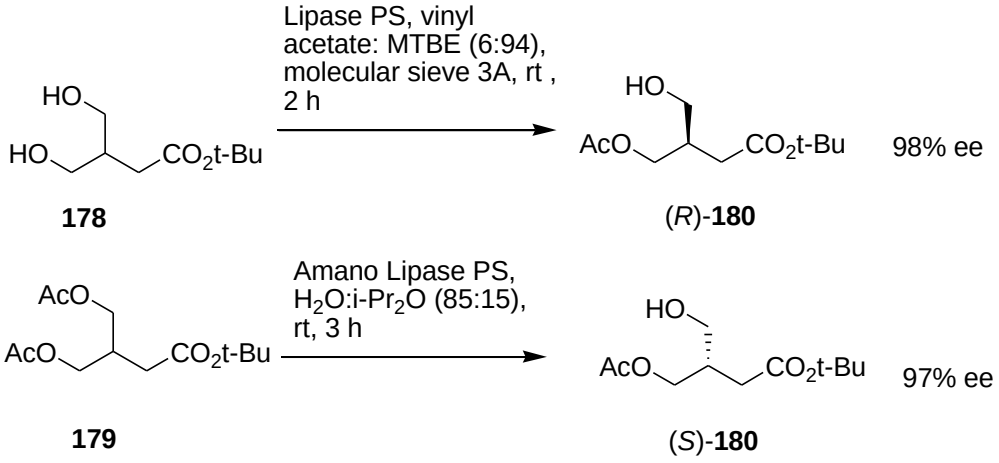

178 (*R*)-**180**

179 (*S*)-**180**

Scheme 51: Access to both enantiomers of monoacetate 180 using lipase PS

Based on the literature examples, vinyl acetate proved to be the best source of acylating agent because the by-product in this reaction is vinyl alcohol (which tautomerize to acetaldehyde) which can be removed easily during work up. However, since our 1,3-diols **43** and **169** are synthetic compounds, their enzymatic reactions are often unpredictable. As such, exhaustive screening of

different lipases and further optimization are normally required for the desymmetrization of a particular diol substrate.

2. Research methodology

Based on our proposed route for the synthesis of piperidone **1** (Scheme 9, chapter I and shown again below), the new chiral center at C5 in piperidone **1** can be obtained by desymmetrization of 1.3-diol **43** through enantioselective acetylation using enzymes.

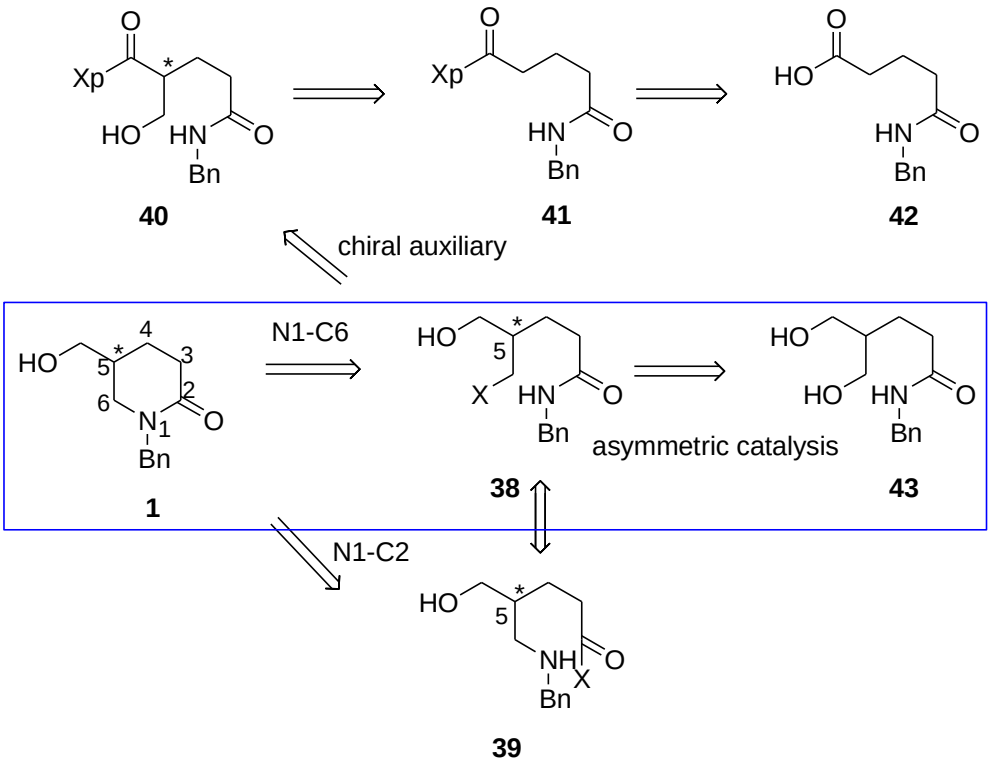

Scheme 9: Retrosynthetic analysis of piperidone 1 (asymmetric catalysis route highlighted in the box)

In chapter III, we have discussed the feasibility of enantioselective acylation of 1,3-diol **39** and **169** using different chiral metal-based ligand catalyst systems. In this chapter, we examine the enantioselective acetylation of 1,3-diols **43** and **169** using different lipases (Scheme 52a,c). In addition, we also investigate the

enantioselective hydrolysis of diacetate **168** using lipase in an attempt to obtain the opposite enantiomer of **133a** (Scheme 52b).

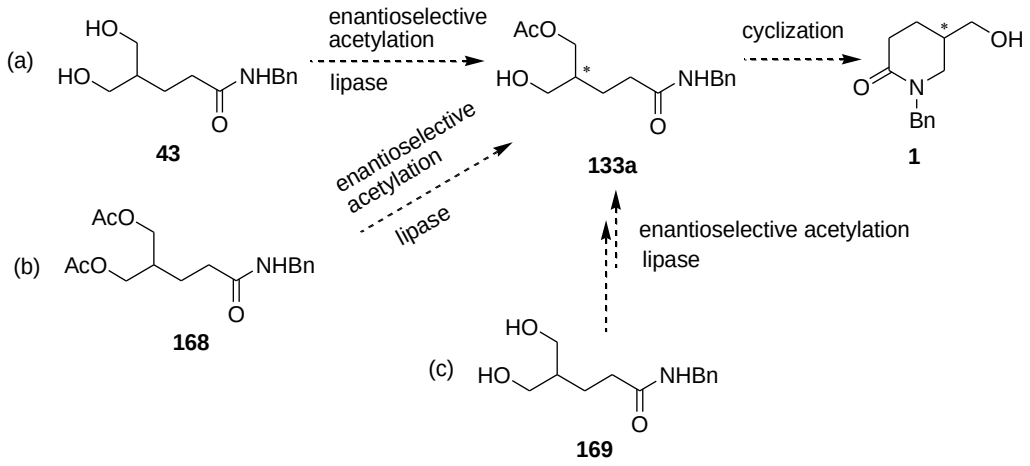

Scheme 52: Strategy for asymmetric synthesis of piperidone 1 *via* desymmetrization using enzyme

3. Enantioselective acetylation of 1,3-diol 43

3.1 Screening of enantioselective acetylation of 1,3-diol 43 with different lipases

The synthesis of 1,3-diol **43** was achieved according to scheme 39 (chapter III). The enantioselective acetylation of 1,3-diol **43** to monoacetate **133a** was examined using five different commercially available lipases: lipase PA, lipase AK, lipase A, lipase G and lipase M (Table 8).

Table 8: Screening of different lipases for the enantioselective acetylation of 1,3-diol 43 [a]

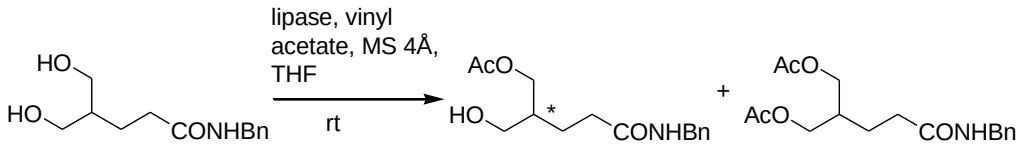

43 **133a** **168**

Entry	Lipase	Time (h)	Monoacetate **133a**		Diacetate **168**
			Yield[b] (%)	*ee*[c] (%)	Yield[b] (%)
1	Lipase PS	21	91	75	4
2	Lipase AK	1	85	87	10
3	Lipase A	12	0	-	-
4	Lipase G	12	0	-	-
5	Lipase M	12	0	-	-

[a]: All the reactions were performed on a 0.2 mmol scale of 1,3-diol **43** in the presence of a given lipase (150 mg/ mmol 1,3-diol **43**), molecular sieve 4Å (10 mg) using vinyl acetate (10.0 equiv) in THF (3.125 mL)
[b]: Isolated yield
[c]: Measured by HPLC :Chiralpak AD-H (hexane: *i*-PrOH, 95: 5), 0.9 ml/ min, 254 nm, t_1: 46.3 min, t_2: 49.8 min

Among the five examined lipases, lipase PS (from *Burkholderia cepacia*) and lipase AK (from *Pseudomonas fluorescens*) catalyzed the formation of monoacetate **133a** in excellent yields of 85% and 91%, respectively (Table 8, entries 1-2). Monoacetate **133a** was obtained as viscous oil after purification by column chromatography (pure EtOAc as the eluent). Along with monoacetate **133a**, diacetate **168** was also obtained in these two reactions in 4% and 10% yield, respectively. On the other hand, reactions using other lipases

such as lipase A (from *Aspergillus niger*), lipase G (from *Penicillium camemberti*), and lipase M (from*Mucor javanicus*) were unsuccessful (Table 8, entries 3-5). Based on these preliminary results, lipase AK (Table 8, entry 2) was selected for further optimization since it also gave the monoacetate **133a** in a much short reaction time of 1 h compared to lipase PS which required 21 h to give monoaceate **133a**.

Though the stability of lipase PS and AK in THF were not examined in this research, it can be implied from their results above that at least their configuration as the active site are retained. While it was shown that enzyme structure tends to denature in the organic solvent, it can only happen in aqueous-organic mixtures where the enzymes have both the proclivity to denature and sufficient conformational flexibility to do so. In anhydrous solvent, the enzyme conformational structures are much more rigid due to the lack of water as the lubricant, thus keeping their native structure.[149]

3.2 Effects of organic solvent

Due to the insolubility of 1,3-diol **43** in many organic solvents such as CH_2Cl_2, $CHCl_3$, EtOAc, PhMe and hexane, a solvent system composed of different ratios of THF and MTBE (which has been reported to be the optimal solvent for desymmetrization of 1,3-diol analogue **178**[132] (Scheme 51)) was examined (Table 9).

Table 9: Effect of co-solvent ratio of THF:MTBE on the enzymatic acetylation of 1,3-diol 43[a]

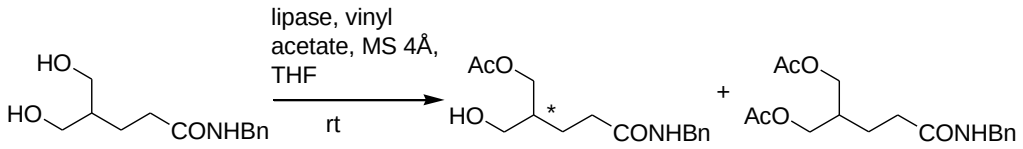

43 **133a** **168**

Entry	THF: MTBE (v/v)	Time (h)	Monoacetate **133a**		Diacetate **168**
			Yield[b] (%)	*ee*[c] (%)	Yield[b] (%)
1	4: 0	1	85	87	10
2	3: 1	1	89	89	8
3	1: 1	1	87	83	12
4	1: 3	1	84	83	14
5	0: 4	1	75	91	20

[a]: All the reactions were performed on a 0.2 mmol scale of 1,3-diol **43** in the presence of lipase AK (150 mg/ mmol 1,3-diol **43**), molecular sieve 4Å (10 mg) using vinyl acetate (10.0 equiv) in the given solvent system (3.125 mL)
[b]: Isolated yield
[c]: Measured by HPLC :Chiralpak AD-H (hexane: *i*-PrOH, 95: 5), 0.9 ml/ min, 254 nm, t_1: 46.3 min, t_2: 49.8 min

We observed that as the ratio of MTBE in the co-solvent mixture increased, the solubility of 1,3-diol **43** decreased significantly. However, the reactions still proceeded smoothly and 1,3-diol **43** was consumed within 1 h to give monoacetate **133a** (Table 9, entries 1-5). No significant variation in the *ee* was observed in these experiments in comparison to that of pure THF. Though the heterogeneous conditions in the reaction may cause mass transfer and diffusion factors become more significant and unfavorable to the reaction rate, the reaction still proceeded and was completed within 1 h to give a mixture of monoacetate **133a** and diacetate **168** (Table 9, entry 5). Furthermore, the

enantioseletivity using pure MTBE was slightly improved to 91% *ee* (Table 9, entries 5).

Since the reaction proceeds under heterogenous conditions, the effects of different organic solvents such as THF, MTBE, *i*-Pr_2O, toluene, $CHCl_3$, CH_2Cl_2, acetone and MeCN were then examined (Table 10). In all cases, the reactions proceeded smoothly under heterogeneous condition to give monoacetate **133a** in good to excellent yields after 1-2 h (Table 10, entries 1-8). In case of ether-type solvents, while THF and MTBE provided similar outcome, reaction in *i*-Pr_2O was less effective and gave the monoacetate **133a** in 65% isolated yield and 78% *ee* (Table 10, entry 3). However, over-acetylation was observed with these solvents as significant amount of diacetate **168** was also obtained (Table 10, entries 1-3). Nonpolar and non-coordinating solvents such as PhMe, $CHCl_3$ and CH_2Cl_2 also provided excellent yield and similar 85% *ee* (Table 10, entries 4-6). In this case, though slightly longer reaction time was needed when compared to ether-type solvents, no diacetate **168** was detected and thus higher overall yields of monoacetate **133a** were obtained. Polar aprotic solvents like acetone and MeCN were also examined (Table 10, entries 7-8). These solvents also provided excellent yields of monoacetate **133a** within 1 h. While acetone only provided up to 82% *ee*, MeCN afforded 88% *ee* and 96% yield within 45 min. Therefore, MeCN is considered to be the optimal solvent for this enzymatic process.

Table 10: Enantioselective acetylation of 1,3-diol 43 in different solvents[a]

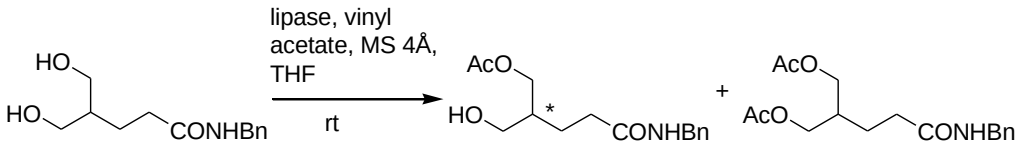

43 **133a** **168**

Entry	Solvent	Time (h)	Monoacetate **133a**		Diacetate **168**
			Yield (%)[b]	*ee*[c] (%)	Yield (%)[b]
1	THF	1	80	87	17
2	MTBE	1	75	91	20
3	*i*-Pr_2O	1	65	78	20
4	toluene	2	88	85	0
5	$CHCl_3$	2	99	85	0
6	CH_2Cl_2	1.5	99	85	0
7	acetone	1	91	82	0
8	MeCN	0.75	96	88	0

[a]: All the reactions were performed on a 0.2 mmol scale of 1,3-diol **43** in the presence of lipase AK (150 mg/ mmol 1,3-diol **43**), molecular sieve 4Å (10 mg) using vinyl acetate (10.0 equiv) in the given solvent (3.125 mL)
[b]: Isolated yield
[c]: Measured by HPLC :Chiralpak AD-H (hexane: *i*-PrOH, 95: 5), 0.9 ml/ min, 254 nm, t_1: 46.3 min, t_2: 49.8 min

3.3 Effects of lipase loadings, equivalents of vinyl acetate, concentration of 1,3-diol 43 and temperature

With MeCN as the optimal solvent, effects of other reaction parameters including lipase loading, equivalent of vinyl acetate, concentration of 1,3-diol **43** and temperature were examined (Table 11).

Interestingly, no major impact on the yield and *ee* were observed by varying the lipase loading (Table 11, entries 1-3) or equivalents of vinyl acetate (Table 11, entries 4-5). Similarly, changing the concentration of 1,3-diol **43** had no significant effect on the yield and *ee* (Table 11, entry 8). When the reaction temperature decreased to 4 °C (ice-bath temperature) or 0 °C (using chiller to control the temperature), the *ee* was improved to 90-92% with 93-94% yield (Table 11, entries 9-10). Further temperature reduction proved ineffective as it severely affected both lipase AK activity and increased the reaction time.

Table 11: Enantioselective acetylation of 1,3-diol 43 under different reaction conditions[a]

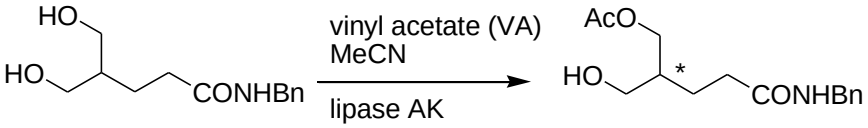

43 **133a**

Entry	Solvent conc. (mM)	Lipase loading (mg/mmol)	VA (equiv.)	Temp. (^oC)	Time (h)	**133a**[b] (%)	*ee*[c] (%)
1	64	150	10	rt	0.75	96	88
2	64	250	10	rt	1	95	87
3	64	100	10	rt	2	96	86
4	64	150	20	rt	1	96	87
5	64	150	15	rt	1	95	88
6	64	150	5	rt	1.5	94	88
7	64	150	3	rt	2	94	86
8	32	150	10	rt	2	95	87
9	64	150	10	4	4	93	92
10	64	150	10	0	4	94	91

[a]: All the reactions were performed on a 0.2 mmol scale of 1,3-diol **43** in the presence of lipase AK (150 mg/ mmol 1,3-diol **43**), molecular sieve 4Å (10 mg) using vinyl acetate in the given solvent (3.125 mL)
[b]: Isolated yield
[c]: Measured by HPLC :Chiralpak AD-H (hexane: *i*-PrOH, 95: 5), 0.9 ml/ min, 254 nm, t_1: 46.3 min, t_2: 49.8 min

In conclusion, an optimal enantioselective acetylation of 1,3-diol **43** using lipase AK which resulted in 93% yield and 92% *ee* of monoacetate **133a** has been established as shown in table 11, entry 9.

Since lipases usually possess the same prochiral selectivity, we envisaged the enantioselective deacetylation (or hydrolysis) of diacetate **168** would lead to the monoacetate **133a** *albeit* opposite absolute configuration. Therefore, the enzymatic hydrolysis of diacetate **168** to give *ent*-**134a** was investigated next.

4. Enantioselective hydrolysis of diacetate 168

4.1 Synthesis of diaceate 168

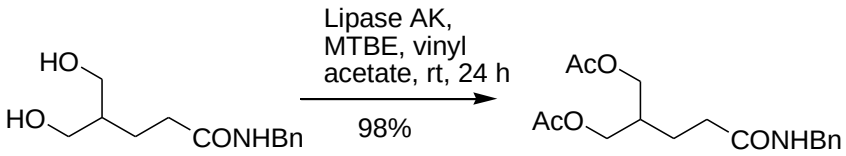

43 **168**

Scheme 53: Synthesis of diacetate 168 from 1,3-diol 43

Synthesis of diacetate **168** was achieved according to scheme 53. Enzymatic acetylation of diol **43** with lipase AK cleanly provided the product as yellow oil in quantitative yield after purification by column chromatography (EtOAc: hexane, 1: 1; v/v).

4.2 Opimization of enantioselective hydrolysis of diacetate 168

A typical enantioselective hydrolysis experiment, involved the addition of lipase AK into a solution of diaceate **168** in pH 7 aqueous buffer at room temperature (Table 12). However, the reaction using lipase AK loading of 150 mg/ mmol of diacetate **168** were sluggish and provided a mixture of monoacetate *ent*-**133a**, 1,3-diol **43** and unreacted diacetate **126** after 24 h (Table 12, entry 1). Purification by column chromatography recovered 42% of the unreacted diacetate **168** and 36% yield of monoacetate *ent*-**133a**. HPLC

analysis of monoacetate *ent*-**133a** confirmed its opposite stereochemistry of in comparison with that of enzymatic acetylation of 1,3-diol **43**. Compared to enzymatic acetylation, control of over-hydrolysis was more difficult, probably due to the enhanced catalytic activity of lipase AK in the aqueous phase.[154]

Table 12: Preliminary screening of enzymatic hydrolysis of diacetate 168[a]

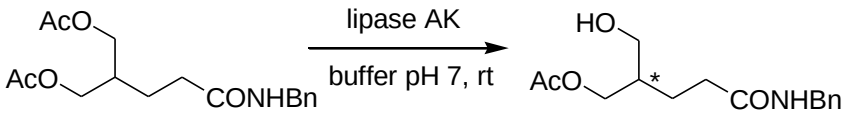

168 *ent*-**133a**

Entry	**168** (mM)	Lipase loading (mg/mmol)	Time (h)	Monoacetate *ent*-**133a** Yield[b] (%)	*ee*[c] (%)	Diacetate **168** Recovery[b] (%)
1	32	150	24	36	66	42
2	32	300	6	63	68	25
3	16	300	5	66	72	21
4	16	600	3	60	59	0

[a]: All the reactions were performed on a 0.2 mmol scale of diacetate **168** in the presence of a lipase AK, in the given buffer solution at room temperature for 24 h
[b]: Isolated yield
[c]: Measured by HPLC :Chiralpak AD-H (hexane: *i*-PrOH, 95: 5), 0.9 ml/ min, 254 nm, t_1: 46.3 min, t_2: 49.8 min

Increasing the enzyme loading to 300 mg per one mmol of diacetate **168** significantly increased the reaction rate and gave 63% yield of *ent*-**133a** with *ee* of 69% (Table 12, entry 2). At lipase Ak loading of 300 mg per one mmol of diacetate **168**, the *ee* can be improved to 72% when the concentration of

diacetate **168** is reduced to 16 mM (Table 12, entry 3). However, increasing the lipase loading to 600 mg per 1 mmol of diacetate **168** severely reduced the *ee* to 0% (Table 12, entry 4). Therefore, the optimal conditions for the hydrolysis reaction is at a diacetate **168** concentration of 16 mM and lipase loading of 300 mg per 1 mmol (Table 12, entry 3).

Next, we examined the effect of organic solvents as additives on the enantioselectivity in the enzymatic hydrolysis of diacetate **168**.

4.2.1 Effect of organic solvents

Preliminary experiments were done using MeCN as co-solvent to determine the percentage of the organic solvent additive that can effectively enhance the hydrolysis reaction. The preliminary experiments were conducted using lipase AK loading of 300 mg per one mmol of diacetate **168** at different ratios of MeCN to aqueous buffer solution (Table 13).

Table 13: Effect of H_2O:MeCN as a cosolvent in the enantioselective hydrolysis of diacetate 168[a]

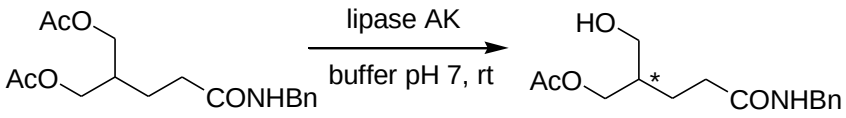

168 *ent*-**133a**

Entry	H_2O: MeCN (v/v)	Monoacetate *ent*-**133a**		Diacetate **168**
		Yield[b] (%)	*ee*[c] (%)	Recovery[b] (%)
1	1:1	-	-	-
2	2:1	-	-	-
3	3:1	-	-	-
4	4:1	-	-	-
5	10:1	41	84	24

[a]:All the reactions were performed on a 0.2 mmol scale of diacetate **168** in the presence of lipase AK (300 mg/ mmol), in the given buffer solution room temperature for 24 h
[b]: Isolated yield
[c]: Measured by HPLC :Chiralpak AD-H (hexane: *i*-PrOH, 95: 5), 0.9 ml/ min, 254 nm, t_1: 46.3 min, t_2: 49.8 min

The results showed that only at MeCN:H_2O ratio of 1:10 that hydrolysis of diacetate **168** can proceed to give monoacetate *ent*-**133a** in 41% yield and 84% *ee* after 24 h (Table 13, entry 5). Higher ratio of MeCN resulted in inhibition of the hydrolysis reaction (Table 13, entries 1-4).

Therefore, the effect of different organic solvents as additives in the lipase AK hydrolysis of diacetate **102** were examined using H_2O:organic solvent of 10:1, (Table 14).

Table 14: Effects of enantioselective hydrolysis of diacetate 168 in different organic solvent additives[a]

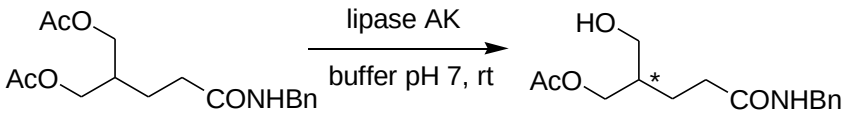

168 *ent*-**133a**

Entry	Solvent	Monoacetate *ent*-**133a**		Diacetate **168**
		Yield[b] (%)	*ee*[c] (%)	Recovered[b] (%)
1	H_2O:MeCN	46	87	38
2	H_2O:acetone	56	24	35
3	H_2O:PhMe	49	82	41
5	H_2O:*i*-Pr_2O	56	9	7
6	H_2O:MTBE	60	63	19
7	H_2O:THF	51	91	39

[a]:All the reactions were performed on a 0.2 mmol scale of diacetate **168** in the presence of lipase AK (300 mg/ mmol), in the given organic solvent with buffer pH 7 solution (10:1, v/v) at room temperature for 24 h
[b]: Isolated yield
[c]: Measured by HPLC :Chiralpak AD-H (hexane: *i*-PrOH, 95: 5), 0.9 ml/ min, 254 nm, t_1: 46.3 min, t_2: 49.8 min

In comparison with enzymatic acetylation in section 3, organic solvents exerted a more dramatic effect on the enantioselectivity in enatioselective hydrolysis (Table 14). Acetone as a polar solvent gave monoacetate *ent*-**133a** in 56% yield but poor 24% *ee* (Table 14, entry 2). On the other hand, toluene provided *ent*-**133a** in 52% yield and 82% *ee* (Table 14, entry 3). Effects of different ether-type solvents were also examined (Table 14, entries 5-7). While hydrolysis in *i*-Pr_2O completely consumed the diacetate **168** as indicated by TLC, a significant amount of 1,3-diol **43** was detected and monoacetate *ent*-**133a** was obtained in 56% yield and only 9% *ee*. In contrast, MTBE seemed to be more effective

additive since it gave 60% yield and 63% *ee* (Table 14, entry 6). When THF was used, the reaction gave *ent*-**133a** in 51% yield and highest of 91% *ee* (Table 14, entry 7). Therefore, further optimization was carried out by examining other reaction parameters including pH value, enzyme ratio and temperature using THF as the solvent.

4.2.2 Effects of pH values

Effects of pH within the optimal range of lipase AK[155] (pH 6.0-7.5) was investigated (Table 15). No significant differences were observed at different pH values since *ent*-**133a** was obtained in 90-91% *ee* and 53-56% yield after 24 h (Table 15).

Table 15: Effects of pH on the enantioselective hydrolysis of diacetate 168[a]

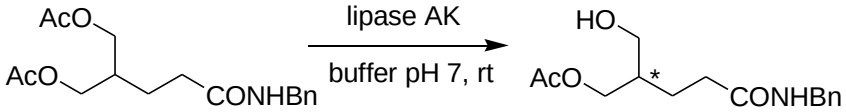

168 *ent*-**133a**

Entry	pH	Temp. (^oC)	Monoacetate *ent*-**133a**		Diacetate **168**
			Yield[b] (%)	*ee*[c] (%)	Yield[b] (%)
1	6.0	rt	55	90	33
2	6.5	rt	53	90	37
3	7.0	rt	56	91	31
4	7.5	rt	54	91	32

a: All the reactions were performed on a 0.2 mmol scale of diacetate **168** in the presence of lipase AK (300 mg/ mmol), in THF and given buffer solution (1:10 v/v) at room temperature for 24 h
b: Isolated yield
c: measured by HPLC :Chiralpak AD-H (hexane: *i*-PrOH, 95: 5), 0.9 ml/ min, 254 nm, t_1: 46.3 min, t_2: 49.8 min

4.2.3 Effect of reaction time, lipase loading and temperature

We suspected that racemization may be taking place as time passes under the reaction conditions used. Therefore, enzymatic hydrolysis of diacetate **168** at different reaction time was examined and the results summarized in table 16. At optimal hydrolysis conditions of diacetate **168** (lipase AK (300 mg/ mmol) in H_2O: THF (10:1 v/v) co-solvent, the yield of monoacetate *ent*-**133a** increased slowly from 21% to 29% to 36% while the enantioselectivity remained nearly unchanged after 5 h, 9 h and 14 h (Table 16, entries 1-3). An increase in the enzyme loading to 450 mg/ mmol gave monoacetate *ent*-**133a** in 41% yield and up to 95% *ee* after 11 h (Table 16, entries 4-5). Attempts to reduce the ratio of THF: H_2O to 20: 1 (Table 16, entry 6) and reduce the reaction temperature to 0 °C led to inferior enantioselectivity (Table 16, entry 7).

Table 16: Effects of reaction time, lipase loading and temperature on the enantioselective hydrolysis of diacetate 168[a]

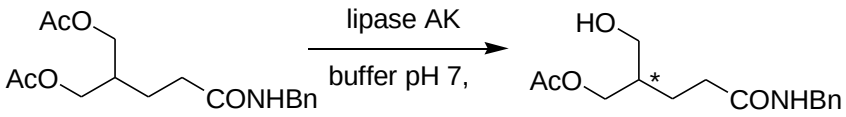

168 *ent*-**133a**

Entry	H_2O: THF	Enzyme loading	Temp. (^oC)	Time (h)	Monoacetate *ent*-**133a**		Diacetate **168**
					Yield[b] (%)	*ee*[c] (%)	Recovery[b] (%)
1	10:1	300	rt	5	21	86	62
2	10:1	300	rt	9	29	91	58
3	10:1	300	rt	14	36	90	55
4	10:1	450	rt	5	34	87	56
5	10:1	450	rt	11	41	95	45
6	20:1	450	rt	5	72	83	11
7	10:1	450	0	18	76	80	6

[a]:All the reactions were performed on a 0.2 mmol scale of diacetate **168** in the presence of a given lipase AK, in THF and given buffer solution (1:10 v/v)
[b]: Isolated yield
[c]: Measured by HPLC :Chiralpak AD-H (hexane: *i*-PrOH, 95: 5), 0.9 ml/ min, 254 nm, t_1: 46.3 min, t_2: 49.8 min

Therefore, the optimal conditions for the enzymatic hydrolysis of diacetate **168** are shown in table 16, entry 5 (enzyme loading of 450 mg/ mmol diacetate **168**; H_2O: THF = 10: 1; room temperature).

Encouraged by positive results obtained from enzymatic desymmetrization of prochiral 1,3-diol **43** and its diacetate **168**, the feasibility of desymmetrization of 1,3-diol **169** using lipase was also investigated.

5. Enantioselective acylation of 1,3-diol 169

The synthesis of 1,3-diol **169** was described in scheme 46, chapter III. Enantioselective acetylation of 1,3-diol **169** was attempted using lipases A, G, M, AK and PS using a reaction procedure similar to the one used for 1,3-diol **43** (Table 17). However, for the purpose of enantioselectivity analysis using chiral HPLC, the crude reaction product was tosylated using *p*-toluenesulfonyl chloride (*p*-TsCl) to introduce chromaphoric moiety prior to HPLC analysis.

Table 17: Screening of lipases for acetylation of 1,3-diol 169 using[a]

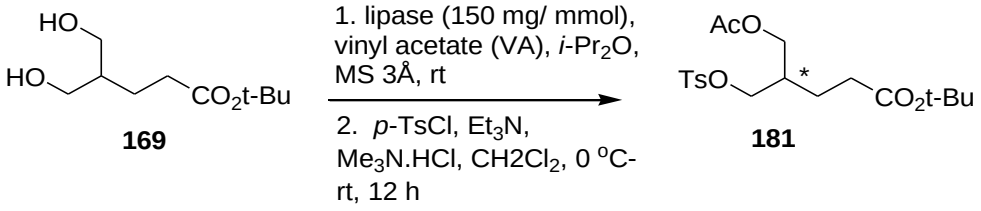

Entry	Enzyme	Time[b] (h)	Yield[c] (%)	*ee*[d] (%)
1	Lipase A	-	-	-
2	Lipase G	-	-	-
3	Lipase M	-	-	-
4	Lipase AK	16	31	46
5	Lipase PS	16	32	55

[a]: All the reactions were performed on a 0.2 mmol scale of 1,3-diol **169** in the presence of a given lipase (150 mg/ mmol 1,3-diol **169**), molecular sieve 4Å (10 mg) using vinyl acetate (10 equiv.) in *i*-Pr_2O (3.125 mL) at room temperature.

[b]: Reaction time of enzymatic reaction
[c]: Isolated yield tosylate product **181**
[d]: Determined by HPLC of **181**: Chiralcel OJ-H (hexane: iPrOH, 90: 10), 1.0 ml/ min, 254 nm, t_1: 36.8 min, t_2: 44.6 min

Unlike the case of 1,3-diol **43**, enantioselective acetylation of 1,3-diol **169** was much slower even when lipase AK or PS were used (Table 17, entries 4-5). Lipases A, G and M failed to give the products (Table 17, entries 1-3).

In order to analyze the products from lipase AK and PS reactions, the crude products were tosylated using *p*-TsCl/Et_3N in CH_2Cl_2 and purified using column chromatography (EtOAc: hexane, 1: 2, v/v; R_f ~ 0.5) to give a viscous oil in 31-32% yields. The FT-IR spectrum of the oil revealed a sharp peak at 1733 cm^{-1} that corresponded to the absorption band of C=O of ester moieties. In addition, a sharp peak was also observed at 1368 cm^{-1} which corresponded to the absorption band of S=O of a sulfonyl moiety. The high resolution ESI-mass spectrum showed a molecular ion *m/z* value of 423.1500 corresponding to $(M+Na)^+$ thus supporting the molecular formula $C_{19}H_{28}O_7S$ (*m/z* calcd for C $C_{19}H_{28}O_7SNa$ $(M+Na)^+$: 423.1453). In comparison with the ^1H NMR of its starting material 1,3-diol **169**, the ^1H NMR of the oil revealed a singlet at δ 2.46 (s, 3H) and two doublets at δ 7.35 (d, *J* = 8.4 Hz, 2H) and δ 7.79 (d, *J*= 8.4 Hz, 2H) which indicated the presence of toluenesulfonyl moiety. In addition, another singlet at δ 1.96 (s, 3H) corresponded to the methyl protons of the acetyl moiety, indicating the successful acetylation. ^{13}C NMR of the oil showed two peaks at δ 170.7 and δ 172.0 corresponding to the carbon signals of two carbonyl carbons from methyl acetoxy and *tert*-butyloxy moieties. In addition, the aromatic carbon signals corresponding to toluenesulfonyl moiety were also found at δ 128.0, δ 129.9, δ 132.7 and δ 145.0. Therefore, the product was

assigned structure **181** (Figure 13). Based on chiral HPLC analysis of tosylate **181**, lipase AK gave 46% *ee* while lipase PS gave 55% *ee*.

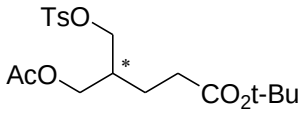

181

Figure 13: Tosylate 181

Optimization of enzymatic acetylation of 1,3-diol **169** was attempted with different solvents using lipase PS (Table 18). *i*-Pr_2O, MTBE, Et_2O, THF CH_2Cl_2 and toluene gave similar results in terms of the enantioselectivity of the tosylated product **181** *albeit* the yields were different (Table 18, entries 1-7). When vinyl acetate was used as both solvent and acylating agent, the tosylated product **181** was also obtained in 50% yield and 54% *ee* (Table 18, entry 5). However, the best result was obtained when the reaction was carried out in MeCN (Table 18, entry 8) since tosylated product **181** was obtained in 75% *ee* (Table 18, entry 8) but in low 29% yield. The unsatisfactory yield (<30%) render this reaction unattractive for further optimization.

Table 18: Effects of solvents in the enantioselective acetylation of 1,3-diol 169[a]

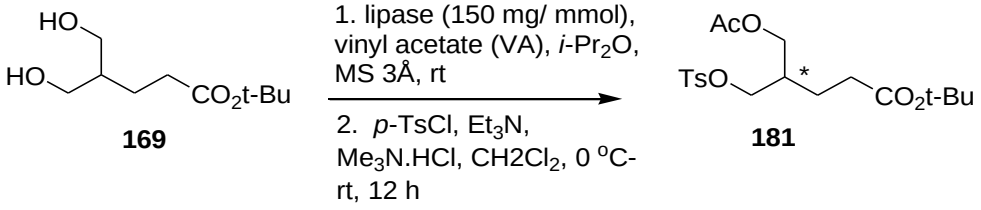

Entry	Solvent	VA (equiv.)	Time[b] (h)	Yield[c] (%)	ee[d] (%)
1	*i*-Pr_2O	10	960	32	55
2	MTBE	10	960	65	55
3	THF	10	240	50	56
4	Et_2O	10	240	47	56
5	VA	-	240	50	54
6	DCM	10	360	21.6	48
7	PhMe	10	360	24.2	55
8	MeCN	10	360	28.5	72

[a]:All the reactions were performed on a 0.2 mmol scale of 1,3-diol **169** in the presence of lipase PS (150 mg/ mmol 1,3-diol **169**), molecular sieve 4Å (10 mg) using vinyl acetate (10.0 equiv) in in a given solvent (3.125 mL) at room temperature.
[b]: Reaction time of enzymatic reaction
[c]: Isolated yield of tosylate product **181**
[d]: Determined by HPLC of **181**: Chiralcel OJ-H (hexane: iPrOH, 90: 10), 1.0 ml/ min, 254 nm, t_1: 36.8 min, t_2: 44.6 min

On the other hand, we examined the enzymatic benzoylation of 1,3-diol **169** using vinyl benzoate (Table 19). Compared to the enzymatic acetylation, the study of the enzymatic benzoylation has been much less developed.[156] The asymmetric benzoylation of 1,3-diol **169** was examined using different lipases under similar enzymatic acetylation conditions except that vinyl benzoate was

used instead of vinyl acetate. Benzoylation reactions proved to be very sluggish and only trace amount of monobenzoate **170b** was obtained (Table 19, entries 1 & 3). Lipase PS and AK gave 40% *ee* and 41% *ee*, resepectively based on the HPLC analysis of monobenzoate **105** (Table 19, entries 1 and 3). Again, lipases A, M and G (Table 19, entries 4-6) did not give any products. Switching the solvent from *i*-Pr_2O to MTBE made no significant difference on the yield but increased the *ee* from 40% to 47% (Table 19, entry 2). In general, the enantioselectivity of the benzoylation was similar to the acetylation *albeit* with much lower yields.

Table 19: Screening of lipases for enzymatic benzoylation of diol 169[a]

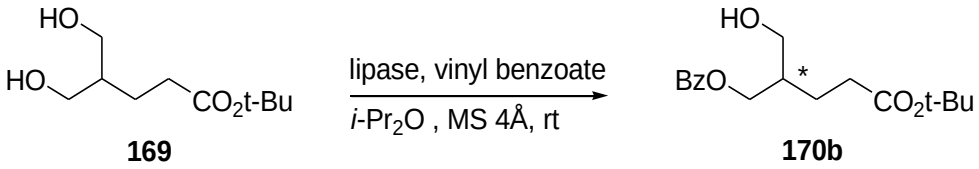

169 **170b**

Entry	Enzyme	Solvent	Time (h)	Yield (%)	*ee*[b] (%)
1	Lipase PS	*i*-Pr_2O	16	trace	40
3	Lipase PS	MTBE	24	trace	47
2	Lipase AK	*i*-Pr_2O	16	trace	41
4	Lipase A	*i*-Pr_2O	16	-	-
5	Lipase M	*i*-Pr_2O	16	-	-
6	Lipase G	*i*-Pr_2O	16	-	-

[a]: All the reactions were performed on a 0.2 mmol scale of 1,3-diol **169** in the presence of lipase PS (150 mg/ mmol 1,3-diol **169**), molecular sieve 4Å (10 mg) using vinyl benzoate (10.0 equiv) in in a given solvent (3.125 mL) at room temperature.
[b]: Determined by HPLC, Chiralcel OD-H (hexane: *i*-PrOH, 90: 10), 1.0 ml/ min, 254 nm, t1: 21.6 min, t2: 29.8 min.

6. Synthesis of piperidone 1

Our successful enzymatic acetylation of 1,3-diol **43** and enzymatic hydrolysis of diacetate **168** provided us with access to both enantiomer of monoacetate **133a** in 90-95% *ee*, and 93% yield (in acetylation) and 41% yield (in hydrolysis). Based on our planned synthetic route described in scheme 50, chiral piperidone **1** can then be synthesized by intramolecular cyclization of monoacetate **133a**.

Cyclization of monoacetate **133a** to piperidone **1** was achieved according to scheme 54. The monoacetate **133a**, was first tosylated to activate its free hydroxyl group. However, this tosylated product was found to be unstable and therefore was immediately subjected to intramolecular amide alkylation. The alkylation was accomplished using *n*-Bu_4NHSO_4 as phase transfer catalyst in the presence of K_2CO_3 and NaOH in toluene at 100 °C. This two-step process effectively provided the corresponding chiral piperidone **1** in 80% yield. The ^{1}H and ^{13}C NMR of this product matched the literature values[38] and the data of the chiral piperidone **1** we obtained in chapter II. The newly obtained chiral piperidone **1** showed optical rotation value of $\alpha_D^{22} = +42.5$ (c, 1.0, CH_2Cl_2), and therefore it was assigned piperidone (*R*)-**1**. We can also deduce based on these results that the enantioselective acetylation of 1,3-diol **43** gave monoacetate (*R*)-**133a** while the enantioselective hydrolysis of diacetate **168** gave the complementary enantiomer monoacetate (*S*)-**133a**

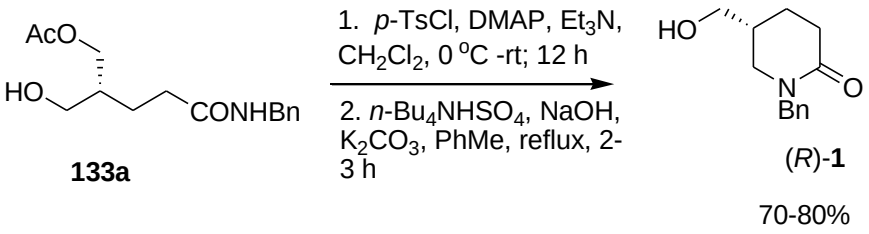

Scheme 54: Synthesis of chiral (*R*)-1 by intramolecular cyclization of monoacetate 133a

7. Conclusion

The feasibility of asymmetric synthesis of piperidone **1** using enzymatic catalysis was investigated. In particular, both 1,3-diol **43** and 1,3-diol **169** were examined for asymmetric acetylation using different lipases. After optimization, enantioselective acetylation of 1,3-diol **43** using lipase AK in MeCN at 4 ^{o}C gave monoacetate (*R*)-**133a** in 93% yield and up to 92% *ee* (Table 11, entry 9), while asymmetric acetylation of 1,3-diol **169** only gave up to 72% *ee* (Table 18, entry 8). Access to monoacetate (*S*)-**133a** was also established by enantioselective hydrolysis of diacetate **168** using lipase AK which resulted in monoacetate (*S*)-**133a** with 41% yield and up to 95% *ee* (Table 16, entry 5).

Synthesis of both enantiomers of chiral piperidone **1** was achieved by intramolecular amide alkylation reaction from both monoacetate (*R*)-**133a** and (*S*)-**133a**. For example, intramolecular cyclization of monoacetate (*R*)-**133a** to chiral piperidone (*R*)-**1** was achieved in two steps in 70-80% yield (Scheme 52).

With the availability of both piperidone (*R*)-**1** and (*S*)-**1**, entry to various enantiopure bioactive compounds (Chapter I, Scheme 1) can be pursued. For example, we can look forward to the asymmetric synthesis of (-)-cytisine **2** following Gallagher's approach[18], or (-)-paroxetine using Jew's approach.[21]

Chapter V: Synthesis of chiral C1-functionalized tetrahydroisoquinoline and C_2-bi-tetrahydroisoquinolines and application in asymmetric Henry reactions*

1. Introduction

Privileged C_2-symmetric chiral ligands such as TADDOL **102**,[157] PyBOX 164, BINOL **2**,[158] (-)-sparteine **165**,[159] Salen **166**,[160] BINOL **167**,[161] (Figure 9, chapter III and shown below) have been used in various enantioselective reactions such as hydrogenation of carbonyl, alkene and imino double bonds,[159b, 162] Diels-Alder reactions,[163] aldol and Mannich-type reactions,[164] aziridination reactions[165] and allylic alkylation reactions.[166] C_2-symmetric ligands preclude complications due to competing diastereomeric states.[167]

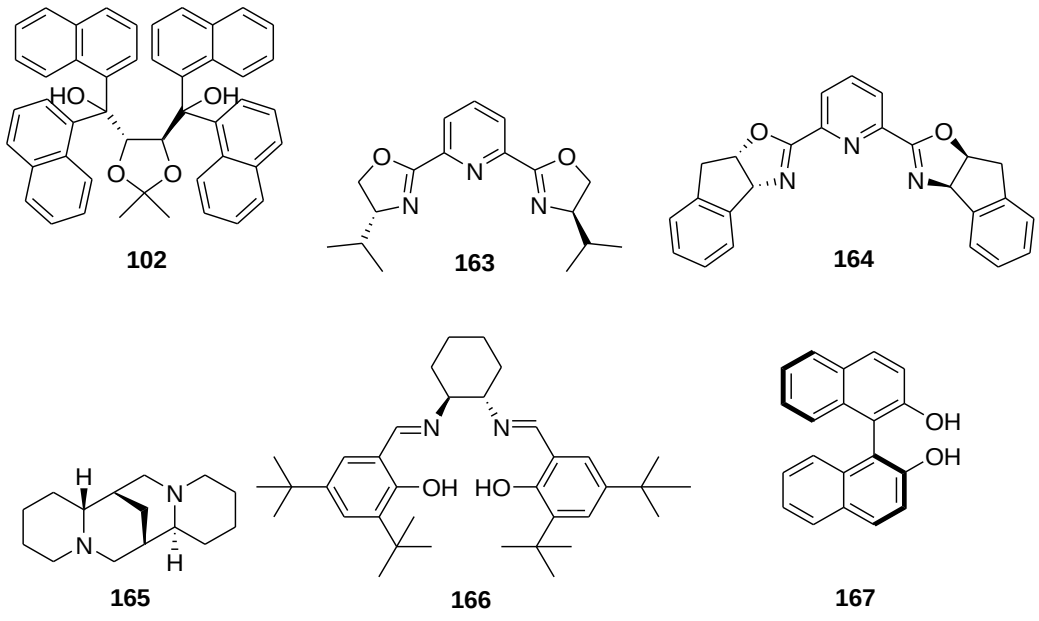

Figure 9: Commercially available chiral ligands to be used for desymmetrization of 1,3-diol 43

* Part of this chapter was published in Synthesis DOI: 10.1055/s-0034-1378892

We have been interested in the synthesis of chiral C_2-symmetric 1,1′-bitetrahydroisoquinolines (C_2-BIQs) **182** (and also C_1-BIQs) and have successfully employed them in asymmetric Henry and alkylation reactions (Scheme 55).[168] We proposed that they hold remarkable potential as chiral ligands for various metal-based and organocatalysis enantioselective reactions due to their excellent coordinating and H-bonding abilities.[169] However, the synthesis and resolution of C_2-BIQs proved to be challenging[168b, 168h, 170] thus limiting their widespread application as chiral catalysts. For example, the synthesis of enantiopure C_2-BIQs **182** was achieved in several steps from phenethylamine **183** through Bischler-Napieralski cyclization of bisoxamide **184**, followed by reduction of bisimine **185** and chiral resolution of *rac*-**182** (Scheme 55). This protocol is tedious, lengthy and difficult to make modular. Moreover, chiral resolution is based on trial and error.

Consequently, optimization of chiral C_2-BIQ ligands has relied mostly on modifications at the nitrogens of C_2-BIQ **182** through derivatization.[168d-g] The effects of C3- and C3′-substituents and the nature/type of the moiety bridging C1 and C1′ (as in C_2-BIQ **188**, Scheme 56) on enantioselectivity have not been elucidated.

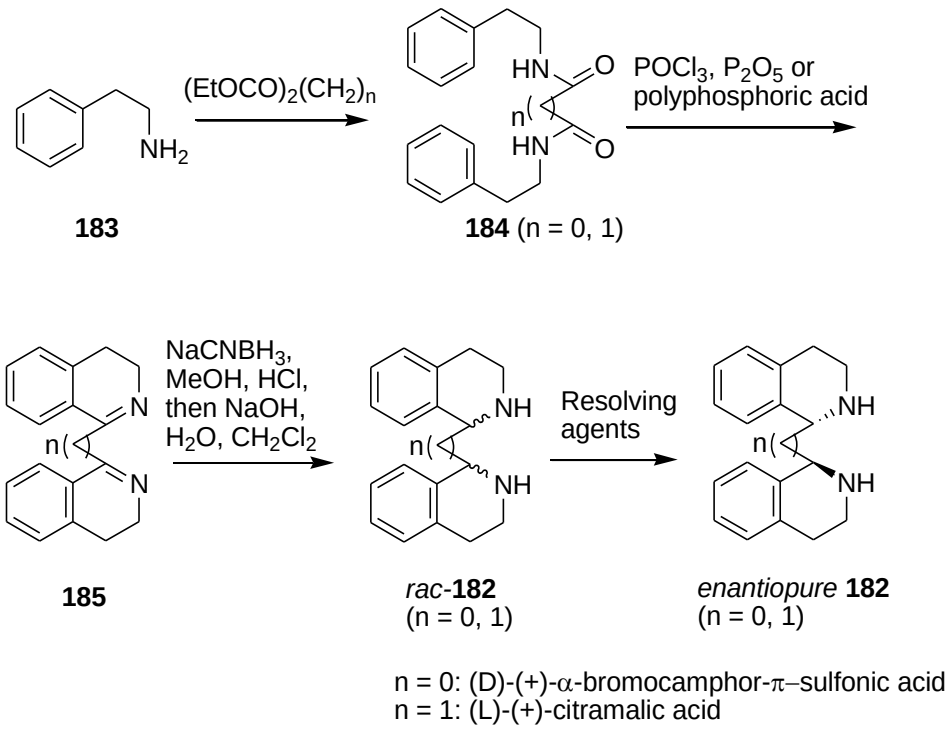

Scheme 55: Synthesis of Chiral C_2-BIQs 182

On the other hand, chiral tetrahydroisoquinoline (THIQ) ligands[77e-g] such as THIQ **190** (Scheme 56) have been successfully used for various asymmetric reactions including transfer hydrogenation,[162d, 171] aluminum- and borane-mediated reductions,[77h, 172] alkynylations[173] and nitro-aldol reactions.[174] However, while the quest to obtain excellent enantioselectivity has so far relied on the optimization at the alcohol and/or amine moieties of THIQ **190**, the effect of substituents at C1 have largely remained uninvestigated.[77d, 77f-h]

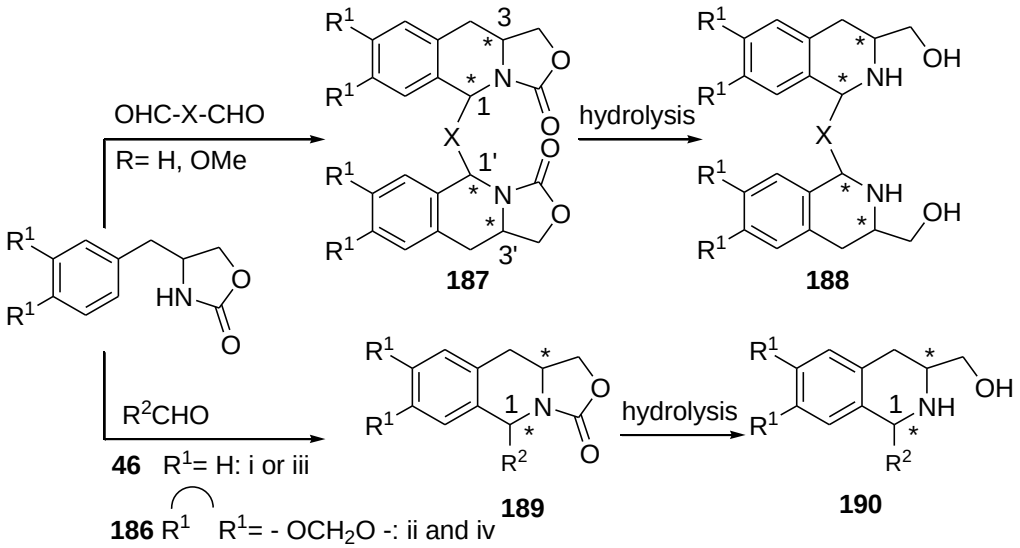

i. (a) Benzotriazole, TsOH, toluene; (b) $TiCl_4$ or $AlCl_3$;
ii. (a) $PhSO_2H$, $MgSO_4$, CH_2Cl_2, r.t.; (b) $TiCl_4$, CH_2Cl_2, -79°C;
iii. TMSOTf, toluene, rt.;
iv. CF_3SO_3H, AcOH, CH_2Cl_2, 4°C or H_2SO_4, CH_2Cl_2

R^2 = alkyl, aromatic, heteroaromatic
X = -, alkyl, aromatic, heteroaromatic

* Chiral centers

Scheme 56: Strategy for the synthesis of chiral *C_2*-BIQs 188 and THIQs 190 from oxazolidinone 46 and 186

We therefore desired a simple, direct and efficient synthetic entry to construct chiral *C_2*-BIQs **188** and THIQs **190** (Scheme 56) to fully explore their potential in asymmetric reactions. We envisioned that a modular double diasteroselective Pictet-Spengler cyclization[74b] between oxazolidinone **46** (or **186**) and various dialdehydes would give bisoxazolidinones **187** which, upon hydrolysis of the oxazolidinone moieties, would provide a direct entry to highly functionalized chiral *C_2*-BIQs **188** (Scheme 56). We also recognized that the same strategy with monoaldehydes would provide the required chiral THIQs **190** (Scheme 56). The key oxazolidinone **189** have been synthesized earlier by reacting oxazolidinone **46** or **186** with suitable aldehydes either in a one-step process

mediated by TMSOTf,[133a] CF_3COOH[175] or H_2SO_4;[175] or in two-step process using benzotriazole/$TiCl_4$[176] or benzenesulphinic acid/$TiCl_4$[177] (Scheme 56).

In the first part of this chapter we describe a direct and modular stereoselective synthesis of highly functionalized C_2-BIQs **188** and THIQs **190**. In the second part, applications of C_2-BIQs **188** and THIQs **190** as chiral ligands in enantioselective Henry reactions will be investigated.

2. Diastereoselective synthesis of chiral THIQs and C_2-BIQs

2.1 Optimization of *N*-acyl Pictet Spengler reaction between oxazolidinone 46 and benzladehyde 191a

As discussed earlier in chapter II, scheme 13, oxazolidinone **46** was obtained in high yields. We started our investigation with the synthesis of THIQs **190** using the diastereoselective Pictet-Spengler cyclization between oxazolidinone **46** and benzaldehyde **191a** by screening different acids and solvents (Table 20).

Table 20: Diastereoselective Pictet-Spengler cyclization between oxazolidinone 46 and benzaldehyde 191a catalyzed by various acids[a]

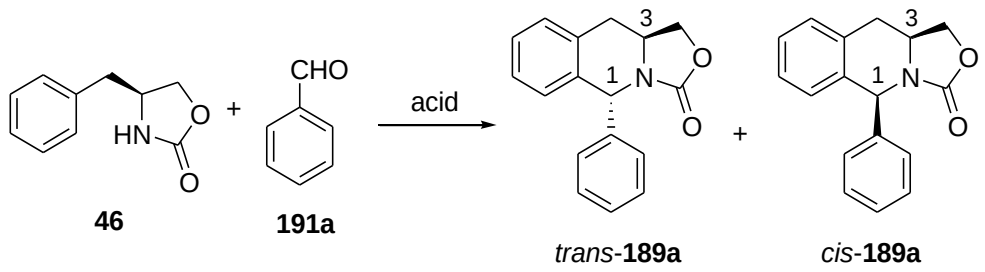

46 **191a** *trans*-**189a** *cis*-**189a**

Entry	Acid	Solvent	Temp.	Time (h)	Conversion[b] (%)	*d.r.*[c]
1	TFA	CH_2Cl_2	rt	48	-	-
2	PPTS	CH_2Cl_2	rt	48	-	-
3	TsOH	CH_2Cl_2	rt	48	-	-
4	H_2SO_4	CH_2Cl_2	rt	12	100	25:1
5	H_2SO_4	$CHCl_3$	rt	12	100	>99:1
6	H_2SO_4	PhMe	rt	12	100	33:1
7	H_2SO_4	PhMe	reflux	3	100	16:1
8	$AlCl_3$	PhMe	reflux	12	86	>99:1
9	$TiCl_4$	PhMe	reflux	12	53	>99:1
10	$ZnCl_2$	PhMe	reflux	12	55	50:1
11	$FeCl_3$	PhMe	reflux	12	100	4:1
12	$CuCl_2$	PhMe	reflux	12	-	-

[a]: All the reactions started with 0.2 mmol of oxazolidinone **46** with benzaldehyde **191a** (2 equiv.) using a given acid (2.0 equiv.) in CH_2Cl_2 or $CHCl_3$ or PhMe (5 mL)
[b,c]: Determined by crude ^{1}H NMR

Our initial attempts at direct one-step synthesis of oxazolidinone **189a** through cyclocondensation between oxazolidinone **46** and benzaldehyde **191a** using trifluoroacetic acid (TFA), pyridinium *p*-toluenesulfonate (PPTS) or 4-

toluenesulfonic acid (TsOH) were fruitless (Table 20, entries 1-3). This may be due to the low nucleophilicity of the aromatic ring of oxazolidinone **46** due to the lack of activating groups (methoxy or methylenedioxy). Nevertheless, we found that this cyclization could be achieved successfully at room temperature using H_2SO_4 in CH_2Cl_2, $CHCl_3$ or toluene (Table 20, entries 4-7) but not in MeOH, CH_3CN or THF (not shown in the table) to give two diastereomeric products *cis*- and *trans*-**189a**. The two diastereomers were separated by by column chromatography (using EtOAc: hexane, 1: 1 v/v as the eluent).

The major diastereomer was obtained as white crystals in 94% yield (Table 1, entry 4), 154-156 ^oC. The FT-IR spectrum of the major diastereomer revealed a sharp peak at 1737 cm^{-1} corresponding to the absorption band of C=O bond of the oxazolidinone moiety. The high resolution ESI-MS showed a molecular ion *m/z* value of 288.0995 corresponding to $(M+Na)^+$ thus supporting the molecular formula $C_{15}H_{19}NO_5$ (*m/z* calcd for $C_{15}H_{19}NO_2Na$ $(M+Na)^+$: 316.1161). The ^1H NMR spectrum showed aromatic proton signals at δ 7.00 (d, *J*=7.5 Hz, 1H) and δ 7.16-7.36 (m, 8H) indicating the presence of two phenyl rings, each from the starting material oxazolidinone **46** and benzaldehde **191a**. In addition, a characteristic *C*1-proton signal was found at δ 6.06 (s, 1H). The ^{13}C NMR spectrum revealed five additional carbon signals in comparison with its starting material oxazolidinone **46**, comprising of four aromatic carbon signals and one *C*1-carbon signal at δ 56.3, indicating the successful condensation of oxazolidinone **46** and benzaldehyde **191a**. By comparison with the literature data,[133a, 176] the major diastereomer was assigned (1*R*,3*S*) and structure *trans*-**189a**.

The minor diastereomer was also obtained as white crystals in 4% yield (Table 1, entry 4). The FT-IR spectrum of the minor diastereomer revealed a sharp peak at 1737 cm^{-1} corresponding the absorption band of the C=O of the oxazolidinone moiety. The high resolution ESI-MS showed a molecular ion *m/z* value of 288.0995 corresponding to $(M+Na)^+$ thus supporting the molecular formula $C_{15}H_{19}NO_5$ (*m/z* calcd for $C_{15}H_{19}NO_2Na$ $(M+Na)^+$: 316.1161). The ^1H NMR spectrum showed nine aromatic proton signals at δ 7.08-7.34 (m, 9H). In addition, the characteristic proton of *C*1-proton was found at δ 5.70 (s, 1H), which was shifted upfield in comparison to that of *C*1-proton of *trans*-**189a**. This indicated the shielding effect from the proton at C3, revealing that these two hydrogen atoms are in *cis*-relationship. The ^{13}C NMR spectrum revealed five new carbon signals in comparison to oxazolidinone **46**, corresponding to four new aromatic carbon signal and one *C*1-carbon signal (at δ 59.5). These results indicated the successful condensation of oxazolidinone **46** and benzaldehyde **191a**. Therefore, the minor diastereomer product was assigned *cis*-**189a**.

Results from table 20 showed that the best conversion of 100% and *d.r*. of >99:1 was obtained in $CHCl_3$ (Table 20, entry 5). Attempts to increase the rate of the reaction by increasing the temperature resulted in a decrease in the diastereoselectivity by almost 50% (Table 20, entries 6 *vs* 7). We also attempted the cyclization using several Lewis acids such as $AlCl_3$, $TiCl_4$, $ZnCl_2$, $FeCl_3$ and $CuCl_2$, and found the reaction to be sluggish at room temperature. However, at reflux (Table 20, entries 8-12), these Lewis acids (except $CuCl_2$) successfully gave the products **189a** in varying degrees of diastereoselectivities and yields. $AlCl_3$ gave the best results with excellent >99% diastereoselectivity and very

good 86% conversion followed by $TiCl_4$ which gave >99% diastereoselectivity and 53% conversion (Table 20, entry 8 and 9, respectively). Clearly, the use of H_2SO_4 not only shortened the synthetic route but also offered several advantages over the TMSOTf protocol (Scheme 56) including avoiding strictly dry reaction conditions and the use of expensive TMSOTf.

With the optimal conditions established (Table 20, entry 5), we then examined the scope of this cyclization using various aldehydes **191a-j** (Table 21). The cyclization preceded smoothly with aromatic **191a-d**, aliphatic **191e-g** and cyclic **191h** aldehydes. The expected products **189a-h** were obtained in high diastereoselectivities and isolated yields. Even cyclization with trimethyl acetaldehyde **191g**, which previously failed using the benzotriazole method,[176] proceeded to give **191g** in excellent >99% diastereoselectivity and 83% yield (Table 21, entry 7). Sterically congested *o*-aldehydes **191b** and **191c** also gave the oxazolidinone products **189b** and **189c**, respectively, in good yields but lower diastereoselectivity (Table 21, entries 2 and 3). However, very congested *o*-benzaldehydes such as *o*-methoxy-1-naphthaldehyde **191i** and *o*-benzyl salicylaldehyde **191j** failed to cyclize (Table 21, entries 9-10). Based on these results, we can conclude that the presence of *o*-substituents on the aldehyde can greatly impact the success and diastereoselectivity of the reaction.

Table 21: Scope of the diastereoselective Pictet-Spengler cyclization between oxazolidinone 46 and aldehydes 191a-h for the synthesis of chiral THIQs 190a-h[a]

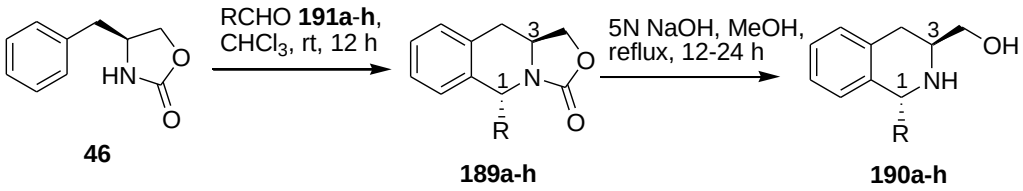

Entry	Aldehyde **191**	Oxazolidinone **189**			THIQ **190**	
		Number	Yield[b] (%)	*d.r.*[c]	Number	Yield[a] (%)
1	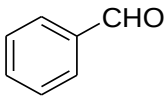 **191a**	**189a**	85	>99:1	**190a**	93
2	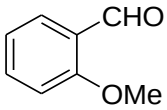 **191b**	**189b**	76	20:1	**190b**	81
3	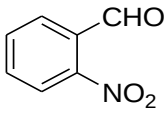 **191c**	**189c**	72	10:1	**190c**	-
4	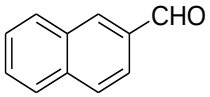 **191d**	**189d**	79	25:1	**190d**	92
5	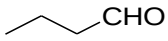 **191e**	**189e**	92	>99:1	**190e**	85
6	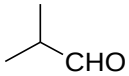 **191f**	**189f**	87	>99:1	**190f**	72
7	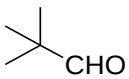 **191g**	**189g**	83	>99:1	**190g**	89
8	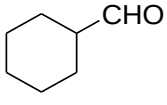	**189h**	83	17:1	**190h**	75

	191h					
9	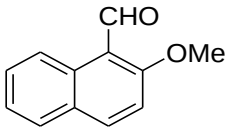	**189i**	-	-	**190i**	-
	191i					
10	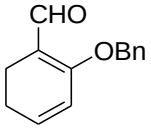	**189j**	-	-	**190j**	-
	191j					

[a]: All the Pictet-Spengler reactions started with 0.2 mmol of oxazolidinone **46** with a given aldehyde (2.0 equiv.) using H_2SO_4 (2.0 equiv.) in $CHCl_3$ (5 mL) at room temperature
[b]: Isolated yield
[c]: Determined by crude $_1$H NMR

The major diastereomer cycloadduct oxazolidinone **189a-h** were fully characterized by melting point measurement, optical rotation, FT-IR, ESI-MS, ^{1}H NMR and ^{13}C NMR (See chapter VII: Experimental procedure). The characteristic proton signal and carbon signal at C1 of oxazolidinone **189a-h** in NMR were tabulated in table 22.

Table 22: The characteristic proton signal and carbon signal at C1 of oxazolidinone 189a-h in NMR

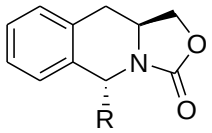

189a-h

R	mp (°C)	ESI-MS $(M+Na)^+$	C1-*H* (ppm)	C1-*C* (ppm)
189a: Ph	145-154	288.0995	6.06 (s, 1H)	56.3
189b: *o*-OMePh	115	318.1101	6.25 (s, 1H)	49.5
189c: *o*-NO_2Ph	230	333.0486	6.60 (s, 1H)	49.6
189d: 2-naph	152-153	338.1151	6.22 (s, 1H)	56.5
189e: *n*-Pr	92	254.1151	4.55 (t, *J*=8.25 Hz, 1H)	48.3
189f: *i*-Pr	118	254.1151	4.82 (d, *J*=3.9 Hz, 1H)	57.9
189g: *t*-Bu	169	268.1308	4.65 (s, 1H)	61.3
189h: Cy	143	294.1465	4.78 (d, *J*=3.9 Hz, 1H)	57.6

Conversion of oxazolidinone **189a-h** (Table 21) to their corresponding THIQs **190a-h** was achieved smoothly by heating a suspension of **189a-h** at reflux in a 1:1 mixture of MeOH and aqueous 5N NaOH.[74a] The THIQs **190a,b,d-h** were obtained in 72-93% yields after purification by flash column chromatography

(EtOAc: hexane, 3:1, v/v). These THIQs **16a,b,d-h** were fully characterized by melting point measurement (where applicable), optical rotation, high resolution ESI-MS, ^{1}H NMR and ^{13}C NMR (See chapter VII: Experimental procedure). The characteristic proton signal and carbon signal at *C*1 of THIQs **15a,b,d-h** are shown in table 23. No isomerization was observed under these conditions as evident from NMR analysis.

Table 23: The characteristic proton signal and carbon signal at *C*1 of THIQ 190a,b,d-h in NMR

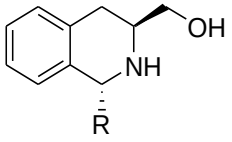

190a,b,d-h

R	mp (°C)	ESI-MS $(M+H)^{+}$	C1-*H* (ppm)	C1-*C* (ppm)
190a: Ph	98	240.1383	5.25 (s, 1H)	59.1
190b: *o*-OMePh	134	270.1489	5.63 (s, 1H)	49.1
190d: 2-naph	105	290.1539	5.39 (s, 1H)	59.2
190e: *n*-Pr	59	206.1539	3.43 (t, *J*=9 Hz, 1H)	48.7
190f: *i*-Pr	-	206.1539	3.43 (d, *J*=8.4 Hz, 1H)	59.8
190g: *t*-Bu	60	220.1696	3.69 (s, 1H)	63.1
190h: Cy	82-83	246.1852	3.40 (d, *J*= 9.3 Hz, 1H)	59.5

However, hydrolysis of **189c** resulted in an inseparable complex mixture. We speculate that, under basic conditions, the strong electron withdrawing NO_2 group significantly increased the acidity of the labile C1-*H* resulting in the formation of several products.

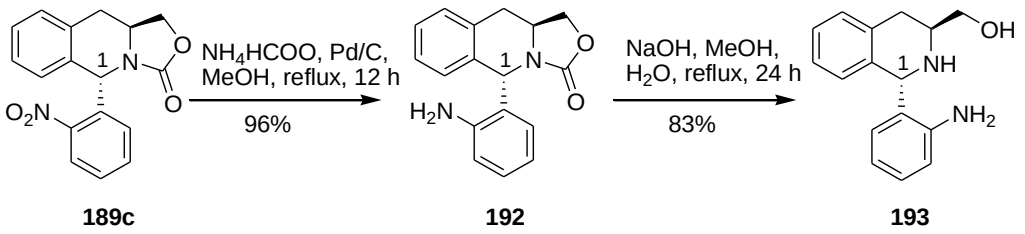

Scheme 57: Synthesis of THIQ 193 from oxazolidinone 189c

However, since our purpose eventually was to reduce the nitro group of **189c** to amine group to obtain the tridentate NNO-THIQ **193**, an indirect approach towards THIQ **193** was pursued according to scheme 57. Oxazolidinone **189c** was hydrogenated using Pd/C catalyst to give oxazolidinone **192** as white solid in quantitave yield, mp 201 ^{o}C. The FT-IR spectrum of the product displayed a sharp peak at 1719 cm^{-1} corresponding to the absorption band of C=O bond of the oxazolidinone moiety. In addition, the FT-IR spectrum also revealed two sharp peaks at 1603 cm^{-1} and 1260 cm^{-1} corresponding to the absorption bands of N-H and C-N, respectively, of the aromatic primary moiety. The high resolution ESI-MS showed a molecular ion *m/z* value of 303.1117 corresponding to $(M+Na)^+$ thus supporting the molecular formula $C_{17}H_{16}N_2O_2$ (*m/z* calcd for $C_{17}H_{16}N_2O_2Na$ $(M+Na)^+$: 303.1109). In comparison with the ^{1}H NMR spectrum of the starting material **189c**, the ^{1}H NMR of the product showed the characteristic proton signal of C1-proton upfield at δ 6.19 (s, 1H) due to the induction effect of an amine group. In addition, two proton signals corresponding to the primary amine moiety –N*H*$_2$ were also found at δ 4.70 (br

s, 2H). The ^{13}C NMR revealed the carbon signal for C1-carbon at δ 47.7. Therefore, the product was confirmed and assigned structure **192**.

In the subsequent step, hydrolysis of oxazolidinone **192** by reflux in a 1:1 mixture of MeOH and aqueous 5N NaOH provided THIQ **193** in in 83% yield as a gummy solid after purification by column chromatography (using pure EtOAc as eluent). FT-IR spectrum of the compound showed the disappearance of an absorption band corresponding to the carbonyl of oxazolidinone moiety and the appearance of strong broad OH and NH absorption at 3324 cm^{-1}. The high resolution-ESI-MS showed a molecular ion *m/z* value of 255.1498 corresponding to $(M+H)^+$ thus supporting the molecular formula $C_{16}H_{18}N_2O$ (*m/z* calcd for $C_{16}H_{19}N_2O$ $(M+H)^+$: 255.1497). In comparison with the ^1H NMR of its starting material oxazolidinone **192**, the ^1H NMR of the product showed the characteristic proton signal of C1-proton shifted upfield at δ 5.33 (s, 1H). The ^{13}C NMR spectrum of the product showed the disappearance of carbon signal of the carbonyl carbon from oxazolidinone moiety, indicating complete hydrolysis. In addition, the carbon signal corresponding to C1-carbon was also found at δ 49.9. Therefore, the product was assigned to be THIQ **193**.

2.2 Diastereoselective synthesis of C_2-BIQs

To synthesize C_2-BIQs **188**, we attempted the double Pictet-Spengler cyclization between oxazolidinone **46** and dialdehydes (and acetals) **194a-c** under the optimized conditions mentioned in table 20, entry 5 (Table 24).

Table 24: Double Pictet-Spengler cyclization for the synthesis of C_2-BIQs[a]

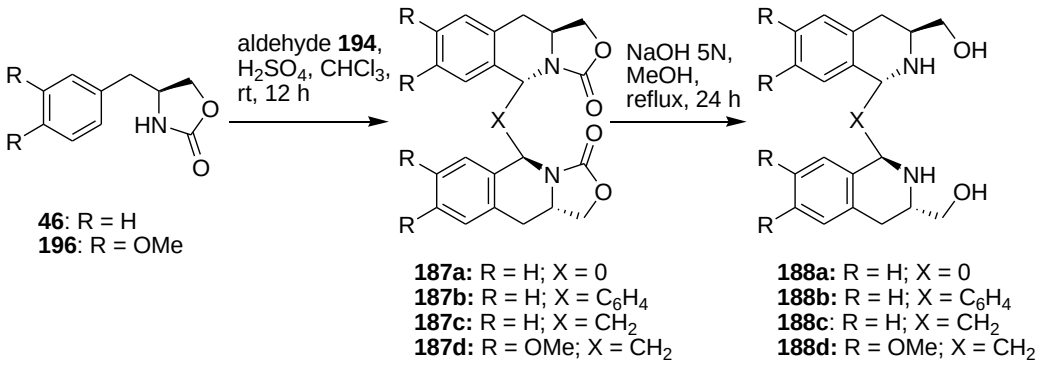

Entry	Aldehyde	Bisoxazolidinone **187**			C_2-BIQ **188**	
		Number	*d.r.*	Yield (%)[b]	Number	Yield (%)[b]
1	aqueous glyoxal **194a**	-	-	-	-	-
2	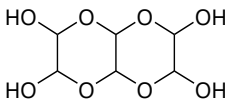 **194a**	**187a**	>99:1	82	**188a**	67
3	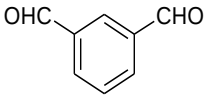 **194b**	**187b**	>99:1	98	**188b**	55
4	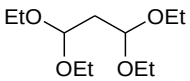 **194c**	**187c**	-	-	**188c**	-
5	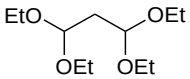 **194c**	**187d**	>99:1	98	**188d**	21

[a]: See chapter VII: Experimental procedures for detailed experiments
[b]: Isolated yields.

Preliminary cyclization between oxazolidinone **46** and aqueous glyoxal **194a** was not successful, probably due to the high water content that could have reduced the dehydration power of H_2SO_4 (Table 24, entry 5). However, to our delight, when aqueous glyoxal **194a** was replaced by its hydrate trimer form **194a**, oxazolidinone **46** was consumed gradually and bisoxazolidinone **187a** was obtained as a pure diastereomer in 82% yield as white crystal, mp 306 ^{o}C (Table 24, entry 5). The FT-IR spectrum of the product displayed a sharp peak at 1754 cm^{-1} corresponding to the absorption band of C=O bond of the oxazolidinone moiety. The high resolution-ESI-MS showed a molecular ion *m/z* value of 399.1315 corresponding to $(M+Na)^+$ thus supporting the molecular formula $C_{22}H_{20}N_2O_4$ of bisoxazolidinone **187** (*m/z* calcd for $C_{22}H_{20}N_2O_4Na$ $(M+Na)^+$: 399.1321). The ^{1}H NMR spectrum of this product revealed a symmetric compound in which the proton signals at C1-proton and C1'-proton were both found at δ 5.00 (s, 2H). ^{13}C NMR spectrum revealed only 11 carbon signals; only half of its supposed total number of 22 carbons thus confirming the presence of symmetric structure. The carbon signals corresponding to C1-carbon and C1'-carbon were both found at δ 56.0. In addition, recrystallization of this product from CH_2Cl_2/EtOAc gave crystals suitable for single X-ray crystallography. X-ray crystallographic analysis revealed a highly constrained dimeric structure where the aromatic rings are *trans* to each other and the absolute configuration of the two newly created chiral centers is (*S*,*S*). The *trans* arrangement of the two chiral centers within each heterocyclic ring is also

evident (Figure 14). Therefore, the product was assigned to be bisoxazolidinone **187a**.

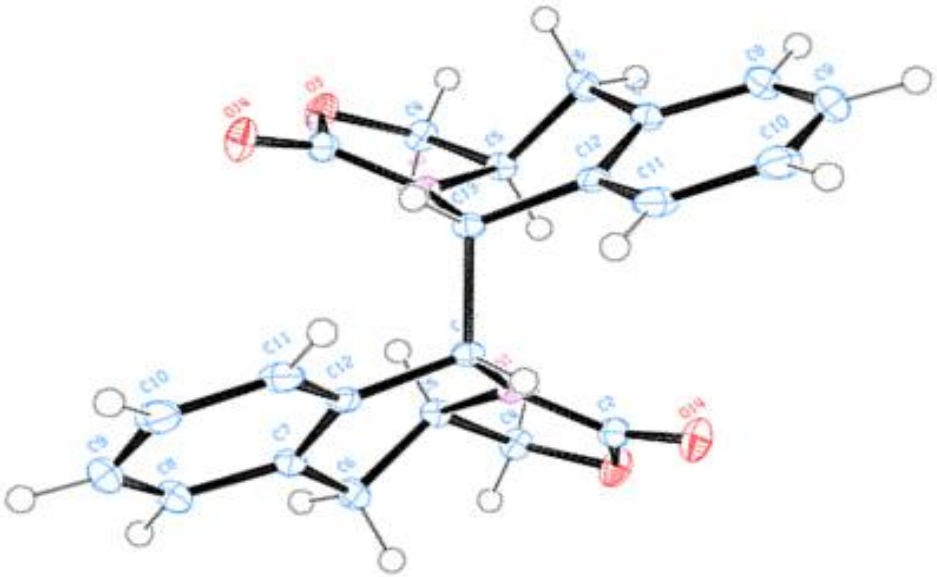

Figure 14: Single X-ray structure of bisoxazolidinone 187a

Extension of this strategy to other dialdehydes proved very successful. Double Pictet-Spengler cyclization between oxazolidinone **46** and isophthalic dialdehyde **194b** provided bisoxazolidinone **187b** as a pure diastereomer in 92% yield (Table 24, entry 5) after 12 h, mp 325 °C. FT-IR spectrum of this product showed a sharp peak at 1751 cm^{-1} corresponding to the absorption band of C=O of oxazolidinone moiety. The high resolution ESI-mass spectrum showed a molecular ion *m/z* value of 475.1628 corresponding to $(M+Na)^+$ thus supporting the molecular formula $C_{28}H_{24}N_2O_4$ of bisoxazolidinone **187b** (*m/z* calcd for $C_{28}H_{24}N_2O_4Na$ $(M+Na)^+$: 475.1634). ^1H NMR of this product revealed a symmetric spectrum in which the proton signals of C1-proton and C1'-proton were both found at δ 5.83 (s, 2H). ^{13}C NMR spectrum revealed only 14 carbon signals; only half of its supposed total number of 28 carbons thus indicating the presence of symmetric structure. In addition, the carbon signals of C1-carbon

and C1'-carbon were also found at δ 56.4. Therefore, the product was assigned as bisoxazolidinone **187b**.

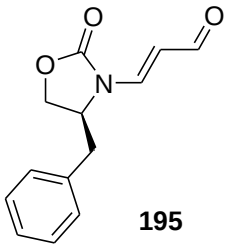

195

Figure 15: Oxazolidinone 195

On the other hand, reaction between oxazolidinone **46** and malondialdehyde **194c** did not provide the corresponding bisoxazolidinone product **187c** (Table 24, entry 4). Instead, chiral α,β-unsaturated aldehyde **195** was obtained in quantitative yield as a light yellow solid, mp 90 °C (Figure 15). FT-IR spectrum of this product showed two sharp peaks at 1753 cm^{-1} and 1675 cm^{-1} corresponding to the absorption bands of the C=O bonds of oxazolidinone and unsaturated aldehyde moieties. Besides, another sharp peak at 1631 cm^{-1} was also observed which corresponded to the absorption band of the C=C stretching. The presence of an aldehyde group was also supported by the detection of a weak absorption band for H-C=O stretch at 2750 cm^{-1}. The high resolution ESI-mass spectrum showed a molecular ion *m/z* value of 254.0788 corresponding to $(M+Na)^+$ thus supporting the molecular formula $C_{13}H_{13}NO_3$ of oxazolidinone **195** (*m/z* calcd for $C_{13}H_{13}NO_3Na$ $(M+Na)^+$: 254.9793). The ^1H NMR of this product revealed five aromatic proton signals at δ 7.16-7.19 (m, 2H) and δ 7.32-7.37 (m, 3H), indicating no cyclization. In addition, a proton signal corresponding to the aldehyde proton was found at δ 9.51 (d, *J*=7.5 Hz, 1H). Two proton signals corresponding to two alkenyl protons were also found at δ 5.76 (dd, *J*=7.8, 14.7 Hz, 1H) and δ 7.73 (d, *J*=14.4 Hz, 1H). With the coupling

constant greater than 11 Hz, these two alkenyl protons were assigned *trans* geometry to each other. The ^{13}C NMR of this product revealed a carbon signal at δ 191.1 corresponding to the carbonyl carbon, and two carbon signals at δ 112.2 and δ 144.8 corresponding to the two alkenyl carbons of the α, β-unsaturated aldehyde moiety. Therefore, the oxazolidinone product was assigned structure **195** (Figure 15).

We suspect that the *N*-acyliminium ion intermediate obtained during this cyclization exhibited a higher propensity to undergo elimination to give product **195** rather than cyclization through nucleophilic attack by an unactivated nucleophilic aromatic ring to give **187c**. Therefore, double cyclization proceeded smoothly between electron rich oxazolidinone **196** (aromatic ring activated with MeO) and malondialdehyde **194c** to give bisoxazolidinone **187d** in quantitative yield as a white solid after 4 h by trituration in hexane, mp 324 ^{o}C (Table 24, entry 5). FT-IR spectrum of this product displayed a sharp peak at 1774 cm-1 corresponding to the absorption band of C=O of oxazolidinone moiety. The high resolution-ESI-MS showed a molecular ion *m/z* value of 533.1894 corresponding to $(M+Na)^+$ thus supporting the molecular formula $C_{27}H_{30}N_2O_8$ of bisoxazolidinone **187d** (*m/z* calcd for $C_{27}H_{30}N_2O_8Na$ $(M+Na)^+$: 533.1900). In comparison with the ^1H NMR of its oxazolidinone starting material **196**,[178] the ^1H NMR of the product revealed a symmetric spectrum in which the proton signals corresponding to C1-proton and C1'-proton were both found at δ 4.97 (t, *J*=6.3 Hz, 2H). The proton signal corresponding to the methylene bridge –CH_2- protons were found at δ 2.55 (t, *J*= 6.2 Hz, 2H). In addition, ^{13}C NMR of this product also revealed a relatively weak carbon signal at δ 40.5 corresponding to bridging methylene carbon –*C*H_2-, and a carbon

signals at δ 48.9 corresponding to the C1-carbon and C1'-carbon. Therefore, the product was assigned structure **187d**.

Subsequently, chiral C_2-BIQs **188a,b,d** were then obtained by heating a suspension of bisoxazolidinone **187a, 187b** and **187d** at reflux in a 1:1 mixture of MeOH and aqueous 5N NaOH. After purification using column chromatography (CH_2Cl_2: MeOH, 95:5, v/v), the viscous oils obtained were triturated with hexane to give wet solids in moderate to good overall yields. C_2-BIQs **188a,b,d** were characterized by FT-IR, optical rotation, high resolution-ESI-MS, ^{1}H and ^{13}C NMR (See Chapter VIII: Experimental procedure). The characteristic proton signal and carbon signal at *C*1 and C1' of C_2-BIQs **188a,b,d** as shown in table 25. No isomerization was observed under these conditions as evident from NMR analysis.

Table 25: The characteristic proton signal and carbon signal at *C*1 and C1' of C_2-BIQs 188a,b,d

	HR-ESI-MS $(M+H)^+$	C1-*H* and C1'-*H* (ppm)	C1-*C* and C1'-*C* (ppm)
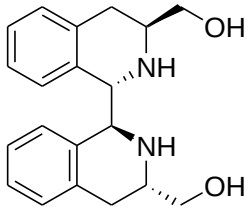 **188a**	325.1911	4.17 (s, 2H)	60.8
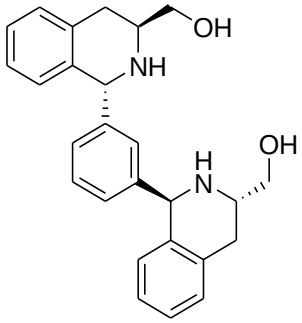 **188b**	401.2224	5.17 (s, 2H)	59.1
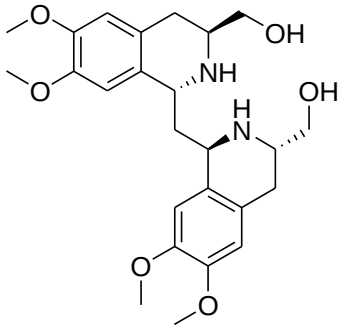 **188d**	459.2490	4.24 (t, *J*=7.2 Hz, 2H	49.6

In conclusion, we have successfully established a direct, modular and high yielding diastereoselective synthesis of highly functionalized oxazolidinone **189a-h** and bisoxazolidinone **187a,b**,**d** using H_2SO_4-catalysed Pictet-Spengler

cyclization. Hydrolysis of oxazolidinones **189** and bisoxazolidinones **187** gave a new family of chiral polydentate-amino alcohol ligands **188** and **190**. Application of these THIQs and C_2-BIQs in the asymmetric Henry reaction was investigated in the next section.

3. Application of THIQs and C_2-BIQs ligands in asymmetric Henry reaction.

The Henry (or nitroaldol) reaction is a classical organic reaction between nitroalkane and aldehyde to give β-nitroalcohol adduct (Scheme 56),[179] a synthetically versatile compounds that can be converted into intermediates such as nitroalkene,[180] β-aminoalcohol,[181] β-aminoacids,[180] α-nitroketones.[182]

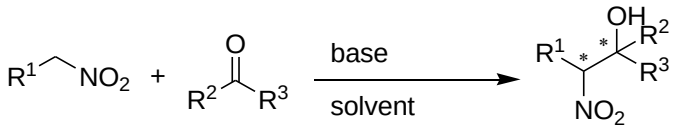

Scheme 58: Typical Henry reaction

The asymmetric version of Henry reaction was first reported by Shibasaki[183] using rare earth metal alkoxide as the chiral catalyst. Since then, research and development in asymmetric Henry reaction has resulted in a wide array of effective metal based and non-metal based catalysts which offer excellent results in terms of conversion, enantioselectivity and substrate specificity.[184] Among the metal-based catalysts, copper is the most commonly used due to its excellent chelating properties to bi- and poly-dentate ligands. Chiral copper complexes derived from ONO type tridentate chiral ligands formed nitro aldols adducts with excellent enantioselectivities.[184b] In addition, majority of chiral ligands developed for this reaction contain nitrogen atoms donor such as

bisoxazolines,[185] bisoxazolidines,[186] diamines,[187] aminopyridines,[188] tetrahydrosalens,[189] The application of β-amino alcohols as chiral ligands in asymmetric Henry reaction has been less investigated, though several ligands such as **111**,[126a] **197**,[174b] **198**,[174a] and **199**[174c] (Figure 16) have been reported with varied success.[174d]

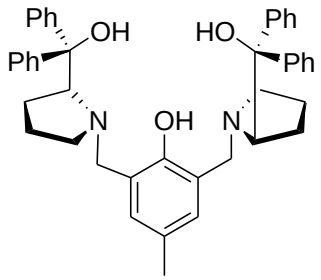

111

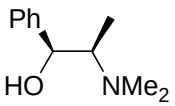

198

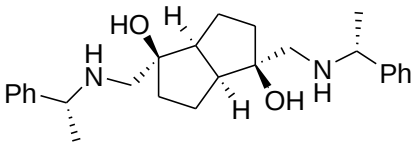

197

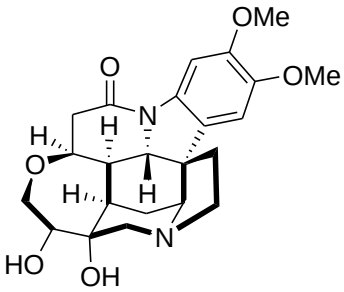

199

Figure 16: Examples of amino alcohols as chiral ligands in asymmetric Henry reactions

The application of chiral THIQ scaffold in Henry reaction had been earlier reported to give good enantioselectivity.[77e] While structural modification of chiral THIQ ligands had been mainly accomplished at the alcohol group,[77e] the effects of modification at *C*1 have not been investigated. As described in the first half of this chapter, we have successfully synthesized a series of novel bidentate and tridentate THIQ aminoalcohols **190a,b,d-h** and **193**; and tetradentate (or C_2-BIQs) aminoalcohols **18a,b,d** (Figure 17).[190] We therefore decided to investigate the effect of substitution at *C*1 on the enantioselectivity in Henry reaction using our ligands.

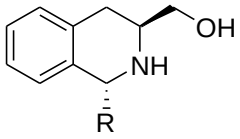

190a,b, d-h, 193

190a: R = Ph
190b: R = *o*-OMe-C_6H_4-
190d: R = 2-naphthyl
190e: R = *n*-Pr
190f: R = *i*-Pr
190g: R = *t*-Bu
190h: R = Cy
193: R = *o*-NH_2-C_6H_4-

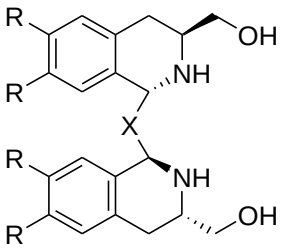

188a, b, d

188a: R = H, X = 0
188b: R = H, X = 3,5-Ph
188d: R = OMe, X = -CH_2-

Figure 17: THIQs and *C_2*-BIQs as chiral ligand in asymmetric Henry reaction.

3.1 Screening of asymmetric Henry using different $Cu(OAc)_2.H_2O$ complexes with THIQ and *C_2*-BIQ ligands

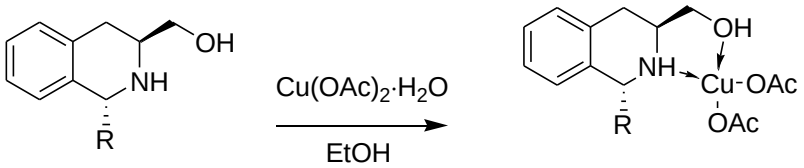

190a,b,d-h, 193 — $Cu(OAc)_2$-THIQ **190a,b, d-h, 193**

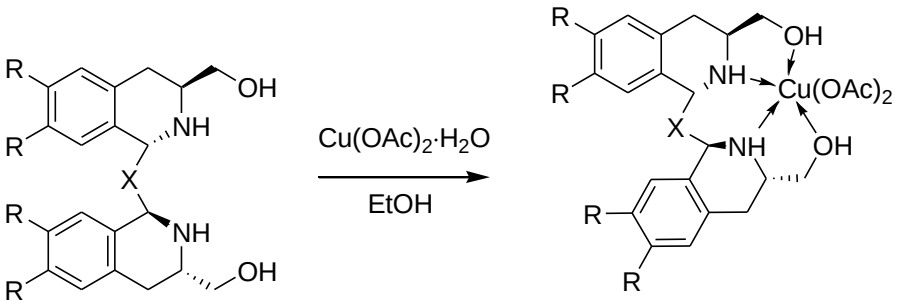

14a, b, d — $Cu(OAc)_2$-*C_2*-BIQ **188a,b,d**

Scheme 59: Complexes of THIQ or *C_2*-BIQs with $Cu(OAc)_2 \cdot H_2O$ for the asymmetric Henry reaction between benzaldehyde 191a and nitromethane 200

Complexes of THIQs **190a,b,d-h, 19** and *C_2*-BIQs **188a,b,d** with $Cu(OAc)_2 \cdot H_2O$ were screened for the asymmetric Henry reaction between benzaldehyde **191a** and nitromethane **200** (Scheme 59) and the results are shown in table 26.

The chiral complexes (10 mol%) were prepared *in situ* by mixing the respective ligand with $Cu(OAc)_2 \cdot H_2O$ in 1:1 molar ratio in EtOH at room temperature. To complete the reaction, benzaldehyde **191a** (1 equiv.) and nitromethane **200** (10 equiv.) were added successively to the *in situ* catalyst solution and the reaction was allowed to stir at room temperature for 48 h. The β-nitroalcohol **201** was obtained by purification using column chromatography (EtOAc: hexane, 5: 1 v/v). Its structure was confirmed by comparing its ^{1}H NMR to the literature values.[168f] The *ee* of the product was measured by HPLC using Chiralcel OD-H column (hexane: IPA = 85:15, flow rate = 1.0 ml/min, wavelength = 215 nm, t_1 = 16.7 min for (*R*), t_2=20.9 min for (*S*)).[168f]

Table 26: Screening of enantioselective Henry reaction using $Cu(OAc)_2.H_2O$ with THIQs and C_2-BIQs[a]

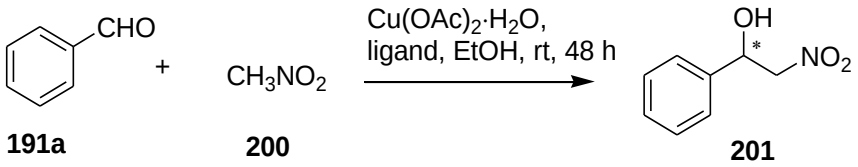

191a **200** **201**

Entry	Ligand	Yield[b] (%)	*ee*[c] (%)
1	**190a**	73	34 (*R*)
2	**190b**	78	36 (*S*)
3	**190d**	74	34 (*R*)
4	**190e**	78	22 (*R*)
5	**190f**	70	2 (*S*)
6	**190g**	71	34 (*S*)
7	**190h**	67	5 (*S*)
8	**193**	42	27 (*S*)
9	**188a**	80	55 (*S*)
10	**188b**	93	11 (*R*)
11	**188d**	85	6 (*S*)

[a]: All the reactions were performed on a 0.2 mmol scale of benzaldehyde **191a** in the presence of ligand (10 mol%) and $Cu(OAc)_2.H_2O$ (10 mol%) using $MeNO_2$ **200** (10.0 equiv) in EtOH (2 mL)
[b]: Isolated yields
[c]: measured by HPLC: Chiralcel OD-H column hexane: IPA = 90:10, flow rate = 0.8 ml/ min, wavelength = 215 nm, t_1 = 18.1 for (*R*), t_2 = 22.2 min for (*S*)

In general, the reactions proceeded smoothly to provide the β-nitroalcohol **201** in good yield (42-78%) after 48 h. The following observation can be concluded from table 26 with respect to the enantioinduction:

1. The bulkiness of the aryl C1 substituents seems to have no effect on the *ee* of the β-nitroalcohol **201** since both THIQs **190a** and **190d** gave the product in 34% *ee* (*R*) (Table 26, entries 1 and 3). No major variation in the

ee with other aryl C1 substituents as in case of THIQ **190b** and THIQ **193** since the ee stayed around the 34% level (Table 26, entries 2 and 8).

2. A dramatic change in the *ee* of the β-nitroalcohol **201** was observed in the case of the aliphatic C1 substituents. In particular, as the steric size of the C1 alkyl substituents increased from *n*-Pr (THIQ **190e**) to *i*-Pr (THIQ **190f**) and to *t*-Bu (THIQ **190g**), the enantioselectivity changed from being pro-(*R*) with 22% *ee* to pro-(*S*) with 2% and 34% *ee*, respectively (Table 26, entry 4-6). THIQ **190h** where C1 substituent is Cy provided similar results to THIQ **190f** where C1 substituent is *i*-Pr-C1 (Table 26, entries 5 vs 7).
3. The presence of oxygen or nitrogen donor atoms at the *ortho* position of the aromatic C1 substituents allows for possible additional chelation to the Cu(II) species. Henry reaction using tridentate THIQ **190b** and THIQ **193** provided the β-nitro alcohol product (*S*)-**201** in only 36% *ee* and 27% *ee*, respectively (Table 26, entries 2 and 8).
4. A relationship between the relative distance of the two amino alcohol groups and the enantioselective was also observed for C_2-BIQs **188a,b,d**. As the relative distance between the two amino groups increased, as can be seen from **188a** to **188d** to **188b**, the enantioseletivity and stereospecificity were shifted from 55% ee (*S*) (Table 26, entry 9) to 6% *ee* (*S*) (Table 26, entry 11) and to 11% *ee* (*R*) (Table 26, entry 10).

In conclusion, the enantioselectivity of the $Cu(OAc)_2$-catalyzed Henry reaction showed a strong dependence on the nature of the *C*1 substituent of THIQs and the types of C_2-BIQs. It should also be noted that it is the conformation of Cu(II)-THIQ complex that determine the enantioselectivity of the reaction. Factors which affect the conformation of Cu(II)-THIQ complex include not

only the steric effects but also the electronics effects and chelating groups. For example, since the C1-phenyl substituent (**190a**) and C1-*t*-butyl substituent (**190g**) are both bulky and have steric effects,[191] the resulting *N*-heterocyclic rings would adopt a similar half-chair conformation where the *C*1-substiuent is at the pseudoequatorial position. However, the β-nitroalcohol product **201** obtained from the reaction with those two THIQs surprisingly gave the opposite enantioselectivity (Table 26, entries 1 vs 6). Though conformational analysis of Cu(II)-THIQ complex is beyond the scope of this work, we speculate that modest *ee* obtained in these cases were probably due to the "less rigid" conformation of the Cu(II)-THIQ complex. With the low energy barrier for the *N*-inversion for the heterocyclic secondary amine,[192] Bowen *et al*[193] demonstrated a significant presence of two conformers of THIQ derivatives in which the N-H bond was at the pseudoaxial or pseudoequatorial positions (Scheme 60).[194] We believe that restricted *N*-inversion by methylation of the amine group would give a more rigid THIQ catalyst that will lead to improvement of enantioselectivity.

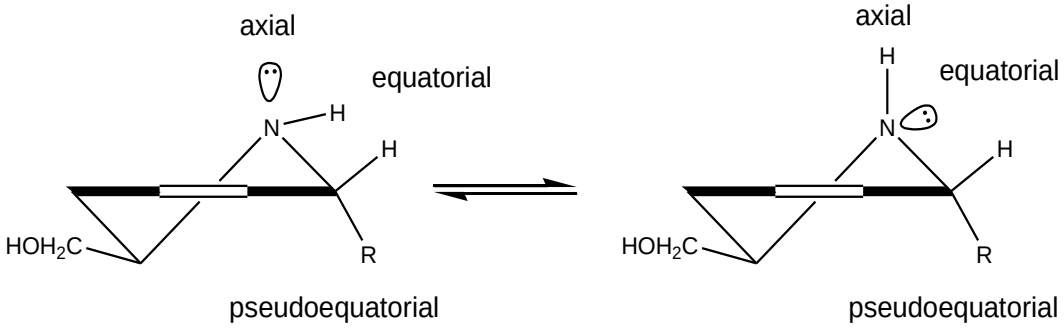

Scheme 60: Possible conformations of THIQ 190 due to *N*-inversion with C1-R substituent at pseudoequatorial

In the next section, the effect of *N*-methylation of THIQs and C_2-BIQs on the enantioselectivity in the Henry reaction will be investigated. This would require

us to synthesize the required ligands through *N*-methylation of THIQs and C_2-BIQs

3.2 Effects of enantioselective Henry reaction by *N*-methylation of THIQs and C_2-BIQs

3.2.1 *N*-methylation of THIQs and C_2-BIQs

N-methylation of THIQs **190a,b,d-h**, **193** and C_2-BIQ **188a,b,d** were carried out by using reductive amination with HCHO/$NaCNBH_3$[195] or nucleophilic aliphatic substitution with MeI[168h, 170b] (Scheme 61).

N-methylation of THIQs **190a,b,d-h** by reductive amination provided the corresponding *N*-methylated THIQs **202a,b,d-h** in 90-99% yield after purification by column chromatography (Scheme 61a). These products were analyzed by melting point measurement (where applicable), optical rotation, high resolution-ESI-MS, ^1H and ^{13}C NMR (See Chapter VII: Experimental procedure). In all cases, high resolution ESI-MS of products **202a,b,d-h** indicated an increment of 14 a.m.u, indicating the addition of the methyl group. In addition, the proton signals corresponding to the new methyl group of THIQ **202a,b,d-h** were found in the range of δ 2.05-2.46 in ^1H NMR.

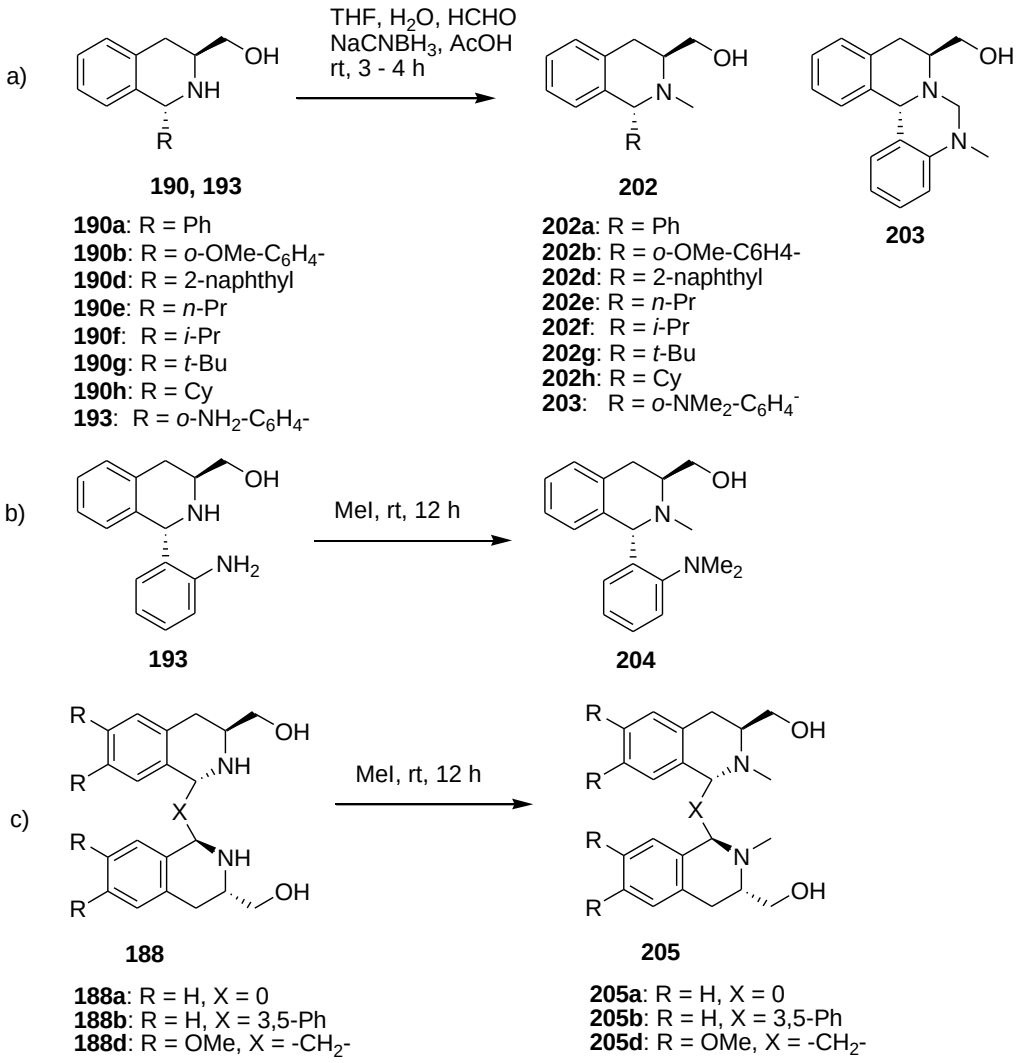

Scheme 61: *N*-methylation of THIQs 190a,b,d-h, 193 and *C*$_2$-BIQs 188a,b,d

However, *N*-methylation of THIQ **193** did not provide the corresponding THIQ **204** (Scheme 61c), but instead, a cyclic THIQ **203** (Scheme 58a) was obtained in quantitative yield as a white solid after purification by column chromatography (EtOAc: henxane, 1:1, v/v), mp 179 ^{o}C. The high resolution-ESI-MS spectrum of the white solid showed a molecular ion *m/z* value of 281.1659 corresponding to $(M+H)^+$ thus supporting the molecular formula $C_{18}H_{20}N_2O$ (*m/z* calcd for $C_{18}H_{21}N_2O$ $(M+H)^+$: 281.1654). In comparison with the ^{1}H NMR spectrum of its starting material THIQ **193**, the ^{1}H NMR spectrum of this product revealed a singlet corresponding to the *N*-methyl protons at δ

2.88 (s, 3H). In addition, two new doublets appeared at δ 4.03 (d, *J*= 10.8 Hz, 1H) and δ 4.3 (d, *J*= 10.8 Hz, 1H) corresponding to the methylene proton bridging two nitrogens.[196] The ^{13}C NMR spectrum of this product revealed two additional carbon signals at δ 70.2 and δ 36.5 respectively corresponding to the *N*-methyl carbon and the methylene carbon bridging two nitrogens. Therefore, the product was assigned structure **203**.

Nevertheless, synthesis of THIQ **204** from its starting material THIQ **193** by methylation using MeI provided the product in 72% yield as a white solid after purification by column chromatography, mp 155-156 ^{o}C (Scheme 58b). The high resolution-ESI-MS showed a molecular ion *m/z* value of 297.1973 corresponding to $(M+H)^+$ and supporting the molecular formula $C_{19}H_{24}N_2O$ (*m/z* calcd for $C_{19}H_{25}N_2O$ $(M+H)^+$: 297.1967). In comparison with the ^{1}H NMR spectrum of its starting material THIQ **193**, the ^{1}H NMR spectrum of this product revealed two singlets corresponding to the proton signals of the aliphatic *N*-methyl protons and aromatic *N*-methyl protons at δ 2.42 (s, 3H) and δ 2.85 (s, 6H) respectively. The ^{13}C NMR spectrum of this product revealed two additional carbon signals at δ 61.3 and δ 35.1 corresponding to two aliphatic *N*-methyl carbon and aromatic *N*-methyl carbons, respectively. Therefore, this product was assigned to structure **204**.

N-methylation of *C*$_2$-BIQ **188a** using MeI[170b] resulted in complicated mixture which showed only trace amount of the possible *N*-methylated product *C*$_2$-BIQ **205a** according to crude ^{1}H NMR spectral analysis. On the other hand, *N*-methylation of **188b** and **188d** gave the corresponding *N*-methylated *C*$_2$-BIQs **205b** and **205d** respectively, as amorphous solid in modest yields after

purification by column chromatography (CH_2Cl_2: MeOH, 95: 5, v/v) (Scheme 58c). *C_2*-BIQs **205b** and **205d** were characterized by melting point, high resolution HR-MS, ^{1}H and ^{13}C NMR spectroscopy. Their structures were confirmed by comparing with the spectroscopic data of their respective starting materials. In the ^{1}H NMR spectrum, the proton signals corresponding to *N*-methyl protons of *C_2*-BIQ **205b** and **205d** were found at δ 2.38 and δ 2.32, respectively.

Based on ^{1}H NMR analysis, it can be inferred that the newly formed methyl group adapted the equatorial position which in turn forced the nitrogen lone pair electron into the axial orientation (Scheme 62).

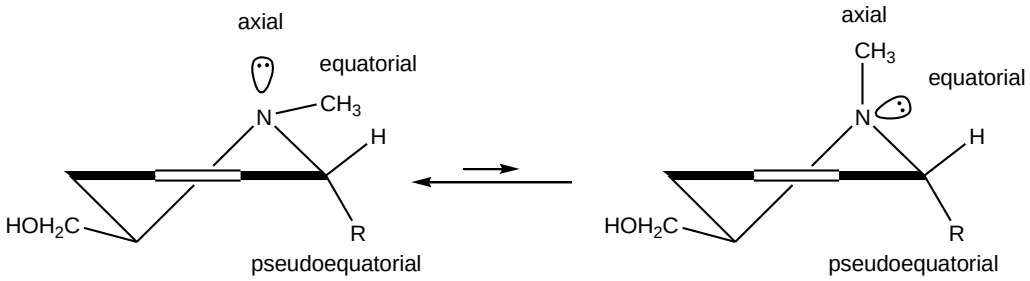

Scheme 62: Possible conformations of *N*-methylated THIQ 202 due to *N*-inversion with C1-R substituent at pseudoequatorial

Before *N*-methylation, the chemical shift of the proton at *C*1 (at pseudoaxial position)[197] of THIQ **190a** was found at δ 5.25. The ^{1}H NMR spectrum of the corresponding *N*-methylated THIQ **202a** showed the proton signal of *C*1-proton shifted upfield to δ 4.89, due to the shielding effect from the axial nitrogen lone pair. Such observation was also found in other THIQs **202a,b,d-h, 33** and *C_2*-BIQs **205b,d** (Table 27) except for the case of *n*-Pr substituent THIQ **190e** and THIQ **202e**.

Table 27: Proton chemical shifts at C1 of THIQs and C_2-BIQs before and after *N*-methylation

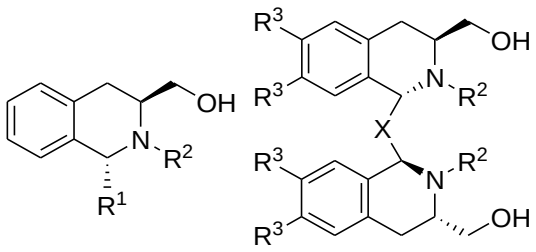	Before *N*-methylation R^2 = H	After *N*-methylation R^2 = Me
R^1 = Ph	5.25 (s, 1H) (**190a**)	4.89 (s, 1H) (**202a**)
R^1 = *o*-OMe-Ph	5.63 (s, 1H) (**190c**)	5.35 (s, 1H) (**202b**)
R^1 = *o*-NH_2-Ph	6.19 (s, 1H) (**193**)	5.59 (s, 1H)[a] (**204**)
R^1 = 2-naphth	5.39 (s, 1H) (**190d**)	5.02 (s, 1H) (**202d**)
R^1 = *n*-Pr	3.43 (t, *J*=9 Hz, 1H) (**190e**)	3.54-3.66 (m, 3H)[b] (**202e**)
R^1 = *i*-Pr	3.43 (d, *J*=8.4 Hz, 1H) (**190f**)	3.14 (d, *J*=9.3 Hz, 1H (**202f**)
R^1 = *t*-Bu	3.69 (s, 1H) (**190g**)	3.39 (s, 1H) (**202g**)
R^1 = Cy	3.40 (d, *J*= 9.3 Hz, 1H) (**190h**)	3.13 (d, *J*= 9Hz, 1H) (**202g**)
X = 3,5-C_6H_4, R^3 = H	5.17 (s, 2H) (**188b**)	4.87 (s, 2H) (**205b**)
X = -CH_2-, R^3 = OMe	4.24 (t, *J*=7.2 Hz, 2H) (**188d**)	3.98 (t, *J*= 7.8 Hz, 2H) (**205d**)

[a]: R^1 = *o*-NMe_2-Ph
[b]: The proton signal overlapped with hydroxymethyl group at *C*3

3.2.2 Enantioselective Henry reaction using $Cu(OAc)_2.H_2O$ complexes of *N*-methylated THIQs and C_2-BIQs

The *N*-methylated THIQ **202a,b,d-h, 203, 204** and C_2-BIQ **205b,d** ligands were screened for the enantioselective Henry reaction between benzaldehyde **191a** and nitromethane **200** in presence of Cu(OAc)2.H2O following the same procedure described in table 26. The results are presented in table 28. The reactions proceeded smoothly to give the desired β-nitroalcohol **201** in good to excellent 67-86% yields. As expected, *N*-methylation significantly improved the enantioselectivity of the β-nitroalcohol **201**. The following observation can be concluded from table 28

1. Bidentate THIQs **202a,d-h** offered the β-nitroalcohol **201** with *R*-selectivity while tridentate THIQs **202b, 203,** and **204** offered the β-nitroalcohol **201** with *S*-selectivity.
2. For reactions involving bidentate THIQs **202a,d-h**, THIQs with *C*1-aryl substituents (e.g. **202a** and **202d**) gave similar enantioselectivities to their precursors, **190a** and **190d** (Table 28, entries 1 and 3 vs Table 26, entries 1 and 3). On the other hand, the enantioselectivity of the β-nitroalcohol **201** increased significantly to 43-70% *ee* for THIQs with *C*1-alkyl substituents (e.g. **202e-h**) (Table 28, entries 4-7). The *ee* was observed to increase as the steric size of the *C*1-alkyl substituents increased from *n*-Pr to *i*-Pr (or Cy) and then to *t*-Bu.

3. Among the bidentate THIQs **202a,d-h**, THIQ **202g** with *C*1-*t*-Bu substituent offered the highest *ee* of 70% with *R*-selectivity.
4. In case of tridentate THIQs **202b**, **203** and **204**, the nature of the third chelating group exerted a substantial effect on the enantioselectivity. While the ONO THIQ **202b** improved the *ee* to 73% (Table 28, entry 2), the NNO *C*1-THIQ **204** (Table 28, entry 9) only provided 28% ee of the β-nitroalcohol **201**, similar to its precursor THIQ **193**.
5. Interestingly, the cyclic aminal NNO THIQ **203** offered the highest *ee* of 76% with pro-*S* selectivity (Table 28, entry 8).
6. Reactions using *N*-methylated C_2-BIQs **205b** and **205d** only resulted in modest *ee* of 26% and 14%, respectively (Table 28, entries 10-11).

Table 28: Enantioselective Henry reaction using $Cu(OAc)_2 \cdot H_2O$ complexes of *N*-methylated THIQs and C_2-BIQs[a]

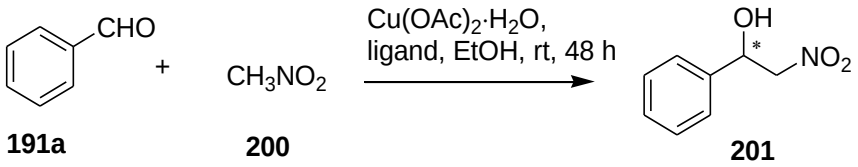

191a **200** **201**

Entry	Ligand	Yield[b] (%)	*ee*[c] (%)
1	**202a**	75	39 (*R*)
2	**202b**	83	73 (*S*)
3	**202d**	78	44 (*R*)
4	**202e**	86	43 (*R*)
5	**202f**	67	59 (*R*)
6	**202g**	71	70 (*R*)
7	**202h**	70	60 (*R*)
8	**203**	74	76 (*S*)
9	**204**	80	28 (*S*)
10	**205b**	85	26 (*R*)
11	**205d**	85	14 (*R*)

[a]: All the reactions were performed on a 0.2 mmol scale of benzaldehyde **191a** in the presence of ligand (10 mol%) and $Cu(OAc)_2.H_2O$ (10 mol%) using $MeNO_2$ **200** (10.0 equiv) in EtOH (2 mL)
[b]: Isolated yields
[c]: Measured by HPLC: Chiralcel OD-H column hexane: IPA = 90:10, flow rate = 0.8 ml/ min, wavelength = 215 nm, t_1 = 18.1 for (*R*), t_2 = 22.2 min for (*S*)

Since the cyclic aminal THIQ **203** gave the highest *ee* (Table 28, entry 8), we wanted to examine the effect of additional steric at the hydroxyl group on the enantioselectevity of the Henry reaction.

3.2.3 Effect of *O*-silylation of THIQ 203

O-Silylations of THIQ **203** with trimethylsilyl chloride (TMSCl) and tert-butyldimethylsilyl chloride (TBDMSCl) using 1H-imidazole[198] in CH_2Cl_2

gave the *O*-silylated *C*1-THIQs **206a** as white solid and **206b** as viscous oil in 72% and 76% yields, respectively (Scheme 63). The products were characterized by FT-IR, high resolution ESI-MS, ^{1}H and ^{13}C NMR spectroscopy. In particular, the ^{1}H NMR spectra of THIQs **206a** and THIQs **206b** revealed the proton signals corresponding to the presence of silyl groups at δ 0.1 (s, 9H) (for THIQs **206a**); and at 0.1 (s, 6H) and 0.86 (s, 9H) (for THIQs **206b**).

203

206a: R = TMS (72% yield)
206b: R = TBDMS (76% yield)

Scheme 63: *O*-silylations of THIQ 203

Next, the *O*-silylated THIQs **206a** and **206b** were examined in the enantioselective Henry reaction following the same procedure described in table 26. The results are presented in table 29. The reactions proceeded smoothly to give the desired β-nitroalcohol product **201** in 75-82% yield. The results showed that the steric hindrance at the hydroxyl group also influenced the enantioselectivity of the Henry reaction. In particular, while introduction of a moderately bulky group TMS as in THIQs **206a** improved the *ee* to 80% (*S*) (Table 29, entry 1), the presence of bulkier group TBDMS in THIQs **206b** severely reduced the *ee* to 52% (Table 29, entry 2).

Table 29: Enantioselective Henry reaction using $Cu(OAc)_2 \cdot H_2O$ complexes of *O*-silylated THIQ 206a,b[a]

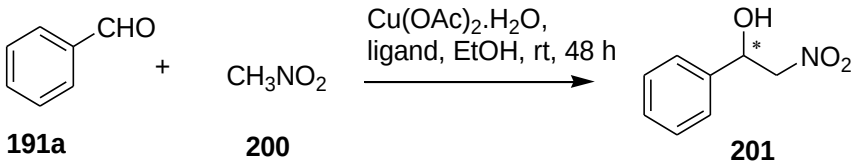

191a **200** **201**

Entry	Ligand	Yield[b] (%)	*ee*[c] (%)
1	**206a**	82	80 (S)
2	**206b**	75	52 (S)

[a]: All the reactions were performed on a 0.2 mmol scale of benzaldehyde **191a** in the presence of ligand (10 mol%) and $Cu(OAc)_2.H_2O$ (10 mol%) using $MeNO_2$ **200** (10 equiv) in EtOH (2 mL)
[b]: isolated yields
[c]: Measured by HPLC: Chiralcel OD-H column hexane: IPA = 90:10, flow rate = 0.8 ml/ min, wavelength = 215 nm, t_1 = 18.1 for (*R*), t_2 = 22.2 min for (*S*)

With the THIQ **206a** as the optimal ligand, the effects of metal salts, solvents and catalyst loading to the enantioselective in the Henry reaction were examined.

3.2.4 Effects of metal salts, solvents and catalyst loading on the enantioselective Henry reaction using THIQ 206a as chiral ligand

3.2.4.1 Effects of metal salts

Different metal acetates including $Co(OAc)_2$, $Mn(OAc)_2$, $Cu(OAc)_2$, CuOAc, $Zn(OAc)_2 \cdot 2H_2O$ and $Ni(OAc)_2 \cdot 4H_2O$ were examined (Table 30, entries 1-7). The Henry reactions between benzaldehyde **191a** and nitromethane **200** were carried out according to the optimized condition in table 29, entry 1. The results showed that all the metal acetate complexes with THIQ **206a** catalyzed the reaction to give 54-85% yield of the β-nitroalcohol **201** (Table 30, entries 1-7). However**,** only the Cu(II) and Cu(I) complexes can effectively induce the

stereoinduction into the reaction (Table 30, entries 3-5). All the other metal complexes resulted in racemic product (Table 30, entries 1-2, 6-7). Besides, Cu(II) in its hydrate form proved to be the optimal metal salt (Table 30, entry 4).

Table 30: Effects of metal salts in the enantioselective Henry reaction using THIQ 206a as chiral ligand[a]

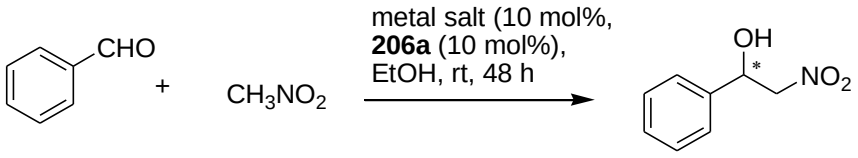

191a **200** **201**

Entry	Metal salts	Yield[b] (%)	*ee*[c] (%)
1	$Co(OAc)_2$	65	1
2	$Mn(OAc)_2$	54	1
3	$Cu(OAc)_2$	78	76
4	$Cu(OAc)_2 \cdot H_2O$	82	80
5	CuOAc	76	72
6	$Zn(OAc)_2 \cdot 2H_2O$	85	0
7	$Ni(OAc)_2 \cdot 4H_2O$	80	1
8	$Cu(acac)_2$	-	-
9	$CuCl_2$	35	14
10	CuCl	56	68
11	CuI	-	-
12	$Cu(NO_3)_2 \cdot 2.5H_2O$	-	-
13	$Cu(OTf)_2$	73	3

[a]: All the reactions were performed on a 0.2 mmol scale of benzaldehyde **191a** in the presence of ligand THIQ **206a** (10 mol%) and metal salt (10 mol%) using $MeNO_2$ **200** (10.0 equiv) in EtOH (2 mL)
[b]: Isolated yields
[c]: Measured by HPLC: Chiralcel OD-H column hexane: IPA = 90:10, flow rate = 0.8 ml/ min, wavelength = 215 nm, t_1 = 18.1 for (*R*), t_2 = 22.2 min for (*S*)

The effects of the counter ion of the copper salts, including $Cu(acac)_2$, $CuCl_2$, CuCl, CuI, $Cu(NO_3)_2 \cdot 2.5H_2O$, $Cu(OTf)_2$, were examined (Table 30, entries 8-13). It was observed that the complexes of $Cu(acac)_2$, CuI or $Cu(NO_3)_2 \cdot 2.5H_2O$, of THIQ **206a** were barely soluble in EtOH and the reaction failed to give β-nitroalcohol **201** (Table 30, entries 8, 11-12). On the other hand, complexes with $CuCl_2$, CuCl, $Cu(OTf)_2$, (Table 30, entries 9, 10 and 13) managed to catalyze the reaction to some extent and gave moderate 35-73% yield and inferior *ee* in comparison with the reaction catalyzed by $Cu(OAc)_2 \cdot H_2O$. Therefore, $Cu(OAc)_2 \cdot H_2O$ was used for further optimization.

3.2.4.2 Effects of the catalyst loadings

To investigate the effect of catalyst loading on the enantioselectivity, the asymmetric Henry reactions between benzaldehyde **191a** and nitromethane **200** carried out using 2.5, 5, 10, 15 and 20 mol% of $Cu(OAc)_2 \cdot H_2O$-THIQ **206a** (Figure 18) (Table 31). Interestingly, the enantioselectivity gradually increased from 67% to 80% *ee* as the loading increased from 2.5 to 10 mol% (Table 31, entries 1-3). However, while the yield improved over a catalyst loading of 10 mol%e, the *ee* remained constant and reached the maximum value of 80%. Therefore, an optimal catalyst loading of 10 mol% was deemed optimal.

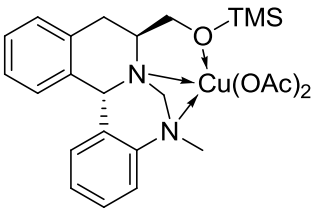

$Cu(OAc)_2$-THIQ **206a**

Figure 18: Proposed complex structure of Cu(OAc)2-THIQ 206a

Table 31: Effects of the catalyst loading in the enantioselective Henry reaction using $Cu(OAc)_2 \cdot H_2O$-THIQ 206a as the catalyst[a]

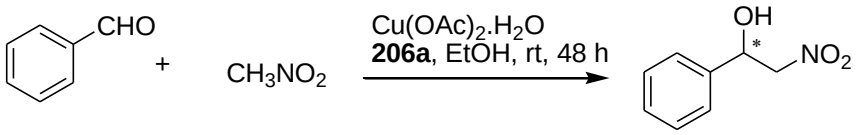

191a **200** **201**

Entry	catalyst (mol%)	Yield[b] (%)	*ee*[c] (%)
1	2.5	56	67
2	5	65	73
3	10	82	80
4	15	87	80
5	20	91	79

[a]: All the reactions were performed on a 0.2 mmol scale of benzaldehyde **191a** in the presence of THIQ **206a** (10 mol%) and $Cu(OAc)_2.H_2O$ (10 mol%) using $MeNO_2$ **200** (10.0 equiv.) in EtOH (2 mL)
[b]: Isolated yields
[c]: Measured by HPLC: Chiralcel OD-H column hexane: IPA = 90:10, flow rate = 0.8 ml/ min, wavelength = 215 nm, t_1 = 18.1 for (*R*), t_2 = 22.2 min for (*S*)

3.2.4.3 Effect of reaction solvents

Effects of different organic solvents on the enantioselectivity of the Henry reaction between benzaldehyde **191a** and nitromethane **200** examined (Table 32). The results showed that polar protic solvents such as MeOH, EtOH and *i*-PrOH afforded the highest yields of 85-86% of β-nitroalcohol **201** (Table 32,

entries 1-3). However, the enantioselectivity was still at its optimum when EtOH was used (80% *ee*) (Table 32, entry 2). MeOH and *i*-PrOH provided lesser *ee* of 63% and 70%, respectively (Table 32 entries 1, 3).

Ether-like solvents such as THF, Et_2O, MTBE and *i*-Pr_2O caused the reactions to be very sluggish (Table 32, entries 4-7). After seven days, only modest yields of 12-31% of the β-nitroalcohol **201** were obtained with inferior *ee* (Table 32, entries 4-7). Other solvents including CH_2Cl_2, MeCN, $MeNO_2$ and PhMe (Table 32, entries 8-11) also gave similar results to the ether solvents. Therefore, EtOH remained as the optimal solvent choice.

Table 32: Effects of organic solvents in the enantioselective Henry reaction using $Cu(OAc)_2.H_2O$-THIQ 206a complex[a]

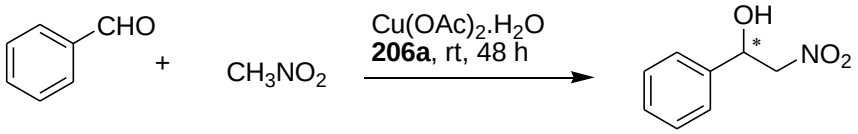

191a **200** **201**

Entry	Solvent	Yield[b] (%)	*ee*[c] (%)
1	MeOH	85	63
2	EtOH	82	80
3	*i*-PrOH	86	70
4*	THF	25	58
5*	Et_2O	31	74
6*	MTBE	-	-
7*	*i*-Pr_2O	12	63
8*	DCM	21	68
9*	MeCN	15	28
10	$MeNO_2$	79	71
11	Toluene	-	-

[a]: All the reactions were performed on a 0.2 mmol scale of benzaldehyde **191a** in the presence of THIQ **206a** (10 mol%) and $Cu(OAc)_2.H_2O$ (10 mol%) using $MeNO_2$ **200** (10.0 equiv.) in the given solvent (2 mL)
[b]: Isolated yield
[c]: Measured by HPLC: Chiralcel OD-H column hexane: IPA = 90:10, flow rate = 0.8 ml/ min, wavelength = 215 nm, t_1 = 18.1 for (*R*), t_2 = 22.2 min for (*S*)
*: Reaction was kept for seven days

3.2.5 Scope of the enantioselective Henry reaction catalyzed by $Cu(OAc)_2 \cdot H_2O$- THIQ 206a complex

The scope and limitation of the Henry reaction using $Cu(OAc)_2 \cdot H_2O$-THIQ **206a** complex under the optimized condition (Table 32, entry 2) was examined using various aldehydes (Table 33). The results showed that a broad range of aromatic aldehydes **191a**, **207-218** reacted smoothly with $MeNO_2$ **200** to give the corresponding β-nitroalcohols **201**, **219-230** in high yields (67-96%) and moderate to high enantioselectivities (54-80% *ee*). Aromatic aldehydes with electron-withdrawing (Table 33, entries 2-6) and electron-donating (Table 33, entries 7-11) substituents gave similar yields (up to 96%) and enantioselectivities (up to 80% *ee*). An exception to this is 4-nitrobenzaldehyde (Table 33, entry 2), which due to its strong electron-withdrawing nitro group; it exerted a much faster reaction rate that led to higher yield (91%) and lower enantioselectivity (54% *ee*). Interestingly, the substitution pattern (Table 33, entries 3-4, entries 7-9) at the aromatic rings had no major effect on the enantioselectivity or yield of the products. Other aromatic aldehydes such as 2-naphthaldehyde **217** and *trans*-cinnamaldehyde **218** also gave the corresponding products **229** and **230** in good yields and *ee* (Table 33, entries 12-13)

Table 33: Scope of the enantioselective Henry reaction using $Cu(OAc)_2 \cdot H_2O$-THIQ 206a catalyst[a]

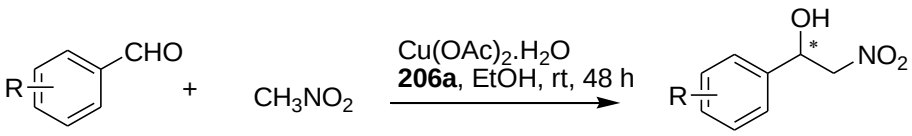

191a, 207-218 **200** **201, 219-230**

Entry	Aldehyde		Product	Yield[b] (%)	*ee*[c] (%)
1	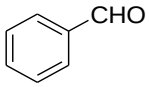	**191a**	**201**	82	80 (*S*)
2	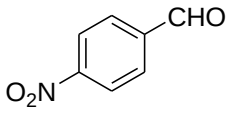	**207**	**219**	91	54 (*S*)
3	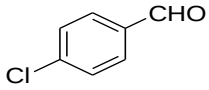	**208**	**220**	88	77 (*S*)
4	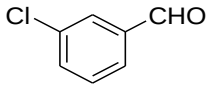	**209**	**221**	80	71 (*S*)
5	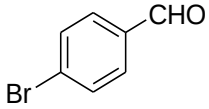	**210**	**222**	95	80 (*S*)
6	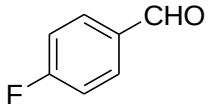	**211**	**223**	67	78 (*S*)
7	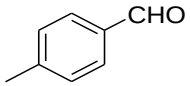	**212**	**224**	83	74 (*S*)
8	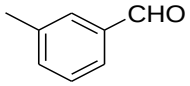	**213**	**225**	61	71 (*S*)
9	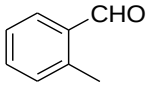	**214**	**226**	96	78 (*S*)
10	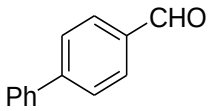	**215**	**227**	93	68 (*S*)
11	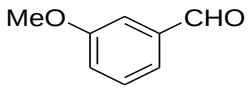	**216**	**228**	80	64 (*S*)
12	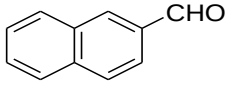	**217**	**229**	93	78 (*S*)

13	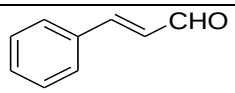	**218**	**230**	76	61 (*S*)

[a]: All the reactions were performed on a 0.2 mmol scale of aromatic aldehyde in the presence of THIQ **206a** (10 mol%) and $Cu(OAc)_2.H_2O$ (10 mol%) using $MeNO_2$ **200** (10.0 equiv.) in the EtOH (2 mL)
[b]: Isolated yields
[c]: Measured by HPLC

4. Conclusion

In conclusion, we have successfully established a direct, modular and high yielding diastereoselective synthesis of highly functionalized oxazolidinones **189a-h** and C_2-symmetric bisoxazolidinones **187a,b,d** using simple H_2SO_4-catalyzed Pictet-Spengler cyclization. Hydrolysis of these oxazolidinones and bisoxazolidinones gave a new family of chiral bi-, tridentate THIQs **190a,b,d-h** and **193**; and tetradentate C_2-BIQs **188a,b,d** in excellent yields.

Application of the THIQs **190a,b,d-h** and **193** and C_2-BIQs **188a,b,d** together with their *N*-methylated derivatives THIQs **202a,b,d-h, 203, 204** and C*2*-BIQs **205b,d** as chiral ligands in enantioselective Cu(II)-catalyzed Henry reactions have been examined. The results indicated strong dependence of the enantioselectivity on the nature of *C*1-substituent of THIQs and C_2-BIQs. After optimization, the *O*-silylated THIQ **206a** was found to be the optimal ligand. *O*-silylated THIQ **206a** complex with $Cu(OAc)_2 \cdot H_2O$ catalyzed a broad range of aromatic aldehydes to give the corresponding β-nitroalcohols in good yields and *ee* up to 80%.

Chapter VI: Future Works

1. Enzymatic desymmetrization of 1,3-diols using lipases immobilized on magnetic nanoparticles

With the successful use of lipase for the desymmetrization of 1,3-diols and 1,3-diaceatate, we envisage an immobilized system of lipase on magnetic nanoparticles in an effort to make it heterogeneous reaction for obvious purification and recycling advantages.[199] With the high surface to volume ratio, magnetic nanoparticles are attractive candidates for the highly active and recyclable catalytic systems.[200]

Immobilization of lipase on magnetic nanoparticles[201] can be achieved through crosslinking with glutaraldehyde or epichlorohydrin on chitosan. This system has found applications in kinetic resolution of secondary alcohols[202] and in biodiesel production.[202c, 203] To the best of our knowledge, application of immobilized lipase for desymmetrization of 1,3-diol has not been well investigated.

Therefore, we propose to establish an efficient protocol for immobilization of lipase AK through covalent attachment on amino-silane coated ferromagnetic nanoparticles. The general synthetic route is outlined in scheme 64. This immobilized lipase system will then be examined for catalytic activity in the desymmetrization of 1,3-diol **43** and other 1,3-diol derivatives. The recovery and recycalibity of the immobilized lipase system should also be examined.

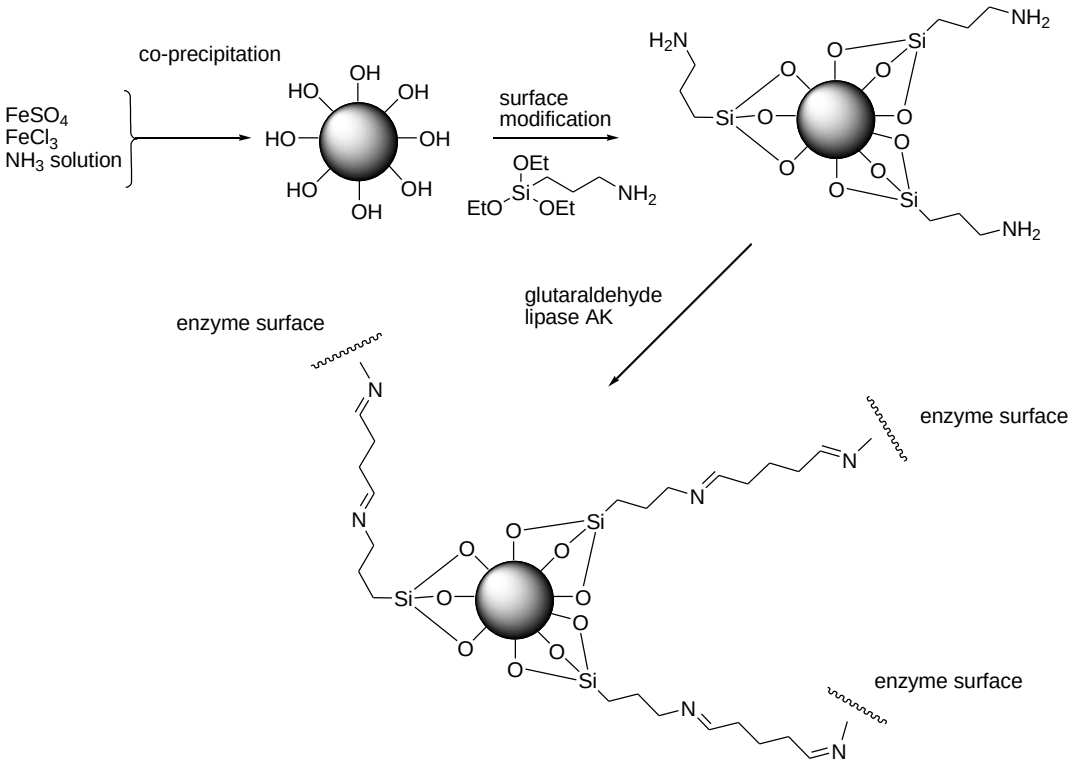

Scheme 64: Strategy for the immobilization of lipase AK on ferromagnetic nanoparticles

2. Further application of THIQs as chiral ligand and chiral catalyst in asymmetric reactions.

We envisage that the application of these THIQs and C_2-BIQs above as chiral ligand is not limited to Henry reaction. These THIQs and C_2-BIQs can potentially find their niche in many other types of asymmetric reactions such as transfer hydrogenation,[162d, 171] aluminum- and borane-mediated reductions,[77h, 172] alkynylations.[173]

In addition, the nature of cyclic secondary amine such as in THIQs **190a,b,d-h** together with their tunable steric directing group at *C*1 as well as *O*-silylether group at C3 make them potential organocatalysts in many asymmetric reactions involved *N*-iminium activation.[204] Therefore, the prospects of these newly

synthesized THIQs and C_2-BIQs in asymmetric catalysis are clearly very promising.

Chapter VII: Experimental procedures

All commercial materials used in the whole project were obtained from Sigma-Aldrich, Merck, Alfa Aesar, Acros and Fisher Scientific, and were used as received unless otherwise indicated. The anhydrous solvents including PhMe, THF and Et_2O were freshly taken from PURE SOLV PS-400-5-MD system. Anhydrous CH_2Cl_2 was distilled using calcium hydride.

Analytical thin layer chromatography (TLC) was performed using Merck 60 F_{254} precoated silica gel plate (0.2 mm thickness) and visualized using UV radiation (254 nm) or by using $KMnO_4$ staining solution. Flash chromatography and column chromatography for purification of compounds were performed using Merck silica gel 60 (230-400 mesh)

FTIR spectra were recorded in KBr thin film on Perkin-Elmer FTIR system Spectrum BS spectrometer. Melting points were tested by Buchi Melting Point-B450. The optical rotation values were measured on JASCO P-1020 polarimeter. X-ray single crystal diffraction data were measured on Bruker-AXS Smart Apex CCD single-crystal diffractometer. LC-Mass spectra were recorded on Agilent LC system with Agilent Mass selective detector. High resolution mass spectra were recorded on Finigan MAT 95*P spectrometer. HPLC was performed on Agilent 1100 using Diacel chiralcel OD-H, OJ-H, and chiralpak AD-H chiral columns.

^1H NMR spectra were recorded at 300 MHz on a Bruker Advanced DPX 300. 1H NMR multiplicities were assigned as singlet (s), doublet (d), triplet (t), triplet of doublet (td), doublet of doublet (dd), quartet (q), multiplet (m), and broad (br). ^{13}C NMR spectra were recorded at 75.47 MHz on a Bruker

Advanced DPX 300. Unless stated, all the experiments were run in $CDCl_3$ solvent with the TMS as internal reference.

Chapter II

*Synthesis of carboxylic acid **42*** (Scheme 12):

dihydro-3*H*-pyran-2,6-dione 62[64]

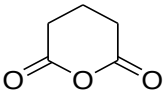

62

A solution of glutaric acid **61** (2 g, 15.1 mmol) in Ac_2O (3.16 mL, 44.3 mmol) was refluxed for 2 h. Acetic anhydride was then removed by distillation (oil bath temperature 140 °C, vacuum) to give an oily residue which was recrystallized from 220 mL of a 1:1 mixture of hexane and Et_2O. Glutaric anhydride **62** was separated from the filtrate by suction filtration. The remaining filtrate was evaporated to 1/3 of its initial volume and cooled down to 0 °C. The resulting precipitate was filtrated by suction filtration to give a total amount of 1.31 g, 95% yield glutaric anhydride **161** (95 %). ^{1}H NMR δ: 1.82-2.19 (m, 2H), 2.75 (t, J=6.7 Hz, 4H). ^{13}C NMR δ: 15.1, 30.0, 168.8. The spectroscopic data was matched with literature values.[64]

5-(benzylamino)-5-oxopentanoic acid 42[66]

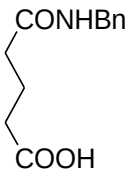

42

To a solution of glutaric anhydride **62** (1.30 g, 11.4 mmol) in CH_2Cl_2 (25 mL) was added drop-wise $BnNH_2$ **11** (1.22 g, 11.4 mmol). The mixture was stirred at room temperature for 15 min after which colorless precipitates were formed. The solvent was removed under reduced pressure. The colorless solid residue was recrystallized from 20 mL distilled water, which was filtrated to obtain 2.34 g of acid **90** as the main product in 94% yield. ^{1}H NMR δ: 1.99 (q, *J*= 7.2 Hz, 2H), 2.31 (t, *J*= 7.2 Hz, 2H), 2.43 (t, *J*= 7.2 Hz, 2H), 4.43 (d, *J*= 5.7 Hz, 2H), 5.98 (brs, 1H, N*H*), 7.25-7.36 (m, 5H), *a resonance attributable to O*H *was not*

observed.^{13}C NMR δ: 20.7), 33.0, 35.2, 43.7, 127.6, 127.8, 128.8, 138.0, 172.4, 177.4. The spectroscopic data was matched with literature values. [66]

*Synthesis of oxazolidinone **46*** (Scheme 13)

(*S*)-2-amino-3-phenylpropan-1-ol 65[67-68]

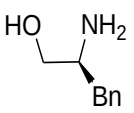

65

To a suspension of *L*-phenylalanine methyl ester hydrochloride **64** (10 g, 46.4 mmol) in MeOH (15 mL) at 0 °C was added drop-wise Et_3N (7.80 mL, 56 mmol) followed by the addition of Et_2O (150 mL) and stirred for 1 h. The reaction mixture was then filtrated and concentrated under reduced pressure. The oily residue was dissolved in MeOH (100 mL) at 0 °C followed by portion-wise addition of $NaBH_4$ (4.65 g, 123 mmol) and stirred for 15 h at room temperature. The mixture was then quenched with DI H_2O (100 mL) and was evaporated to remove MeOH. The resulting aqueous phase was extracted with EtOAc (4 x 100 mL). The combined organic phase was dried over $MgSO_4$, filtrated and concentrated under reduced pressure to give 6.3 g of *L*-phenylalaninol **65** as white solid, yield 90 %. ^{1}H NMR δ: 2.48-2.56 (m, 1H), 2.73-2.78 (m, 1H), 3.10-3.16 (m, 1H), 3.36-3.42 (m, 1H), 3.61-3.66 (m, 1H), 7.17-7.33 (m, 5H). The spectroscopic data was matched with literature values. [67-68]

(*S*)-4-benzyloxazolidin-2-one 46[69, 205]

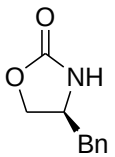

46

To a solution of *L*-phenylalaninol **64** (5 g, 33 mmol) in CH_2Cl_2 (70 mL) was added Et_3N (10 mL, 72 mmol) at ice-bath temperature. A solution of triphosgene **66** (3.43 g, 11.6 mmol) in CH_2Cl_2 (20 mL) was then added drop-wise to the above solution for approximately 30

mins at the same temperature. After 15 h, the reaction mixture was evaporated to remove CH_2Cl_2 followed by the addition of DI H_2O (30 mL) and MeOH (15 mL). The resulting suspension was stirred for 30 min followed by concentration under reduced pressure. Additional DI H_2O (50 mL) was then added and the mixture was stirred for several mins. The resulting white precipitate was filtrated, washed with aqueous 1N HCl solution and with water to give 5.2 g of oxazolidinone **46** as white crystals, yield 89%. ^{1}H NMR δ: 2.82-2.94 (m, 2H), 4.05-4.17 (m, 2H), 4.41-4.46 (m, 1H), 5.86 (br s, 1H, N*H*), 7.17-7.37 (m, 5H). ^{13}C NMR δ: 41.3, 53.8, 69.6, 127.18, 128.9, 129.1, 136.0, 159.8. The spectroscopic data was matched with literature values.[69, 205]

*Synthesis of oxazolidinone **57*** (Scheme 17)

(*S*)-*N*-benzyl-5-(4-benzyl-2-oxooxazolidin-3-yl)-5-oxopentanamide 57

To a solution of carboxylic acid **42** (300 mg, 1.36 mmol) in anhydrous THF (3.7 mL) in a flame-dried Schlenk tube at -50 °C was added

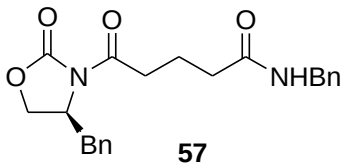

57

Et_3N (151 mg, 1.50 mmol) followed by the drop-wise addition of PivCl (170 µL, 1.36 mmol). The resulting mixture was stirred for 1 h while being slowly cooled down to 0 °C. In a separate flask, a solution of oxazolidinone **46** (241 mg, 1.36 mmol) in anhydrous THF (3 mL) at -50 °C was added drop-wise a solution of *n*-BuLi (0.85 mL, 1.36 mmol, 1.60 M). After being stirred for 15 mins, the resulting mixture was allowed to warm to rt and to stir for additional 45 mins and then cooled down to -50 ^{o}C again. The resulting yellow suspension was then transferred to , the mixture was added to the mixture of **90** via cannula at -50 °C. The reaction was stirred for 15 min then warmed to 0 °C

and stirred for 1 h. DI H_2O (3 mL) was added and the aqueous layer was extracted with EtOAc (3 x 10 mL). The combined organic phase was washed with brine, dried over $MgSO_4$ and concentrated under reduced pressure to yield the crude product as yellow oil which was purified by column chromatography (EtOAc: hexane, 1:1 v/v) to obtain 425 mg of oxazolidinone **57** as white solid, yield 82%, mp: 81-83 ^oC. $[\alpha]_D^{23} = +50$ (*c*, 1.0, CH_2Cl_2). FTIR (KBr) ν_{max}: 1790, 1699, 1643, 1550, 1395, 1198, 702, 504. ^1H NMR δ: 2.03-2.12 (m, 2H), 2.31-2.36 (t, *J*= 7.2 Hz, 2H), 2.71-2.79 (dd, *J*= 13.5, 9.75 Hz, 1H), 2.97-3.03 (m, 2H), 3.25-3.31 (dd, *J*= 13.5, 3.3 Hz, 2H), 4.13-4.23 (m, 2H), 4.44-4.46 (d, *J*= 6 Hz, 2H), 4.61-4.69 (m, 1H), 5.90 (br s, 1H, N*H*), 7.18-7.37 (m, 10H).^{13}C NMR δ: 20.2, 34.9, 35.5, 37.9, 43.7, 55.2, 66.3, 127.4, 127.5, 127.9, 128.8, 129.0, 129.4, 135.2, 138.3, 153.5, 172.0, 172.6. HRMS (ESI-positive mode): *m/z* calcd. for $C_{22}H_{24}N_2O_4$ 380.1736; found 403.1628 $[M+Na]^+$.

*Unsucessful diastereoselective aldol reaction between oxazolidinone **57** and 1,3,5-trioxane **58*** (Scheme 18):

To a solution of oxazolidinone **57** (380 mg, 1 mmol) in anhydrous CH_2Cl_2 (10 mL) under inert condition at 0^oC was added drop-wise the solution of $TiCl_4$ 1M in CH_2Cl_2 (1.1 mL, 1.1 mmol). After that, the resulting yellow suspension was stirred for 5 min at 0 °C followed by the addition of Et_3N (150 µL, 1.1 mmol) to furnish a dark red solution which turned to brown after stirring for 1 h at 0 °C. A solution of 1,3,5-trioxane **58** (100 mg, 1.1 mmol) in anhydrous CH_2Cl_2 (1 mL) was then added, followed by $TiCl_4$ (1.1 mL, 1.1 mmol). After stirring for 5 h at 0 °C, the reaction was quenched with saturated NH_4Cl solution (40 mL). The organic layer was separated and the aqueous layer was extracted

with CH_2Cl_2 (3 x 45 mL). The combined organic phase was washed with sat. $NaHCO_3$ solution, then wash with brine, and dried over $MgSO_4$, filtrated and concentrated under reduced pressure to give a brown oil which was purified by column chromatography (Hex:EA, 7: 3) to obtain oxazolidinone **46** (23% yield), cyclic imide 67 (91% yield), tricyclic oxazolidinone **69** (52% yield).

1-benzylpiperidine-2,6-dione 67[206]

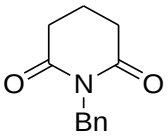

67

The cyclic imide **67** as yellow oil was formed in the experiment above. ^{1}H NMR δ: 2.40 (q, *J*= 6.5 Hz, 2H), 2.69 (t, J=6.5 Hz, 4H), 4.95 (s, 2H), 7.32-7.35 (m, 5H). ^{13}C NMR δ: 17.0, 32.8, 42.6, 127.4, 128.3, 128.8, 136.8, 173.5. The spectroscopic data was matched with literature value.[206]

(*S*)-10,10a-dihydro-1*H*-oxazolo[3,4-b]isoquinolin-3(5*H*)-one 69[74a]

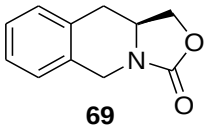

69

The compound **69** as white crystal was formed in the experiment above. ^{1}H NMR δ: 2.86 (dd, *J*= 10.8, 15.3 Hz, 1H), 2.94 (dd, *J*= 4.4, 15.3 Hz, 1H), 3.93-4.00 (m, 1H), 4.14 (dd, *J*= 5.1, 8.5 Hz, 1H), 4.37 (d, *J*= 16.7 Hz, 1H), 4.58 (t, *J*= 8.5 Hz, 1H), 4.82 (d, *J*= 16.7 Hz, 1H), 7.13-7.27 (m, 4H). ^{13}C NMR δ: 34.0, 43.0, 51.1, 68.4, 126.4, 126.8, 127.0, 129.4, 131.4, 131.6, 157.3. The spectroscopic data was matched with literature value.[74a]

*Synthesis of oxazolidinone **80** (Scheme 25, method C)*

(*S*)-methyl 5-(4-benzyl-2-oxooxazolidin-3-yl)-5-oxopentanoate 80

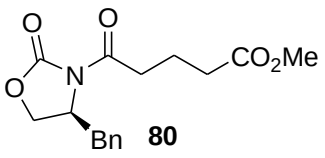

80

To a solution of mono-methyl glutarate **84** (3.9 mL, 31. mmol) in THF (50 mL) at 0 ^{o}C was added Et_3N (8 mL, 57.6 mmol) followed by PivCl (3.8 mL, 31 mmol) and was stirred for 1 h. LiCl (1.12 g, 26.3 mmol) was then added to the reaction mixture followed by oxazolidinone **46** (3.9 g, 22.1 mmol) and the reaction was stirred for 12 h. After the reaction completion, the reaction was quenched with 0.1N HCl (50 mL) solution and was concentrated under reduced pressure. The aqueous phase was extracted with CH_2Cl_2 (20 mL x 3). The combined organic phase was washed with brine, dried over $MgSO_4$, filtrated and evaporated. The oily crude residue was purified by column chromatography (Hex:EA = 3 : 1) to obtain 7.4 g of oxaozolidinone **80** as white solid, yield 85%, mp 71 ^{o}C. $[\alpha]_D^{23} = +51$ (*c*, 1.0, $CHCl_3$). FTIR (KBr) ν_{max}: 1770, 1727, 1693, 1402, 1219, 764 cm^{-1}. ^{1}H NMR δ: 2.00-2.10 (q, *J*= 7.2 Hz, 2H), 2.43-2.48 (t, *J* = 7.2 Hz, 2H), 2.75-2.83 (dd, *J*= 9.9, 13.5 Hz, 1H), 2.93-3.11 (m, 2H), 3.29-3.35 (dd, *J*= 3.9, 13.5 Hz, 1H), 3.71 (s, 3H), 4.16-4.26 (m, 2H), 4.65-4.72 (m, 1H), 7.21-7.38 (m, 5H). ^{13}C NMR δ: 19.4, 33.0, 34.7, 37.9, 51.6, 55.2, 66.3, 127.4, 129.0, 129.4, 135.3, 153.5, 172.5, 173.4. HRMS (ESI, positive mode): $C_{16}H_{19}NO_5$ calculated 305.1263, found 328.1225 $[M+Na]^+$. The spectroscopic data was matched with literature value.[78a]

*Diastereoselective aldol reaction between oxazolidinone **80** and 1,3,5-trioxane **58*** (Scheme 26):

To a solution of oxazolidinone **80** (2 g, 6.55 mmol) in anhydrous CH_2Cl_2 (65 mL) under inert condition at 0^oC was added drop-wise the solution of $TiCl_4$ 1M in CH_2Cl_2 (7.3 mL, 7.3 mmol). After that, the resulting yellow suspension was stirred for 5 min at 0 °C followed by the addition of Et_3N (1.2 mL, 7.3 mmol) to furnish a dark red solution which was stirred for 1 h at 0 °C. A solution of 1,3,5-trioxane **58** (650 mg, 7.255 mmol) in anhydrous CH_2Cl_2 (1 mL) was then added, followed by $TiCl_4$ (7.3 mL, 7.3 mmol). After stirring for 5 h at 0 °C, the reaction was quenched with saturated NH_4Cl solution (40 mL). The organic layer was separated and the aqueous layer was extracted with CH_2Cl_2 (3 x 45 mL). The combined organic phase was washed with sat. $NaHCO_3$ solution, then wash with brine, and dried over $MgSO_4$, filtrated and concentrated under reduced pressure to give a brown oil which was purified by column chromatography (EtOAc: henxae, 7: 3 v/v) to obtain 1.58 g of aldol adduct **81** as wet yellow solid, yield 63%, and 180 mg of lactone **85** as a viscous gum, yield 9%. The compound was slowly decomposed despite being kept in closed atmosphere at low temperature.

(*R*)-methyl 5-((*S*)-4-benzyl-2-oxooxazolidin-3-yl)-4-(hydroxymethyl)-5-oxopentanoate 81

$[\alpha]_D^{21} + 113$ (c, 0.43, $CHCl_3$). FT-IR (KBr) ν_{max}: 1785, 1742, 1704, 1398, 1225, 1118, 1056, 706 cm^{-1}. ^1H NMR δ: 1.79-1.89 (m, 1H), 1.91-2.03 (m, 1H), 2.31 (t, *J*= 7.5 Hz, 2H), 2.71 (dd, *J*= 9.5, 13.2 Hz, 1H), 3.19 (dd, *J*= 3, 13.2 Hz,

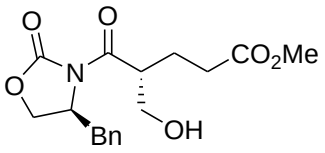

81

1H), 3.58 (s, 3H), 3.78 (d, *J*= 7.8 Hz, 2H), 3.89-3.92 (m, 1H), 4.12-4.20 (m, 2H), 4.56-4.67 (m, 1H), 7.14-7.28 (m, 5H). ^{13}C NMR δ: 24.0, 31.5, 37.8, 42.6, 51.7, 55.3, 66.0, 68.4, 127.3, 128.9, 129.5, 135.3, 153.3, 173.3, 173.9. HRMS (ESI, positive mode): calculated $C_{17}H_{11}NO_6$ 335.1369, found 358.1328 $[M+Na]^+$.

(*S*)-4-benzyl-3-((*R*)-2-oxo-tetrahydro-2*H*-pyran-5-carbonyl)oxazolidin-2-one 85

$[\alpha]_D^{21}$+157 (*c*, 0.6, $CHCl_3$). FT-IR (KBr) ν_{max}: 1782, 1764 1700, 1396, 1220, 1076, 765, 708 cm^{-1}. ^{1}H NMR δ: 2.18-2.25 (m, 2H), 2.55-2.66 (m, 1H), 2.73-2.81 (m, 1H), 2.84-2.88 (m, 1H), 3.25 (d, *J*= 13.2 Hz, 1H), 4.05-4.13 (m, 1H), 4.24-4.32 (m, 2H), 4.52 (d, *J*= 5.7 Hz, 2H), 4.69-4.75 (m, 1H), 7.18-7.37 (m, 5H). ^{13}C NMR δ: 21.4, 28.0, 37.5, 37.7, 55.2, 66.6, 68.6, 127.5, 129.0, 129.4, 134.7, 153.1, 170.9, 171.9. HRMS, calculated $C_{16}H_{17}NO_5$ 303.1107, found 326.1063 $[M+Na]^+$.

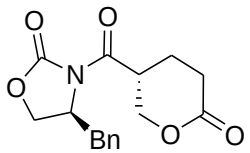

85

*Hydrolysis and bromination of aldol adduct **81** and lactone **85*** (Scheme 29)

(*S*)-5-((*S*)-4-benzyl-2-oxooxazolidin-3-yl)-4-(bromomethyl)-5-oxopentanoic acid 86

To a solution of 8**1** and **85** (1.5 g) in HBr solution (10 mL, 33 wt% in AcOH) was stirred at 40 ^{o}C for 5 h. The mixture was then diluted with excess PhMe followed by evaporation to remove the AcOH. The crude residue was purified by column chromatography (EtOAc: hexane, 1: 1 v/v) to obtain carboxylic acid **86** as the viscous oil (~85% yield). $[\alpha]_D^{21}$+25.6, (*c*, 0.54, $CHCl_3$). FT-IR (KBr)

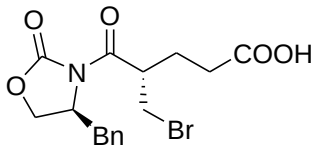

86

ν_{max}: 1781, 1737, 1709, 1395, 1219, 765, 707 cm^{-1}. ^{1}H NMR δ: 1.89-2.05 (m, 1H), 2.13-2.20 (m, 1H), 2.44 (t, J= 6.6 Hz, 2H), 2.78 (dd, *J*= 9.6, 13.5 Hz, 1H), 3.35 (dd, J= 3.3, 13.5 Hz, 1H), 3.58-3.73 (m, 2H), 4.14-4.20 (m, 2H), 4.21-4.31 (m, 1H), 4.70-4.76 (m, 1H), 7.23-7.37 (m, 5H). ^{13}C NMR δ: 25.8, 30.8, 32.4, 37.9, 44.1, 55.4, 66.4, 127.4, 129.0, 129.4, 129.5, 135.1, 153.3, 172.6, 177.9. HRMS (ESI, positive mode): calculated $C_{16}H_{18}BrNO_5$ 383.0368, found 406.0294 $[M+Na]^+$.

(*S*)-*N*-benzyl-5-hydroxy-4-methylpentanamide 88 (Scheme 30)

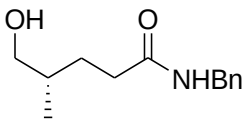

88

To a solution of oxazolidinone acid **86** (1 g, 2.61 mmol) in CH_2Cl_2 (10 mL) at 0 ^oC was added DMF (10 µL, 0.13 mmol) followed by drop-wise addition of $(COCl)_2$ (250 µL, 2.86 mmol) under inert condition. The resulting solution was warmed to rt and stirred for 1 h until the gas evolution ceased. The mixture was concentrated under reduced pressure then redissolved in anhydrous THF (10 mL). The resulting solution was then added drop-wise to the solution of $BnNH_2$ **11** (340 µL, 3.13 mmol) and Et_3N (730 µL, 5.22 mmol) in anhydrous THF (10 mL) at 0 ^oC. The resulting mixture was stirred for additional 15 min then concentrated under reduced pressure to remove THF. The crude residue was redissolved in a biphasic mixture of EtOAc (20 mL) and DI H_2O (20 mL). The two phases were then separated. The aqueous phase was extracted with EtOAc (2 x 15 mL). The combined organic phase was washed with brine, dried over $MgSO_4$, filtrated and evaporated under reduced pressure. The crude residue was redisolved in dry THF (10 mL) and MeOH (1.7 mL, 4.2 mmol). $LiBH_4$ 2M solution in THF (2.2 mL, 4.2 mmol) was then added drop-wise to the reaction mixture at 0 ^oC under inert condition. After stirring for 30 min, the reaction was quenched with

saturated NH_4Cl aq. solution. The biphasic mixture was separated. The aqueous phase was extracted with CH_2Cl_2 (10 mL x 2). The combined organic phase was washed with brine, dried over $MgSO_4$, filtrated and evaporated under reduced pressure. The crude residue was purified by column chromatography (EtOAc: hexane, 1: 2) to give the 378 mg of product **88** as the colorless oil, yield 81%. $\alpha_D^{23} - 5$ (c, 0.14, CH_2Cl_2). FT-IR (KBr) ν_{max}: 3455, 1649, 1555, 1456, 1386 cm^{-1}. ^1H NMR δ: 0.89 (d, *J*= 6.6 Hz, 3H), 1.52-1.59 (m, 1H), 1.62-1.72 (m, 1H), 1.74-1.81 (m, 1H), 2.18-2.34 (m, 2H), 3.35-3.49 (m, 2H), 4.39 (d, *J*= 6.0 Hz, 2H), 7.24-7.35 (m, 5H). ^{13}C NMR δ: 15.6, 27.7, 32.7, 34.3, 42.6, 66.0, 126.4, 126.7, 127.1, 127.6, 127.7, 137.3. HRMS (ESI-positive mode): *m/z* calcd. for $C_{13}H_{19}NO_2$ 221.1416; found 222.1578 $[M+H]^+$, 244.1388 $[M+Na]^+$.

(*S*)-*N*-benzyl-4-(bromomethyl)-5-hydroxypentanamide 89 (Scheme 30)

To a solution of oxazolidinone acid **86** (1 g, 2.61 mmol) in CH_2Cl_2 (10 mL) at 0 ^oC was added DMF (10 µL, 0.13 mmol) followed by drop-wise addition of $(COCl)_2$ (250 µL, 2.86 mmol) under inert condition. The resulting solution was warmed to rt and stirred for 1 h until the gas evolution ceased. The mixture was concentrated under reduced pressure then redissolved in anhydrous THF (10 mL). The resulting solution was then added drop-wise to the solution of $BnNH_2$ **11** (340 µL, 3.13 mmol) and Et_3N (730 µL, 5.22 mmol) in anhydrous THF (10 mL) at 0 ^oC. The resulting mixture was stirred for additional 15 min then concentrated under reduced pressure to remove THF. The crude residue was redissolved in a biphasic mixture of EtOAc (20 mL) and DI H_2O (20 mL). The two phases were then separated. The aqueous phase was extracted with EtOAc (2 x 15 mL). The combined organic phase was washed with brine, dried

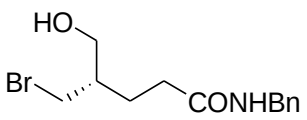

89

over MgSO4, filtrated and evaporated under reduced pressure. The crude residue was redisolved in the mixture of THF/ H_2O (3:1, 10 mL) followed by the slow addition of $NaBH_4$ (155 mg, 4.2 mmol) at 0 ^oC and stirred overnight at room temperature. The reaction was quenched with saturated NH_4Cl aq. followed by extraction with EtOAc (10 mL x 3). The combined organic phase was washed with brine, dried over MgSO4, filtrated and concentrated under reduced pressure. The crude residue was purified by column chromatography (EtOAc: hexane, 2:1) to obtain 320 mg of 89 as the colorless oil, yield 86%. $\alpha_D^{23} = -12$ (c, 0.2, CH_2Cl_2). FT-IR (KBr) ν_{max}: 1638, 1499, 1450, 1381 cm^{-1}. ^1H NMR δ: 1.74-1.90 (m, 3H), 2.24-2.41 (m, 2H), 3.49-3.51 (m, 2H), 3.60-3.70 (m, 2H), 4.44 (d, *J*= 5.7 Hz, 2H), 7.26-7.38 (m, 5H). ^{13}C NMR δ: 24.8, 33.4, 35.6, 42.3, 43.8, 62.8, 127.7, 127.9, 128.8, 138.0, 172.6. HRMS (ESI, positive mode): *m/z* calcd. for $C_{13}H_{18}BrNO_2$ 299.0521, found 301.1310 $[M+2H]^{2+}$.

(***R*)-1-benzyl-4-(hydroxymethyl)piperidin-2-one 1** (Scheme 30)

To a solution of **89** (500 mg, 1.67 mmol) in anhydrous THF (10 mL) was added NaH (167 mg, 4.18 mmol). The mixture was refluxed for 12 h (overnight). After cooling to rt, the reaction mixture was quenched with MeOH at 0 ^oC, and then evaporated under reduced pressure to remove the organic solvent. The residue was diluted with EtOAc and DI H_2O. The aqueous phase extracted with EtOAc (10 mL x 2). The combined organic phase was washed with brine, dried over MgSO4, filtrated and evaporated under reduced pressure. The crude residue was purified by column chromatography (EtOAc: hexane, 1: 1) to give the 282 mg of piperidone **1** as the colorless oil, yield 89%. $\alpha_D^{22} + 43$ (c, 1.0, CH_2Cl_2). ^1H

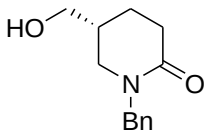

(*R*)-**1**

NMR δ: 1.46-1.52 (m,1H), 1.79-1.89 (m, 1H), 1.90-2.05 (m, 1H), 2.39-2.51 (m, 2H), 2.99 (t, *J*= 11.25 Hz, 1H), 3.27-3.33 (m, 1H), 3.40-3.46 (m, 1H), 3.51-3.56 (m, 1H), 4.56 (q, *J*= 14.7 Hz, 2H), 7.20-7.33 (m, 5H). ^{13}C NMR δ: 23.8, 31.2, 36.4, 49.9, 50.4, 64.3, 127.5, 128.0, 136.9, 170.2. HRMS (ESI, positive mode) *m/z* calcd. for $C_{13}H_{17}NO_2$ 219.1259, found 220.1329 $[M+H]^+$. The spectroscopic data was match with literature value.[18, 44]

Chapter III

Synthesis of 1,3-diol **43** (Scheme 41)

3-*tert*-butyl 1,1-dimethyl propane-1,1,3-tricarboxylate 136To a mixture of NaH (60 % in oil, 1.48 g, 37 mmol) in dry THF (100 mL) was added dimethyl malonate **135** (15.0 g, 114 mmol) at ice-bath temperature under inert condition. The mixture was stirred for 30 min followed by drop-wise addition of *tert*-butyl acrylate **134** (14.56 g, 114 mmol) for 15 min under the same condition. The mixture was gradually warmed to room temperature and stirred for 20 h when TLC showed the complete consumption of the starting materials **134** and **135**. DI H_2O (20 mL) and Et_2O (20 mL) were added successively to the reaction mixture and the biphasic mixture was separated. The aqueous layer was extracted with Et_2O (3 x 20 mL). The combined organic phase was washed with brine (10 mL), dried over $MgSO_4$, filtrated and concentrated under reduced pressure to obtain 26.8 g triester **136** as colourless oil was used for the next step without further purification, yield 91%. ^{1}H NMR δ: 1.45 (s, 9H), 2.13-2.21 (m, 2H), 2.31 (t, *J*= 7.2 Hz, 2H), 3.49 (t, *J*= 7.5 Hz, 1H), 3.75 (s, 6H). ^{13}C NMR δ: 23.9, 27.98, 32.5, 50.4, 52.4, 80.6, 169.4, 171.5. The spectroscopic data was matched with literature value.[207]

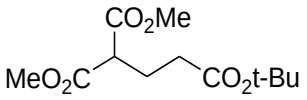

136

5-methoxy-4-(methoxycarbonyl)-5-oxopentanoicacid 137[119a, 120]

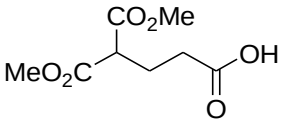

137

To a solution of triester **136** (5 g, 19.21 mmol) in CH_2Cl_2 (100 mL) was added drop-wise TFA (7.4 mL, 96 mmol) at room temperature. The resulting solution was stirred overnight (12 h) when the TLC showed the complete consumption of the starting material. The resulting brown solution was concentrated under reduced pressure to remove CH_2Cl_2. TFA was removed from the reaction mixture by azeotropic distillation with PhMe. The resulting crude was dried *in vacuo* to obtain 3.7 g of brown oil as acid **137**, yield 95%**.** ^{1}H NMR δ: 2.21-2.28 (m, 2H), 2.50 (t, *J*= 7.35 Hz, 2H), 3.53 (t, *J*= 7.35 Hz, 1H), 3.77 (s, 6H). ^{13}C NMR δ: 23.4, 31.1, 50.3, 52.7, 169.3, 178.3. The spectroscopic data was matched with literature value.[120]

dimethyl 2-(3-(benzylamino)-3-oxopropyl)malonate 138

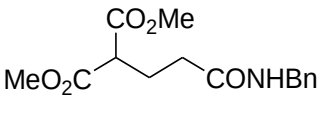

138

To a solution of carboxylic acid **137** (9.75 g, 47.8 mmol) in CH_2Cl_2 (60 mL) and DMF (50 µL) was added drop-wise oxalyl chloride (6.25 mL,71.7 mmol) at 0 ^{o}C under inert condition. After that, the solution was warmed up to room temperature and stirred for 1 h. The solution was evaporated to remove CH_2Cl_2, followed by dilution in THF (50 mL) and Et_3N (13 mL, 95.6 mmol) and cooled down to 0 ^{o}C. A solution of $BnNH_2$ (5.74 mL, 52 mmol) in THF (25 mL) was added drop-wise to the above solution under inert condition. After the addition, the resulting slurry was warmed up to room temperature and stirred for additional 1 h. DI H_2O (50 mL) was then added slowly to the reaction. The biphasic mixture was separated. The aqueous phase was CH_2Cl_2 (40 mL x 3).

The combined organic phase was washed with brine, dried over $MgSO_4$, and concentrated under reduced pressure. The crude residue was purified by column chromatography (EtOAc: hexane, 1:3) to obtain 12.86 g of **138** as light yellow oil, yield 91%. FTIR (KBr) ν_{max}: 1741, 1661, 1556, 1442, 1268, 1035, 699. ^{1}H NMR δ: 2.23-2.35 (m, 4H), 3.53 (t, *J*= 6.75 Hz, 1H), 3.75 (s, 6H), 4.44 (d, *J*= 15 Hz, 2H, d, J= 15 Hz, PhC*H*$_2$NH), 5.83 (br s, 1H), 7.28-7.38 (m, 5H). ^{13}C NMR δ: 24.5, 33.3, 43.5, 50.5, 52.6, 127.4, 127.7, 128.6, 138.3, 169.6, 171.5.HRMS (ESI-positive mode): *m/z* calcd. for $C_{15}H_{19}NO_5$ 293.1263; found 316.1174 $[M+Na]^+$.

_N_-benzyl-5-hydroxy-4-(hydroxymethyl)pentanamide 43

To a solution of amide **138** (5.87 g, 20 mmol) in of anhydrous THF (200 mL) and MeOH (3.8 mL) was added drop-wise a solution of $LiBH_4$ 2M in THF (40 mL, 80 mmol) under inert atmosphere at 0 ^{o}C. After that, the reaction was warmed up to room temperature and stirred for addition 1 h when TLC showed complete consumption of the starting material amide **138**. The reaction was then cooled down to 0 ^{o}C and was quenched by drop-wise addition of saturated aqueous NH_4Cl solution (50 mL). The biphasic mixture was separated. The aqueous phase was extracted with a co-solvent of *i*-PrOH and $CHCl_3$ (1/4, v/v) (100 mL x 3). The combined organic phase was washed with brine, dried over MgSO4, and concentrated under reduced pressure. The crude yellow oil was triturated with pure EtOAc to obtain 4.03 g of 1,3-diol **43** as white solid, yield 85%, mp: 90-91 ^{o}C. FTIR (KBr) ν_{max}: 1646, 1558, 1457, 1265, 1052, 700 cm^{-1}. ^{1}H NMR (300MHz, CD_3OD) δ: 1.56-1.67 (m, 3H), 2.28 (t, *J*= 7.65 Hz, 2H),

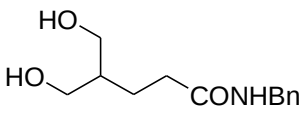

43

3.53 (d, *J*= 5.1 Hz, 4H), 4.32 (s, 2H), 7.16-7.29 (m, 5H). ^{13}C NMR (75 MHz, CD_3OD) δ: 26.9, 36.2, 45.7, 45.8, 64.8, 129.8, 130.1, 131.2, 141.6, 177.6. HRMS (ESI-positive mode): *m/z* calcd. for $C_{13}H_{19}NO_3$ 237.1365; found 260.1261 $[M+Na]^+$.

Synthesis of 1,3-diol **169** (Scheme 48)

***tert*-butyl 5-hydroxy-4-(hydroxymethyl)pentanoate 169**

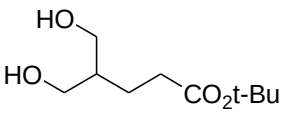

169

To a suspension of $Na(AcO)_3BH$ (340 mg, 1.60 mmol) and $NaBH_4$ (2.38 g, 62.5 mmol) in anhydrous THF (40 mL) was add drop-wise a solution of triester **136** (4.00 g, 15.4 mmol) in anhydrous THF (20 mL) at 35 °C under inert condition. MeOH (10.0 mL, 247 mmol) was then added drop-wise in 4 portions with 15 min interval. The mixture was stirred at 35 °C for 11 h. A solution of HCl 1N (6 mL) was then added and the solution was stirred for 10 min. pH of the mixture was then adjusted to 3 by addition of DI H_2O (30 mL), followed by the addition of EtOAc (50 mL). The biphasic mixture was separated. The aqueous layer was extracted with EtOAc (25 mL x 3). The combined organic phase was washed with brine, dried over $MgSO_4$, filtrated and concentrated under reduced pressure. The oily residue was purified by column chromatography (EtOAc: hexane, 1:1) to 2.44 g of 1,3-diol **169** as colourless oil, yield 78%. FTIR (KBr) ν_{max}: 1731, 1370, 1261, 1159, 1044, 849.^{1}H NMR δ: 1.45 (s, 9H), 1.62-1.75 (m, 3H), 2.29-2.34 (t, *J*= 7.05, 2H), 3.63-3.82 (m, 4H*), a resonance attributable to O<u>H</u> was not observed.* ^{13}C NMR δ: 22.3, 28.1, 33.1, 41.9, 65.2, 80.8, 173.7. HRMS (ESI-positive mode): *m/z* calcd. for $C_{10}H_{20}O_4$ 204.1362; found 227.1261 $[M+Na]^+$.

*Synthesis of Trost ligand **111, 151-154, 158, 160*** (Scheme 44 and scheme 46)

(*S*)-1-ethyl 2-methyl pyrrolidine-1,2-dicarboxylate 150

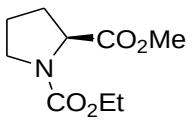

150

To a mixture of *L*-Proline **148** (10 g, 87 mmol) and K_2CO_3 (12 g, 87 mmol) in MeOH (100 mL) at 0 ^oC was added drop-wise $ClCO_2Et$ **149** (19 mL, 200 mmol). The resulting mixture was gradually warmed to rt and stirred for 12 h (overnight). After that, the reaction mixture was filtrated and filtrate was concentrated under reduced pressure, dilute with Et_2O, washed with brine, dried over MgSO4, filtrated and concentrated under reduced pressure. The crude residue was purified by column chromatography (EtOAc: hexane, 1: 4) to obtain 13.7 g of product **150** as the light yellow oil, yield 78%. ^1H NMR δ: 1.24 (t, *J*= 16.5 Hz, 3H) 1.88-2.02 (m, 3H), 2.11-2.23 (m, 1H), 3.42-3.60 (m, 2H), 3.74 (s, 3H), 4.08-4.20 (m, 2H), 4.34 (d, *J*= 15 Hz, 1H). ^{13}C NMR δ: 14.6, 22.5, 28.2, 47.7, 52.0, 59.0, 60.5, 158.2, 171.6. The spectroscopic data was matched with literature value.[129]

*General procedure for the synthesis of (S)-α,α-diarylprolinols **140**, **144-147*** (Scheme 44)

To a solution of **150** (2 g, 10 mmol) in anhydrous THF under inert condition at 0 ^oC was added drop-wise the solution of the corresponding arylmagnesium bromide in THF or Et_2O (3 equiv.). The resulting mixture was gradually warmed to rt and stirred for 4 to 6 h which was monitored by TLC. After that, the reaction was cooled to 0 ^oC and was gradually quenched with saturated NH_4Cl solution. The biphasic mixture was separated. The aqueous phase was extracted with CH_2Cl_2 (40 mL x 3). The combined organic phase was washed with brine, dried over MgSO4, filtrated and evaporated under reduced pressure.

The crude residue was re-dissolved in a mixture of KOH (10 equiv.) in MeOH (50 mL). The resulting solution was refluxed for 12 h (overnight). After that, the mixture was evaporated under reduced pressure and then was diluted in a mixture of CH_2Cl_2 (30 mL) and DI H_2O (30 mL). The biphasic mixture was separated. The aqueous phase was extracted with CH_2Cl_2 (30 mL x 2). The combined organic phase was washed with brine, dried over MgSO4, filtrated and evaporated under reduced pressure. The crude residue was purified by column chromatography (EtOAc: hexane, 1: 1) to obtain the desired prolinol derivatives in good yield after two steps. This procedure was used to synthesize the following compounds:

(*S*)-diphenyl(pyrrolidin-2-yl)methanol 140

L-proline ester **150** was reacted with PhMgBr followed by hydrolysis to give α,α'-diphenylprolinol **140** as white solid after purification by column chromatography (EtOAc: hexane, 1:2 v/v), 1.54 g, 61% yield after two steps. $[\alpha]_D^{22} - 45^o$ (c 1.0, MeOH). ^{1}H NMR δ: 1.41-1.67 (m, 4H), 2.82-2.91 (m, 2H), 4.19 (t, *J*= 7.6 Hz, 1H), 7.08-7.25 (m, 6H), 7.41-7.45 (m, 2H), 7.48-7.52 (m, 2H). ^{13}C NMR δ: 25.6, 26.1, 46.8, 64.4, 77.1, 125.6, 125.9, 126.4, 126.5, 128.1, 128.3, 145.4, 148.1. The spectroscopic data was in accordance with the literature value.[125]

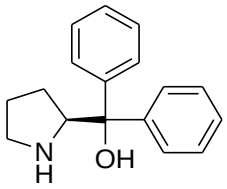

140

(*S*)-dibiphenyl(pyrrolidin-2-yl)methanol 144

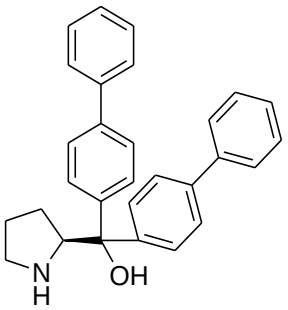

144

L-proline ester **150** was reacted with biphenylmagnesium bromide followed by hydrolysis to give α,α'-di(4-biphenyl)prolinol **144** as white solid after purification by column chromatography (EtOAc: hexane, 1:2 v/v), 1.5 g, 39% after two steps. $[\alpha]_D^{22} - 48^o$ (c 1.0, CH_2Cl_2). ^{1}H NMR δ: 1.60-1.90 (m, 4H), 2.90-3.10 (m, 2H), 4.33 (t, *J*= 7.6 Hz, 1H), 7.22-7.30 (m, 18H). ^{13}C NMR δ: 25.5, 26.4, 46.8, 64.5, 77.4, 125.9, 126.3, 126.8, 127.0, 127.1, 127.2, 128.6, 128.7, 139.2, 139.4, 140.8, 140.9, 144.4, 147.2. The spectroscopic data was in accordance with the literature value.[126]

(*S*)-dinaphthalen-2-yl(pyrrolidin-2-yl)methanol 145

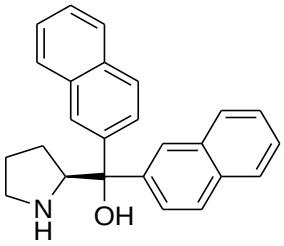

145

L-proline ester **150** was reacted with naphthalylmagnesium bromide followed by hydrolysis to give α,α'-dinaphthylprolinol **145** as white solid after purification by column chromatography (EtOAc: hexane, 1:2 v/v), 1.73 g, 49% after two steps. $[\alpha]_D^{22} - 95^o$ (c 1.0, MeOH). ^{1}H NMR δ: 1.45-1.75 (m, 4H), 2.85-2.98 (m, 2H), 4.5 (t, *J*= 7.4 Hz, 1H), 7.4-7.9 (m, 12H). ^{13}C NMR δ: 25.6, 26.5, 46.9, 64.1, 77.6, 123.8, 124.1, 124.5, 125.3, 125.7, 125.8, 125.9, 126.1, 127.5, 127.7, 128.1, 128.2, 128.3, 132.2, 132.3, 133.2, 133.3, 142.7, 145.4. The spectroscopic data was in accordance with the literature value.[127]

(*S*)-pyrrolidin-2-yldim-tolylmethanol 146

L-proline ester **150** was reacted with *m*-tolylmagnesium bromide followed by hydrolysis to give α,α'-di(3-methylphenyl)prolinol **146** as viscous oil after purification by column chromatography (EtOAc: hexane, 1:2 v/v), 1.4 g, 52% yields after two steps. $[\alpha]_D^{22} - 59^o$ (c, 1.0, $CHCl_3$). ^{1}H NMR δ: 1.48-1.64 (m, 4H), 2.22 (s, 6H), 2.80-2.92 (m, 2H), 4.13 (t, *J*= 7.5 Hz, 1H), 6.87-6.89 (m, 2H), 7.03-7.08 (m, 2H), 7.11-7-31 (m, 4H). ^{13}C NMR δ: 21.6, 21.7, 25.5, 26.2, 46.7, 64.5, 122.5, 126.1, 126.6, 127.0, 127.1, 137.4, 137.7, 145.3, 148.1. The spectroscopic data was in accordance with the literature value.[128]

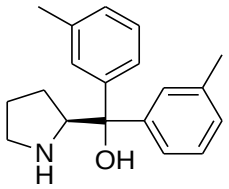

146

(***S*)-bis(3-methoxyphenyl)(pyrrolidin-2-yl)methanol 147**

L-proline ester **150** was reacted with *o*-methoxyphenylmagnesium bromide followed by hydrolysis to give α,α'-di(3-methoxyphenyl)prolinol **147** as viscous oil after purification by column chromatography (EtOAc: hexane, 1:2 v/v), 1.4 g, 46% after two steps. $[\alpha]_D^{22} - 62^o$ (c, 1.0, $CHCl_3$). ^{1}H NMR δ: 1.48-1.63 (m, 4H), 2.75-2.89 (m, 2H), 3.67 (s, 3H), 3.68 (s, 3H), 4.10 (t, *J*= 7.8 Hz, 1H), 6.59-6.63 (m, 2H), 6.95-7.12 (m, 6H). ^{13}C NMR δ: 25.4, 26.2, 46.7, 55.1, 64.6, 76.9, 111.4, 111.5, 112.1, 117.9, 118.0, 128.8, 129.1, 146.9, 149.8, 159.3, 159.5. The spectroscopic data was in accordance with the literature value.[128]

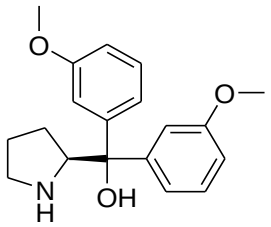

147

*General procedure for synthesis of Trost ligands **111**, **151-154*** (Scheme 44)

To a suspension of the respective α,α'-diarylprolinol (**140**, **144-147**) (2 mmol) and K_2CO_3 (1.1 g, 8 mmol) in dry DMF (5 mL) at 0 ^oC was added dibromide **139** (291 mg, 1 mmol) in one portion. The ice bath was removed and the reaction was stirred at room temperature for 12 – 48 h which was monitored by TLC. After the reaction was completed, the mixture was diluted with DI H_2O (20 mL) and Et_2O (20 mL). The biphasic mixture was separated and the aqueous phase was washed Et_2O (10 mL x 3). The combined organic phase was wash DI H_2O (10 mL x 2), brine, dried over MgSO4, filtrated and evaporated under reduced pressure. The crude residue was purified by column chromatography (EtOAc: hexane, 1: 1) to obtain the product as the crusty foam under vacuum. The procedure was used to synthesize the following compounds:

(*S*,*S*)-2,6-bis[2-(hydroxydiphenylmethyl)-1-pyrrolidinyl-methyl]-4-methylphenol 111

α,α'-diphenylprolinol **140** was reacted with dibromide **139** to give Trost ligand **111** as crusty foam after purification by column chromatography (EtOAc: hexane, 1:2 v/v), 516 mg , 81% yield. $[\alpha]_D^{22} + 49$ (c, 1.0, $CHCl_3$). FTIR (KBr) ν_{max}: 1481, 1449, 911, 875, 749, 705 cm^{-1}. ^1H NMR δ: 1.41-1.79 (m, 8H), 2.06 (s, 3H), 2.30 (q, *J*=12.7 Hz, 2H), 2.63-2.79 (m, 2H), 3.14 (d, *J*= 13.2 Hz, 2H), 3.30 (d, *J*= 13.2 Hz, 2H), 3.87-3.90 (m, 2H), 6.51 (s, 2H), 7.03-7.13 (m, 4H), 7.19-7.25 (m, 8H), 7.48 (d, *J*= 7.2 Hz, 4H), 7.61 (d, *J*= 7.2 Hz, 4H). ^{13}C NMR δ: 20.4, 24.0, 29.6,

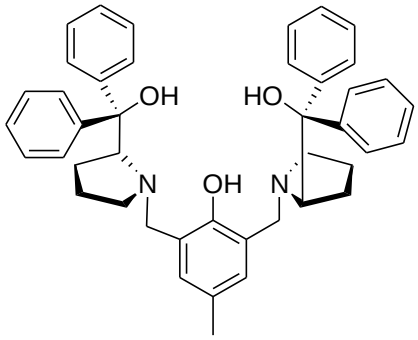

111

55.0, 57.7, 71.4,78.9, 124.0, 125.9,126.0, 126.4, 126.6, 127.1, 128.0, 128.2, 128.8, 146.4, 147.0, 152.6. The spectroscopic data was in accordance with the literature value.[112]

(*S*,*S*)-2,6-bis[2-(hydroxydibiphenylmethyl)-1-pyrrolidinyl-methyl]-4-methylphenol 151

α,α'-di(4-biphenyl)prolinol **144** was reacted with dibromide **139** to give ligand **151** as crusty foam after purification by column chromatography (EtOAc: hexane, 1:2 v/v), 725 mg, 77% yield.

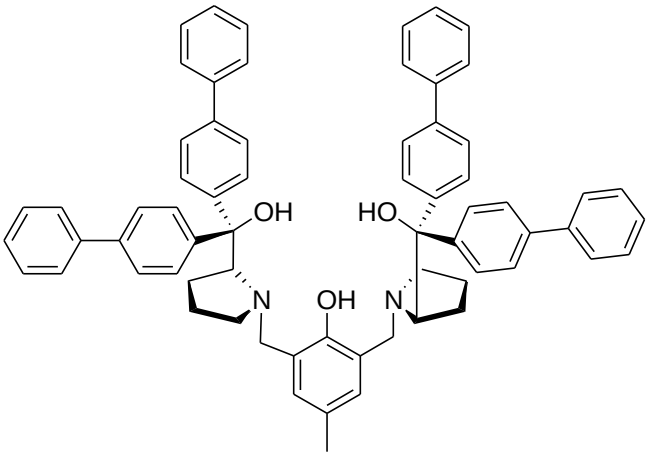

151

$[\alpha]_D^{22} + 85$ (c, 0.6, CH_2Cl_2). FTIR (KBr) ν_{max}: 1601, 1486, 1007, 837, 765, 745, 697 cm^{-1}. ^1H NMR δ: 1.29-1.65 (m, 4H), 1.69-1.82 (m, 2H), 1.87-2.01 (m, 2H), 2.08 (s, 3H), 2.45 (q, *J*= 6.9 Hz, 2H), 3.29 (d, *J*= 12.9 Hz, 2H), 3.64 (d, *J*= 12.9 Hz, 2H), 3.91-4.00 (m, 2H), 6.65 (s, 2H), 7.28-7.47 (m, 14H), 7.55-7.62 (m, 14H), 7.72 (d, *J*= 7.2 Hz, 2H), 7.86 (d, *J*= 7.2 Hz, 2H). ^{13}C NMR δ: 20.4, 23.9, 29.7, 55.0, 57.9, 71.3, 78.7, 124.0, 126.3, 126.4, 126.8, 127.0, 128.6, 128.7, 129.0, 139.2, 139.4, 140.6, 140.8, 145.6, 146.2, 152.8. HRMS (ESI, positive mode): *m/z* calcd. for $C_{67}H_{62}N_2O_3$ 942.4760; found 943.4673 $[M+H]^+$. The spectroscopic data was in accordance with the literature value.[112]

(*S*,*S*)-2,6-bis[2-(hydroxydi-2-naphthylmethyl)-1-pyrrolidinyl-methyl]-4-methylphenol 152

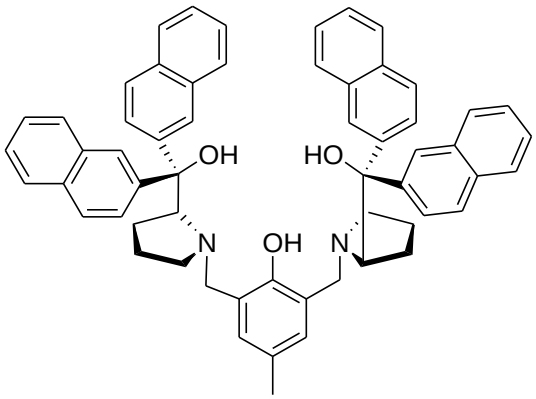

152

α,α'-dinaphthylprolinol **145** was reacted with dibromide **139** to give ligand **152** as crusty foam after purification by column chromatography (EtOAc: hexane, 1:2 v/v), 691 mg, 84% yield. $[\alpha]_D^{22} + 60$ (c, 0.6, CH_2Cl_2). FTIR (KBr) ν_{max}: 2926, 1480, 1360, 1272, 1123, 812, 789, 749, 477 cm^{-1}. ^1H NMR δ: 1.52-1.79 (m, 4H), 1.93-2.20 (m, 8H), 2.15 (s, 3H), 2.43 (q, *J*= 7.8 Hz, 2H), 3.25 (d, *J*= 12.6 Hz, 2H), 3.49 (d, *J*= 12.6 Hz, 2H), 4.17-4.28 (m, 2H), 6.53 (s, 2H), 7.40-7.53 (m, 8H), 7.74-8.05 (m, 16H), 8.23 (s, 1H), 8.51 (s, 1H). ^{13}C NMR δ: 20.2, 24.0, 29.8, 55.1, 57.6, 70.7, 79.2, 123.7, 124.4, 124.5, 124.7, 124.8, 125.7, 125.9, 126.9, 127.3, 127.4, 127.7, 127.8, 127.9, 128.3, 128.4, 128.9, 133.1, 133.2, 143.8, 144.3, 152.8. The spectroscopic data was in accordance with the literature value.[112] HRMS (ESI, positive mode): *m/z* calcd. for $C_{59}H_{54}N_2O_3$ 838.8134; found 839.4086 $[M+H]^+$

(*S*,*S*)-2,6-bis[2-(hydroxydi-*m*-tolylmethyl)-1-pyrrolidinyl-methyl]-4-methylphenol 153

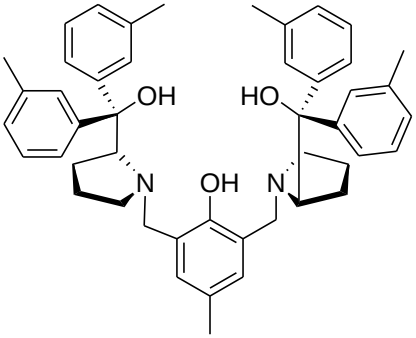

153

α,α'-di(3-methylphenyl)prolinol **146** was reacted with dibromide **139** to give ligand **153** as crusty foam after purification by column chromatography (EtOAc: hexane, 1:2 v/v), 548 mg, 79% yield. $\alpha_D^{22} + 86$ (c, 0.6, CH_2Cl_2). FTIR (KBr) ν_{max}: 2926, 1606, 1483, 1151, 876, 773, 708 cm^{-1}. ^1H NMR δ: 1.51-1.75 (m, 6H), 1.77-1.89 (m, 2H), 1.96-2.10 (m, 2H), 2.17 (s, 3H), 2.31 (s, 6H), 2.40 (s, 6H), 2.82-2.90 (m, 2H), 3.23 (s, 4H), 3.92-3.94 (m, 2H), 6.60 (s, 2H), 6.93 (d, *J*= 7.2 Hz, 2H), 7.02 (d, *J*= 7.2 Hz, 2H), 7.15-7.29 (m, 4H), 7.36-7.45 (m, 6H), 7.55 (s, 2H). ^{13}C NMR δ: 20.4, 21.7, 21.8, 24.1, 29.7, 55.1, 57.3, 71.5, 78.7, 122.8, 123.0, 124.0, 126.4, 126.6, 127.0, 127.1, 127.3, 127.8, 128.0, 128.7, 137.6, 146.3, 147.0, 152.5. HRMS (ESI, positive mode): *m/z* calcd. for $C_{47}H_{54}N_2O_3$ 694.4134; found 695.4180 $[M+H]^+$. The spectroscopic data was in accordance with the literature value.[131]

(*S*,*S*)-2,6-bis[2-(hydroxydi-3-methoxyphenylmethyl)-1-pyrrolidinyl-methyl]-4-methylphenol 154

α,α'-di(3-methoxyphenyl)prolinol **147** was reacted with dibromide **139** to give ligand **154** as crusty foam after purification by column chromatography (EtOAc: hexane, 1:2 v/v), 548 mg, 79% yield. $\alpha_D^{22} + 49$ (*c* , 1.0, CH_2Cl_2). FTIR (KBr) ν_{max}: 1600, 1487, 1255, 1156, 1051, 876, 755 cm^{-1}. ^1H NMR δ: 1.40-1.551 (m, 6H), 1.62-1.84 (m, 2H), 1.85-1.98 (m, 2H), 2.05 (s, 3H), 2.25-2.34 (m, 2H), 2.70-2.79 (m, 2H), 3.12 (d, *J*= 12.9 Hz 2H), 3.26 (d, *J*= 12.9 Hz 2H), 3.67 (s, 6H), 3.68 (s, 6H), 3.78-3.85 (m, 2H), 6.50 (s, 2H), 6.55-6.65 (m, 4H), 7.03-7.17 (m, 10H), 7.24-7.25 (m, 2H). ^{13}C NMR: 20.4, 24.0, 29.7, 55.1, 55.2, 57.4, 71.4, 78.7, 111.5, 111.8, 112.1, 118.3, 118.4, 124.0, 129.0, 129.1, 148.1, 1488, 152.7, 159.3, 159.5. HRMS (ESI, positive mode): *m/z* calcd. for $C_{47}H_{54}N_2O_7$ 758.3931; found 759.3950 $[M+H]^+$.

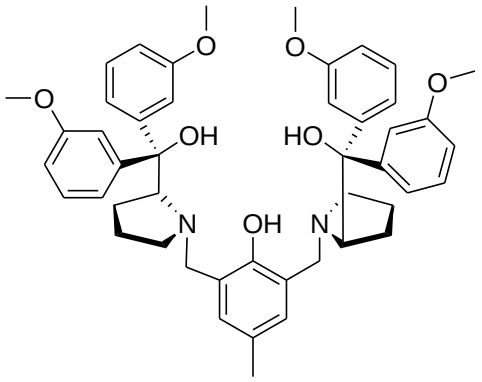

154

*General procedure for synthesis of Trost ligands **158**, **160*** (Scheme 46)

To a suspension of α,α'-diphenylprolinol **140** (2 mmol) and K_2CO_3 (1.1 g, 8 mmol) in dry DMF (5 mL) at 0 ^oC was added dibromide (**155** or **159**) (1 mmol) in one portion. The ice bath was removed and the reaction was stirred at room temperature for 12 – 48 h which was monitored by TLC. After the reaction was completed, the mixture was diluted with DI H_2O (20 mL) and Et_2O (20 mL). The biphasic mixture was separated and the aqueous phase was washed Et_2O (10 mL x 3). The combined organic phase was wash DI H_2O (10 mL x 2), brine, dried over MgSO4, filtrated and evaporated under reduced pressure. The crude residue was purified by column chromatography (EtOAc: hexane, 1: 1) to obtain the product as the crusty foam under vacuum. The procedure was used to synthesize the following compounds:

(*S*,*S*)-2,6-bis[2-(hydroxydiphenylmethyl)-1-pyrrolidinyl-methyl]-4-*tert*-butylphenol 158

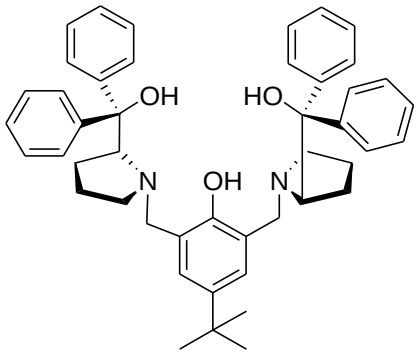

158

α,α'-diphenyl-prolinol **140** was reacted with dibromide **155** to give ligand **158** as crusty foam after purification by column chromatography by column chromatography (EtOAc: hexane, 1:2 v/v), 557 mg, 82% yield. $\alpha_D^{22} + 55$ (c, 1.00, CH_2Cl_2). FTIR (KBr) ν_{max}: 2964, 1485, 1450, 1365, 1308, 1217, 1035, 882, 749, 705 cm^{-1}. ^1H NMR δ: 1.40 (s, 9H), 1.55-1.80 (m, 6H), 1.89-2.00 (m, 2H), 2.06-2.19 (m, 2H), 2.32-2.60 (m, 4H), 2.91-2.89 (m, 2H), 3.42 (d, *J*= 12.6 Hz, 2H), 3.62 (d, *J*= 12.6 Hz, 2H), 4.08-4.17 (m, 2H), 6.96 (s, 2H), 7.26-7.47 (m, 14H), 7.71-7.74

(m, 4H), 7.86-7.89 (m, 4H). 13C NMR δ: 24.1, 29.6, 31.6, 33.8, 55.0, 58.0, 71.3, 78.9, 123.5, 125.3, 125.9, 125.9, 126.4, 126.6, 128.0, 128.2, 140.8, 146.4, 147.0, 152.5. HRMS (ESI, positive mode): *m/z* calcd. for $C_{46}H_{52}N_2O_3$ 680.3978; found 681.3984 $[M+H]^+$. The spectroscopic data was matched with the literature value.[131]

(*S*,*S*)-2,6-bis[2-(hydroxydiphenylmethyl)-1-pyrrolidinyl-methyl]-pyridine 160

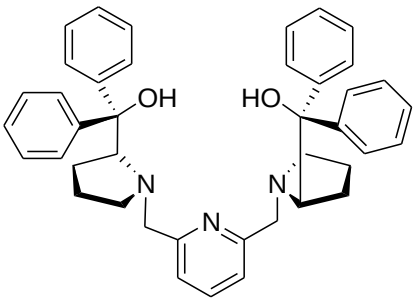

160

α,α'-diphenyl-prolinol **140** was reacted with dibromide **159** to give ligand **160** as white solid after purification by column chromatography (EtOAc: hexane, 1:2 v/v), 396 mg, 65% yield. $[\alpha]_D^{22} + 45$ (c, 0.6, CH_2Cl_2). FTIR (KBr) ν_{max}: 1590, 1450, 1381, 1114, 1034, 874, 748, 706 cm^{-1}. ^1H NMR δ: 1.45-1.71 (m, 6H), 1.81-1.97 (m, 2H), 2.51 (q, *J*= 8.7 Hz, 2H), 2.80-2.90 (m, 2H), 3.34 (q, *J*= 7.2 Hz, 2H), 3.96-4.08 (m, 2H), 5.10 (br s, 1H), 6.88 (d, *J*= 7.5 Hz, 2H), 6.91-7.00 (m, 2H), 7.01-7.24 (m, 10H), 7.59-7.62 (m, 2H), 7.68-7.71 (m, 2H). ^{13}C NMR δ: 24.3, 29.5, 46.3, 46.6, 55.6, 61.7, 70.8, 78.0, 120.8, 121.6, 122.0, 125.5, 125.7, 126.2, 126.3, 126.8, 127.9, 128.0, 137.2, 138.0, 146.3, 147.6, 155.3, 156.2, 159.6. The spectroscopic data was matched with literature value.[133b, 208] HRMS (ESI, positive mode): *m/z* calcd. for $C_{41}H_{43}N_3O_2$ 609.3355; found 610.3481 $[M+H]^+$.

*Synthesis of sulfonamide **119*** (Scheme 47)

(1*R*,2*R*)-*N*,*N*-dimethyl-*N*'-3,5-bis(trifluoromethyl)benzenesulfonyl-1,2-diphenyl-1,2-ethanediamine 119[114, 209]

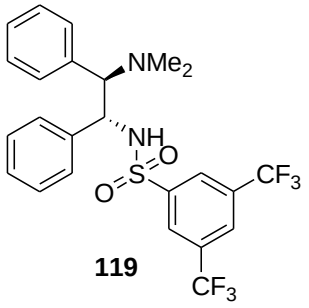

119

The synthesis was proceeded according to the established procedure.[114] To a solution of (*R*,*R*)-diamine **161** and 3,5-bis(trifluoromethyl)benzenesulfonyl chloride **162** (2.5 g, 8.0 mmol) in CH_2Cl_2 (80 mL) was added Et_3N (1.12 mL, 8.0 mmol) at room temperature. The mixture was stirred 30 min and then treated with 1N NaOH aq. (150 mL) followed by extraction with $CHCl_3$, dried over $MgSO_4$, filtrated, and then the filtrate was evaporated under reduced pressure. The residue was dissolved in THF (80 mL). To the solution was added NaH (60% w/w in mineral oil, 800 mg, 20 mmol) and MeI (1.245 mL, 20 mmol) at room temperature. The mixture was refluxed for 1 h and then treated with H_2O followed by extraction with $CHCl_3$. The organic phase was dried over MgSO4, filtrated, and then the filtrate was evaporated in vacuo. The residue was chromatographed on a silica gel column with AcOEt-hexane (1: 3) to afford compound **119** as colorless needles ($CHCl_3$-hexane), 2.8 g, 68% yield. ^{1}H NMR (300 MHz, DMSO-d6) δ: 1.96 (6s, 1H), 1.96 (s, 6H), 3.86 (d, *J*= 11.2 Hz , 1H), 4.95 (d, *J* = 11.2 Hz, 1H), 6.84-6.73 (m, 3H), 7.15-6.93 (m, 7H), 8.05 (s, 2H), 8.20 (s, 1H), 8.61 (br s, 1H). The spectroscopic data was matched with literature value.[114, 209]

*General procedure for acetylation of 1,3-diol **43** catalyzed by metal Lewis acid (using $Yb(OTf)_3$ as the example)* (Table 1)

To a suspension of 1,3-diol **43** (120 mg, 0.5 mmol) in CH_2Cl_2 (10 mL) was added $Yb(OTf)_3$ (15.5 mg, 0.025 mmol) and Ac_2O (240 µL, 2.5 mmol) at room temperature. The mixture was stirred for 1 – 2 which was monitored by TLC. The mixture was evaporated. The crude residue was purified by column chromatography (EtOAc: hexane, 2: 1) to obtain monoacetate **133a** as colorless oil and of diacetate **168** as the colorless oil (See table 1 for the yields obtained).

rac-5-(benzylamino)-2-(hydroxymethyl)-5-oxopentyl acetate 133a

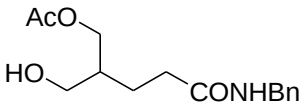

133a

FTIR (KBr) ν_{max}: 1737, 1659, 1556, 1269, 1037, 702 cm^{-1}. ^1H NMR δ: 1.53-1.79 (m, 3H), 1.96 (s, 3H), 2.12-2.32 (m, 2H), 3.45-3.49 (m, 2H), 3.96-4.04 (m, 2H), 4.35 (d, *J*= 5.7 Hz, 2H), 6.17 (br s, 1H), 7.17-7.28 (m, 5H). ^{13}C NMR δ: 20.9, 23.3, 33.6, 40.2, 43.7, 61.7, 64.5, 127.6, 127.8, 128.7, 138.1, 171.6, 173. HRMS (ESI-positive mode): *m/z* calcd. for $C_{15}H_{21}NO_4$ 279.1471; found 302.1373 $[M+Na]^+$. HPLC: Chiralpak AD-H (hexane: iPrOH, 95: 5), 0.9 ml/ min, 254 nm, t_1: 46.3 min, t_2: 49.8 min.

***N*-benzyl-5-acetoxy-4-(acetoxymethyl)pentanamide 168**

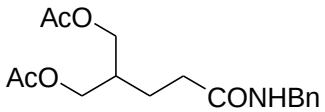

168

FTIR (KBr) ν_{max}: 1741, 1655, 1558, 1248, 1045. ^1H NMR δ: 1.70-1.78 (m, 2H), 1.97-2.08 (m, 1H), 2.04 (s, 6H), 2.27-2.33 (t, *J*= 7.95 Hz, 2H), 4.01-4.11 (m, 4H), 4.41-4.43 (d, *J*= 5.4 Hz, 2H), 6.08 (br s, 1H), 7.26-7.37 (m, 5H). ^{13}C NMR δ: 21.0, 24.4, 33.6, 37.1, 43.8, 63.9, 127.6, 127.8, 128.7, 138.2, 171.2, 172.1.

HRMS (ESI-positive mode): *m/z* calcd. for $C_{17}H_{23}NO_5$ 321.1576; found 344.1481 $[M+Na]^+$.

*General procedure for monoacetylation of diol **43** catalyzed by $Yb(OTf)_3$ in complex with chiral ligands **102, 111, 160-167*** (Table 2)

To a solution of the respective ligand above (0.025 mmol) in CH_2Cl_2 (10 mL) was added $Yb(OTf)_3$ (15.5 mg, 0.025 mmol) at room temperature. The resulting solution was stirred for 1 h followed by the addition of 1,3-diol **43** (120 mg, 0.5 mmol) and Ac_2O (240 µL, 2.5 mmol) at room temperature. The mixture was monitored by TLC. After the completion of the reaction, the mixture was evaporated. The crude residue was purified by column chromatography (EtOAc: hexane, 2: 1) to obtain monoacetate **133a** as colorless oil (See table 2 for the yields obtained).

*General procedure for asymmetric benzoylation of prochiral 1,3-diols **43** and 1,3-diol **169** using Trost catalysts*

To the solution of Trost ligand (**111**, **151-154**, **158**, **160**) (0.05 mmol) in dry PhMe (1.9 mL) was added drop-wise solution of Et_2Zn 1.1 M in PhMe (0.09 mL, 0.1 mmol) under inert condition at room temperature. The mixture was stirred 30 min and then was transferred to the solution of 1,3-diol **43** or **169** (0.5 mmol), vinyl benzoate (350 µL, 2.5 mmol) in dry PhMe (4 mL) under inert condition at room temperature. The reaction mixture was stirred for 12-48 h, followed by the treatment with 5% KH_2PO_4 aq (10 mL) and diluted with Et_2O (20 mL). The biphasic mixture was separated. The aqueous layer was extracted with Et_2O (20 mL x 2). The combined organic phase was washed with water, sat. $NaHCO_3$, brine and dried over $MgSO_4$, filtrated, and evaporated under

reduced pressure. The procedure was only successful give monobenzoate **170b** (See tables 5, 6 and 7 for the yield and *ee* values)

5-*tert*-butoxy-2-(hydroxymethyl)-5-oxopentyl benzoate 170b

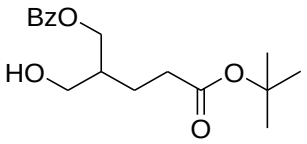

170b

FTIR (KBr) ν_{max}: 3496, 3445, 1725, 1279, 1157, 1129, 715 cm^{-1}. ^{1}H NMR δ: 1.38 (s, 9H), 1.59-1.77 (m, 2H), 1.86-1.94 (m, 1H), 2.24-2.36 (m, 2H), 3.50-3.64 (m, 2H), 4.25-4.39 (m, 2H), 7.35-7.40 (m, 2H), 7.48-7.53 (m, 1H), 7.95-7.98 (2H, m). ^{13}C NMR δ: 22.9, 28.1, 32.9, 40.3, 61.9, 64.7, 80.7, 128.4, 129.6, 123.0, 133.1, 167.0, 173.1. HRMS (ESI-positive mode): *m/z* calcd. for $C_{17}H_{24}O_5$ 308.1264; found 331.1522 $[M+Na]^+$. HPLC: Chiralcel OD-H (exane: *i*-PrOH, 90: 10,, 1.0 ml/ min, 254 nm, t_1: 21.6 min, t_2: 29.8 min.

Chapter IV

*Enantioselective acetylation of 1,3-diol **43** to give (R)-**133a** under optimal condition* (Table 11, entry 4):

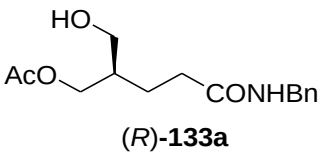

(*R*)-**133a**

To a suspension of 1,3-diol **43** (48 mg, 0.2 mmol) and molecular sieve 4Å (10 mg) in MeCN (3.1 mL) under inert condition at 4 ^{o}C was added lipase AK (30 mg, 150 mg/ mmol). The mixture was stirred for 15 min followed by the addition of vinyl acetate (190 uL, 2 mmol). The reaction was stirred for 4-5 h at 4 ^{o}C which was monitored by TLC. After completion, the reaction was filtrated, evaporated and purified by column chromatography (EtOAc: hexane, 5:1) to obtain (*R*)-**133a** as colorless oil, 52 mg, 93% yield. $[\alpha]_D^{22} - 2.1$ (c, 0.11, CH_2Cl_2). HPLC: Chiralpak AD-H (hexane: iPrOH, 95: 5), 0.9 ml/ min, 254 nm, t_1: 46.3 min, t_2: 49.8 min (92% *ee*).

*Synthesis of diacetate **168** from acetylation of 1,3-diol **43** using lipase AK* (Scheme 53):

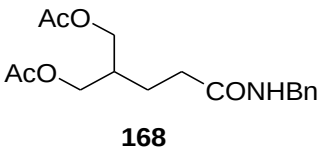

168

To a suspension of 1,3-diol **43** (1.186 g, 5 mmol) in MTBE (30 mL) was added lipase AK (500mg, 100 mg/ mmol). The reaction was stirred for 24 h until all the starting material was converted to diacetate (as shown by TLC). The suspension was filtrated to remove the enzyme. The filtrate was evaporated under reduced pressure. The residue was purified by column chromatography (hexane: EtOAc, 1:1) to give **168** as clear yellow oil, 1.48 g, 92% yield.

*Enantioselective hydrolysis of diacetate **126** under optimal condition* (Table 16, entry 5)

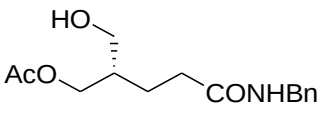

(*S*)-**133a**

To a solution of diacetate **168** (64 mg, 0.2 mmol) in buffer pH 7 (12.5 mL) and THF (1.25 mL) was added lipase AK (90 mg, 450 mg/ mmol) at room temperature. The reaction was stirred for 11 h, followed by extraction with CH_2Cl_2 (10 mL x 3). The organic phase was washed with brine, dried over MgSO4, filtrated and evaporated under reduced pressure. The crude mixture was purified by column chromatography (hexane: EtOAc, 1:1) to obtain (*S*)-**125** as colorless oil, 48 mg, 56% yield. . $[\alpha]_D^{22} + 2.3$ (c, 0.15, CH_2Cl_2). HPLC: Chiralpak AD-H (hexane: iPrOH, 95: 5), 0.9 ml/ min, 254 nm, t_1: 46.3 min, t_2: 49.8 min (95% *ee*)

*Procedure for enzymatic acetylation and tosylation of diol **169** to tosylate **181** under optimal condition* (Table 18, entry 8)

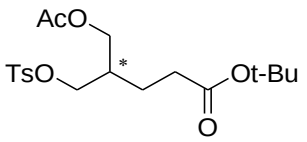

181

To a solution of diol **169** (50 mg, 0.25 mmol) and molecular sieve 4Å (30 mg) in MeCN (3.9 mL) under inert condition at room temperature was added lipase PS (37 mg, 150 mg/ mmol). The mixture was stirred for 30 min at room temperature followed by the addition of vinyl acetate (230 µL, 2.5 mmol). The reaction was then stirred for 4 h at room temperature, filtrated, and evaporated under reduced pressure. The crude mixture was dissolved in CH_2Cl_2 (5 mL), followed by the addition of Et_3N (86 µL, 0.615 mmol), $Me_3N.HCl$ (4.7 mg, 0.049 mmol), and TsCl (117 mg, 0.615 mmol). The reaction was stirred for 12 h (overnight). The mixture was concentrated under reduced pressure and crude

product was chromatographed (Hex: EA = 3:1) to give **181** as colorless oil, 33 mg, 33% yield after two steps. $[\alpha]_D^{22} + 5$ (*c*, 0.13, CH_2Cl_2). FTIR (KBr) ν_{max}: 3435, 1733, 1368, 1234, 1177 cm^{-1}. ^1H NMR δ: 1.43 (s, 9H), 1.58-1.66 (m, 2H), 1.96 (s, 3H), 1.99-2.07 (m, 1H), 2.20-2.25 (t, *J*= 7.8 Hz, 2H), 2.46 (s, 3H), 3.91-4.06 (m, 4H), 7.35 (d, *J* = 8.4 Hz, 2H), 7.79 (d, *J*= 8.4 Hz, 2H). ^{13}C NMR δ: 20.7, 21.7, 23.0, 28.0, 32.5, 36.9, 63.1, 69.3, 80.7, 128.0, 129.9, 132.7, 145.0, 170.7, 172.0. HRMS (ESI, positive mode): *m/z* calcd. for $C_{19}H_{28}O_7S$ 400.1556; found 423.1500 $[M+Na]^+$. HPLC: Chiralcel OJ-H (hexane: iPrOH, 90: 10), 1.0 ml/ min, 254 nm, t_1: 36.8 min, t_2: 44.6 min (72% *ee*).

Chapter V

*General procedure for the Pictet-Spengler cyclization between (S)-4-benzyloxazolidinone **46** and aldehydes **191a-h** using H_2SO_4*: (Table 21, Table 24)

Concentrated H_2SO_4 98% (11.28 mmol, 2 equiv.) was added dropwise to a stirred solution of oxazolidinone **46** (1 g, 5.6 mmol) and aldehyde **191a-h** (11.28 mmol, 2 equiv.) in $CHCl_3$ (10 mL) at room temperature. After reaction completion (TLC), the mixture was diluted with excess water (30 mL), the organic layer was separated and aqueous layer further extracted with CH_2Cl_2 (3 x 10 mL). The combined organic layers were washed with brine, dried over $MgSO_4$ and concentrated under reduced pressure. The crude residue was purified by silica gel column chromatography and recrystallized from CH_2Cl_2/hexane or EtOAc. The general procedure was used to synthesize:

(5*R*,10a*S*)-5-phenyl-10,10a-dihydro-1H-oxazolo[3,4-b]isoquinolinone *trans*-189a

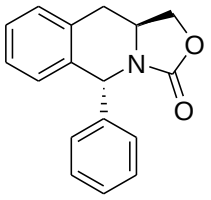

trans-**189a**

Oxazolidinone **46** was reacted with benzaldehyde **191a** and the product was purified by column chromatography (hexane : EtOAc, 3:1 v/v) followed by recrystallization from gradual addition of hexane to saturated solution of *trans*-**189a** in CH_2Cl_2. White crystals, 1.27 g, 85% yield, mp 154-155 ^{o}C. $[\alpha]_D^{22}$ -244 (*c* 1.00, CH_2Cl_2). FTIR (KBr) ν_{max}:, 2913, 1737, 1418, 1264, 1074, 1014, 749, 699, 622, 555 cm^{-1}. ^{1}H NMR δ: 2.99-3.08 (m, 2H), 4.06-4.15 (m, 2H), 4.48 (t, *J*= 8 Hz, 1H), 6.06 (s, 1H), 7.00 (d, *J*= 7.5 Hz, 1H), 7.16-7.36 (m, 8H). ^{13}C NMR δ:

34.3, 48.1, 56.3, 68.5, 126.9, 127.4, 128.0, 128.6, 128.8, 129.3, 132.4, 134.0, 142.1, 156.6. HRMS (ESI-positive mode): *m/z* calcd. for $C_{17}H_{15}NO_2$ 265.1103; found 288.0995 $[M+Na]^+$.

Minor diastereomer *cis*-**189a** was also isolated in approximately 2% yield (30 mg) from the reaction in table 20, entry 4.

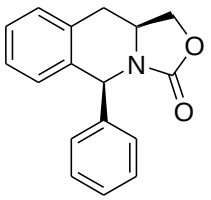

cis-**189a**

^{1}H NMR δ: 3.02-3.19 (m, 2H), 4.08-4.21 (m, 2H), 4.58 (t, *J*= 6.75 Hz, 1H), 5.70 (s, 1H), 7.08-7.34 (m, 9H). ^{13}C NMR δ: 34.4, 54.4, 59.5, 68.5, 127.1, 127.6, 127.6, 128.5, 128.6, 129.1, 131.1, 136.8, 142.5, 156.9. HRMS (ESI-positive mode): *m/z* calcd. for $C_{17}H_{15}NO_2$ 265.1103; found 288.0995 $[M+Na]^+$.

(5*S*,10a*S*)-5-(2-methoxyphenyl)-10,10a-dihydro-1H-oxazolo[3,4-b]isoquinolinone 189b

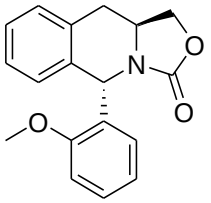

189b

Oxazolidinone **46** was reacted with 2-methoxybenzaldehyde **191b** and the product was purified by column chromatography (hexane: EtOAc, 3:1 v/v) followed by recrystallization from gradual addition of hexane to saturated solution of **189b** in CH_2Cl_2. White crystals, 1.26 g, yield 76%, mp 115 ^{o}C. $[\alpha]_D^{22}$ -255 (*c*, 1.00, CH_2Cl_2). FTIR (KBr) ν_{max}: 2966, 2838, 1756, 1598, 1491, 1404, 1226, 1065, 756, 620 cm^{-1}. ^{1}H NMR δ: 2.98 (d, $J_{H,H}$=7.5 Hz, 2H), 3.73 (s, 3H), 4.10-4.14 (m, 1H), 4.18-4.27 (m, 1H), 4.46 (t, $J_{H,H}$=7.95 Hz, 1H), 6.25 (s, 1H), 6.88-6.93 (m, 3H), 7.06-7.18 (m, 4H), 7.25-7.28 (m, 1H). ^{13}C NMR δ: 34.4, 49.5, 52.8, 55.7, 68.1, 111.7, 120.5, 126.8, 127.6, 129.0, 129.3, 130.5,

130.7, 132.2, 135.4, 156.9, 157.3. HRMS (ESI-positive mode): *m/z* calcd. for $C_{18}H_{17}NO_3$ 295.1208; found 318.1101 $[M+Na]^+$.

(5*S*,10a*S*)-5-(2-nitrophenyl)-10,10a-dihydro-1H-oxazolo[3,4-b]isoquinolinone 189c

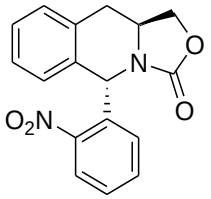

189c

Oxazolidinone **46** was reacted with 2-nitrobenzaldehyde **191c** and the product **189c** was purified by column chromatography (CH_2Cl_2: EtOAc, 99: 1 v/v), followed by recrystallization in EtOAc. White crystals, 1.26 g, yield 72%, mp 230 ^oC. $[\alpha]_D^{23}$ +140 (*c* 1.00, CH_2Cl_2). FTIR (KBr) ν_{max}: 1754, 1741, 1523, 1418, 1348, 1268, 1083, 1016, 968, 856, 752, 740 cm^{-1}. ^1H NMR δ: 2.91-3.12 (m, 2H), 4.14-4.25 (m, 2H), 4.581 (t, *J* =8 Hz, 1H), 6.60 (s, 1H), 7.01 (d, *J*= 7.5Hz, 1H), 7.17-7.29 (m, 4H), 7.42-7.61 (m, 2H), 7.86-7.89 (m, 1H). ^{13}C NMR δ: 34.8, 49.6, 52.1, 68.7, 124.5, 127.5, 127.7, 128.1, 128.8, 129.2, 131.0, 132.4, 132.9, 133.4, 136.5, 157.1. HRMS (ESI-positive mode): *m/z* calcd. for $C_{17}H_{14}N_2O_4$ 310.0954; found 333.0486 $[M+Na]^+$.

(5*R*,10a*S*)-5-(naphthalen-2-yl)-10,10a-dihydro-1H-oxazolo[3,4-b]isoquinolinone 189d

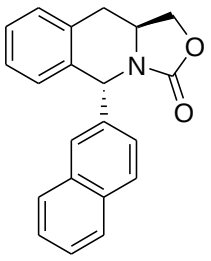

189d

Oxazolidinone **46** was reacted with 2-naphthaldehyde **191d** and the product **189d** was purified by column chromatography (hexane : EtOAc, 3:1 v/v). White crystals, 1.4 g, yield 79%, mp 152-153 ^oC. $[\alpha]_D^{22}$ -242 (*c*, 1.00, CH_2Cl_2). FTIR (KBr) ν_{max}: 3055, 2926, 1740, 1415, 1253, 1071, 797, 747, 480 cm^{-1}. ^1H NMR δ: 2.97-3.12 (m, 2H), 4.08-4.16 (m, 2H),

4.42-4.48 (m, 1H), 6.22 (s, 1H), 7.04 (m, 1H), 7.17-7.31 (m, 3H), 7.39-7.50 (m, 3H), 7.65 (s, 1H), 7.74-7.83 (m, 3H). ^{13}C NMR δ: 34.4, 48.3, 56.5, 68.5, 126.3, 126.4, 127.0, 127.5, 127.6, 127.7, 128.2, 128.7, 128.9, 129.4, 132.5, 132.9, 133.1, 133.9, 139.4, 156.7. HRMS (ESI-positive mode): *m/z* calcd. for $C_{21}H_{17}NO_2$ 315.1259; found 338.1151 $[M+Na]^+$.

(5*R*,10a*S*)-5-propyl-10,10a-dihydro-1H-oxazolo[3,4-b]isoquinolinone 189e

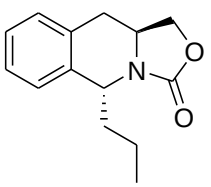

189e

Oxazolidinone **46** was reacted with butyraldehyde **170e** and the product **189e** was purified by column chromatography (hexane : EtOAc, 3:1 v/v). White crystals, 1.2 g, yield 92%, mp 92 ^{o}C. $[\alpha]_D^{22}$ -149 (*c*, 1.00, CH_2Cl_2). FTIR (KBr) ν_{max}: 2938, 1750, 1438, 1427, 1270, 1072, 749 cm^{-1}. ^{1}H NMR δ: 0.98 (t, *J*= 7.4 Hz, 3H), 1.46-1.51 (m, 2H), 1.71-1.89 (m, 2H), 2.9 (d, *J*=7.5 Hz, 2H), 4.04-4.08 (m, 1H), 4.14-4.18 (m, 1H), 4.55 (t, *J*= 8.25 Hz, 1H), 4.89-4.93 (m, 1H), 7.09-7.24 (m, 4H). ^{13}C NMR δ: 13.9, 19.4, 33.9, 39.4, 48.3, 52.6, 68.2, 126.8, 126.9, 127.0, 129.4, 131.4, 136.4, 157.3. HRMS (ESI-positive mode): *m/z* calcd. for $C_{14}H_{17}NO_2$ 231.1259; found 254.1151 $[M+Na]^+$.

(5*R*,10a*S*)-5-isopropyl-10,10a-dihydro-1H-oxazolo[3,4-b]isoquinolinone 189f

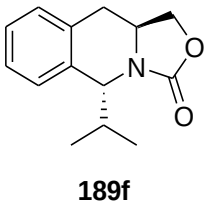

189f

Oxazolidinone **46** was reacted with isobutyraldehyde **191f** and the product **189f** was purified by column chromatography (hexane : EtOAc, 3:1 v/v). White crystals, 1.1 g yield 87%, mp 118 ^{o}C. $[\alpha]_D^{21}$ -152 (*c*, 1.00, CH_2Cl_2). FTIR (KBr) ν_{max}: 2963, 1750, 1412, 1245, 1063, 763 cm^{-1}. ^{1}H NMR δ: 0.78 (d, *J*= 6.9 Hz, 3H),

1.17 (d, *J*= 6.9 Hz, 3H), 2.32-2.42 (m, 1H), 2.9 (d, *J*= 6.9 Hz, 2H), 4.03-4.16 (m, 2H), 4.55 (t, *J*= 8.1, 1H), 4.82 (d, *J*= 3.9 Hz, 1H), 7.10 -7.26 (m, 4H). ^{13}C NMR δ: 17.6, 20.3, 33.7, 35.0, 50.6, 57.9, 67.9, 126.8, 126.9, 129.3, 132.2, 135.2, 158.0. HRMS (ESI-positive mode): *m/z* calcd. for $C_{14}H_{17}NO_2$ 231.1259; found 254.1151 $[M+Na]^+$.

(5*R*,10a*S*)-5-*tert*-butyl-10,10a-dihydro-1H-oxazolo[3,4-b]isoquinolinone 189g

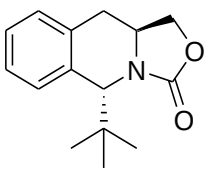

189g

Oxazolidinone **46** was reacted with trimethylacetaldehyde **191g** and the product **189g** was purified by column chromatography (hexane : EtOAc, 4:1 v/v). White crystals, 1.14 g, yield 83%, mp 169 ^{o}C. $[\alpha]_D^{23}$ = -64 (*c* 1.00, CH_2Cl_2). FTIR (KBr) ν_{max}: 2960, 1746, 1424, 1273, 1071, 753 cm^{-1}. ^{1}H NMR δ: 1.05 (s, 9H), 2.78-2.86 (m, 1H), 3.1-3.18 (m, 1H), 3.98-4.03 (m, 1H), 4.44-4.49 (m, 1H), 4.50-4.60 (t, *J*= 8.0 Hz, 1H), 4.65 (s, 1H), 7.10-7.24 (m, 4H). ^{13}C NMR δ: 28.3, 32.7, 38.0, 49.4, 61.3, 69.3, 125.7, 127.3, 128.7, 129.3, 131.9, 134.3, 157.8. HRMS (ESI-positive mode): *m/z* calcd. for $C_{15}H_{19}NO_2$ 245.1416; found 268.1308 $[M+Na]^+$.

(5*R*,10a*S*)-5-cyclohexyl-10,10a-dihydro-1H-oxazolo[3,4-b]isoquinolinone 189h

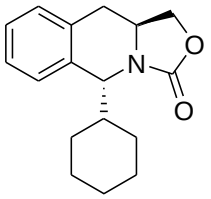

189h

Oxazolidinone **46** was reacted with cyclohexanecarbaldehyde **191h** and the product **189h** was purified by column chromatography (hexane : EtOAc, 3:1). White crystals, 1.27 g, yield 83%, mp 143 ^{o}C. $[\alpha]_D^{22}$ -133 (*c*, 1.00, CH_2Cl_2). FTIR (KBr) ν_{max}: 2934, 2856, 1754, 1420, 1241, 1072, 969, 760 cm^{-1}. ^{1}H NMR δ:

0.96-1.99 (m, 11H), 2.85-2.89 (m, 2H), 4.03-4.15 (m, 2H), 4.60 (t, *J*= 8 Hz, 1H), 4.78 (d, *J*= 3.9 Hz, 1H), 7.09-7.26 (m, 4H). ^{13}C NMR δ: 26.3, 26.4, 26.6, 28.2, 31.0, 33.8, 45.2, 50.5, 57.6, 67.9, 126.8, 127.0, 129.3, 132.3, 134.9, 158.1. HRMS (ESI-positive mode): *m/z* calcd. for $C_{17}H_{21}NO_2$ 271.1572; found 294.1465 $[M+Na]^+$.

(5*S*,10a*S*)-5-(2-aminophenyl)-10,10a-dihydro-1H-oxazolo[3,4-b]isoquinolinone 192

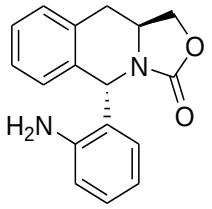

192

To a suspension of **189c** (500 mg, 1.35 mmol) in MeOH (10 mL) was added Pd/C (135 mg, 100 mg of Pd/C for 1 mmol of 2h) and $HCOONH_4$ (510 mg, 8 mmol). The mixture was refluxed for 12 h, then filtered through a pad of Celite. The filtrate was concentrated. The resulting residue was then diluted with DCM (20 mL) and washed with DI H2O (20 mL). The organic layer was separated, washed with brine, dried over MgSO4, filtrated and evaporated. The crude residue was purified by column chromatograpy (EtOAc: hexane, 1:1 v/v) to afford 320 mg of **192**. Off-white solid, yield 95%, mp 201 ^{o}C. $[\alpha]_D^{23} - 98$ (c 1.00, CH_2Cl_2). FTIR (KBr) ν_{max}:1719, 1603, 1493, 1431, 1260, 1082, 756 cm^{-1}. ^{1}H NMR δ: 3.01-3.04 (m, 2H), 4.05-4.08 (m, 1H), 4.14-4.18 (m, 1H), 4.47 (t, *J*= 8 Hz, 1H), 4.70 (s, 2H, NH2), 6.19 (s, 1H), 6.48-6.57 (m, 2H), 6.71-6.74 (m, 1H), 6.98-7.01 (m, 1H), 7.05-7.10 (m, 1H), 7.15-7.25 (m, 3H). ^{13}C NMR δ: 34.0, 47.7, 51.3, 68.9, 116.4, 117.5, 126.3, 127.0, 127.4, 129.0, 129.1, 129.7, 132.4, 134.0, 146.2, 157.7. HRMS (ESI-positive mode): *m/z* calcd. for $C_{17}H_{16}N_2O_2$ 271.1572; found 280.1212; found 303.1117 $[M+Na]^+$.

(5*S*,10a*S*)-5-((5*S*,10a*S*)-3-oxo-3,5,10,10a-tetrahydro-1H-oxazolo[3,4-b]isoquinolin-5-yl)-10,10a-dihydro-1H-oxazolo[3,4-b]isoquinolinone 187a

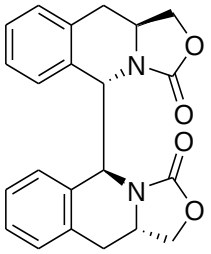

187a

Concentrated H_2SO_4 98% (11.28 mmol, 2 equiv.) was added dropwise to a stirred suspension of oxazolidinone **46** (1 g, 5.64 mmol) and glyoxal trimer dihydrate **194a** (197 mg, 0.167 equiv.) in $CHCl_3$ (10 mL) at room temperature. After reaction completion (TLC), the mixture was diluted with excess water (30 mL), the organic layer was separated and the aqueous layer further extracted with CH_2Cl_2 (3 x 10 mL). The combined organic layers were washed with brine, dried over $MgSO_4$ and concentrated under reduced pressure. Bisoxazoline **187a** was recrystallized by slow addition of EtOAc into hot saturated solution of crude **187a** in CH_2Cl_2. White crystals, 0.87 g, yield 82%, 306 ^{o}C. $[\alpha]_D^{23}$ -103 (*c* 1.00, CH_2Cl_2). FTIR (KBr) ν_{max}: 2959, 1754, 1414, 1229, 1078, 757, 647 cm^{-1}. ^{1}H NMR δ: 2.89-2.97 (m, 2H), 3.19-3.26 (m, 2H), 4.06-4.14 (m, 2H), 4.63-4.69 (m, 4H), 5.00 (s, 2H), 6.35 (d, *J*= 7.8 Hz, 2H), 6.97-7.02 (m, 2H), 7.17-7.27 (m, 4H). ^{13}C NMR δ: 33.4, 48.0, 56.0, 69.5, 125.3, 128.3, 129.5, 130.5, 130.7, 132.5, 157.3. HRMS (ESI-positive mode): *m/z* calcd. for $C_{22}H_{20}N_2O_4$ 376.1423; found 399.1315 $[M+Na]^+$. CCDC-992907 contains the supplementary crystallographic data for this paper. These data can be obtained free of charge from The Cambridge Crystallographic Data Centre via www.ccdc.cam.ac.uk/data_request/cif.

(5*R*,10a*S*)-5-(3-((5*R*,10a*S*)-3-oxo-3,5,10,10a-tetrahydro-1H-oxazolo[3,4-b]isoquinolin-5-yl)phenyl)-10,10a-dihydro-1H-oxazolo[3,4-b]isoquinolinone 187b

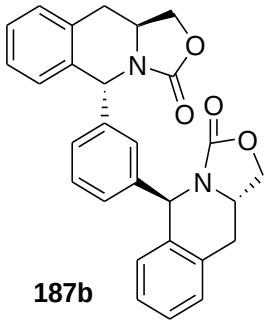

187b

Concentrated H_2SO_4 98% (11.28 mmol, 2 equiv.) was added dropwise to a stirred solution of oxazolidinone **46** (1 g, 5.64 mmol) and isophthalaldehyde **187b** (378 mg, 0.5 equiv.) in $CHCl_3$ (10 mL) at room temperature. After reaction completion (TLC), the mixture was diluted with excess water (30 mL), the organic layer was separated and aqueous layer further extracted with CH_2Cl_2 (3 x 10 mL). The combined organic layers were washed with brine, dried over $MgSO_4$ and concentrated under reduced pressure. Bisoxazoline **187b** was purified by column chromatography (CH_2Cl_2: EtOAc, 99:1 v/v) and recrystallized by slow addition of hexane into hot saturated solution of **187b** in CH_2Cl_2. White crystals, 1.24 g, yield 98%, mp 325 ^oC. $[\alpha]_D^{20}$ -298 (*c*, 1.00, CH_2Cl_2). FTIR (KBr) ν_{max}: 2905, 1751, 1413, 1268, 1060, 1019, 741, 715, 622 cm^{-1}. ^1H NMR δ: 2.80-3.10 (m, 4H), 3.99-4.08 (m, 4H), 4.33-4.39 (m, 2H), 5.83 (s, 2H), 6.84 (d, $J_{H,H}$=7.5 Hz, 2H), 7.05-7.19 (m, 10H). ^{13}C NMR δ: 34.5, 48.2, 56.4, 68.7, 127.0, 127.4, 128.2, 128.7, 128.9, 129.3, 132.4, 134.0, 142.6, 156.6. HRMS (ESI-positive mode): *m/z* calcd. for $C_{28}H_{24}N_2O_4$ 452.1736; found 475.1628 $[M+Na]^+$.

(5*R*,10a*S*)-5-(((5*R*,10a*S*)-7,8-dimethoxy-3-oxo-3,5,10,10a-tetrahydro-1H-oxazolo[3,4-b]isoquinolin-5-yl)methyl)-7,8-dimethoxy-10,10a-dihydro-1H-oxazolo[3,4-b]isoquinolinone 187d

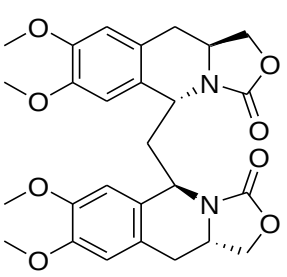

187d

Concentrated H_2SO_4 98% (9 mmol, 2 equiv.) was added dropwise to a stirred solution of oxazolidinone **196** (1 g, 4.52 mmol) and 1,1,3,3-tetraethoxypropane **194c** (540 µL, 0.5 equiv.) in $CHCl_3$ (10 mL) at room temperature. After reaction completion (TLC), the mixture was diluted with excess water (30 mL), the organic layer was separated and the aqueous layer further extracted with CH_2Cl_2 (3 x 10 mL). The combined organic layers were washed with brine, dried over $MgSO_4$ and concentrated under reduced pressure. Bisoxazoline **187d** was recrystallized by slow addition of hexane into hot saturated solution of **187d** in CH_2Cl_2 Light yellow crystal, 1.05 g, yield 98%, mp 324 ^oC. $[\alpha]_D^{20}$ -198 (*c*, 1.00, CH_2Cl_2). FTIR (KBr) ν_{max}: 2945, 2837, 1774, 1521, 1420, 1226, 1111, 988, 756 cm^{-1}. ^1H NMR δ: d, 2.81 (d, *J*= 7.5 Hz, 4H), 3.83 (s, 6H), 3.86 (s, 6H), 4.11-4.12 (m, 4H), 4.50 (t, *J*= 7.7 Hz, 2H), 4.97 (t, *J*= 6.3 Hz, 2H), 6.57 (s, 4H). ^{13}C NMR δ: 32.5, 48.9, 49.8, 55.9, 56.0, 68.5, 109.1, 111.9, 123.9, 127.3, 148.1, 148.3, 157.3. HRMS (ESI-positive mode): *m/z* calcd. for $C_{27}H_{30}N_2O_8$ 510.2002; found 533.1894 $[M+Na]^+$.

(*S*,*E*)-3-(4-benzyl-2-oxooxazolidin-3-yl)acrylaldehyde 195

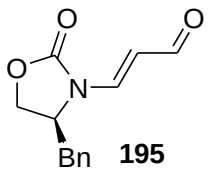

195

Concentrated H_2SO_4 98% (11.28 mmol, 2 equiv.) was added dropwise to a stirred solution of oxazolidinone **46** (1 g, 5.64

mmol) and malionaldehyde **194c** (5.64 mmol, 1 equiv.) in $CHCl_3$ (10 mL) at room temperature. After reaction completion (TLC), the mixture was quenched with saturated $NaHCO_3$ solution, the organic layer was separated and aqueous layer further extracted with CH_2Cl_2 (3 x 10 mL). The combined organic layers were washed with brine, dried over $MgSO_4$ and concentrated under reduced pressure. The product **195** was recrystallized into yellow needles by slow mixing of hexane into saturated solution of the crude residue in CH_2Cl_2. 1.27 g, yield: 99%, mp 90 ^oC. $[\alpha]_D^{23}$ +89 (*c* 1.00, CH_2Cl_2). FTIR (KBr) ν_{max}: 3077, 2930, 2750, 1753, 1675, 1631, 1416, 1142, 761, 707 cm^{-1}. ^1H NMR δ: 2.82-2.86(m, 1H), 3.2 (d, *J*=14 Hz, 1H), 4.35-4.36 (m, 3H), 5.76 (dd, $J_{H,H}$=7.8, 14.7 Hz, 1H), 7.16-7.19 (m, 2H), 7.32-7.37 (m, 3H), 7.73 (d, $J_{H,H}$=14.4 Hz, 1H), 9.51 (d, *J*=7.5 Hz, 1H) . ^{13}C NMR δ: 36.3, 55.0, 67.1, 112.2, 127.9, 129.3, 133.9, 144.8, 154.0, 191.1. HRMS (ESI-positive mode): *m/z* calcd. for $C_{13}H_{13}NO_3$ 231.0895; found 254.0788 $[M+Na]^+$.

*General procedure for hydrolysis of oxazolidinones **189a,b,d-h, 192,** and **187a, b,d***

A suspension of the respective oxazolidinone **189a,b,d-h, 192,** and **187a, b,d** (5 mmol) in MeOH (15 mL) and aqueous NaOH 5N (15 mL) was heated at reflux under strong stirring. The reaction mixture gradually became clear. After reaction completion (TLC), MeOH was evaporated at low pressure and the resulting aqueous mixture was extracted with CH_2Cl_2 (3 x 15 mL). The combined organic layers were washed with brine, dried over $MgSO_4$, filtrated and evaporated under reduced pressure. The crude mixture was purified by

silica gel column chromatography to give the pure products **190a**,**b**,**d-h**,**193** and **188a,b,d**.

((1*R*,3*S*)-1-phenyl-1,2,3,4-tetrahydroisoquinolin-3-yl)methanol 190a

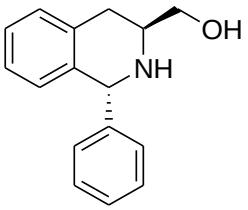

190a

Hydrolysis of oxazolidinone **189a** and purification using column chromatography (EtOAc: hexane, 3: 1 v/v) gave the product **190a** as white solid in 1.11 g, 93% yield, mp 98 ^{o}C . $[\alpha]_D^{22}$ = -20 (*c* 1.00, CH_2Cl_2). FTIR (KBr) ν_{max}: 2828, 1486, 1450, 1260, 1039, 945, 739 cm^{-1}. ^{1}H NMR δ: 2.05 (br s, 2H, NH and OH), 2.59-2.68 (m, 1H), 2.77-2.84 (m, 1H), 3.08-3.16 (m, 1H), 3.42-3.49 (m, 1H), 3.60-3.65 (m, 1H), 5.25 (s, 1H), 6.93 (d, $J_{H,H}$=7.5 Hz, 1H), 7.09-7.31 (m, 8H). ^{13}C NMR δ: 31.0, 48.9, 59.1, 65.7, 125.8, 126.7, 127.1, 128.3, 128.4, 128.7, 129.3, 134.8, 136.6, 144.7. HRMS (ESI-positive mode): *m/z* calcd. for $C_{16}H_{17}NO$ 239.1310; found 240.1383 $[M+H]^+$.

((1*S*,3*S*)-1-(2-methoxyphenyl)-1,2,3,4-tetrahydroisoquinolin-3-yl)methanol 190b

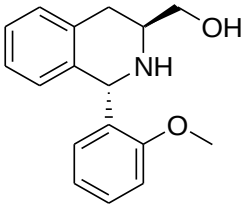

190b

Hydrolysis of oxazolidinone **189b** and purification using column chromatography (pure EtOAc) gave product **190b** as light yellow solid, 1.09 g, yield 81%, mp 134 ^{o}C. $[\alpha]_D^{23}$ = +11.3 (*c* 1.00, CH_2Cl_2). FTIR (KBr) ν_{max}: 2928, 1597, 1486, 1241, 1024, 752, 612 cm^{-1}. ^{1}H NMR δ: 2.05 (br s, 2H, NH and OH), 2.71-2.74 (m, 2H), 3.02-3.05 (m, 1H), 3.46-3.52 (m, 1H), 3.62-3.67 (m, 1H), 3.92 (s, 3H), 5.63 (s, 1H), 6.50-6.53 (m, 1H), 6.73-6.79 (m, 1H), 6.90-6.94 (m, 2H), 7.09-7.13 (m, 1H), 7.18-7.25 (m, 3H). ^{13}C NMR δ: 31.14, 49.1, 53.83,

55.5, 66.1, 110.4, 119.7, 125.6, 126.6, 128.3, 128.4, 129.0, 130.2, 132.6, 135.4, 136.3, 157.2. HRMS (ESI-positive mode): *m/z* calcd. for $C_{17}H_{19}NO_2$ 269.1416; found 270.1489 $[M+H]^+$.

((1*R*,3*S*)-1-(naphthalen-2-yl)-1,2,3,4-tetrahydroisoquinolin-3-yl)methanol 190d

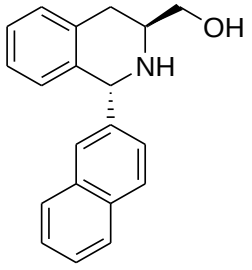

190d

Hydrolysis of oxazolidinone **189d** and purification using column chromatography (EtOAc: hexane, 3: 1 v/v) gave the product **190d** as white solid, 1.33 g, yield 92%, mp 105 ^oC. $[\alpha]_D^{23}$ = -44 (*c* 1.00, CH_2Cl_2). FTIR (KBr) ν_{max}: 2913, 1598, 1425, 1274, 1122, 1034, 860, 750, 748, 476 cm^{-1}. ^1H NMR: 2.14 (br s, 2H, NH and OH), 2.59-2.68 (m, 1H), 2.77-2.84 (m, 2H), 3.09-3.15 (m, 1H), 3.41-3.47 (m, 1H), 3.56-3.61 (m, 1H), 5.39 (s, 1H), 6.97 (d, $J_{H,H}$=7.5 Hz, 1H), 7.10-7.25 (m, 3H), 7.39-7.46 (m, 4H), 7.68-7.71 (m, 1H), 7.76-7.83 (m, 2H). ^{13}C NMR δ: 31.0, 49.0, 59.2, 65.6, 125.8, 125.9, 126.1, 126.8, 126.9, 127.5, 127.6, 128.0, 128.2, 128.6, 129.4, 132.6, 133.0, 134.9, 136.5, 142.1. HRMS (ESI-positive mode): *m/z* calcd. for $C_{29}H_{19}NO$ 289.1467; found 290.1539 $[M+H]^+$.

((1*R*,3*S*)-1-propyl-1,2,3,4-tetrahydroisoquinolin-3-yl)methanol 190e

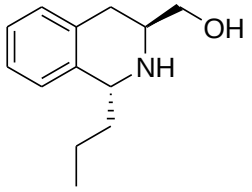

190e

Hydrolysis of oxazolidinone **189e** and purification using column chromatography (EtOAc: hexane, 3: 1 v/v) gave the product **190e** as white solid, 0.87 g, yield 85%, mp 59 ^oC. $[\alpha]_D^{22}$ = -6.3 (*c* 1.00, CH_2Cl_2). FTIR (KBr) ν_{max}: 3312, 2932, 2874, 1492, 1450, 1049, 1025, 745, 734 cm^{-1}. ^1H NMR δ: 0.98 (t, *J*=

7.05 Hz, 3H), 1.44-1.48 (m, 1H), 1.57-1.65 (m, 2H), 1.72-1.78 (m, 1H), 2.44-2.53 (m, 1H), 2.65-2.72 (m, 1H), 3.18-3.27 (m, 1H), 3.43 (t, *J*=9 Hz, 1H), 3.70-3.74 (m, 1H), 3.93-3.98 (m, 1H), 7.05-7.14 (m, 4H), *the resonance attributable to NH and OH were not observed*. ^{13}C NMR δ: 14.0, 20.0, 31.2, 38.7, 48.7, 54.7, 65.8, 125.8, 126.1, 126.7, 129.3, 133.7, 140.3. HRMS (ESI-positive mode): *m/z* calcd. for $C_{13}H_{19}NO$ 205.1467; found 206.1539 $[M+H]^+$.

((1*R*,3*S*)-1-isopropyl-1,2,3,4-tetrahydroisoquinolin-3-yl)methanol 190f

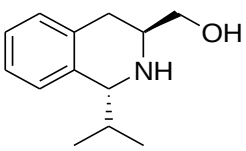

190f

Hydrolysis of oxazolidinone **189f** and purification using column chromatography (EtOAc: hexane, 3: 1 v/v) gave the product **190f** as light yellow viscous oil, 0.74 g, yield 72%. $[\alpha]_D^{22}$ = +15 (*c* 0.70, CH_2Cl_2). FTIR (KBr) ν_{max}: 2966, 1669, 1457, 1388, 1091, 1052, 746 cm^{-1}. ^{1}H NMR δ: 0.95 (d, *J*= 6.9 Hz, 3H), 1.06 (d, *J*= 6.9 Hz, 3H), 2.06-2.19 (m, 1H), 2.24 (br s, 2H, NH and OH), 2.42-2.51 (m, 1H), 2.76-2.83 (m, 1H), 3.32-3.42 (m, 1H), 3.43 (d, *J*=8.4 Hz, 1H), 3.61-3.68 (m, 2H), 7.07-7.15 (m, 4H). ^{13}C NMR δ: 18.5, 20.9, 30.9, 32.4, 50.0, 59.8, 65.6, 125.2, 126.2, 127.3, 129.3, 134.3, 138.7. HRMS (ESI-positive mode): *m/z* calcd. for $C_{13}H_{19}NO$ 205.1467; found 206.1539 $[M+H]^+$.

((1*R*,3*S*)-1-*tert*-butyl-1,2,3,4-tetrahydroisoquinolin-3-yl)methanol 190g

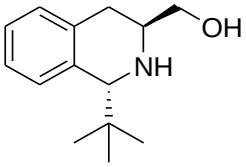

190g

Hydrolysis of oxazolidinone **189g** and purification using column chromatography (EtOAc: hexane, 3: 1 v/v) gave the product **190g** as light yellow solid, 0.97 g, yield 89%, mp 60 ^{o}C. $[\alpha]_D^{21}$ = +28 (*c* 1.00, CH_2Cl_2). FTIR (KBr) ν_{max}: 2933, 1493, 1398, 1364, 1142, 1025, 946, 752 cm^{-1}. ^{1}H NMR δ: 1.00 (s,

9H), 2.03 (br s, 2H, NH and OH), 2.46-2.51 (m, 1H), 2.87-2.94 (m, 1H), 3.18-3.25 (m, 1H), 3.50-3.57 (m, 2H), 3.69 (s, 1H), 7.07-7.18 (m, 4H). ^{13}C NMR δ: 28.3, 30.8, 37.3, 50.5, 63.1, 66.0, 124.8, 126.3, 128.5, 129.1, 134.9, 137.0. HRMS (ESI-positive mode): *m/z* calcd. for $C_{14}H_{21}NO$ 219.1623; found 220.1696 $[M+H]^+$.

((1*R*,3*S*)-1-cyclohexyl-1,2,3,4-tetrahydroisoquinolin-3-yl)methanol 190h

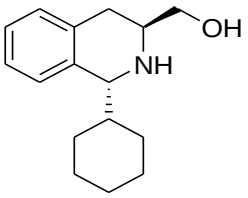

190h

Hydrolysis of oxazolidinone **189h** and purification using column chromatography (EtOAc: hexane, 3: 1 v/v) gave the product **190h** as light yellow solid, 0.92 g, yield 75%, mp 82-83 ^{o}C. $[\alpha]_D^{23}$ = +3 (*c* 1.00, CH_2Cl_2). FTIR (KBr) ν_{max}: 2921, 2854, 1447, 1024, 766, 623 cm^{-1}. ^{1}H NMR δ: 1.15-1.30 (m, 5H), 1.68-1.86 (m, 6H), 2.16 (br s, 2H, NH and OH), 2.42-2.51 (m, 1H), 2.75-2.82 (m,1H), 3.28-3.37 (m, 1H), 3.40 (d, *J*= 9.3 Hz, 1H), 3.61-3.70 (m, 2H), 7.07-7.14 (m, 4H). ^{13}C NMR δ: 26.4, 26.5, 26.6, 29.0, 30.7, 31.3, 42.1, 49.7, 59.5, 65.9, 125.0, 126.2, 127.6, 134.2, 138.4. HRMS (ESI-positive mode): *m/z* calcd. for $C_{16}H_{23}NO$ 245.1780; found 246.1852 $[M+H]^+$.

((1S,3S)-1-(2-aminophenyl)-1,2,3,4-tetrahydroisoquinolin-3-yl)methanol 193

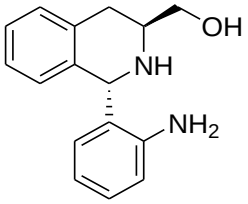

193

Hydrolysis of oxazolidinone **192** and purification using column chromatography (EtOAc: hexane, 5: 1 v/v) gave the product **172** as light yellow crusty foam, 0.92 g, yield 83%, mp 74.5 ^{o}C. $[\alpha]_D^{22}$ = +80 (*c* 0.74, CH_2Cl_2). FTIR (KBr) ν_{max}: 3324, 2921, 1613, 1492, 1457, 1035, 754 cm^{-1}. ^{1}H NMR δ: 2.61

(dd, *J*= 10.2, 16.6 Hz, 1H), 2.84 (dd, *J*= 4.8, 16.6 Hz, 1H), 3.06-3.10 (m, 1H), 3.49 (dd, *J*= 7.8, 10.8 Hz, 1H), 3.65 (dd, *J*= 4.2, 10.8 Hz, 1H), 5.33 (s, 1H), 6.45 (dd, *J*= 1.4, 7.7 Hz, 1H), 6.58 (td, *J*= 1.4, 7.7 Hz, 1H), 6.70 (dd, *J*= 1.4, 7.7 Hz, 1H), 7.00-7.09 (m, 2H), 7.15-7.24 (m, 3H). ^{13}C NMR δ: 30.7, 49.9, 56.5, 65.5, 116.4, 117.8, 125.9, 126.9, 127.9, 128.3, 129.6, 130.3, 134.9, 136.6, 145.8. HRMS (ESI-positive mode): *m/z* calcd. for $C_{16}H_{18}N_2O$ 254.1419; found 255.1498 $[M+H]^+$.

(1*S*,3*R*)-3-hydroxymethyl-1-((1*S*,3*R*)-3-hydroxymethyl-1,2,3,4-tetrahydroisoquinolin-1-yl)-1,2,3,4-tetrahydroisoquinoline 188a

Hydrolysis of bisoxazolidinone **187a** and purified by column chromatography (CH_2Cl_2: MeOH, 90:10 v/v) gave product **188a** as white crystal, 1.09 g, yield 67%, mp 96 ^{o}C. $[\alpha]_D^{21}$ = +8 (*c* 0.45, CH_2Cl_2). FTIR (KBr) ν_{max}: 2922, 1604, 1508, 1328, 1219, 1086, 1015, 742 cm^{-1}. ^{1}H NMR (300 Hz, CD_3OD) δ: 2.45-2.54 (m, 2H), 2.81-2.88 (m, 2H), 3.37-3.46 (m, 4H), 3.52-3.61 (m, 2H), 4.17 (s, 2H), 6.19 (d, *J*= 7.5 Hz, 2H), 6.76 (t, *J*= 6.9 Hz, 2H), 7.00-7.07 (m, 4H), *the resonance attributable to NH and OH were not observed*. ^{13}C NMR (75.6 Hz, CD_3OD) δ: 33.3, 52.2, 60.8, 68.1, 127.1, 129.3, 131.3, 132.3, 137.4, 137.5. HRMS (ESI-positive mode): *m/z* calcd. for $C_{20}H_{24}N_2O_2$ 324.1838; found 325.1911 $[M+H]^+$.

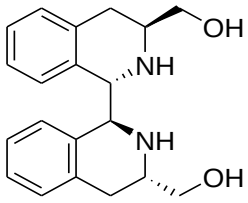

188a

(1*R*,3*R*)-3-hydroxymethyl-1-(3-((1*R*,3*R*)-3-hydroxymethyl-1,2,3,4-tetrahydroisoquinolin-1-yl)phenyl)-1,2,3,4-tetrahydroisoquinoline 188b

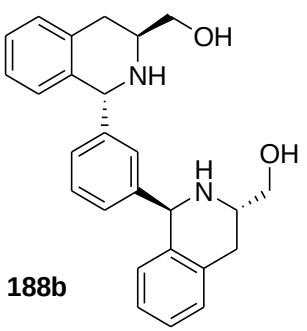

188b

Hydrolysis of bisoxazolidinone **187b** and purified by column chromatography (CH_2Cl_2: MeOH = 91:10 v/v) gave the product **188b** as white needles, 1.1 g, yield 55%, mp 115 ^{o}C. $[\alpha]_D^{22}$ = -29 (*c* 1.00, CH_2Cl_2). FTIR (KBr) ν_{max}: 1663, 1455, 1421, 1387, 1037, 747 cm^{-1}. ^{1}H NMR δ: 2.09 (bs, 4H, NH and OH), 2.51-2.60 (m, 2H), 2.70-2.77 (m, 2H), 3.00-3.06 (m, 2H), 3.34-3.41 (m, 2H), 3.57-3.62 (m, 2H), 5.17 (s, 2H), 6.86-6.89 (m, 2H), 6.93-6.96 (m, 2H), 7.08-7.21 (m, 8H). ^{13}C NMR δ: 31.0, 49.2, 59.1, 65.4, 125.8, 126.9, 127.7, 127.9, 128.5, 129.3, 134.7, 136.2, 144.8. HRMS (ESI-positive mode): *m/z* calcd. for $C_{26}H_{28}N_2O_2$ 400.2151; found 401.2224 $[M+H]^+$.

bis((1*S*,3*S*)-6,7-dimethoxy-3-hydroxymethyl-1,2,3,4-tetrahydroisoquinolin-1-yl)methane 188d

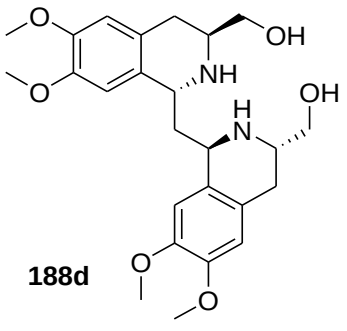

188d

Hydrolysis of oxazolidinone **187d** and purified by column chromatography (CH_2Cl_2: MeOH = 85:15 v/v) gave product **188d** as yellow powder when triturated in diethyl, 0.52 g, yield 21%. $[\alpha]_D^{22}$ = -38.5 (*c* 1.00, CH_2Cl_2).). FTIR (KBr) ν_{max}: 3471, 2948, 1614, 1517, 1242, 1110, 733 cm^{-1}. ^{1}H NMR δ: 2.08 (t, *J*= 6.9 Hz, 2H), 2.35-2.43 (m, 2H), 2.62-2.69 (m, 2H), 3.26-3.38 (m, 2H), 3.52 (t, *J*= 9.9 Hz, 2H), 3.70-3.74 (m, 2H), 3.77 (s, 6H), 3.81 (s, 6H), 4.24 (t, *J*= 7.2 Hz, 2H), 6.49 (s, 2H), 6.51 (s, 2H), *the resonance attributable to NH and OH were not*

observed. ^{13}C NMR δ: 30.3, 41.0, 49.6, 50.7, 55.8, 56.0, 64.9, 109.0, 111.8, 125.4, 130.6, 147.4, 147.6. HRMS (ESI-positive mode): *m/z* calcd. for $C_{25}H_{34}N_2O_6$ 458.2417; found 459.2490 $[M+H]^+$.

General procedure for N-methylation using reductive amination:

To the respective solution of THIQ (1 mmol, 1 equiv.) in THF (5 mL) was added the aq. HCHO 37 wt% (0.75 mL, 10 equiv.). The mixture was stirred for 15 min at room temperature, followed by the addition of $NaCNBH_3$ (310 mg, 5 equiv.) and then stirred for additional 15 min. Glacial AcOH (0.6 mL, 10 equiv.) was then added drop-wise to the reaction and stirred for 3 – 4 h followed by treatment with sat. aq $NaHCO_3$ (10 mL), extraction with CH_2Cl_2 (10 mL x 3). The combined organic phase was washed with brine, dried over MgSO4, filtrated and evaporated under reduced pressure. The crude mixture was purified by column chromatography to obtain **202a, b, d-h** and **203** as pure product.

((*1R,3S*)-2-methyl-1-phenyl-1,2,3,4-tetrahydroisoquinolin-3-yl)methanol 202a

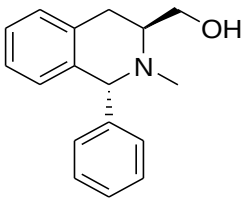

202a

The crude product from *N*-methylation of THIQ **190a** was purified by column chromatography (hexane: EtOAc, 1 : 3 v/v) to obtain THIQ **202a** as white solid, 230 mg, 91% yield, mp 137 ^{o}C. $[\alpha]_D^{21}$-144, (c, 1.0, MeOH). FTIR (KBr) ν_{max}: 709, 2917, 1459, 1050, 753, 709 cm^{-1}. ^{1}H NMR δ: 2.41 (s, 3H), 2.61-2.80 (m, 2H), 3.17-3.23 (m, 1H), 3.47-3.53 (m, 1H), 3.59-3.66 (m, 1H), 4.89 (s, 1H), 6.99 (d, J = 7.5 Hz, 1H), 7.12-7.29 (m, 8H). ^{13}C NMR δ: 26.0, 35.7, 53.0, 61.3,

67.8, 76.6, 77.0, 77.5, 126.0, 126.7, 127.1, 128.1, 129.2, 129.3, 129.7, 133.9, 134.9, 143.4. HRMS (ESI-positive mode): *m/z* calcd. for $C_{17}H_{19}NO$ 253.1467; found 254.1536 $[M+H]^+$

((*1S*,*3S*)-1-(2-methoxyphenyl)-2-methyl-1,2,3,4-tetrahydroisoquinolin-3-yl)methanol 202b

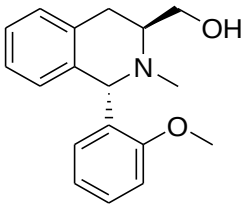

202b

The crude product from *N*-methylation of THIQ **190b** was purified by column chromatography (hexane: EtOAc, 1 : 3 v/v) to obtain THIQ **202b** as white solid, 260 mg, 92% yield, mp 95 ^oC. $[\alpha]_D^{22}$-140, (c, 1.0, MeOH). FTIR (KBr) ν_{max}: 1594, 1484, 1241, 1098, 1027, 746 cm^{-1}. ^1H NMR δ: 2.39 (s, 3H), 2.66-2.82 (m, 2H), 3.32 (s, 1H), 3.51-3.65 (m, 2H), 3.91 (s, 3H), 5.35 (s, 1H), 6.61 (d, *J*= 7.2 Hz, 1H), 6.74-6.79 (m, 1H), 6.92(d, *J* = 7.8 Hz, 2H), 7.10-7.26 (m, 5H). ^{13}C NMR δ: 25.9, 35.3, 53.3, 55.8, 60.8, 61.2, 76.6, 77.0, 77.5, 110.7, 119.9, 126.1, 126.4, 128.4, 129.0, 129.4, 130.7, 131.6, 134.3, 135.9, 157.9. HRMS (ESI-positive mode): *m/z* calcd. for $C_{18}H_{21}NO_2$ 283.1572; found 284.1713 $[M+H]^+$.

((*1R*,*3S*)-2-methyl-1-(naphthalen-2-yl)-1,2,3,4-tetrahydroisoquinolin-3-yl)methanol 202d

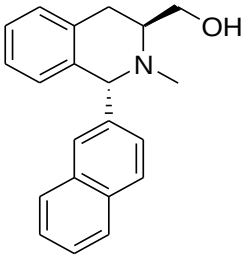

202d

The crude product from *N*-methylation of THIQ **190d** was purified by column chromatography (hexane: EtOAc, 1 : 3 v/v) to obtain THIQ **202d** as white solid, 285 mg, 94% yield, mp 127-129 ^oC. $[\alpha]_D^{22}$-197, (c, 1.0, MeOH). FTIR (KBr) ν_{max}: 2926, 1454, 1042, 747 cm^{-1}. ^1H NMR δ: 2.46

(s, 3H), 2.66-2.84 (m, 2H), 3.21-3.27 (m, 1H), 3.46-3.51 (m, 1H), 3.62-3.69 (m, 1H), 5.02 (s, 1H), 7.03 (d, *J*= 7.5 Hz, 1H), 7.14-7.32 (m, 3H), 7.39-7.51 (m, 3H), 7.66-7.69 (m, 1H), 7.76-7.81(m, 2H). ^{13}C NMR δ: 26.1, 36.0, 53.3, 61.12, 67.9, 76.6, 77.0, 77.5, 125.8, 125.9, 126.1, 126.8, 127.3, 127.6, 128.0, 128.0, 129.4, 129.8, 132.7, 132.9, 133.9, 134.8, 141.1. HRMS (ESI-positive mode): *m/z* calcd. for $C_{21}H_{21}NO$ 303.1623; found 304.1701 $[M+H]^+$.

((*1R,3S*)-2-methyl-1-propyl-1,2,3,4-tetrahydroisoquinolin-3-yl)methanol 202e

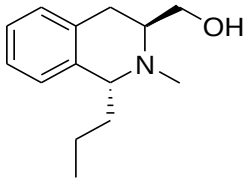

202e

The crude product from *N*-methylation of THIQ **190e** was purified by column chromatography (hexane: EtOAc, 1 : 3 v/v) to obtain THIQ **202e** as yellow oil, 186 mg, 85% yield. $[\alpha]_D^{22}$-27, (c, 1.0, MeOH). FTIR (KBr) ν_{max}: 1962, 1456, 1035, 752 cm^{-1}. ^{1}H NMR δ: 0.95-1.00 (m, 3H), 1.53-1.65 (m, 3H), 1.74-1.83 (m, 1H), 2.22 (3H, s), 2.40-2.50 (m, 1H), 2.56-2.65 (m, 1H), 3.34-3.43 (m, 1H), 3.54-3.66 (m, 3H), 7.06-7.26 (m, 4H). ^{13}C NMR δ: 14.0, 20.2, 24.5, 34.5, 37.9, 52.3, 61.8, 63.6, 76.6, 77.0, 77.2, 77.5, 126.1, 126.1, 128.1, 129.0, 133.1, 138.7. HRMS (ESI-positive mode): *m/z* calcd. for $C_{14}H_{21}NO$ 219.1623; found 220.1701 $[M+H]^+$.

((*1R,3S*)-1-isopropyl-2-methyl-1,2,3,4-tetrahydroisoquinolin-3-yl)methanol 202f

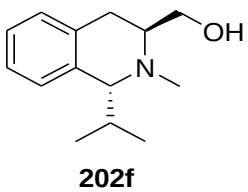

202f

The crude product from *N*-methylation of THIQ **190f** was purified by column chromatography (hexane: EtOAc, 1 : 3 v/v) to obtain THIQ **202f** as yellow oil, 177 mg, 81%

yield. $[\alpha]_D^{22}$-14, (c, 1.0, MeOH). FTIR (KBr) ν_{max}: 2967, 1457, 1241, 1033 cm^{-1}. ^1H NMR δ: 1.01 (d, *J*= 6.6 Hz, 3H), 1.09 (d, *J*= 6.6 Hz, 3H), 1.89-1.99 (m, 1H), 2.15 (s, 3H), 2.52 (d, *J*= 8.4 Hz, 2H), 3.13 (d, *J*= 9.3 Hz, 1H), 3.40-3.48 (m, 1H). 3.55-3.63 (m, 2H), 7.07-7.19 (m, 4H). ^{13}C NMR δ:20.7, 21.3, 24.9, 32.0, 34.6, 52.7, 62.2, 70.7, 125.2, 126.2, 129.0, 129.8, 133.5, 136.5. HRMS (ESI-positive mode): *m/z* calcd. for $C_{14}H_{21}NO$ 219.1623; found 220.1698 $[M+H]^+$.

((*1R*,*3S*)-1-*tert*-butyl-2-methyl-1,2,3,4-tetrahydroisoquinolin-3-yl)methanol 202g

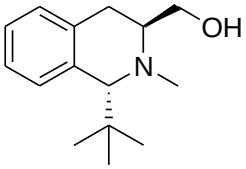

202g

The crude product from *N*-methylation of THIQ **198g** was purified by column chromatography (hexane: EtOAc, 1 : 3 v/v) to obtain THIQ **202g** as yellow solid, 205 mg, 88% yield, mp 67 ^oC. $[\alpha]_D^{21}$-3, (c, 1.0, MeOH). FTIR (KBr) ν_{max}: 2978, 2887, 1091, 1041, 756 cm^{-1}. ^1H NMR δ: 1.03 (s, 9H), 2.18 (s, 3H), 2.51 (d, *J*= 7.5 Hz, 2H), 3.39 (s, 1H), 3.56-3.68 (m, 3H), 7.07-7.26 (m, 4H). ^{13}C NMR δ: 24.5, 29.8, 35.0, 36.6, 52.6, 62.5, 73.2, 76.6, 77.0, 77.5, 125.3, 126.3, 129.1, 129.8, 133.8, 135.6. HRMS (ESI-positive mode): *m/z* calcd. for $C_{15}H_{23}NO$ 233.1780; found 234.1858 $[M+H]^+$.

((*1R*,*3S*)-1-cyclohexyl-2-methyl-1,2,3,4-tetrahydroisoquinolin-3-yl)methanol 202h

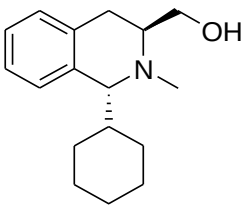

202h

The crude product from *N*-methylation of THIQ **190h** was purified by column chromatography (hexane: EtOAc, 1 : 3 v/v) to obtain THIQ **202h** as yellow oil, 233 mg, 90% yield. $[\alpha]_D^{22}$-49.5 (c, 1.0, MeOH). FTIR (KBr) ν_{max}: 2936,

2857, 1759, 1453, 1037, 754 cm^{-1}. ^{1}H NMR δ: 1.05-1.18 (m, 5H), 1.46-1.67 (m, 5H), 2.05 (s, 3H), 2.43-2.49 (m, 2H), 3.13 (d, *J*= 9Hz, 1H), 3.33-3.47 (m, 1H), 3.50-3.55 (m, 2H), 6.97-7.11 (m, 4H). ^{13}C NMR δ: 24.8, 26.4, 26.5, 26.5, 30.8, 31.5, 34.5, 41.4, 52.4, 62.3, 69.7, 76.7, 77.1, 77.51, 125.0, 126.3, 129.1, 130.0, 133.5, 136.2. HRMS (ESI-positive mode): *m/z* calcd. for $C_{17}H_{25}NO$ 259.1936; found 260.2018 $[M+H]^{+}$.

((*8S,13bS*)-5-methyl-6,8,9,13b-tetrahydro-5H-isoquinolino[2,1-c]quinazolin-8-yl)methanol 203

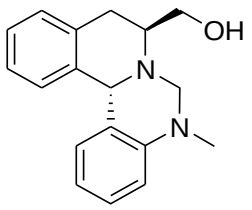

203

The crude product from *N*-methylation of THIQ **193** was purified by column chromatography (hexane: EtOAc, 1: 1 v/v) to obtain THIQ **203** as white solid, 270 mg, 96% yield, mp 179 ^{o}C. $[\alpha]_D^{23} + 260$ (c, 1.0, CH_2Cl_2). FTIR (KBr) ν_{max}: 1605, 1328, 1219, 1087, 1016, 742 cm^{-1}. ^{1}H NMR δ: 2.67-2.84 (m, 2H), 2.88 (s, 3H), 3.23-3.28 (m, 1H), 3.44-3.49 (m, 1H), 3.66-3.71 (m, 1H), 4.03 (d, *J*= 10.8 Hz, 1H), 4.3 (d, *J*= 10.8 Hz, 1H), 5.23 (s, 1H), 6.58-6.77 (m, 3H), 7.10-7.25 (m, 4H). ^{13}C NMR δ: 30.6, 36.6, 56.0, 59.9, 65.1, 70.2, 111.5, 117.1, 122.4, 125.6, 127.4, 127.8, 128.0, 128.3, 128.4, 134.5, 137.6, 145.8. HRMS (ESI-positive mode): *m/z* calcd. for $C_{18}H_{20}N_2O$ 280.1576; found 281.1659 $[M+H]^{+}$.

General procedure for N-methylation using MeI

A solution of the respective THIQ or *C_2*-BIQ (1 mmol) in MeI (4 mL) was stirred for 12 h. The reaction mixture was evaporated under reduced pressure followed by the addition of CH_2Cl_2 (5 mL) and aqueous NaOH 5N solution (5

mL) to the crude mixture. The resulting mixture was stirred for 1 h. The biphasic mixture was separated. The aqueous phase was extracted with CH_2Cl_2 (10 mL x 3). The combined organic phase was washed with brine, dried over $MgSO_4$, filtered, evaporated under reduced pressure, followed by purification by column chromatography. The procedure was used to synthesize the following compounds:

((*1S*,*3S*)-1-(2-(dimethylamino)phenyl)-2-methyl-1,2,3,4-tetrahydroisoquinolin-3-yl)methanol 204

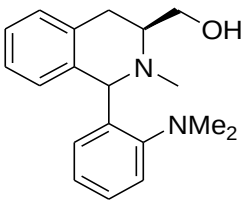

204

The crude mixture was purified by column chromatography (hexane: EtOAc, 1 : 1 v/v) to obtain compound **204** as white solid, 200 mg, 67% yield, mp 155-156 ^{o}C. $[\alpha]_D^{22}$-88 (c, 1.0, MeOH). FTIR (KBr) ν_{max}: 2939, 1488, 1454, 1102, 947, 744 cm^{-1}. ^{1}H NMR δ: 2.41 (s, 3H), 2.75 (d, *J*= 6.9 Hz, 2H), 2.85 (s, 6H), 3.48-3.70 (m, 3H), 5.59 (s, 1H), 6.70 (d, *J*= 7.2 Hz, 1H), 6.83-6.94 (m, 2H), 7.06-7.10 (m, 1H), 7.11-7.23 (m, 5H). ^{13}C NMR δ: 25.5, 29.7, 35.1, 45.9, 53.2, 61.3, 61.4, 120.6, 123.5, 126.3, 128.0, 128.9, 129.6, 131.2, 133.7. HRMS (ESI-positive mode): *m/z* calcd. for $C_{19}H_{24}N_2O$ 296.1889; found 297.1973 $[M+H]^+$.

(1*R*,3*R*)-2-methyl-3-hydroxymethyl-1-(3-((1*R*,3*R*)-2-methyl-3-hydroxymethyl-1,2,3,4-tetrahydroisoquinolin-1-yl)phenyl)-1,2,3,4-tetrahydroisoquinoline 205b

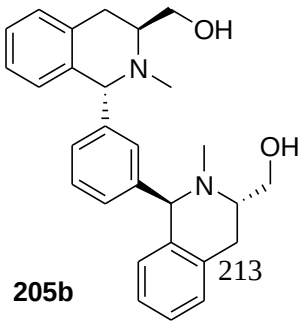

205b

The crude mixture was purified by column chromatography (CH_2Cl_2: MeOH, 95: 5 v/v) to obtain **205b** as the white crustly foam 270 mg, 63% yield.

$[\alpha]_D^{22}$-140, (c, 1.0, MeOH), FTIR (KBr) ν_{max}: 2943, 1738, 1654, 1454, 1243, 1042, 748 cm^{-1}.^{1}H NMR δ: 2.38 (s, 6H), 2.41-2.73 (m, 4H), 3.10-3.16 (m, 2H), 3.46-3.62 (m, 4H), 4.87 (s, 2H), 6.87 (dd, *J*= 7.65, 1.5 Hz, 2H), 7.16 (d, *J*= 7.2 Hz, 2H), 7.09-7.25 (m, 8H). ^{13}C NMR δ: 25.8, 35.6, 52.9, 61.7, 67.9, 126.0, 126.8, 127.6, 128.2, 129.2, 129.6, 130.1, 133.8, 134.6, 142.8. HRMS (ESI-positive mode): *m/z* calcd. for $C_{28}H_{32}N_2O_2$ 428.2464; found 429.2549 $[M+H]^+$.

bis((1*S*,3*S*)-6,7-dimethoxy-2-methyl-3-hydroxymethyl-1,2,3,4-tetrahydroisoquinolin-1-yl)methane 205d

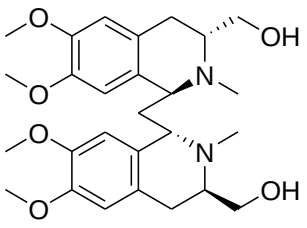

205d

The crude mixture was purified by column chromatography (CH_2Cl_2: MeOH, 95: 5 v/v) to obtain **205d** as the white crustly foam 286 mg, 59% yield, mp 144 ^{o}C. $[\alpha]_D^{22} - 19$, (c, 1.0, MeOH). FTIR (KBr) ν_{max}: 2940, 1514, 1467, 1350, 1242, 1119, 1029 cm^{-1}. ^{1}H NMR δ: 2.12 (t, *J*= 7.5 Hz, 2H), 2.32 (s, 6H), 2.40-2.61 (m, 4H), 3.36-3.42 (m, 2H), 3.57-3.73 (m, 4H), 3.89 (s, 6H), 3.90 (s, 6H), 3.98 (t, *J*= 7.8 Hz, 2H), 6.54 (s, 2H), 6.58 (s, 2H). ^{13}C NMR δ: 23.9, 34.5, 54.7, 55.9, 56.1, 62.1, 109.9, 111.7, 125.0, 129.3, 147.5, 147.6. HRMS (ESI-positive mode): *m/z* calcd. for $C_{27}H_{38}N_2O_6$ 486.2730; found 487.2816 $[M+H]^+$.

*General procedure for O-silylation of THIQ **203***

To a solution of THIQ **203** (280 mg, 1 mmol) in CH_2Cl_2 (5 mL) was added 1H-imidazole (136 mg, 2 mmol) followed by gradual addition of the respective silyl chloride (3 equiv.). After stirring 3 h, the reaction mixture was quenched with DI H_2O (10 mL), followed by the extraction with CH_2Cl_2 (10 mL x 3). The

combined organic phase was washed with brine, dried over MgSO4, filtrated and evaporated under reduced pressure. The crude residue was purified by column chromatography (hexane: EtOAc, 5: 1 v/v) to obtain the *O*-silylated product **206a-b**

(*8S,13bS*)-5-methyl-8-((trimethylsilyloxy)methyl)-6,8,9,13b-tetrahydro-5H-isoquinolino[2,1-c]quinazoline 206a

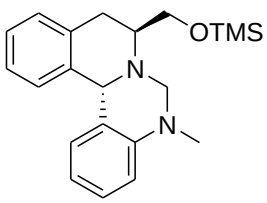

206a

THIQ **203** was reacted with TMSCl to obtain **206a** as white solid after purified from column chromatography, 250 mg, 71% yield, mp 173 ^{o}C. $[\alpha]_D^{22}$+131, (c, 0.4, CH_2Cl_2). FTIR (KBr) ν_{max}: 1726, 1603, 1508, 1322, 1277, 756 cm^{-1}. ^{1}H NMR δ: 0.1 (s, 9H), 2.72-2.83 (m, 2H), 2.88 (s, 3H), 3.22-3.26 (m, 1H), 3.39-3.45 (m, 1H), 3.56-3.61 (m, 1H), 4.09 (d, *J*=11.1 Hz, 1H), 4.46 (d, *J*=11.1 Hz, 1H), 5.33 (s, 1H), 6.49-6.67 (m, 3H), 7.06-7.25 (m, 5H). ^{13}C NMR δ: 0.0, 30.6, 36.3, 55.7, 60.7, 65.1, 70.1, 110.7, 116.4, 122.6, 125.4, 127.2, 127.3, 127.8, 128.4, 128.7, 137.8, 145.9. HRMS (ESI-negative mode): *m/z* calcd. for $C_{21}H_{28}N_2OSi$ 352.1971; found 352.1754 [M]$^-$.

(*8S,13bS*)-8-((tert-butyldimethylsilyloxy)methyl)-5-methyl-6,8,9,13b-tetrahydro-5H-isoquinolino[2,1-c]quinazoline 206b

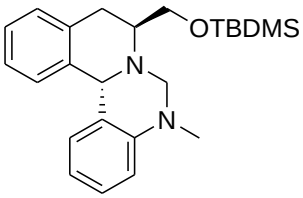

206b

THIQ **203** was reacted with TBDMSCl to obtain **206b** as viscous oil after purified from column chromatography, 299 mg, 76% yield. $[\alpha]_D^{22}$+2, (c, 1.0, CH_2Cl_2). FTIR (KBr) ν_{max}: 1605, 1505, 1258, 1099, 838, 747 cm^{-1}. ^{1}H NMR δ: 0.1 (s, 6H), 0.86 (s, 9H), 2.72-2.83 (m, 2H), 2.88 (s,

3H), 3.22-3.26 (m, 1H), 3.39-3.45 (m, 1H), 3.56-3.61 (m, 1H), 4.09 (d, *J*=11.1 Hz, 1H), 4.46 (d, *J*=11.1 Hz, 1H), 5.33 (s, 1H), 6.49-6.67 (m, 3H), 7.06-7.25 (m, 5H). ^{13}C NMR δ: 0.0, 30.6, 36.3, 55.7, 60.7, 65.1, 70.1, 110.7, 116.4, 122.6, 125.4, 127.2, 127.3, 127.8, 128.4, 128.7, 137.8, 145.9. HRMS (ESI-positive mode): *m/z* calcd. for $C_{24}H_{34}N_2OSi$ 394.2440; found 395.2514 $[M+H]^+$.

*Procedure for enantioselective Henry reaction using Cu(OAc)$_2$.H$_2$O-THIQ **206a** under optimal conditions* (Table 31)

A solution of THIQ **206a** (7 mg, 0.02 mmol) and $Cu(OAc)_2.H_2O$ (4mg, 0.02 mmol) in EtOH was stirred at rt for 2 h followed by the addition of a corresponding aldehyde **191a**, **207**-**218** (0.2 mmol) and nitromethane **200** (125 µL, 2 mmol). The resulting reaction mixture was stirred at room temperature for 48 h. The reaction mixture was then evaporated. The crude mixture was purified by column chromatography (EtOAc: hexane, 1: 5 v/v) to obtain the corresponding β nitroalcohol products.

(*S*)-1-Phenyl-2-nitroethanol 201[168f]

The crude mixture from the reaction of benzaldehyde **191a** and nitromethane **200** was purified by flash chromatography (EtOAc: hexane, 1: 5 v/v) to obtain β-nitroalcohol product **201** as an oil in 82% yield. ^{1}H NMR δ: 2.76 (br s, 1H), 4.39-4.56 (m, 2H), 5.37 (dd, *J*= 9.3, 9.6 Hz, 1H), 7.34-7.40 (m, 5H); ^{13}C NMR δ: 71.0, 81.3, 126.0, 129.0, 129.1, 138.2. The *ee* of 80% was determined by HPLC using Chiralcel OD-H column: hexane: *i*-PrOH = 90:10, flow rate = 0.8 ml/min, wavelength = 215 nm, t_1 = 18.1min for (*R*), t_2=22.2 min for (*S*).[168f]

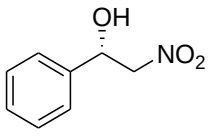

(*S*)-**201**

(*S*)-1-(4-nitrophenyl)-2-nitroethanol 219[168f]

The crude mixture from the reaction of 4-nitrobenzaldehye **207** and nitromethane **200** was purified by flash chromatography (EtOAc: hexane, 3: 7 v/v) to obtain β-nitroalcohol product **219** as yellow solid in 91% yield. ^{1}H NMR δ: 3.28 (br s, 1H), 4.47-4.66 (m, 2H), 5.48-5.56 (m, 1H), 7.63 (d, *J*= 8.7 Hz, 2H), 8.27 (d, *J*= 8.7 Hz, 2H). ^{13}C NMR δ: 70.0, 80.6, 124.1, 127.0, 1455.4 ,148.0. The ee of 54% was determined by HPLC (Chiralcel OD-H column): hexane: *i*-PrOH = 85:15, flow rate = 1.0 ml/min, wavelength = 215 nm, t_1 = 16.7 min for (*R*), t_2 = 20.9 min for (*S*).[168f]

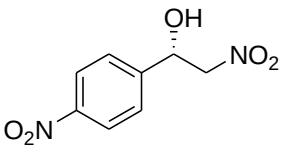

(*S*)-**219**

(*S*)-1-(4-chlorophenyl)-2-nitroethanol 220[168f]

The crude mixture from the reaction of 4-chlorobenzaldehye **208** and nitromethane **200** was purified by flash chromatography (EtOAc: hexane, 1: 5 v/v) to obtain β-nitroalcohol product **220** as an oil in 88% yield. ^{1}H NMR δ: 2.89 (br s, 1H), 4.47-4.62 (m, 2H), 5.44-5.47 (m, 1H), 7.34-7.40 (m, 4H). ^{13}C NMR δ: 70.3, 80.1, 127.3, 129.3, 134.9, 136.5. The ee of 77% was determined by HPLC (Chiralcel OD-H column): hexane: *i*-PrOH = 90:10, flow rate = 1.0 ml/min, wavelength = 215 nm, t_1 = 13.7min for (*R*), t_2=17.5min for (*S*).[168f]

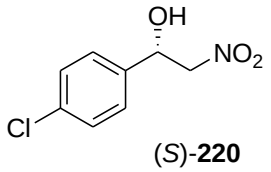

(*S*)-**220**

(*S*)-1-(3-chlorophenyl)-2-nitroethanol 221[168f]

The crude mixture from the reaction of 3-chlorobenzaldehye **209** and nitromethane **200** was purified by flash chromatography (EtOAc: hexane, 1: 5

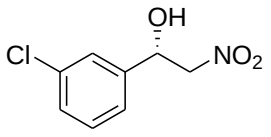

(*S*)-**221**

v/v) to obtain β-nitroalcohol product **221** as an oil in 80% yield. ^{1}H NMR δ: 2.96 (br, s, 1H), 4.49-4.63 (m, 2H), 5.37-5.44 (m, 1H), 7.26-7.73 (4H, m). ^{13}C NMR δ: 70.3, 81.0, 124.0, 126.2, 129.1, 130.3, 135.0, 140.0. The *ee* of 71% was determined by HPLC (Chiralcel OD-H column): *hexane*: IPA = 90:10, flow rate = 01.0 ml/min, wavelength = 215 nm, t_1 = 13.6 min for (*R*), t_2 = 17 min for (*S*).[168f]

(*S*)-1-(4-bromophenyl)-2-nitroethanol 222[168f]

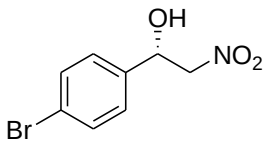

(*S*)-**222**

The crude mixture from the reaction of 4-bromobenzaldehye **210** and nitromethane **200** was purified by flash chromatography (EtOAc: hexane, 1: 5 v/v) to obtain β-nitroalcohol product **222** as an oil in 95% yield. ^{1}H NMR δ: 2.96 (s, 1H), 4.40-4.54 (m, 2H), 5.36-5.39 (m, 1H), 7.19-7.23 (m, 2H), 7.45-7.48 (m, 2H). ^{13}C NMR δ: 70.3, 80.9, 123.0, 127.6, 132.2, 137.1. The ee of 80% was determined by HPLC (Chiralcel OD-H column): hexane: *i*-PrOH = 85:15, flow rate = 0.8 ml/min, wavelength = 215 nm, t_1 = 13.5 min for (R), t_2 = 17.6 min for (S).[168f]

(*S*)-1-(4-fluorophenyl)-2-nitroethanol 223[168f]

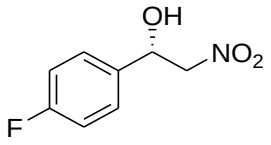

(*S*)-**223**

The crude mixture from the reaction of 4-florobenzaldehye **211** and nitromethane **200** was purified by flash chromatography (EtOAc: hexane, 1: 7 v/v) to obtain β-nitroalcohol product **223** as an oil in 67% yield. ^{1}H NMR δ: 2.89 (s, 1H), 4.46-4.63 (m, 2H), 5.47 (d, *J*=7.5 Hz, 1H), 7.07-7.13 (m, 2H), 7.37-7.42 (m, 2H). ^{13}C NMR δ: 70.3, 81.2, 115.9, 116.1, 127.7, 127.8. The *ee* of 78% was

determined by HPLC (Chiralcel OD-H column): hexane: *i*-PrOH = 90:10, flow rate = 0.8 ml/min, wavelength = 215 nm, t_1 = 14.8 min for (*R*), t_2 = 17.6 min for (*S*).[168f]

(*S*)-1-(4-methylphenyl)-2-nitroethanol 224[168f]

The crude mixture from the reaction of 4-methylbenzaldehye **212** and nitromethane **200** was purified by flash chromatography (EtOAc: hexane, 1: 8 v/v) to obtain β-nitroalcohol product **224** as an oil in 83% yield. ^{1}H NMR δ: 2.36 (s, 3H), 2.48 (s, 1H), 4.46-4.64 (m, 2H), 5.40-5.46 (m, 1H), 7.26-7.30 (m, 4H). ^{13}C NMR δ: 21.2, 70.9, 81.3, 125.9, 129.7, 135.2, 139.0. The ee of 74% was determined by HPLC (Chiralcel OD-H column): hexane: *i*-PrOH = 90:10, flow rate = 0.5 ml/min, wavelength = 215 nm, t_1 = 27.7 min for (*R*), t_2=35.9 min for (*S*).[168f]

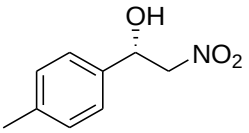

(*S*)-**224**

(*S*)-1-(3-methylphenyl)-2-nitroethanol 225[168f]

The crude mixture from the reaction of 3-methylbenzaldehye **213** and nitromethane **200** was purified by flash chromatography (EtOAc: hexane, 1: 5 v/v) to obtain β-nitroalcohol product **225** as an oil in 61% yield. ^{1}H NMR δ: 2.38 (s, 3H), 2.81 (s, 1H), 4.50-4.65 (m, 2H), 5.37-5.45 (m, 1H), 7.23-7.32 (m, 4H). ^{13}C NMR δ: 21.4, 71.1, 81.8, 123.0, 126.6, 128.9, 129.7, 138.0 ,138.9. The ee of 71% was determined by HPLC (Chiralcel OD-H column): hexane: *i*-PrOH = 90:10, flow rate = 0.5 ml/min, wavelength = 215 nm, t_1 = 23.3 min for (*R*), t_2 = 26.9 min for (*S*).[168f]

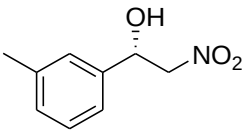

(*S*)-**225**

(*S*)-1-(2-methylphenyl)-2-nitroethanol 226[168f]

The crude mixture from the reaction of 2-methylbenzaldehye **214** and nitromethane **200** was purified by flash chromatography (EtOAc: hexane, 1: 5 v/v) to obtain β-nitroalcohol product **226** as an oil in 96% yield. ^{1}H NMR δ: 2.40 (s, 3H), 2.72 (d, *J*= 3.6Hz, 1H), 4.42-4.60 (m, 2H), 5.67-5.72 (m, 1H), 7.25-7.31 (m, 3H), 7.51-7.56(m, 1H). ^{13}C NMR δ: 18.9, 6.80, 80.2, 125.6, 126.8, 130.9, 134.4 and 136.2. The ee of 78% was determined by HPLC (Chiralcel OD-H column): hexane: *i*-PrOH = 90:10, flow rate = 0.5 ml/min, wavelength = 215 nm, t_1 = 21.9 min for (*R*), t_2 = 33.7 min for (*S*).[168f]

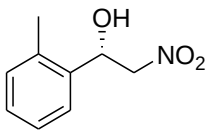

(*S*)-**226**

(*S*)-1-(biphenyl-4-yl)-2-nitroethanol 227[168f]

The crude mixture from the reaction of 4-phenyllbenzaldehye **215** and nitromethane **200** was purified by flash chromatography (EtOAc: hexane, 1: 5 v/v) to obtain β-nitroalcohol product **227** as an oil in 93% yield. ^{1}H NMR δ: 2.88 (d, *J*= 3.3Hz, 1H), 4.36-4.69 (m, 2H), 5.52 (d, *J*= 9.3Hz, 1H), 7.34-7.64 (m, 9H). ^{13}C NMR δ: 70.8, 81.2, 126.4,127.1, 127.7, 127.8, 128.9, 137.0, 140.3, 142.0. The ee of 68% was determined by HPLC (Chiralcel OD-H column): hexane: *i*-PrOH = 85:15, flow rate = 0.8 ml/min, wavelength = 215 nm, t_1 = 19.3 min for (*R*), t_2 = 23.4 min for (*S*).[168f]

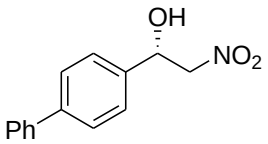

(*S*)-**227**

(*S*)-1-(3-methoxylphenyl)-2-nitroethanol 228[168f]

The crude mixture from the reaction of 3-methoxylbenzaldehye **216** and nitromethane **200** was purified by flash chromatography (EtOAc: hexane, 1: 5 v/v) to obtain β-nitroalcohol product **228** as an oil in 80% yield. ^{1}H NMR δ: 2.97 (br, s, 1H), 3.19 (s, 3H), 4.72-4.84 (m, 2H), 5.42-5.48 (m, 1H), 6.88-6.97 (m, 3H), 7.28-7.57 (m, 1H). ^{13}C NMR δ: 55.3, 70.9, 81.2, 111.5, 114.4, 118.1, 130.1, 139.8, 160.1. The ee of 64% was determined by HPLC (Chiralcel OD-H column): hexane: *i*-PrOH = 90:10, flow rate = 0.5 ml/min, wavelength = 215 nm, t_1 = 45.6 min for (*R*), t_2 = 58.7 min for (*S*).[168f]

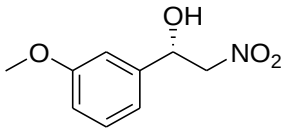

(*S*)-**228**

(*S*)-1-(2-naphthyl)-2-nitroethanol 229[168f]

The crude mixture from the reaction of 2-naphthaldehyde **217** and nitromethane **200** was purified by flash chromatography (EtOAc: hexane, 1: 4 v/v) to obtain β-nitroalcohol product **229** as an oil in 93% yield. ^{1}H NMR δ: 3.04 (br, s, 1H), 4.54 -4.82 (m, 2H), 5.61 (d, *J*= 6.9Hz, 1H), 7.26-7.54 (m, 3H), 7.84-7.88 (m, 4H). ^{13}C NMR δ: 71.2, 81.2, 123.2, 125.3, 126.7, 126.7, 127.8, 128.1, 129.0, 133.2, 133.4, 135.4. The ee of 78% was determined by HPLC (Chiralcel OD-H column): hexane: *i*-PrOH = 85:15, flow rate = 0.8 ml/min, wavelength = 215 nm, t_1 = 34.7 min for (R), t_2 = 50.8 min for (*S*).[168f]

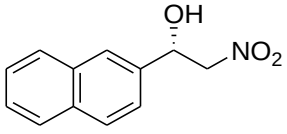

(*S*)-**229**

(*S, E*)-1-Nitro-4-phenyl-3-buten-2-ol 230[168f]

The crude mixture from the reaction of 2-naphthaldehyde **218** and nitromethane **200** was purified by flash chromatography (EtOAc: hexane, 1: 5 v/v) to obtain β-nitroalcohol product **230** as an oil in 76% yield. ^{1}H NMR δ: 2.68 (br s,

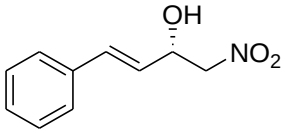

(*S,E*)-**230**

1H), 4.51 -4.61 (m, 2H), 5.02-5.08 (m, 1H), 6.15 (dd, *J*= 6.3, 15.9 Hz, 1H), 6.79 (d, *J*= 15Hz, 1H), 7.30-7.46 (m, 5H). ^{13}C NMR δ: 69.6, 79.9, 124.9, 126.7, 128.6, 128.8, 133.7, 135.5. The ee of 61% was determined by HPLC (Chiralcel OD-H column): hexane: *i*-PrOH = 90:10, flow rate = 0.8 ml/min, wavelength = 215 nm, t_1 = 54.0 min for (*R*), t_2 = 61.3 min for (*S*).[168f]

Appendix: ^{1}H NMR, ^{13}C NMR, MS and FTIR spectra of new compounds

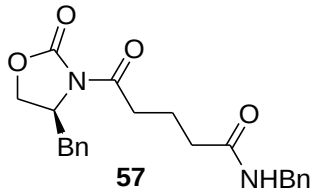

57

^{1}H NMR	^{13}C NMR
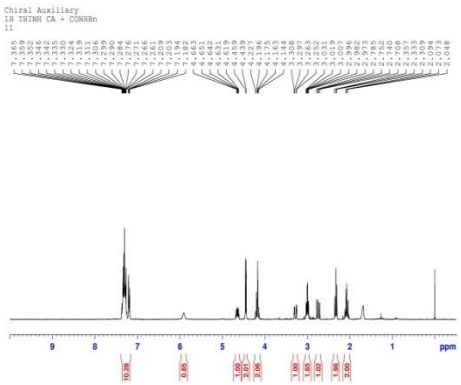	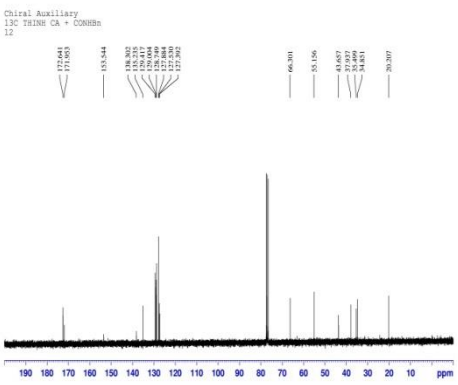
Mass	FTIR
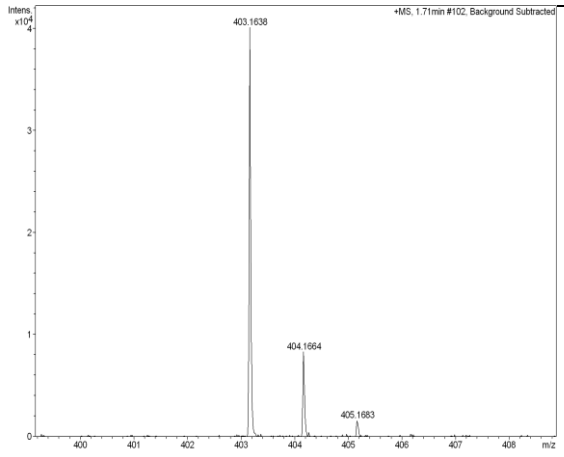	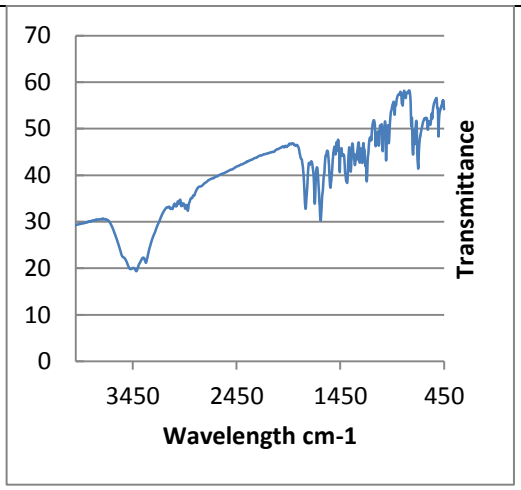

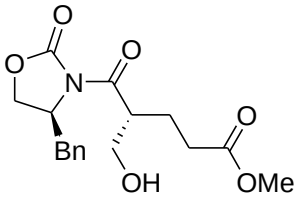

81

^{1}H NMR	^{13}C NMR
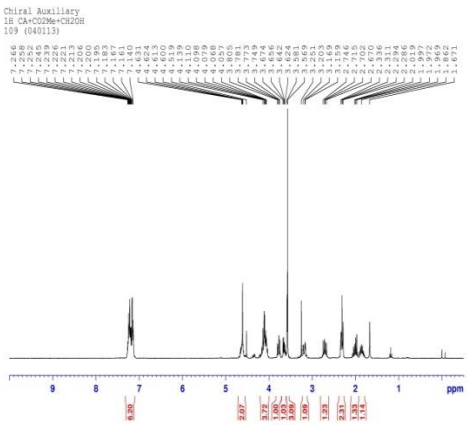	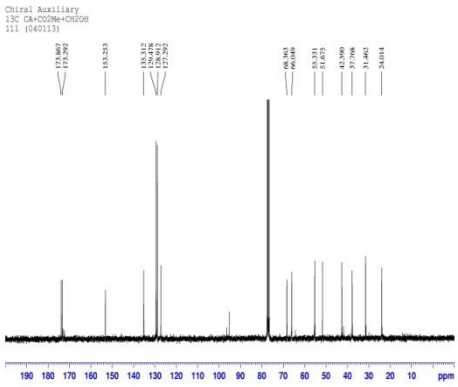
Mass	FTIR
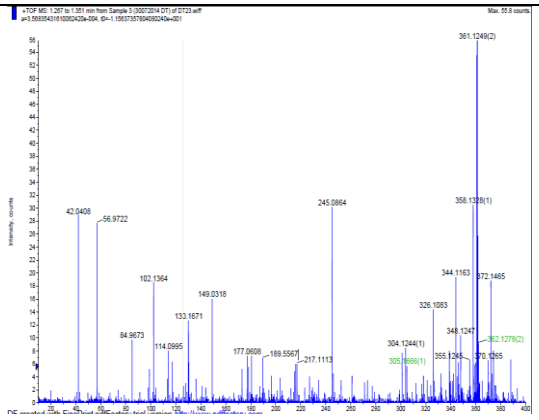	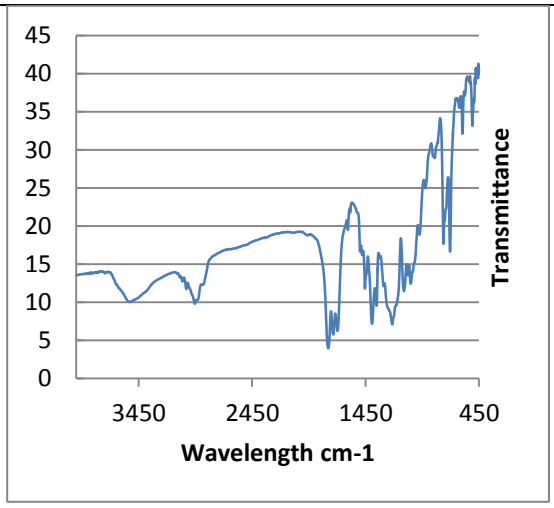

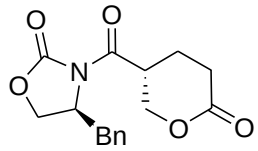

85

^{1}H NMR	^{13}C NMR
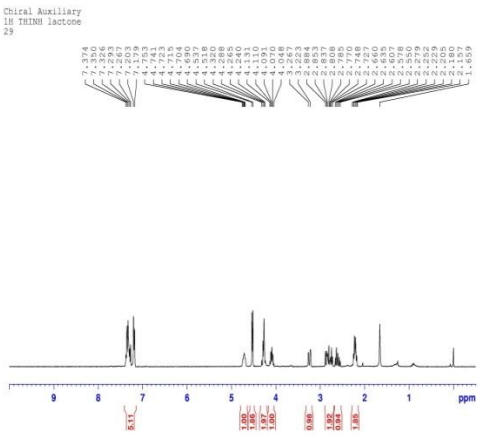	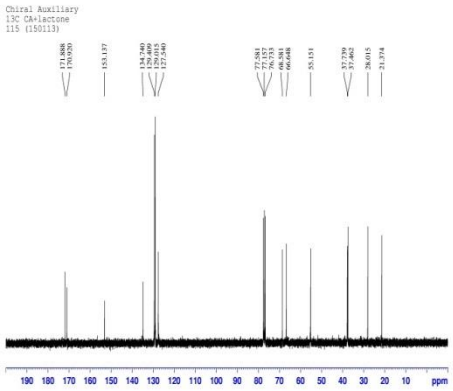
Mass	FTIR
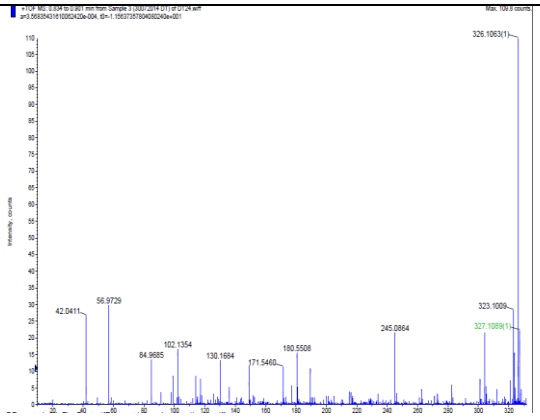	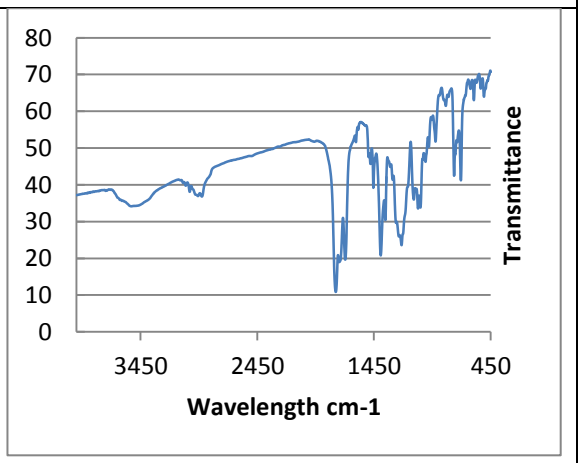

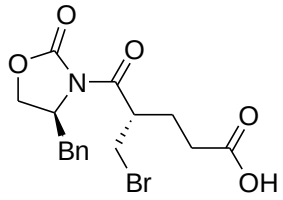

86

^{1}H NMR	^{13}C NMR
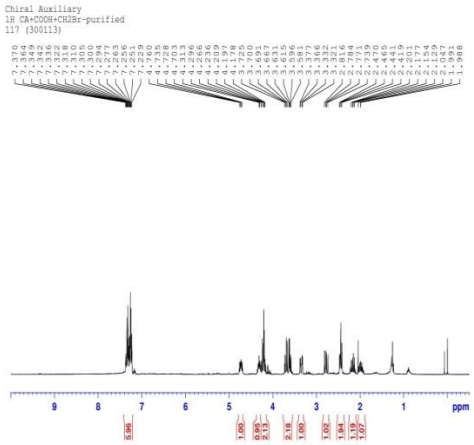	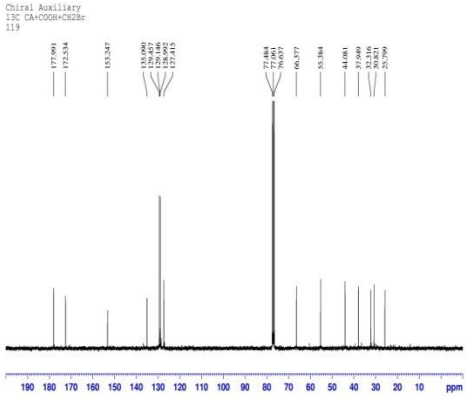
Mass	FTIR
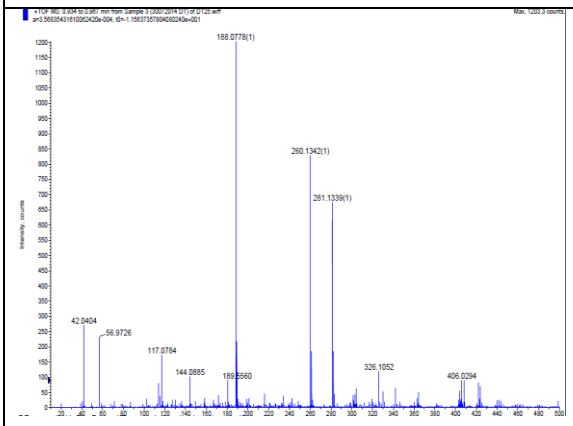	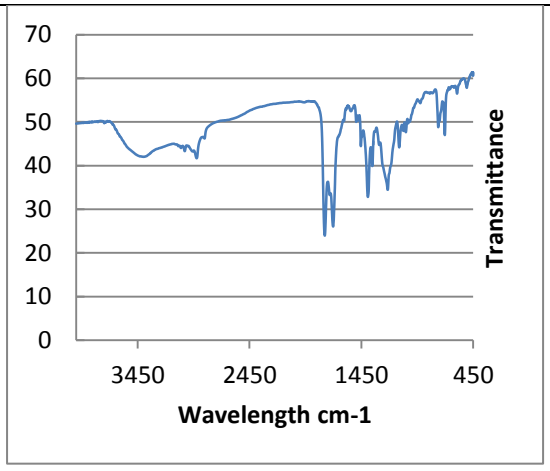

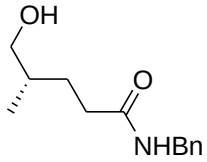

88

^{1}H NMR	^{13}C NMR
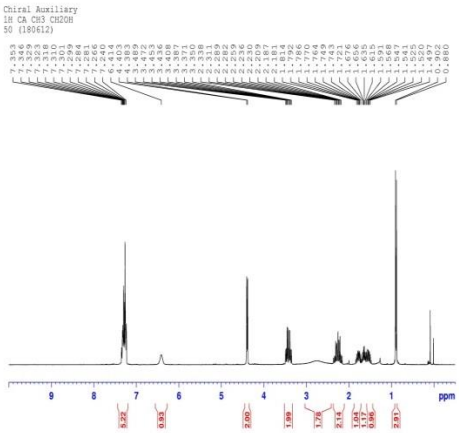	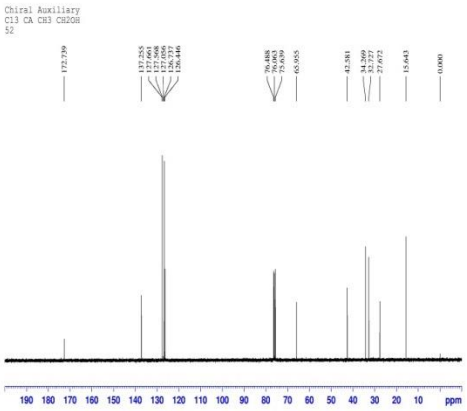
Mass	**FTIR**
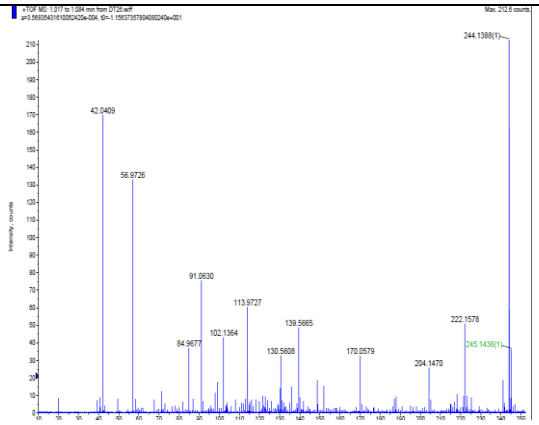	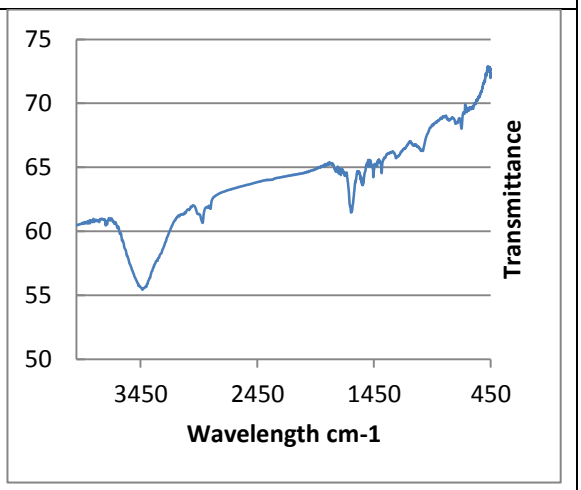

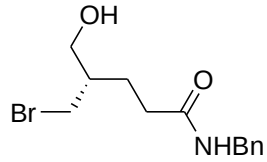

89

^{1}H NMR	^{13}C NMR
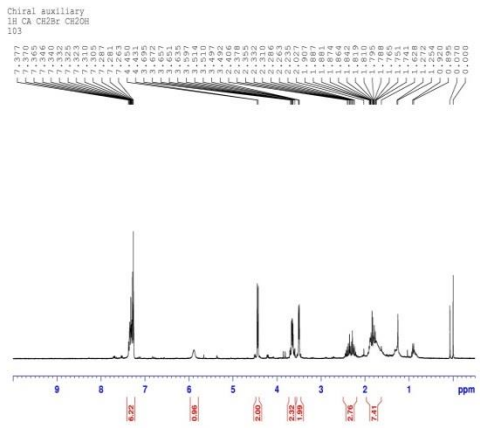	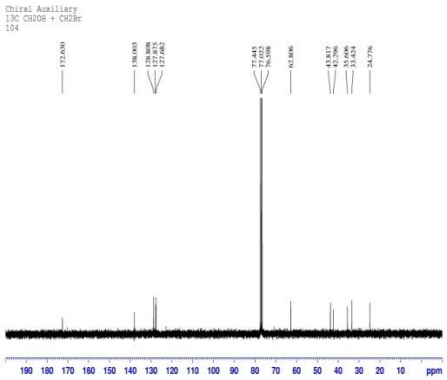
Mass	FTIR
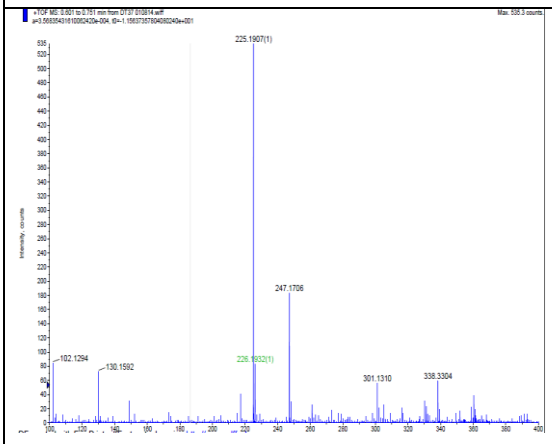	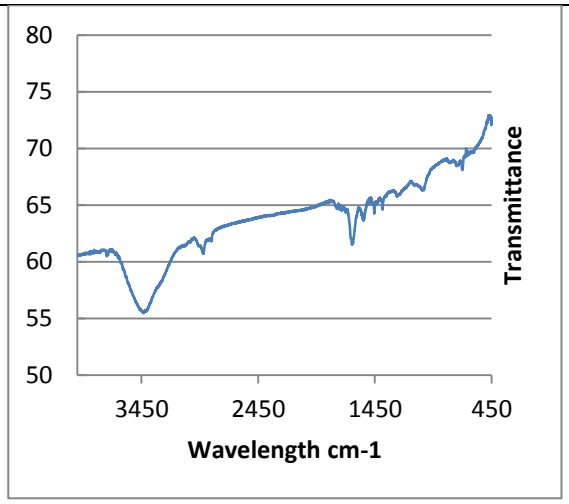

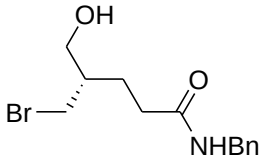

89

^{1}H NMR	^{13}C NMR
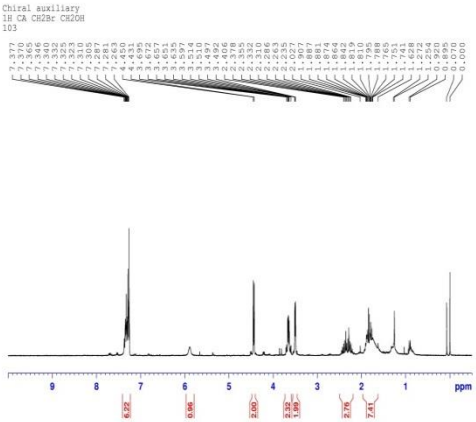	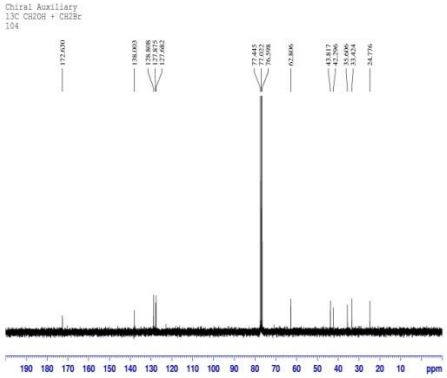
Mass	FTIR
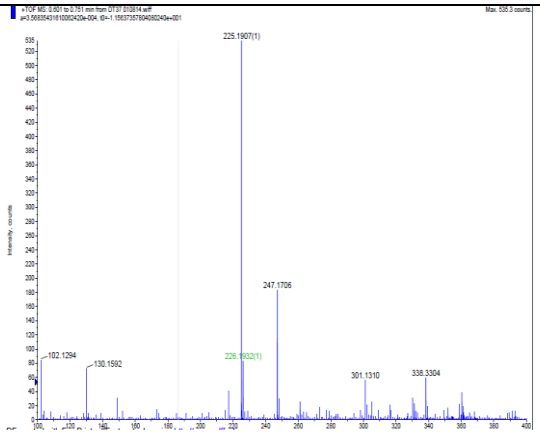	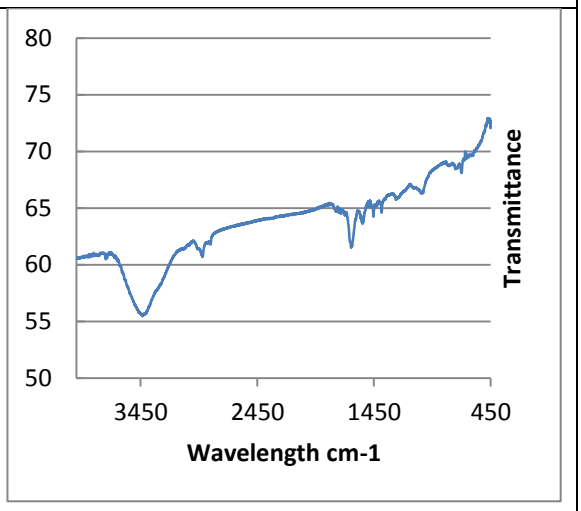

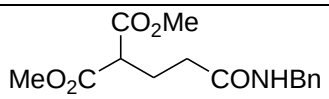

138

^{1}H NMR	^{13}C NMR
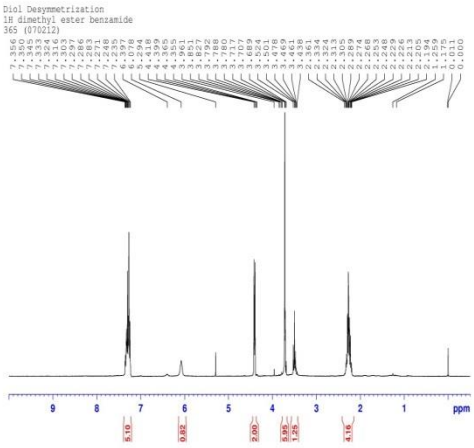	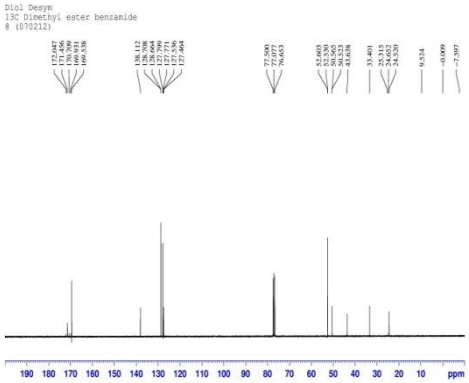
Mass	**FTIR**
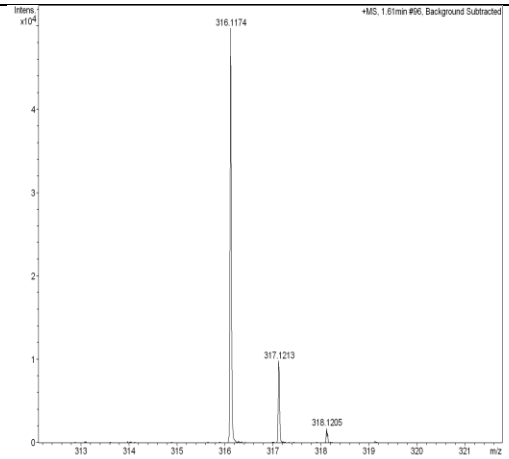	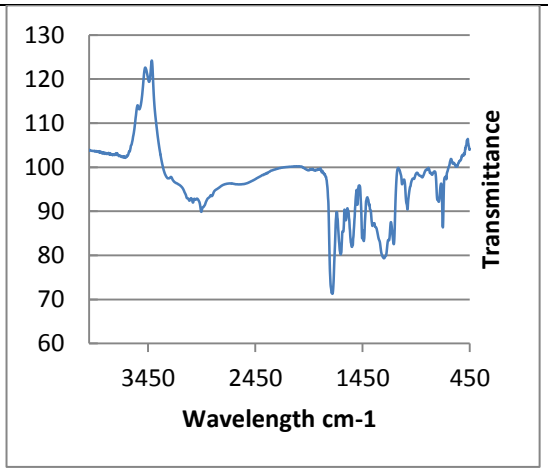

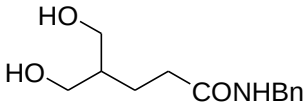

43

^{1}H NMR	^{13}C NMR
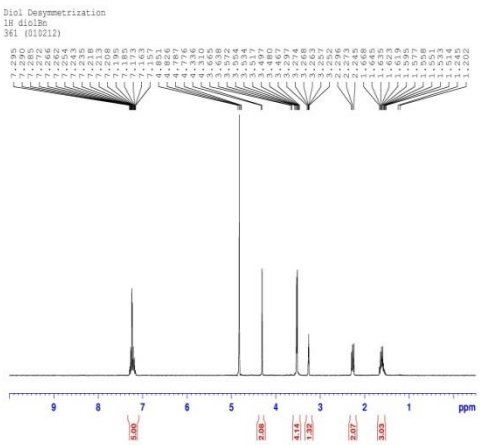	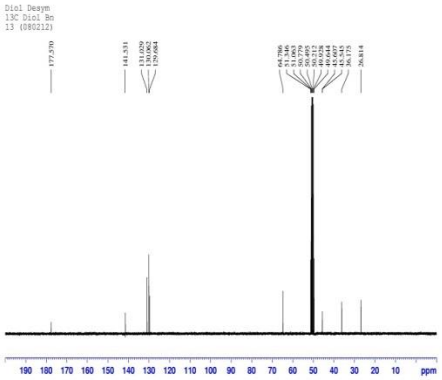
Mass	**FTIR**
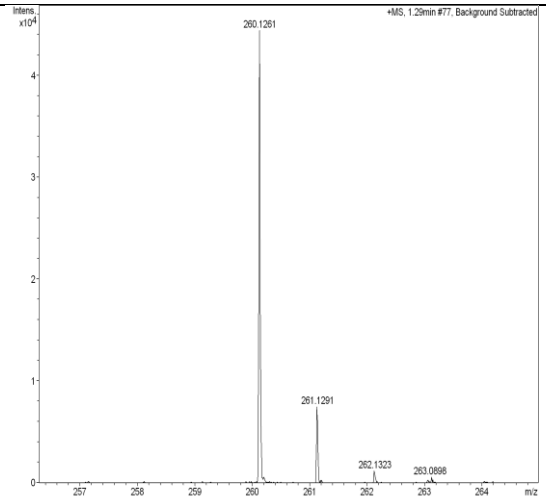	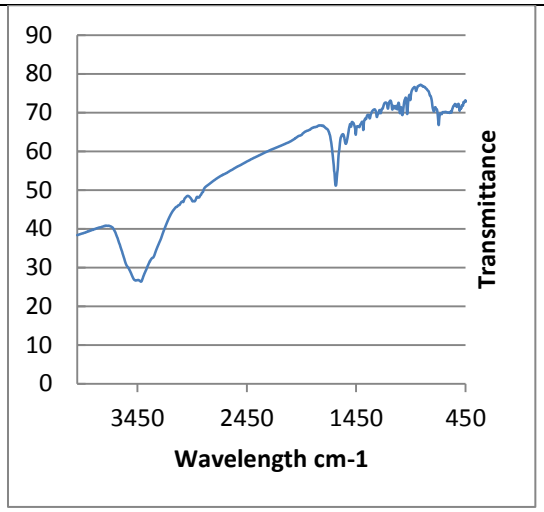

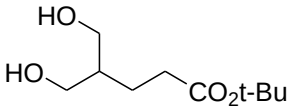

169

^{1}H NMR	^{13}C NMR
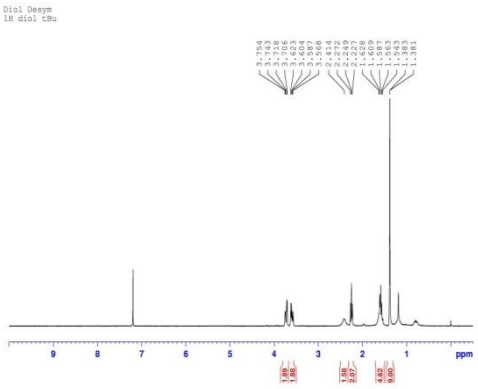	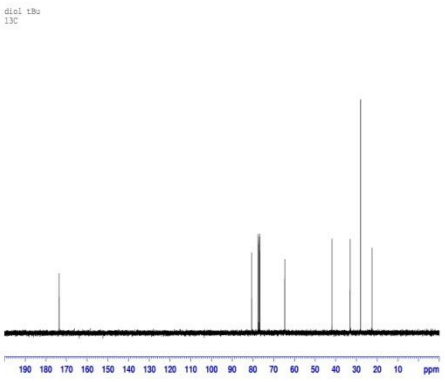
Mass	**FTIR**
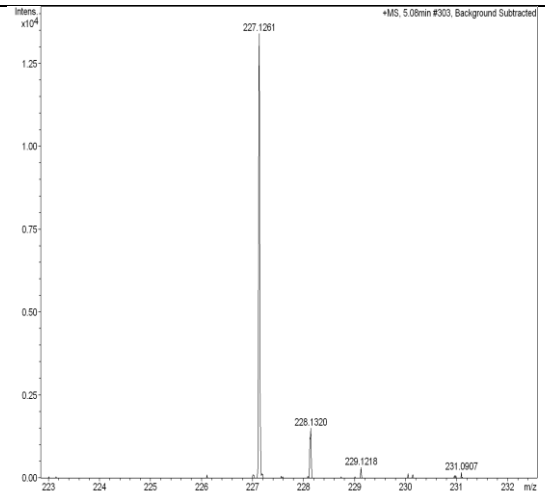	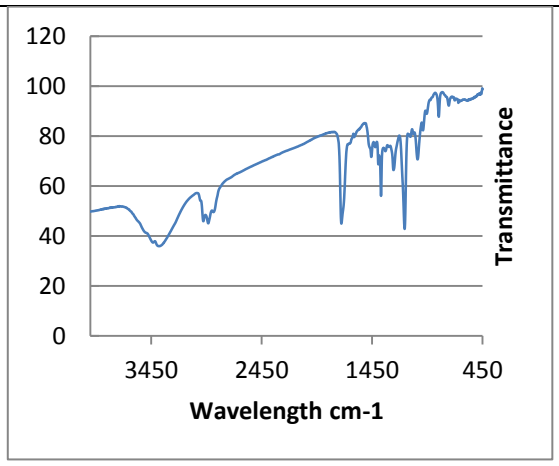

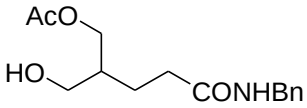

133a

^{1}H NMR	^{13}C NMR
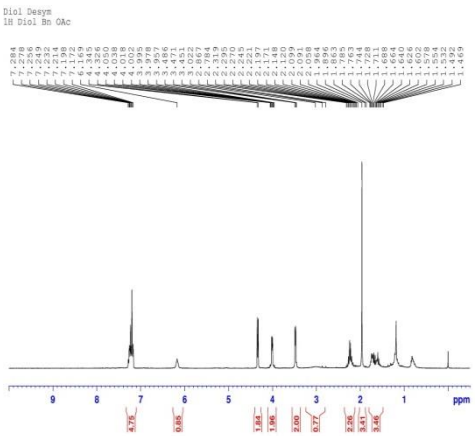	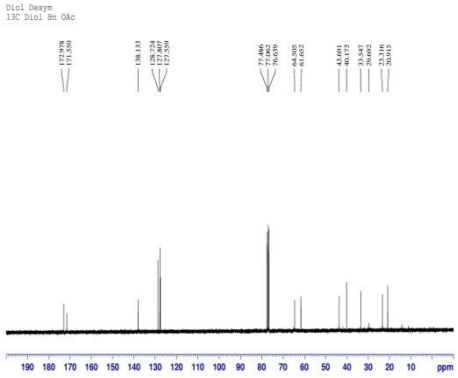
Mass	**FTIR**
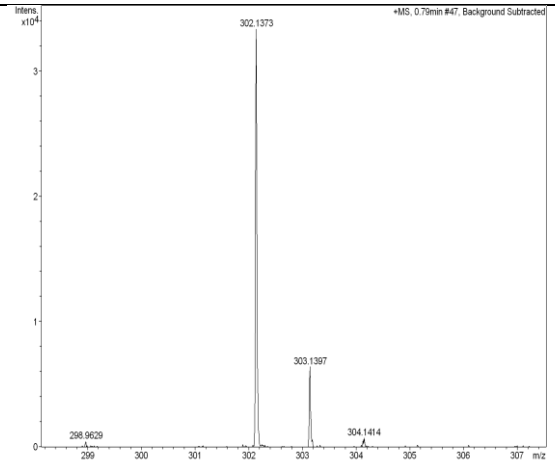	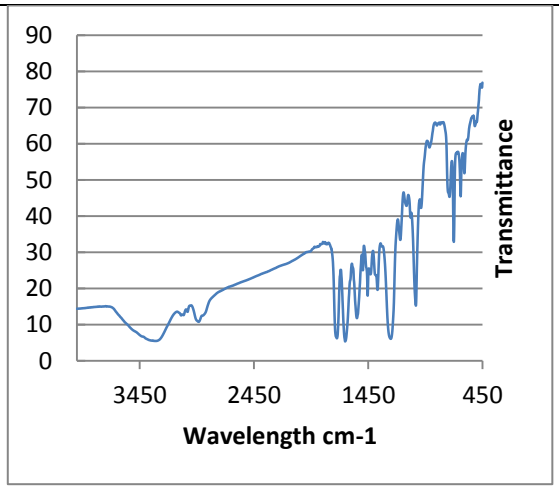

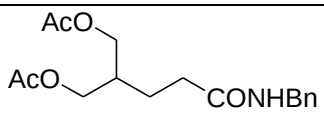

168

^{1}H NMR	^{13}C NMR
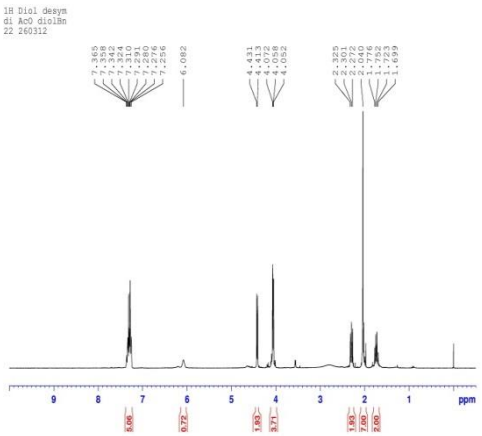	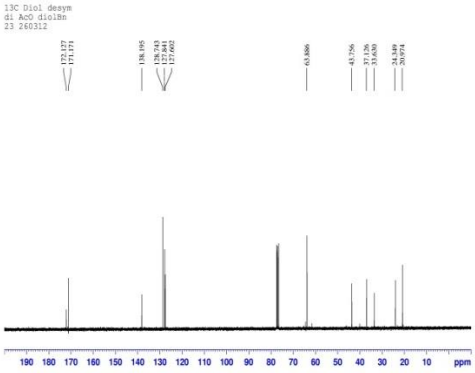
Mass	**FTIR**
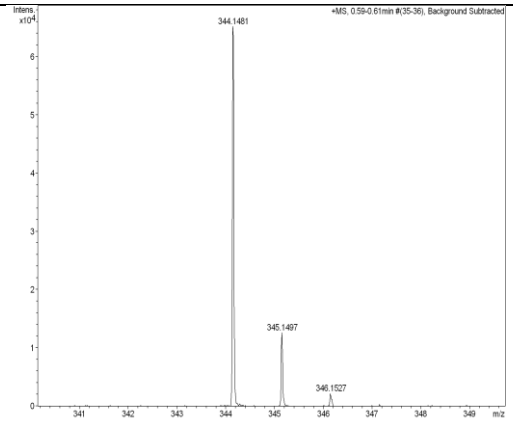	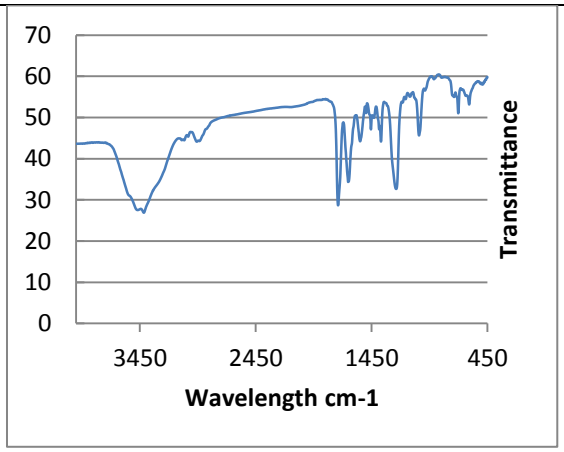

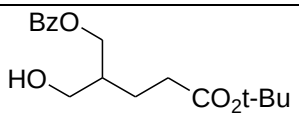

170b

^{1}H NMR	^{13}C NMR
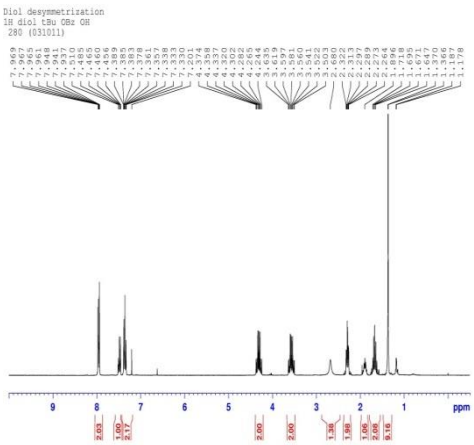	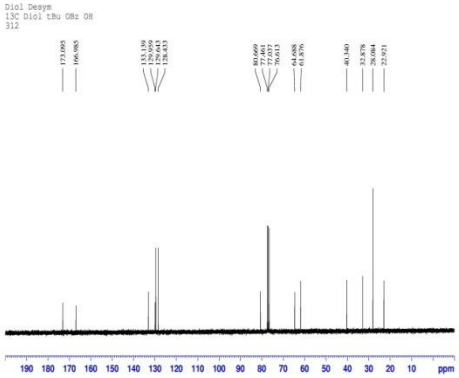
Mass	**FTIR**
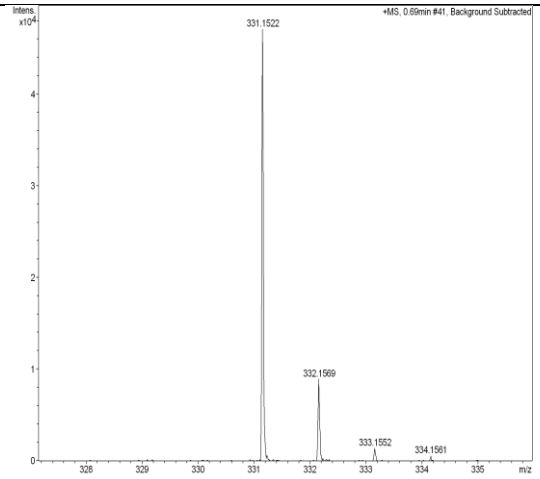	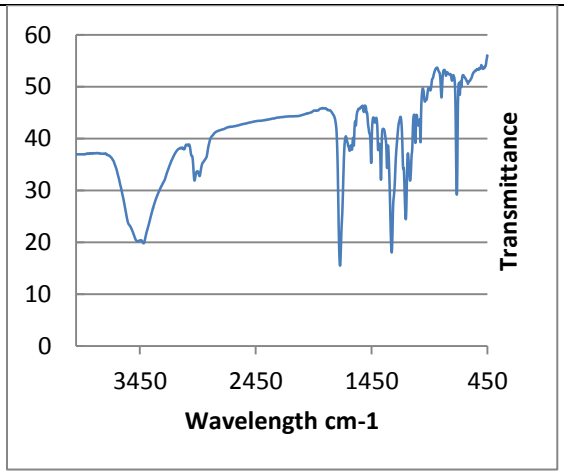

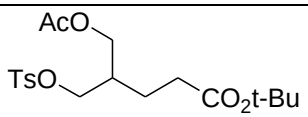

181

^{1}H NMR	^{13}C NMR
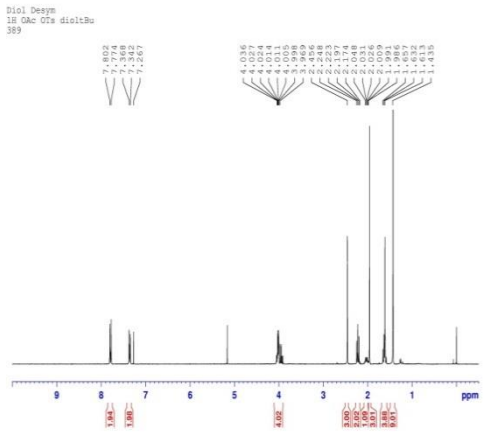	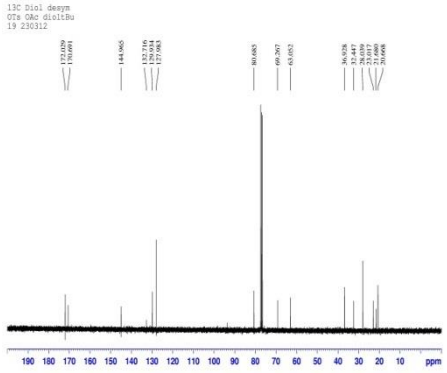
Mass	**FTIR**
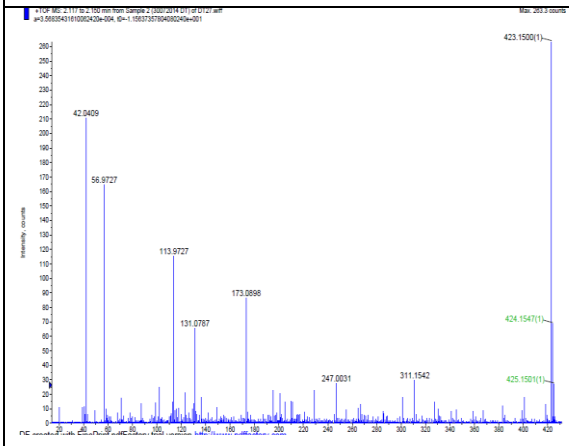	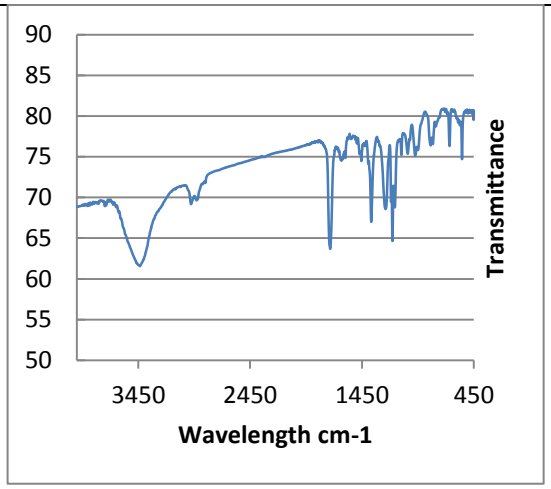

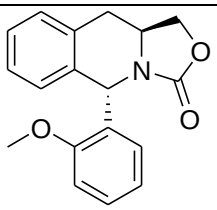

189b

^{1}H NMR	^{13}C NMR
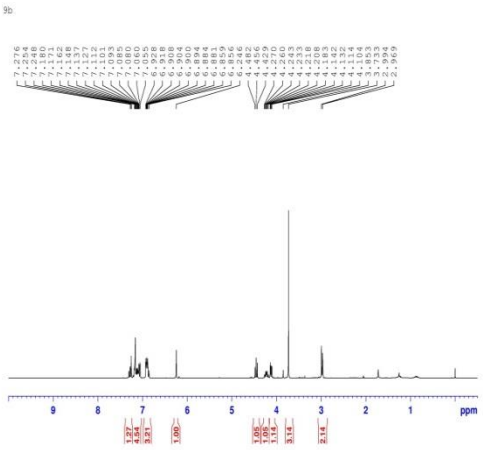	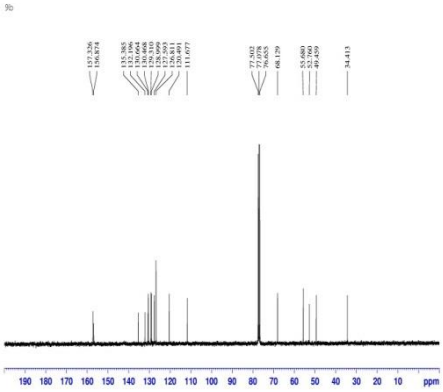
Mass	**FTIR**
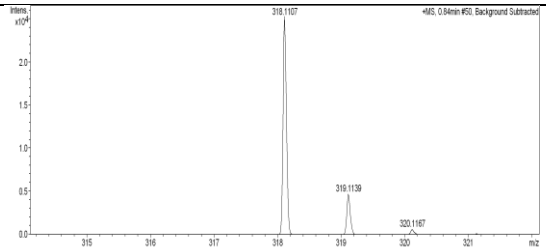	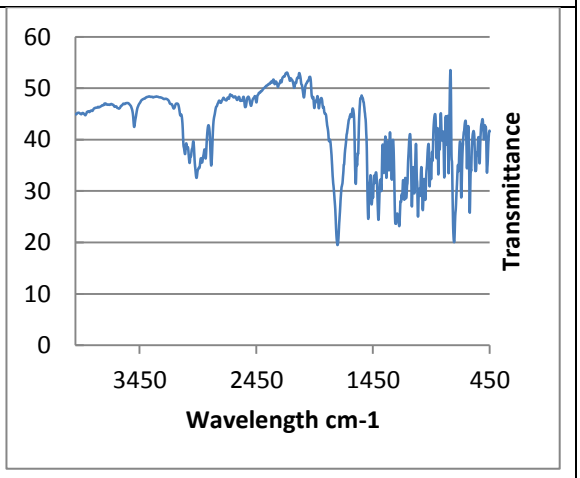

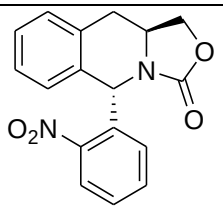

189c

^{1}H NMR	^{13}C NMR
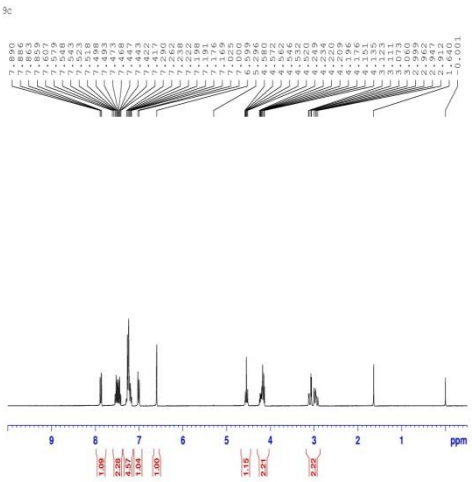	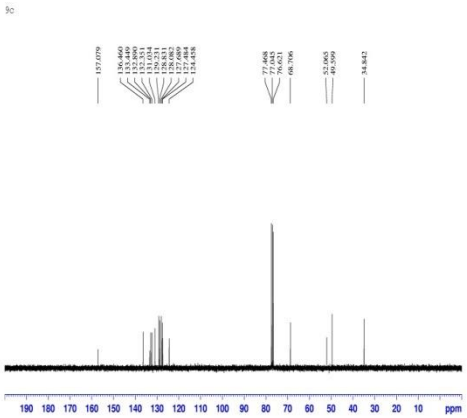
Mass	**FTIR**
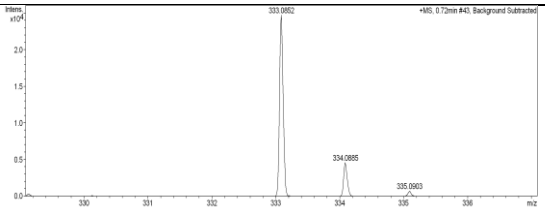	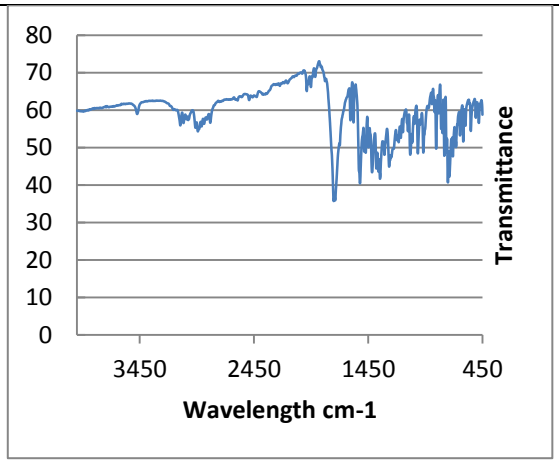

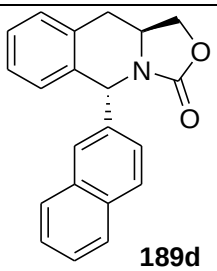

189d

^{1}H NMR	^{13}C NMR
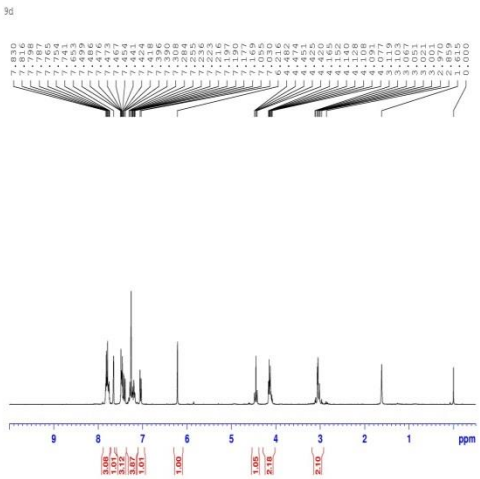	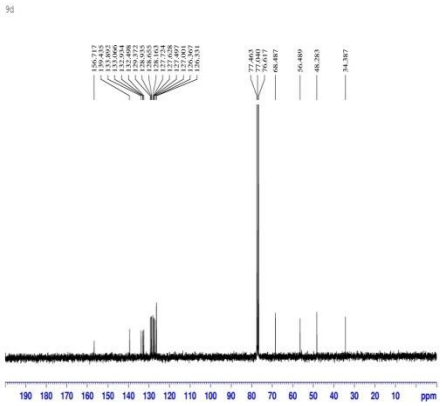

Mass	FTIR
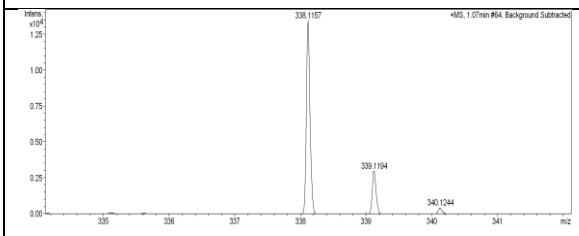	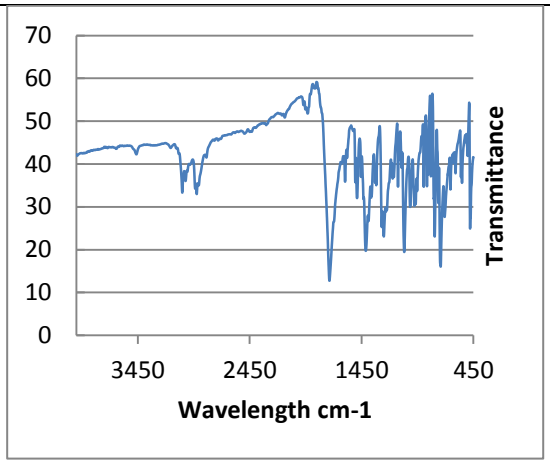

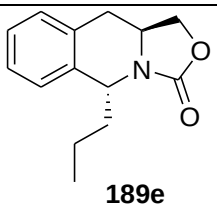

189e

^{1}H NMR	^{13}C NMR
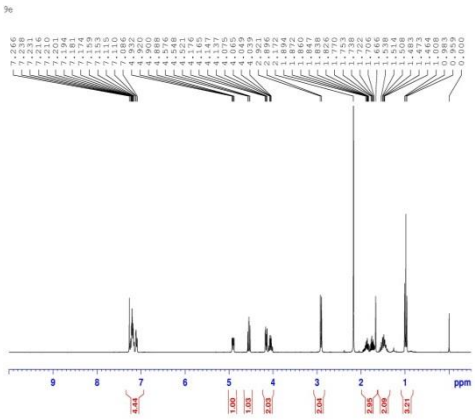	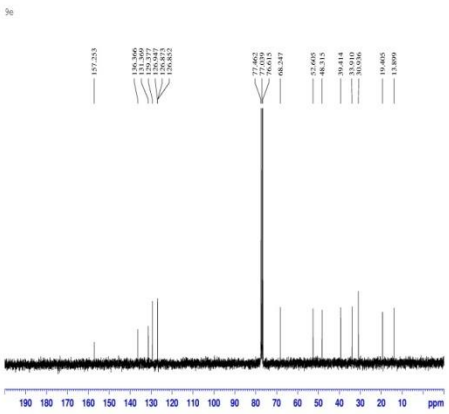
Mass	**FTIR**
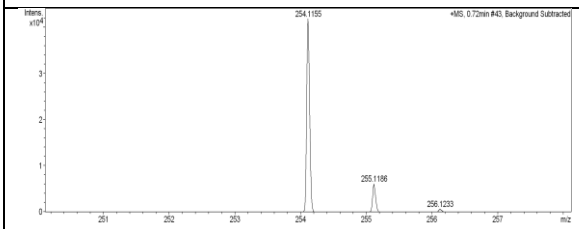	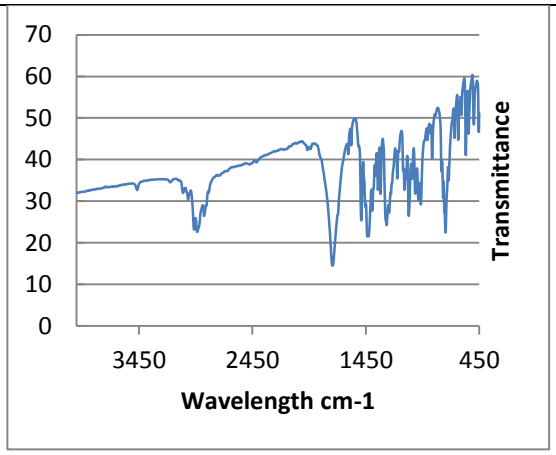

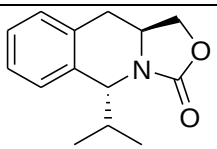

189f

^{1}H NMR	^{13}C NMR
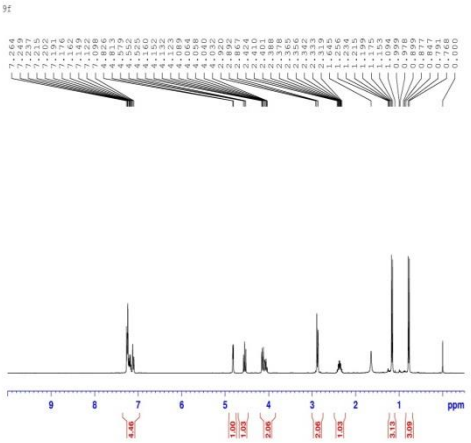	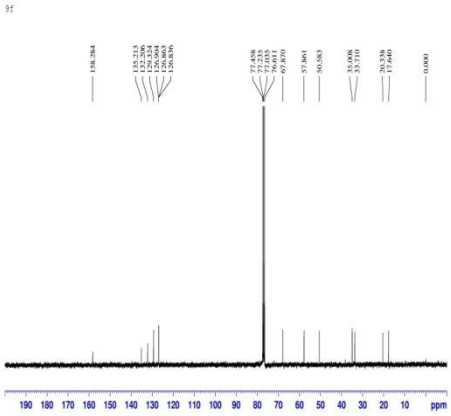
Mass	**FTIR**
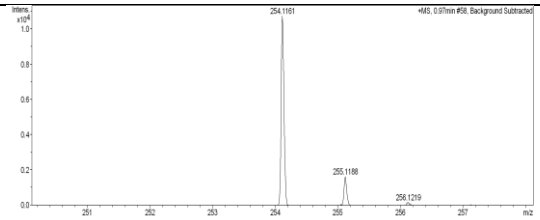	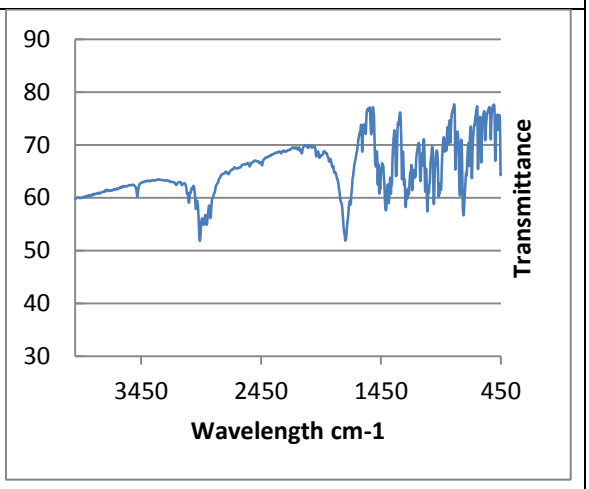

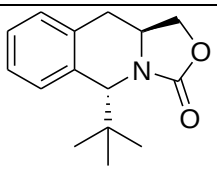

189g

^{1}H NMR	^{13}C NMR
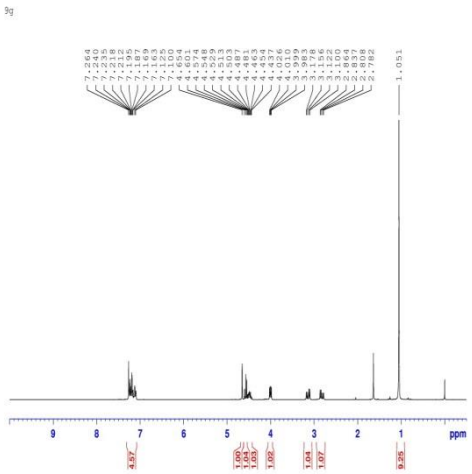	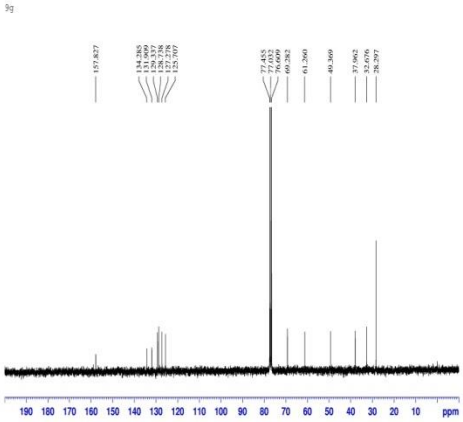
Mass	**FTIR**
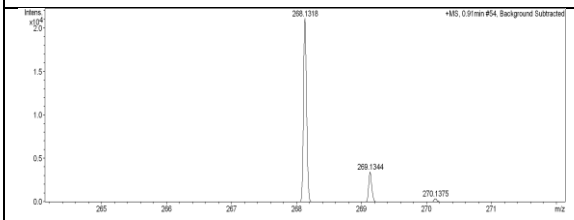	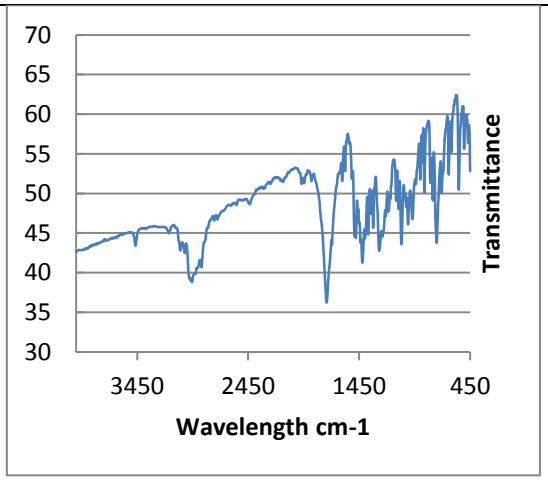

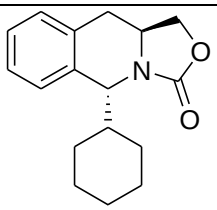

189h

^{1}H NMR	^{13}C NMR
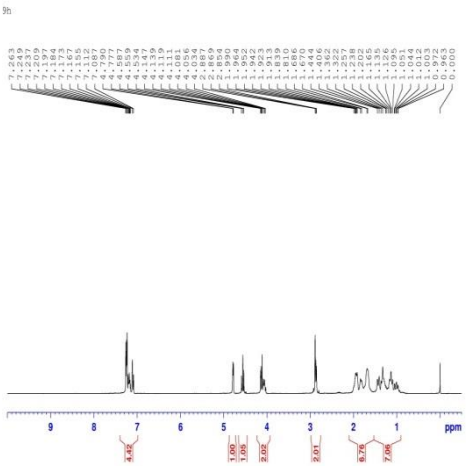	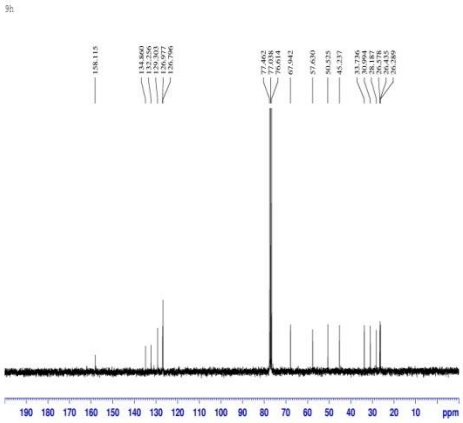
Mass	**FTIR**
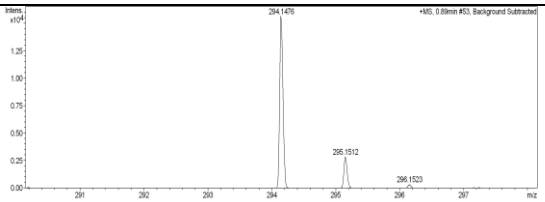	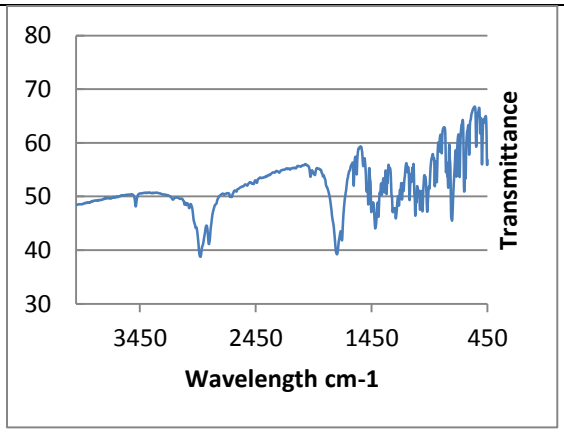

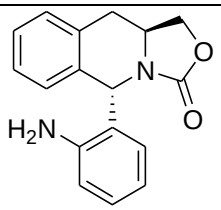

192

^{1}H NMR	^{13}C NMR
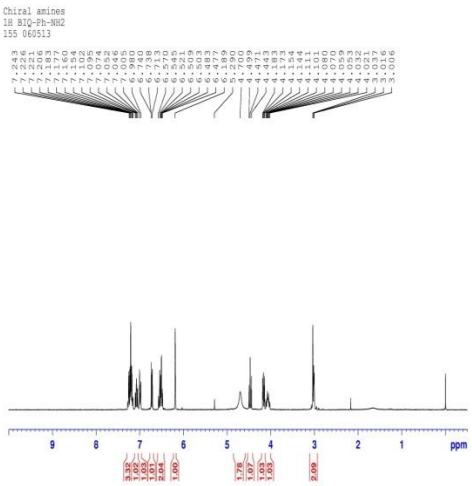	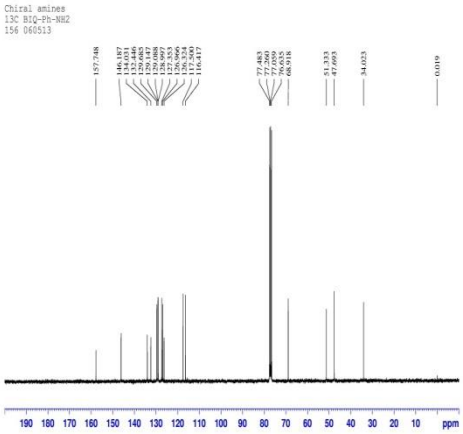
Mass	FTIR
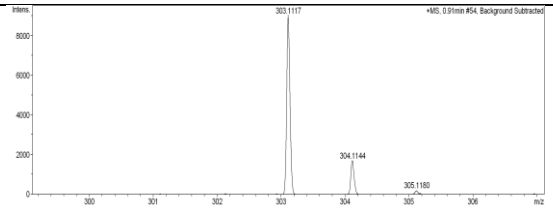	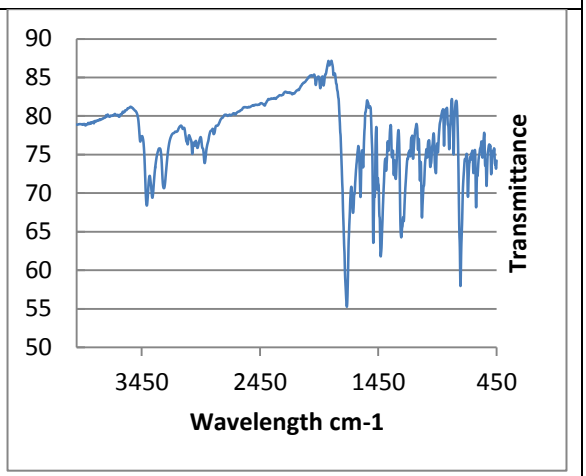

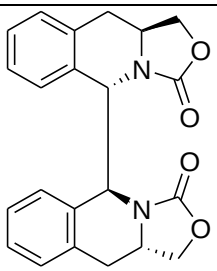

187a

^{1}H NMR	^{13}C NMR
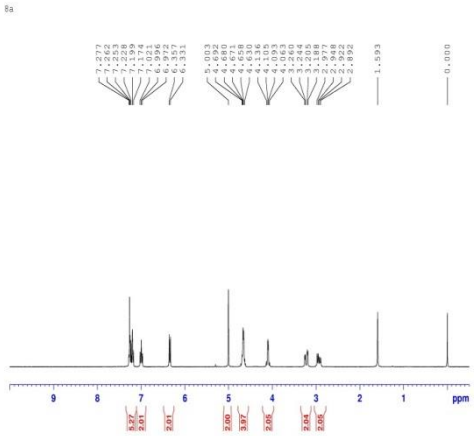	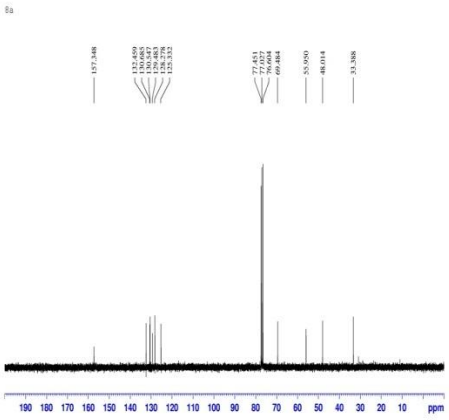
Mass	**FTIR**
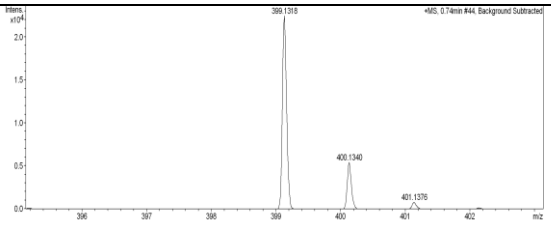	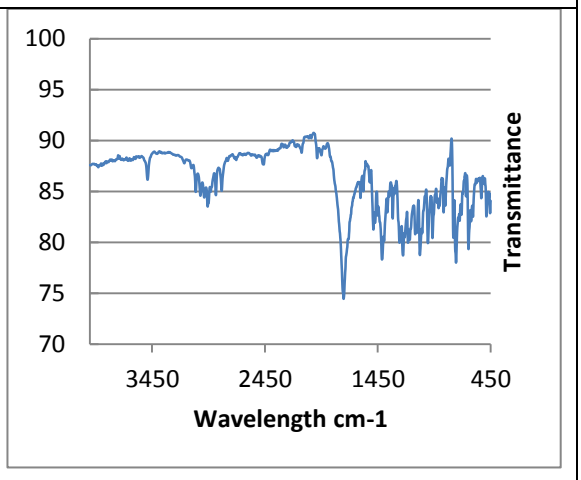

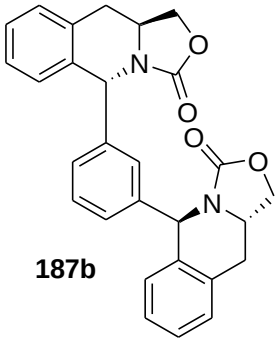

187b

^{1}H NMR	^{13}C NMR
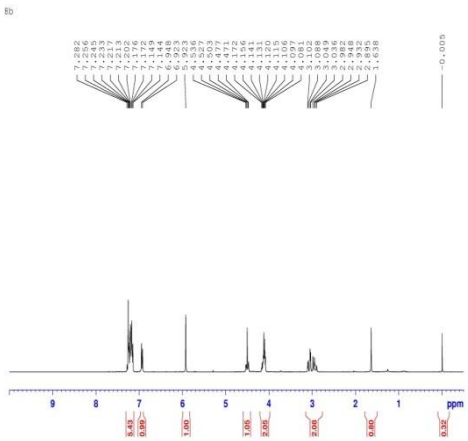	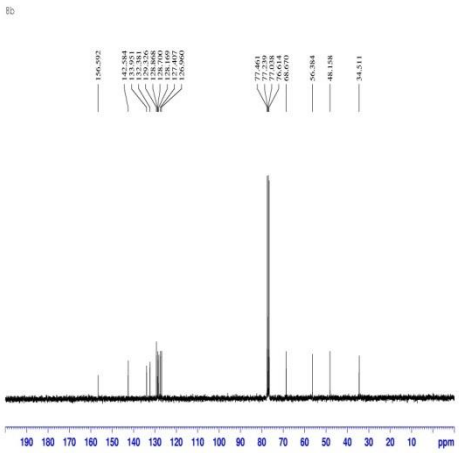
Mass	**FTIR**
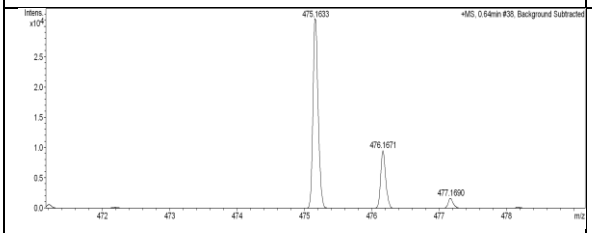	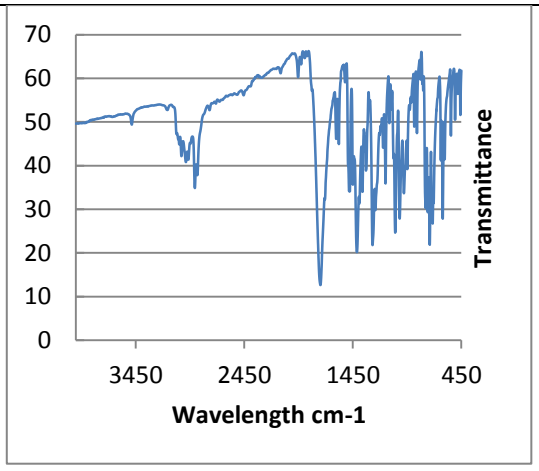

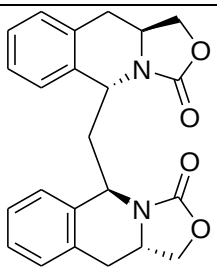

187d

^{1}H NMR	^{13}C NMR
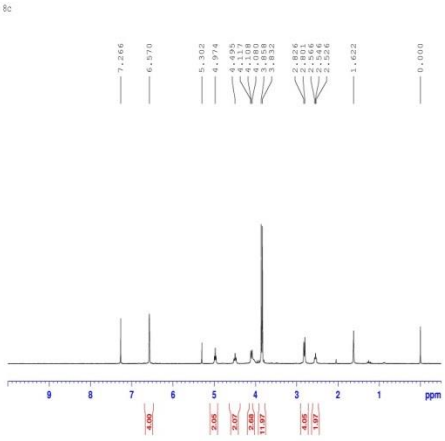	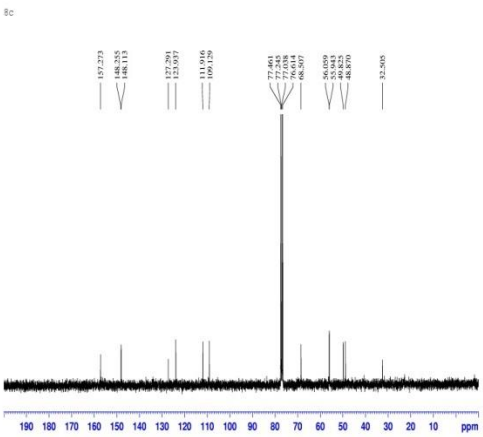
Mass	**FTIR**
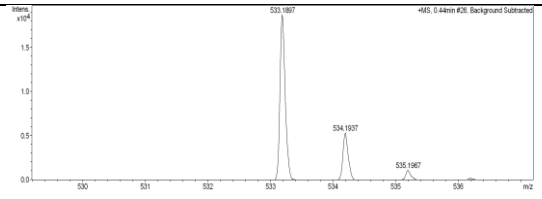	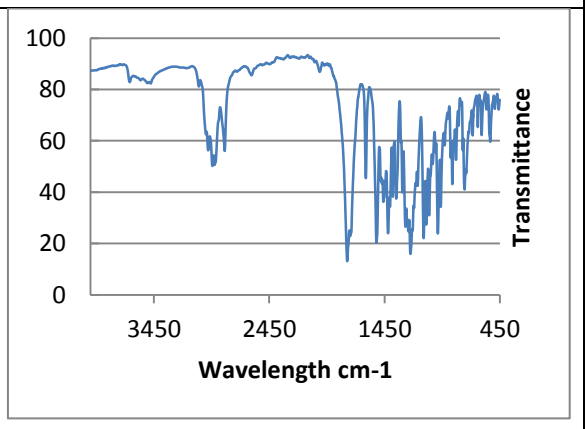

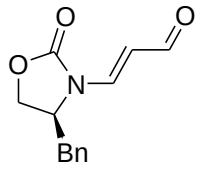

195

^{1}H NMR	^{13}C NMR
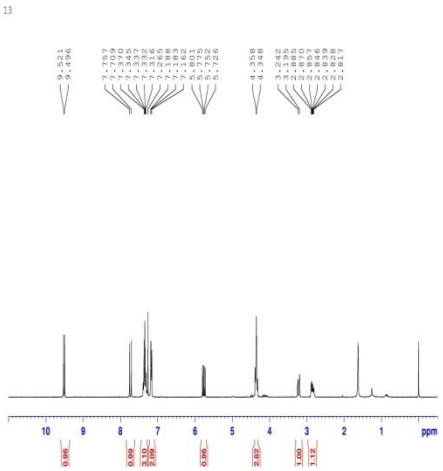	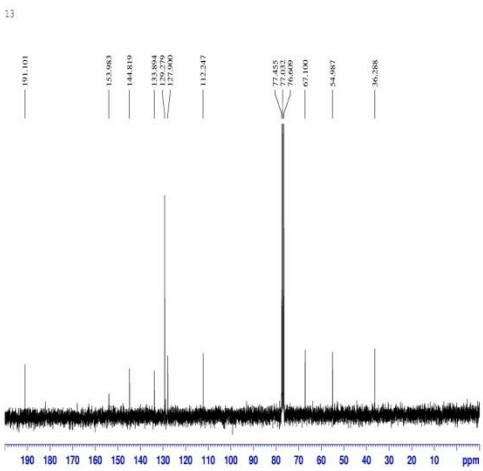
Mass	FTIR
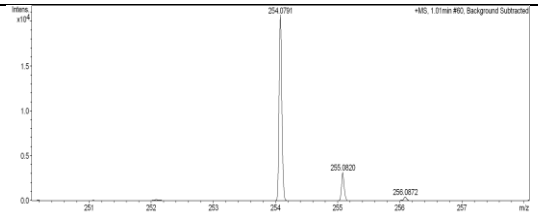	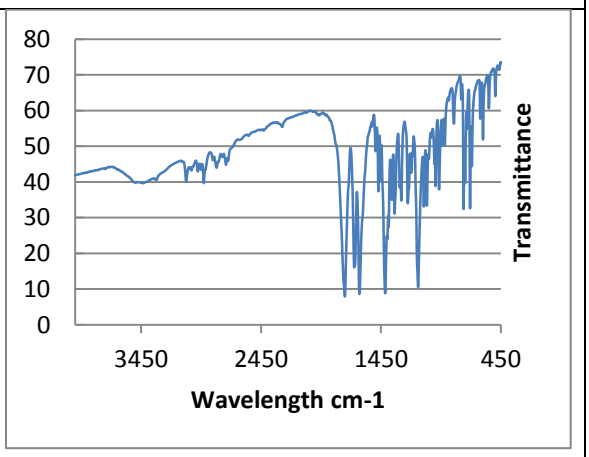

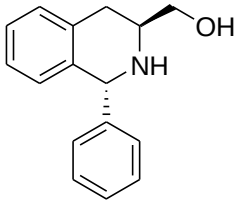

190a

^{1}H NMR	^{13}C NMR
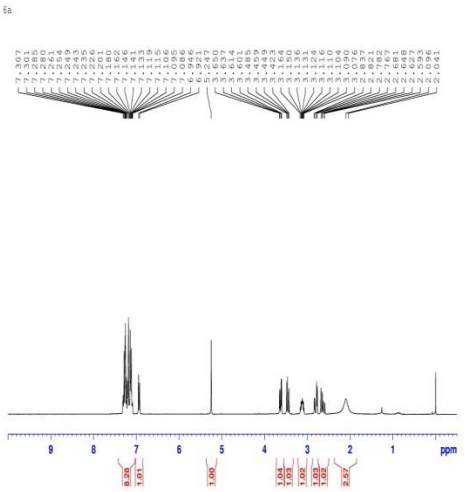	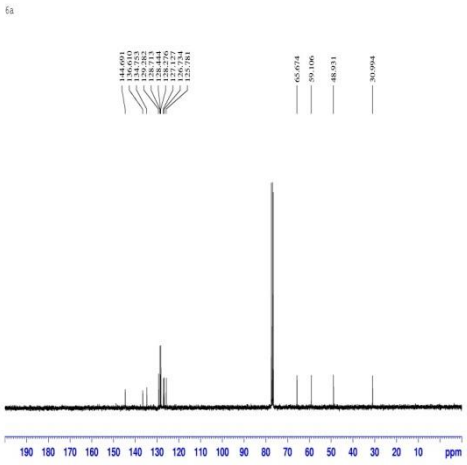

Mass	FTIR
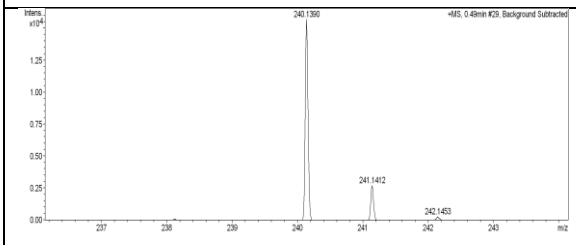	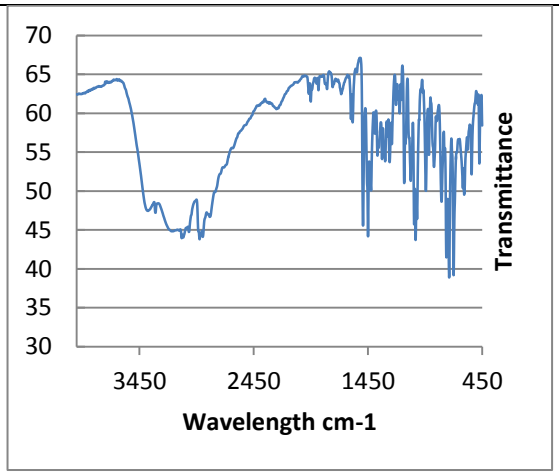

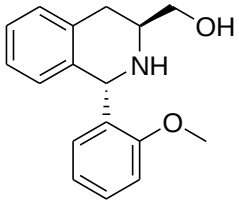

190b

^{1}H NMR	^{13}C NMR
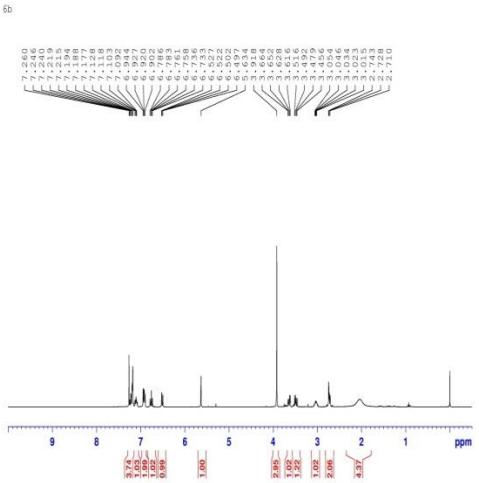	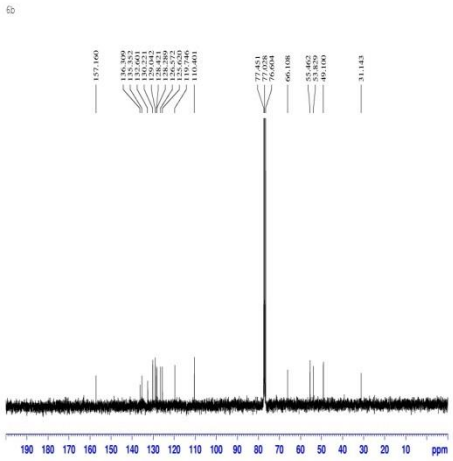

Mass	FTIR
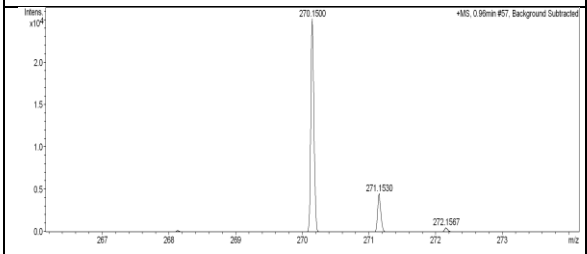	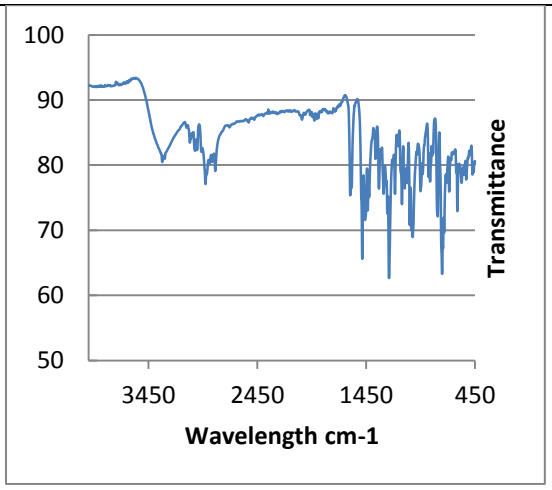

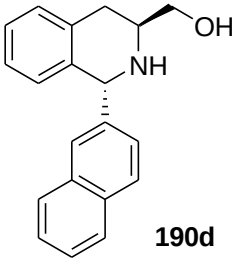

190d

^{1}H NMR	^{13}C NMR
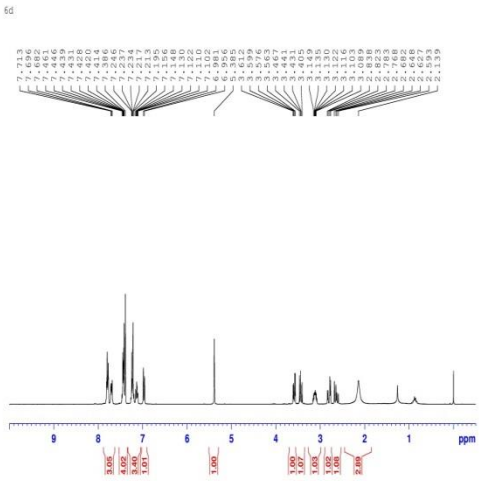	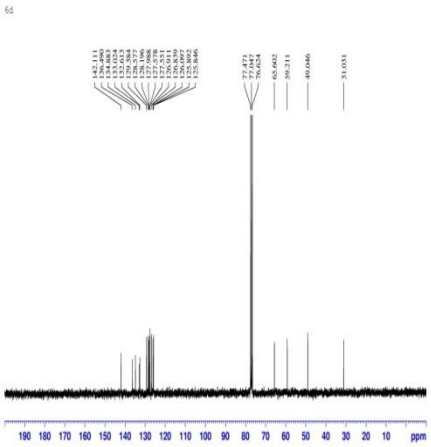
Mass	FTIR
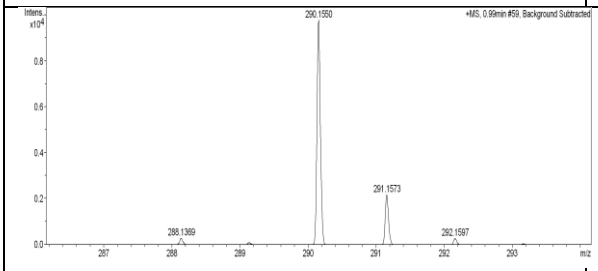	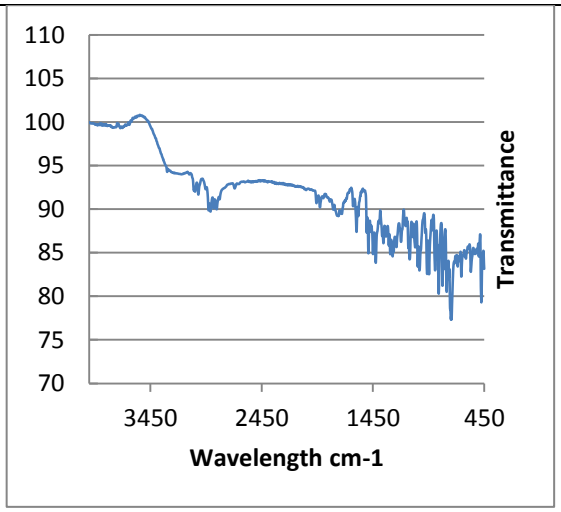

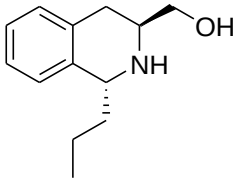

190e

^{1}H NMR	^{13}C NMR
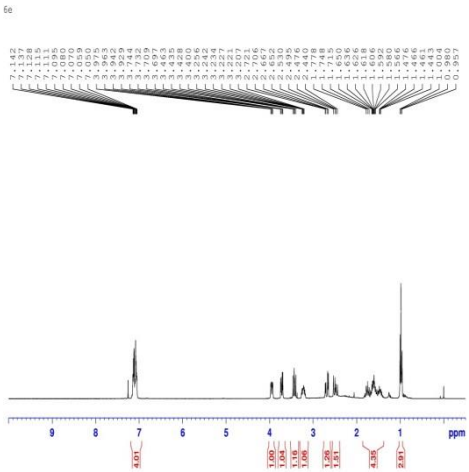	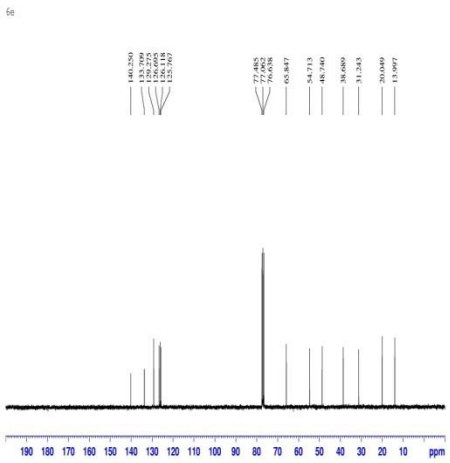
Mass	FTIR
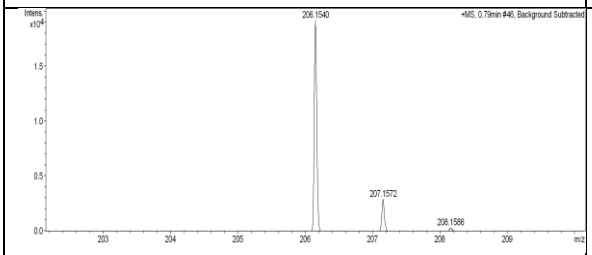	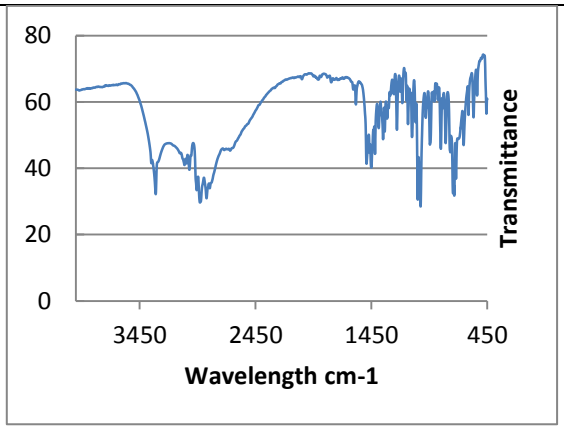

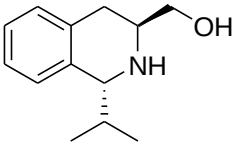

190f

^{1}H NMR	^{13}C NMR
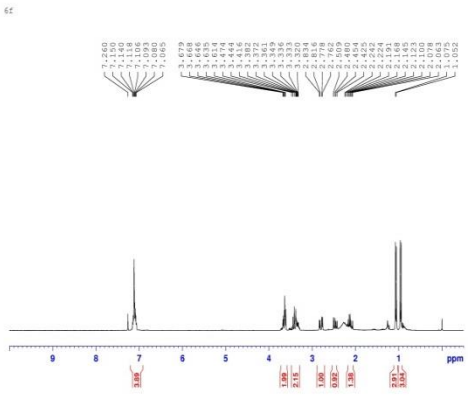	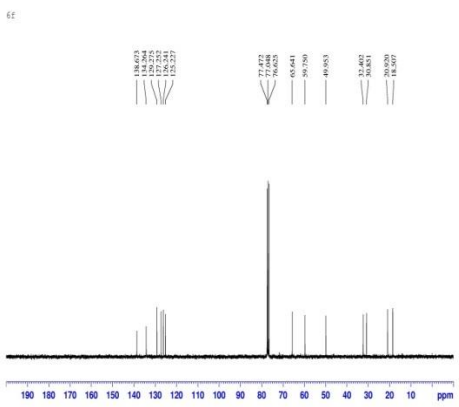
Mass	**FTIR**
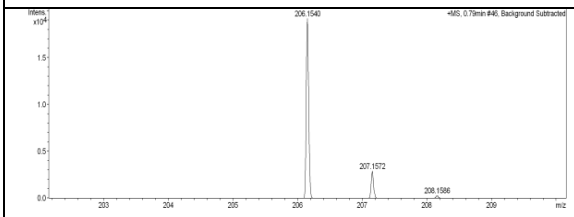	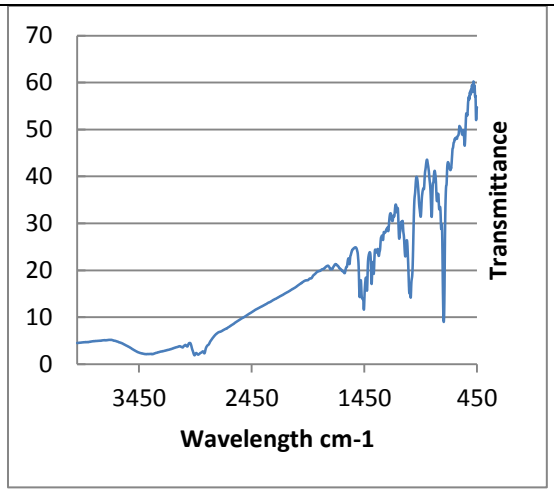

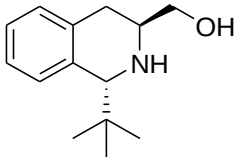

190g

^{1}H NMR	^{13}C NMR
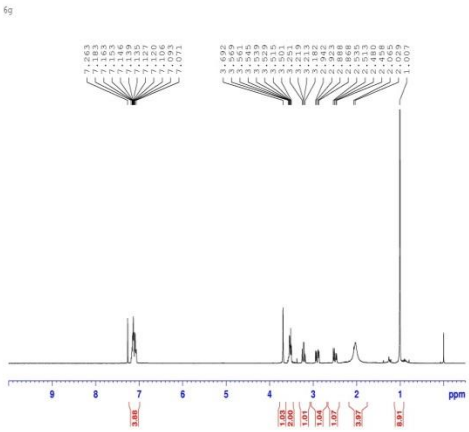	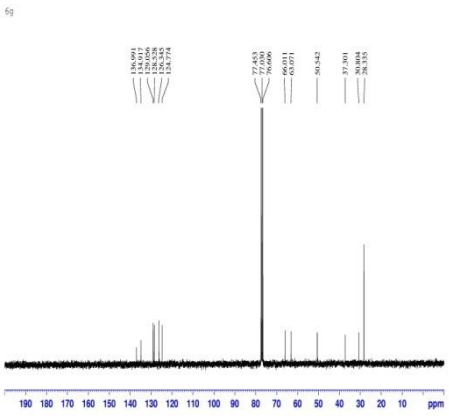
Mass	**FTIR**
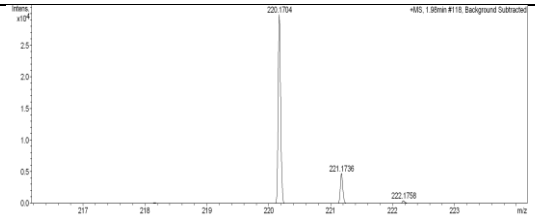	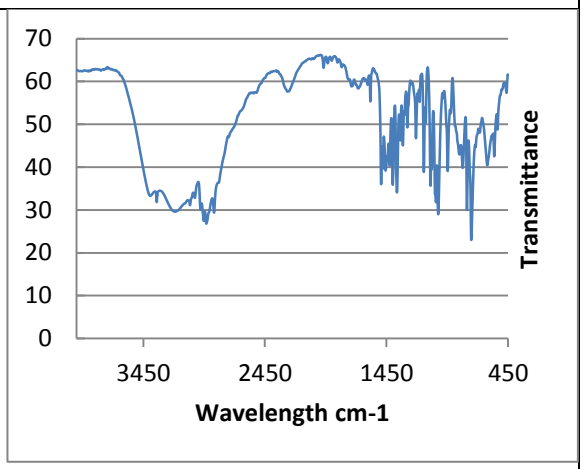

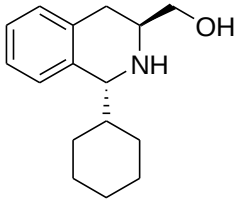

190h

^{1}H NMR	^{13}C NMR
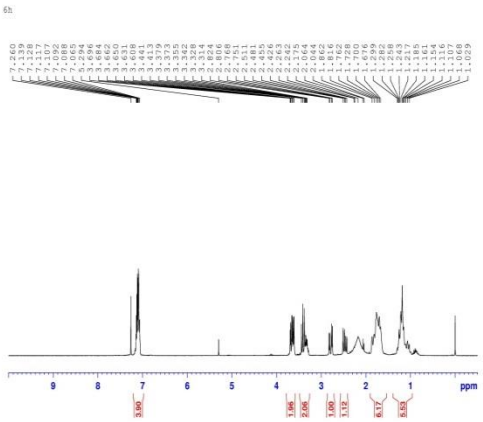	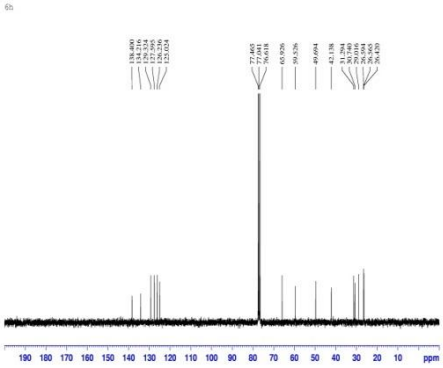
Mass	**FTIR**
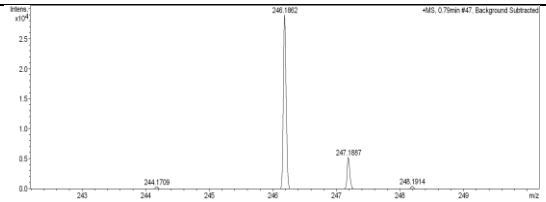	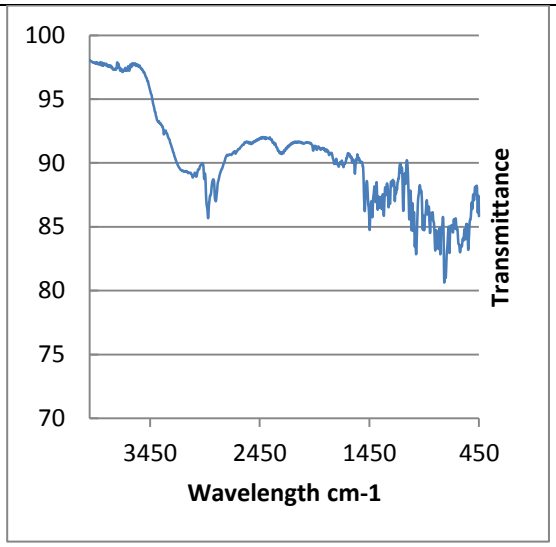

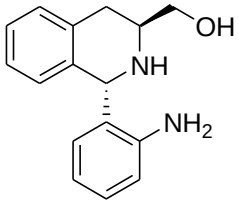

193

^{1}H NMR	^{13}C NMR
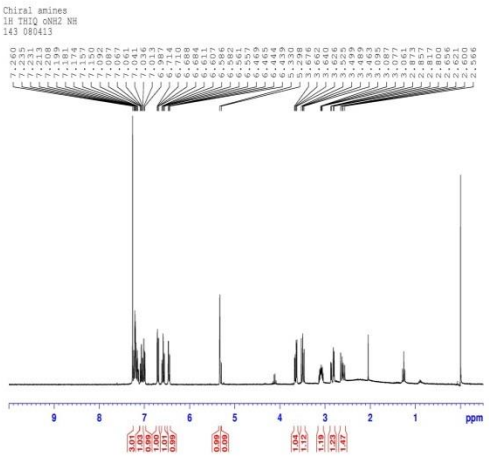	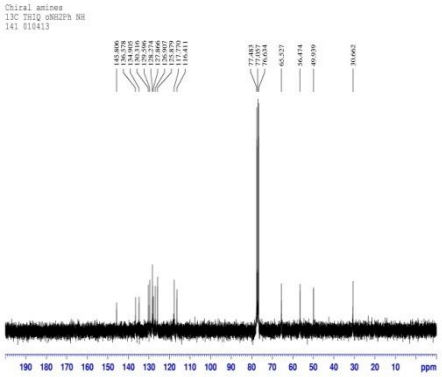
Mass	FTIR
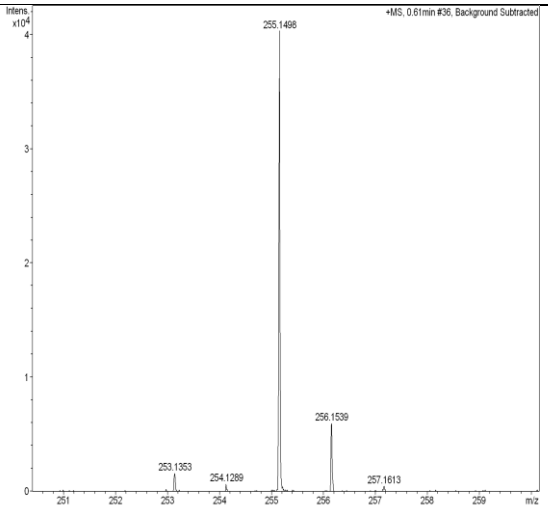	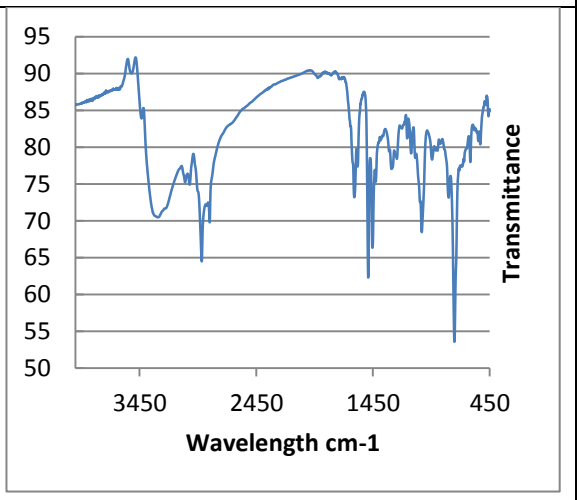

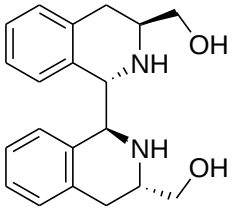

188a

^{1}H NMR	^{13}C NMR
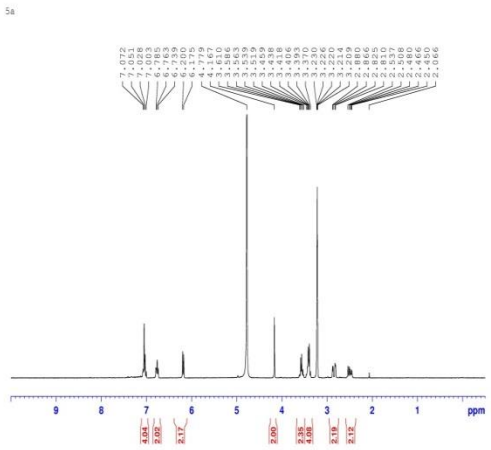	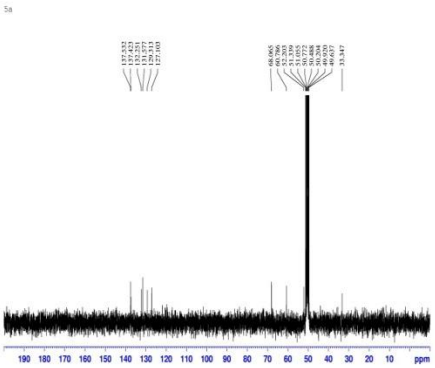
Mass	**FTIR**
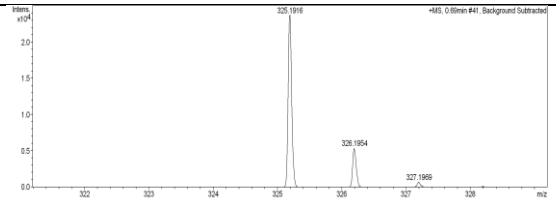	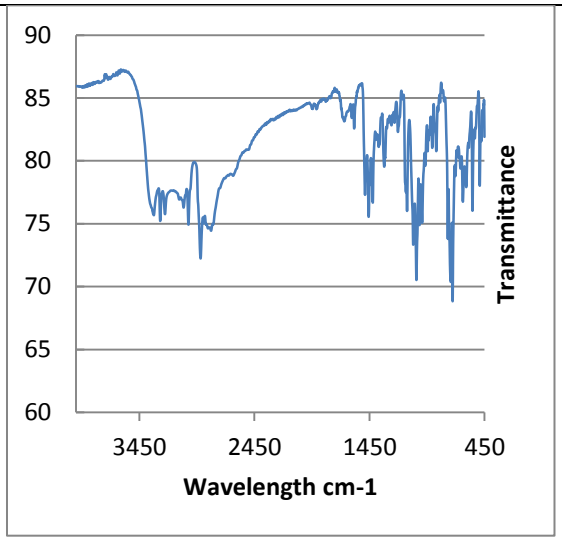

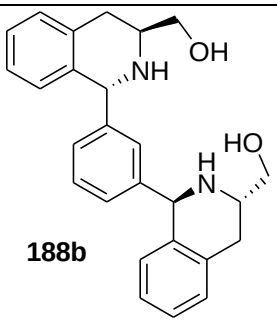

188b

^{1}H NMR	^{13}C NMR
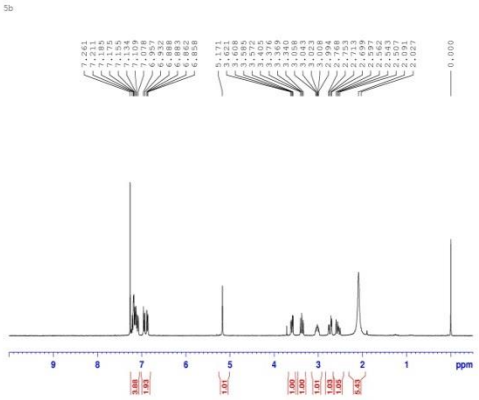	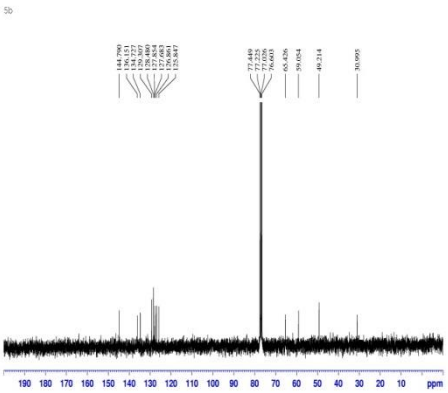
Mass	**FTIR**
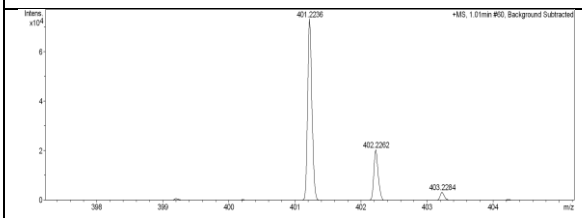	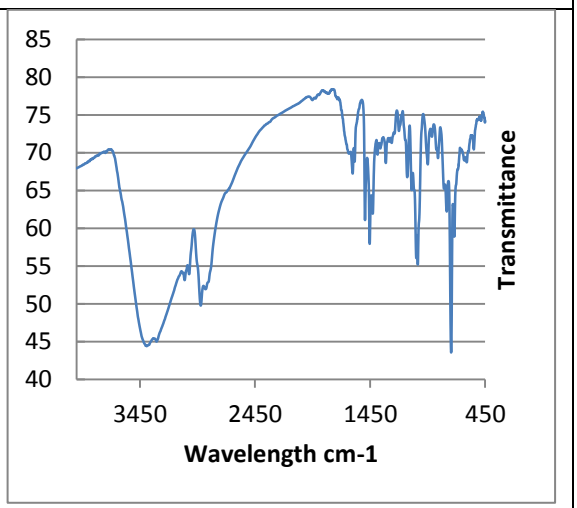

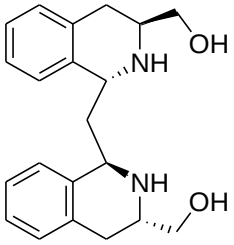

188d

^{1}H NMR	^{13}C NMR
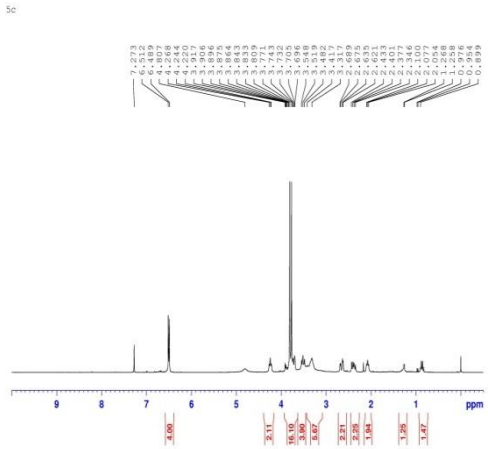	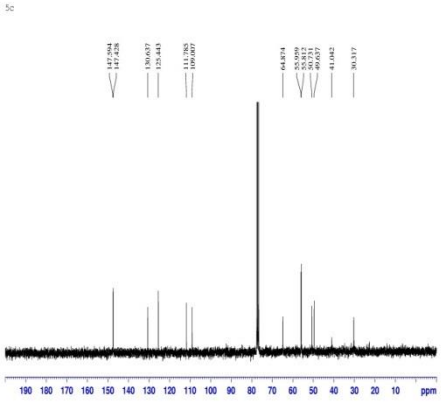
Mass	**FTIR**
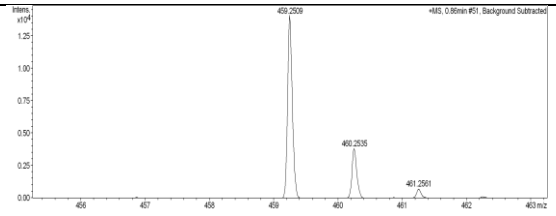	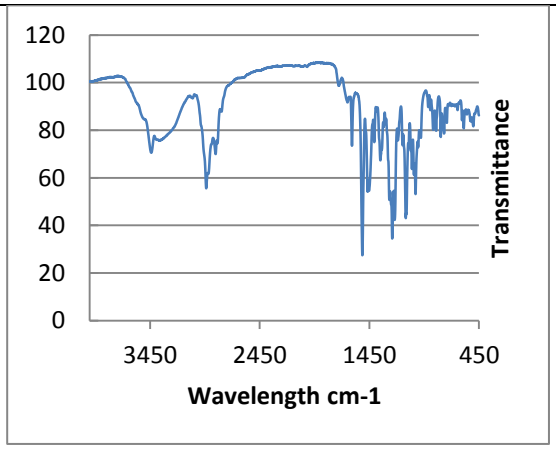

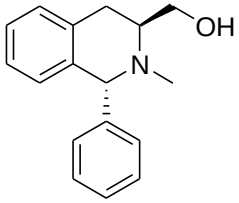

202a

^{1}H NMR	^{13}C NMR
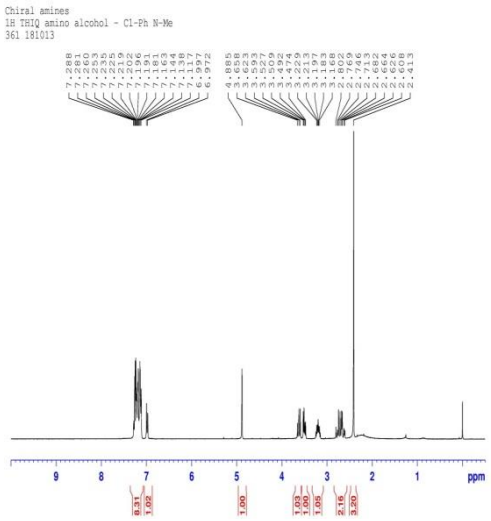	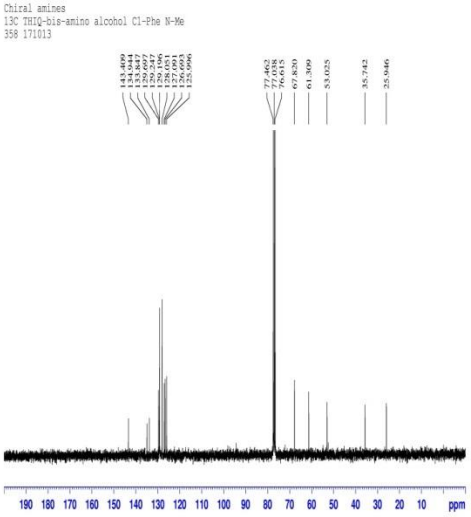
Mass	FTIR
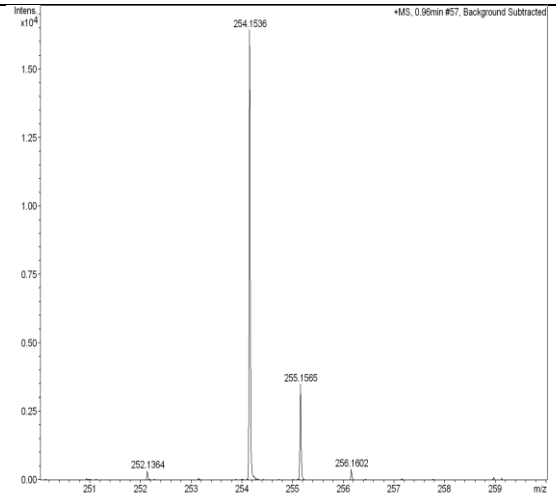	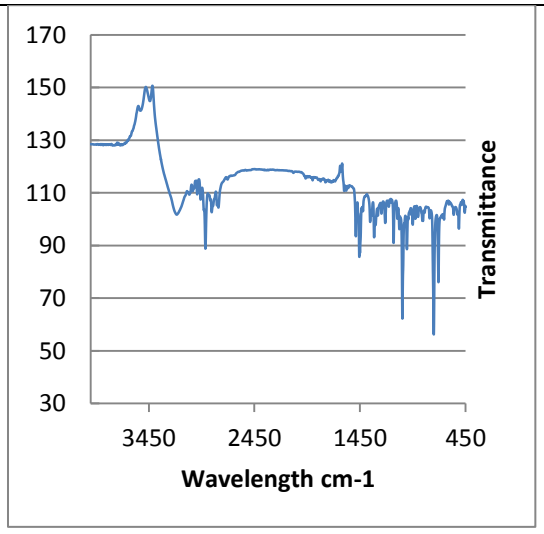

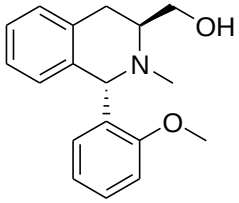

202b

^{1}H NMR	^{13}C NMR
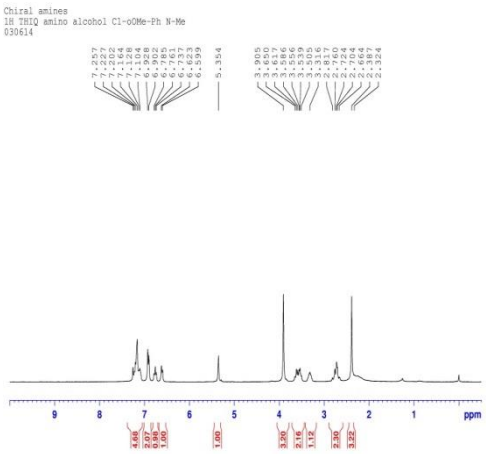	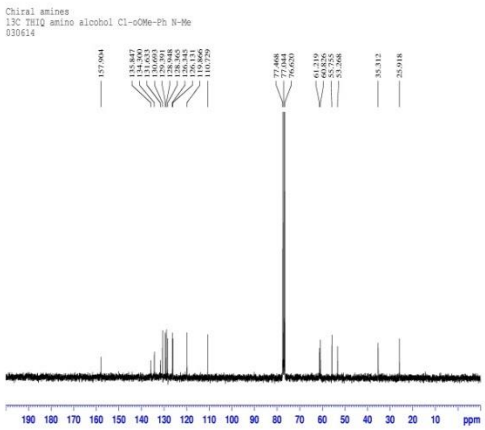
Mass	**FTIR**
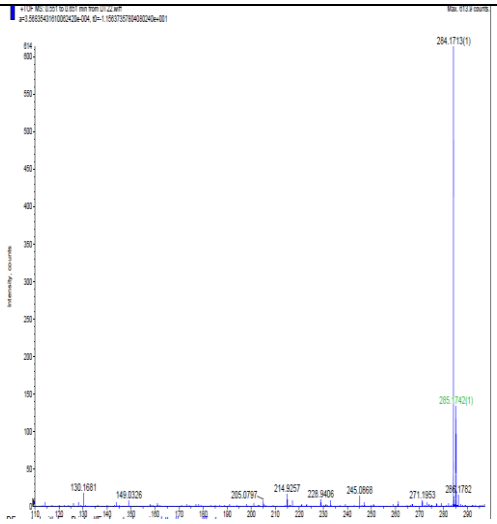	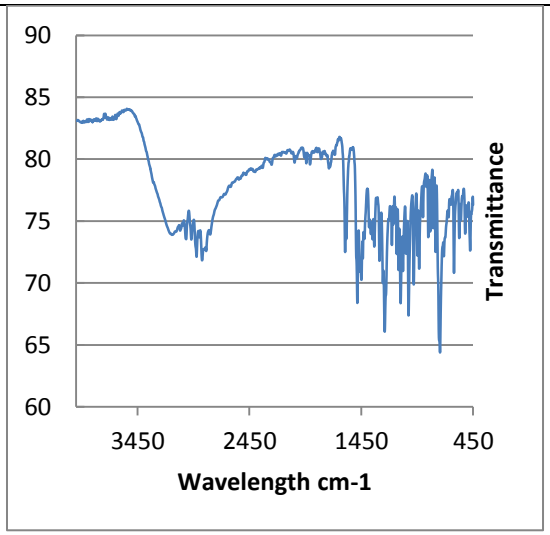

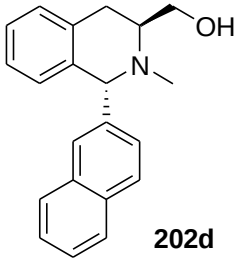

202d

^{1}H NMR	^{13}C NMR
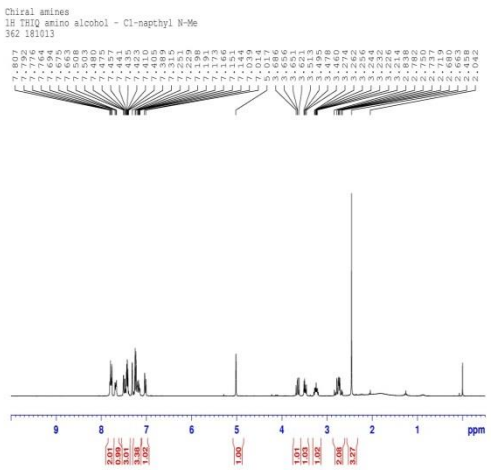	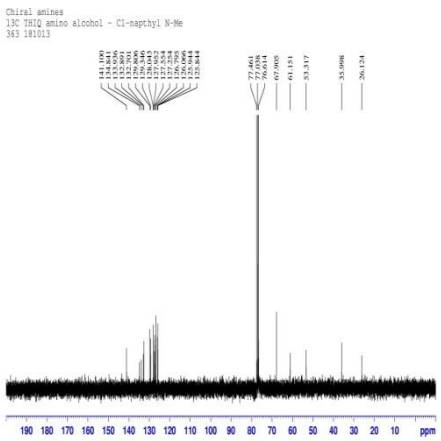

Mass	FTIR
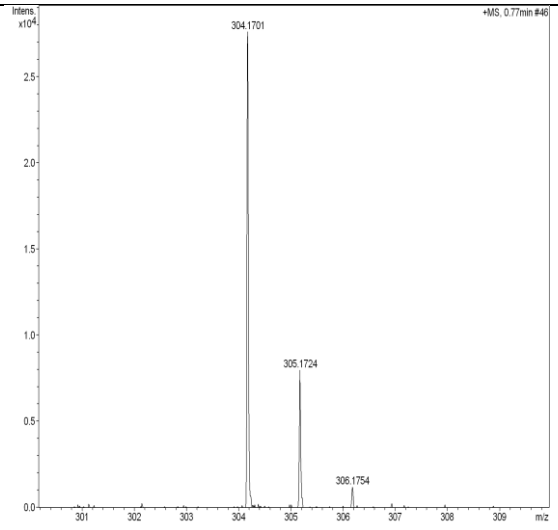	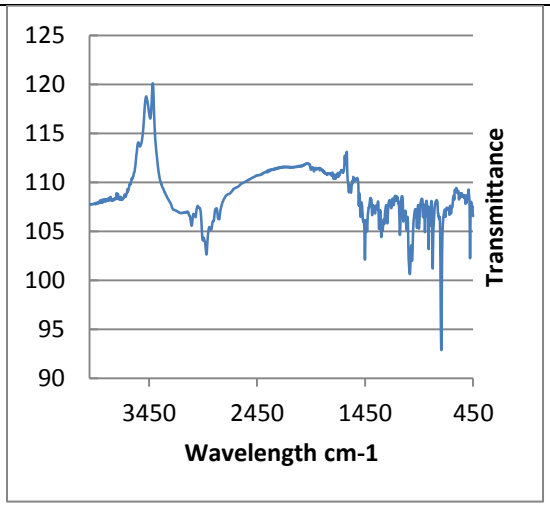

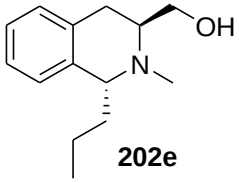

202e

^{1}H NMR	^{13}C NMR
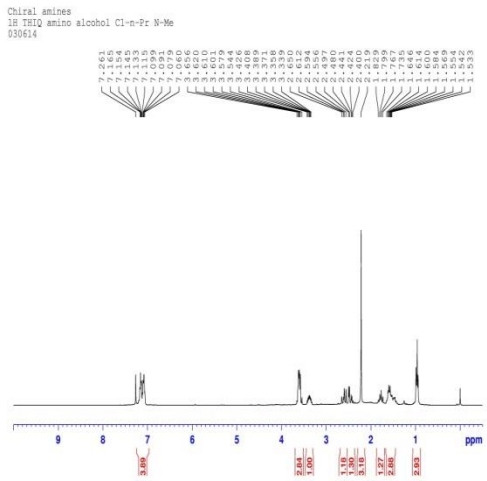	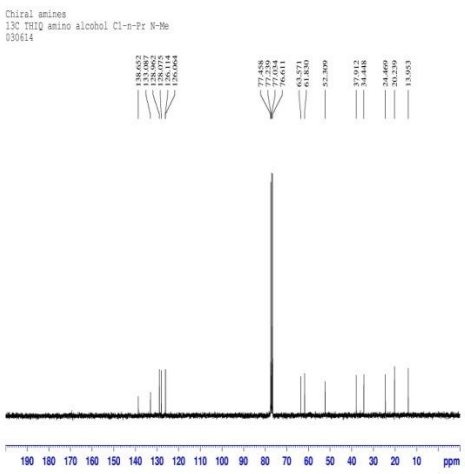

Mass	FTIR
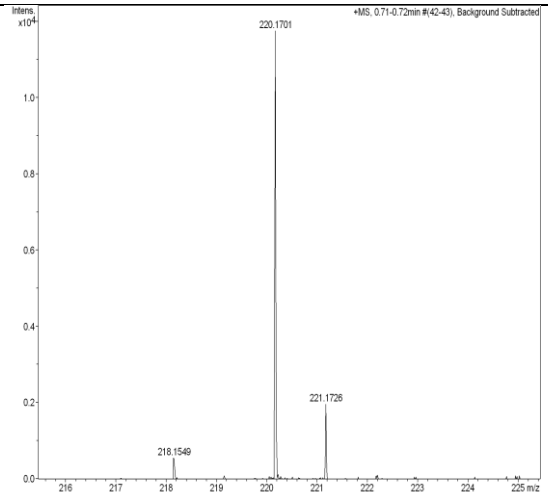	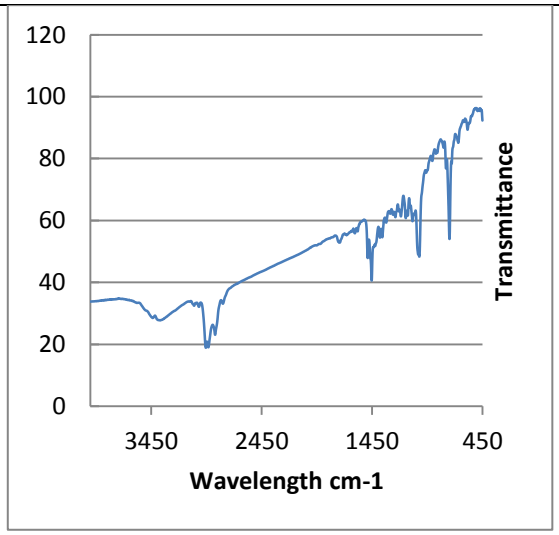

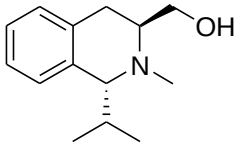

202f

^{1}H NMR	^{13}C NMR
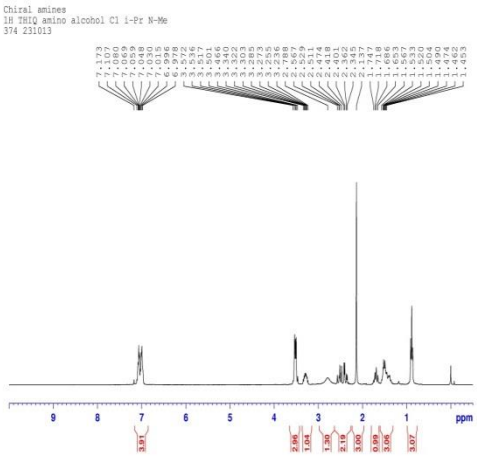	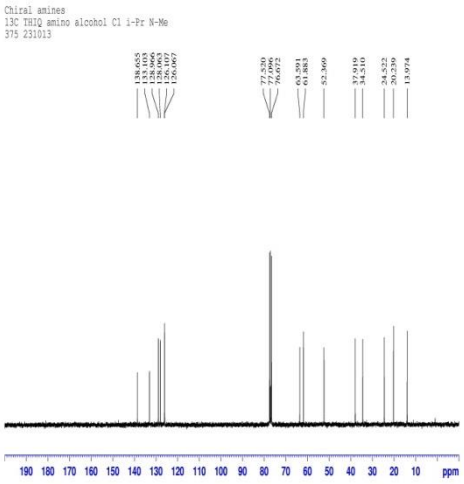
Mass	**FTIR**
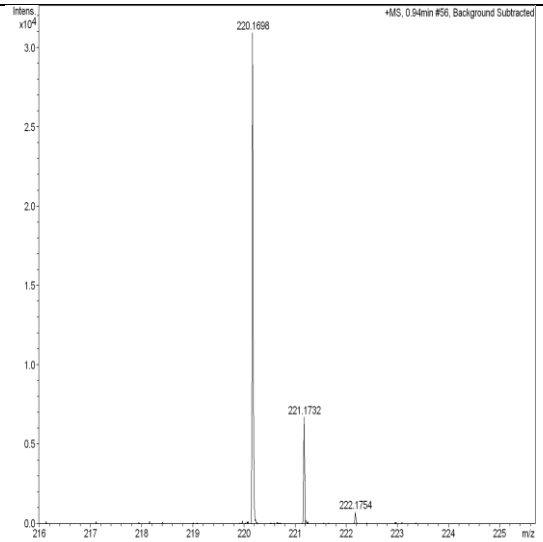	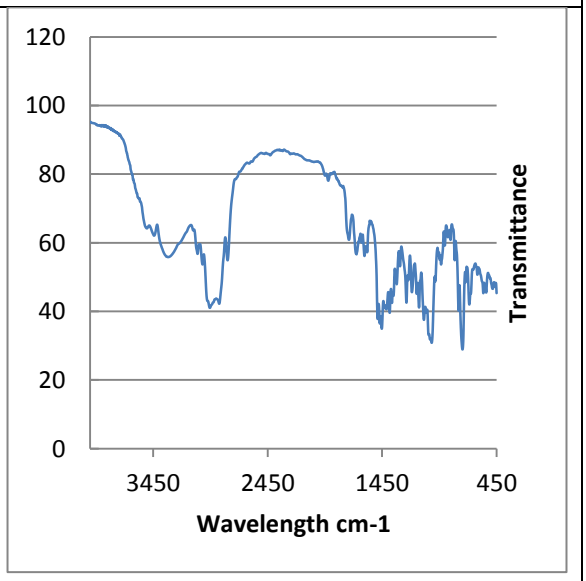

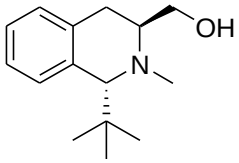

202g

^{1}H NMR	^{13}C NMR
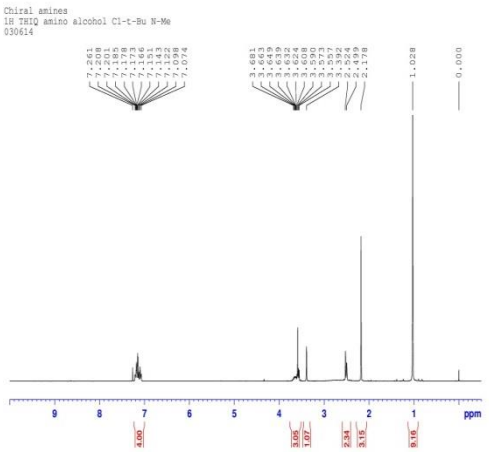	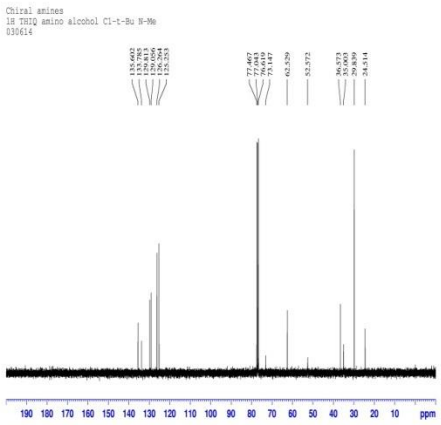
Mass	**FTIR**
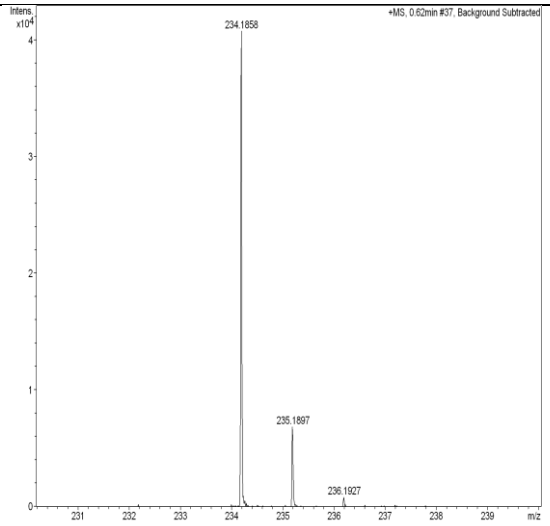	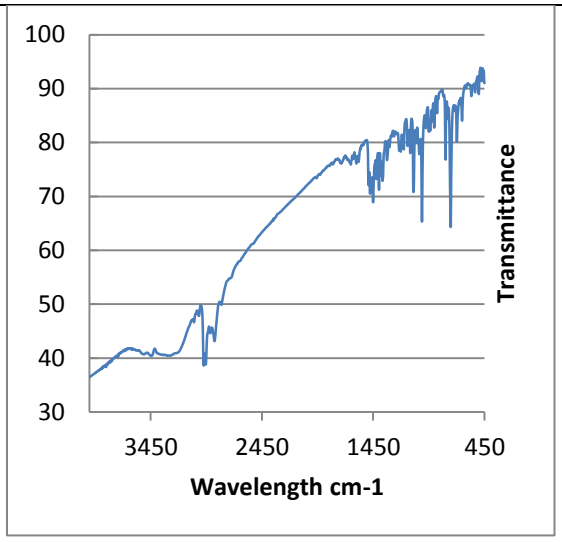

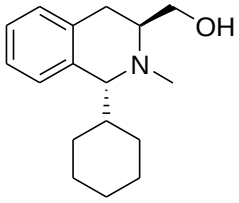

202h

^{1}H NMR	^{13}C NMR
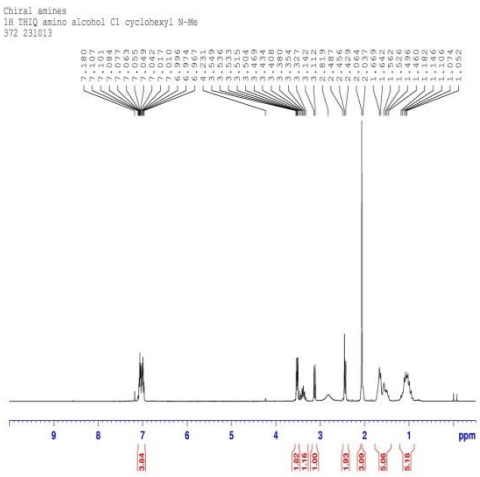	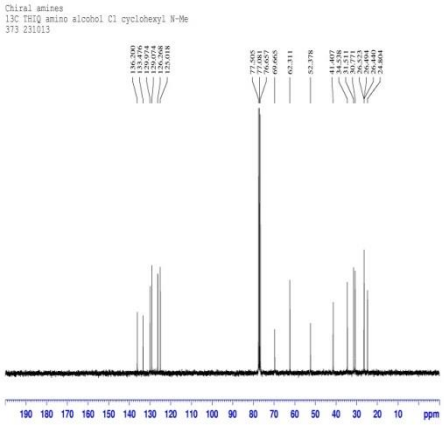
Mass	**FTIR**
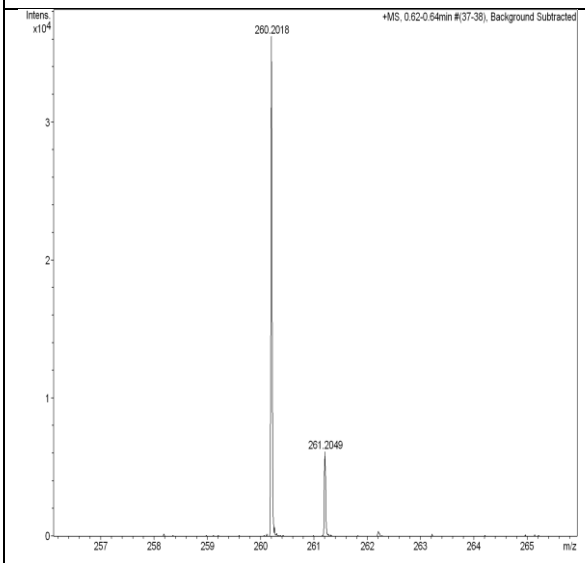	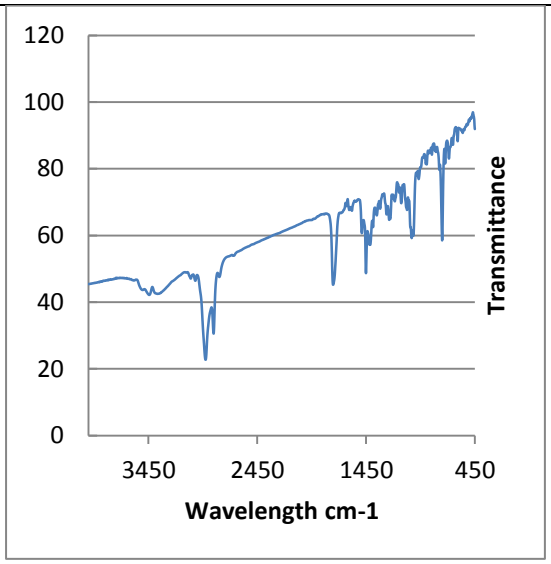

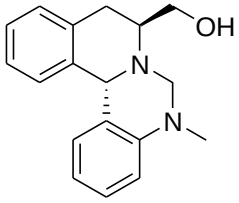

203

^{1}H NMR	^{13}C NMR
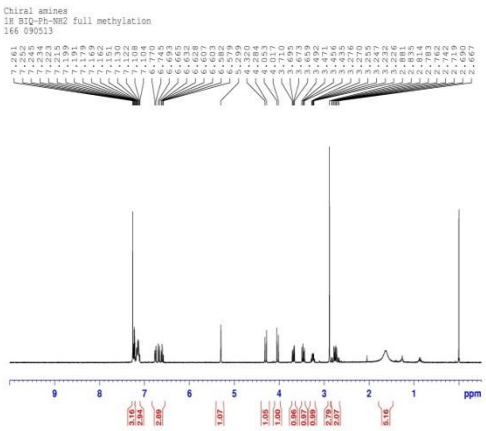	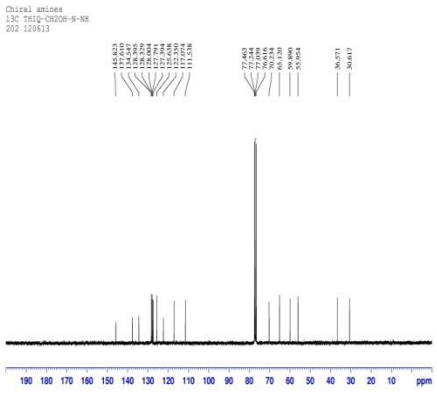
Mass	**FTIR**
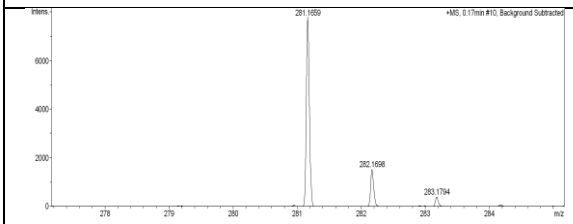	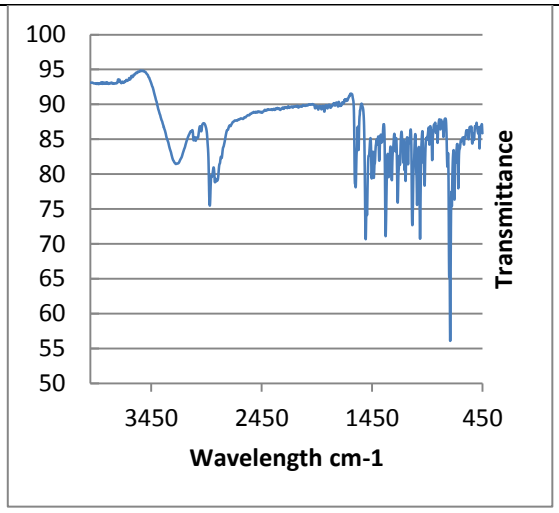

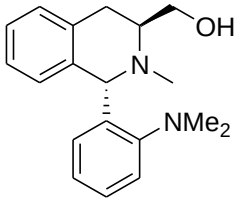

204

^{1}H NMR	^{13}C NMR
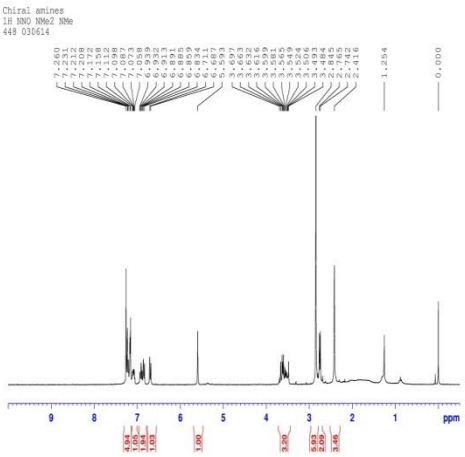	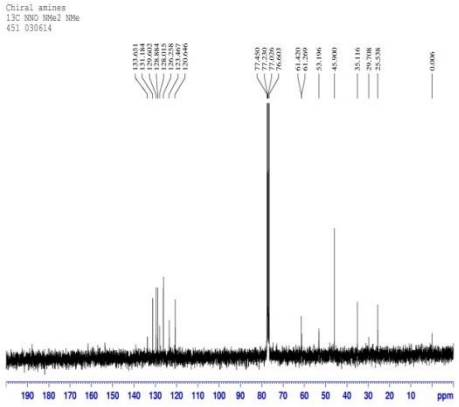
Mass	**FTIR**
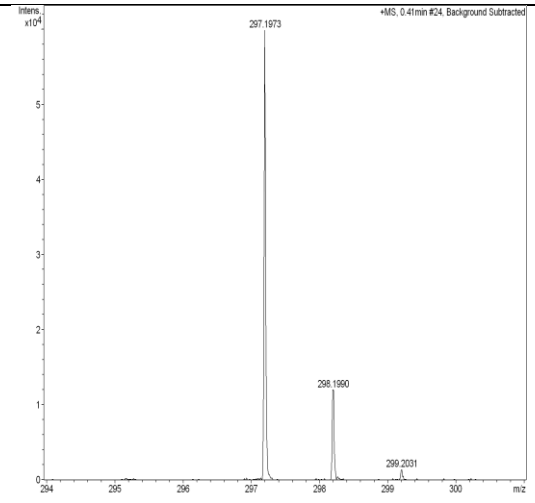	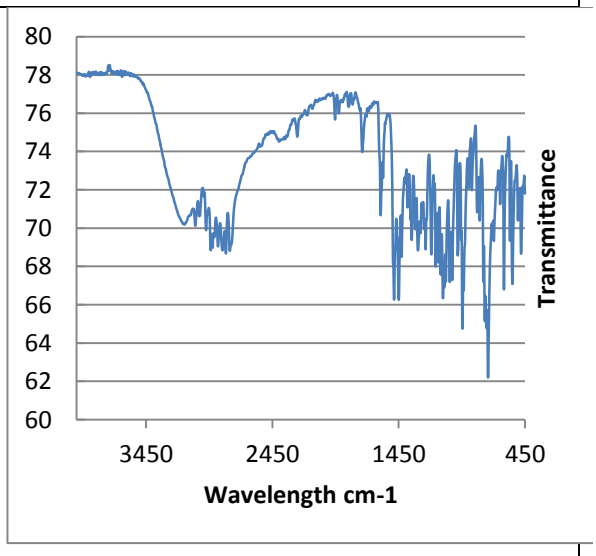

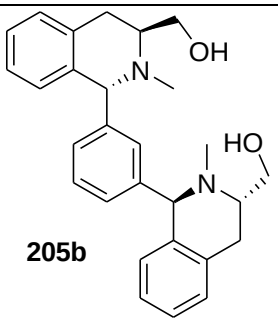

205b

^{1}H NMR	^{13}C NMR
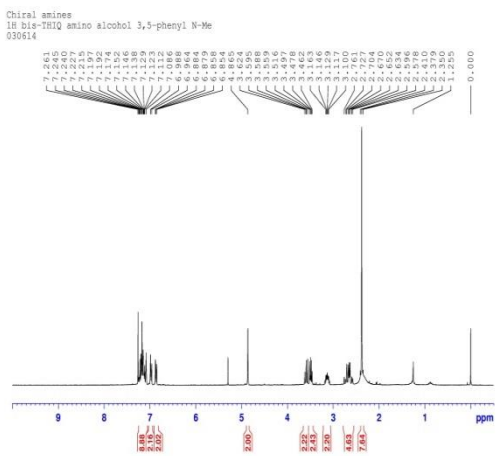	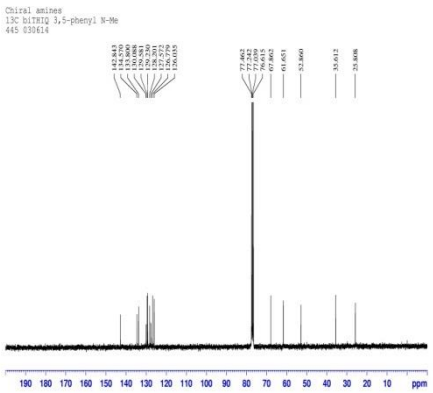
Mass	FTIR
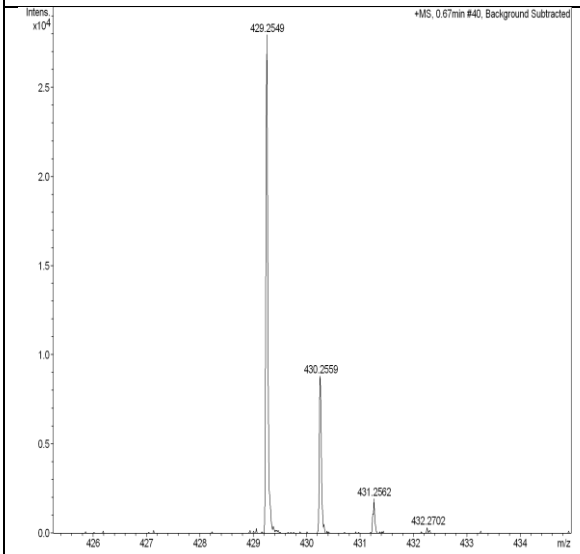	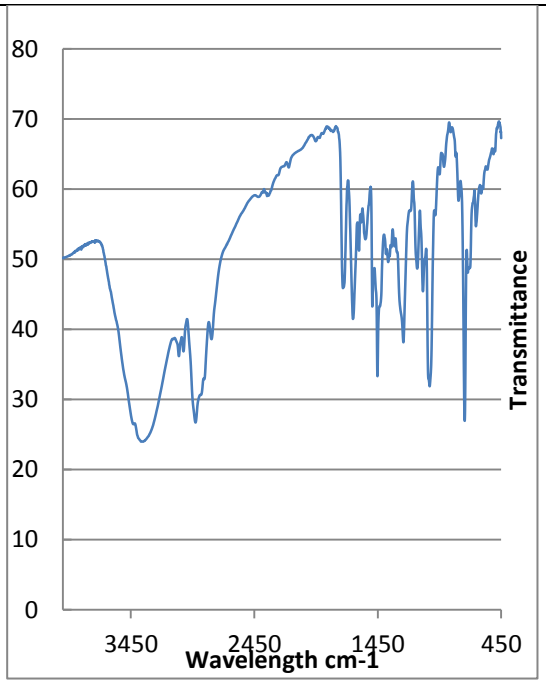

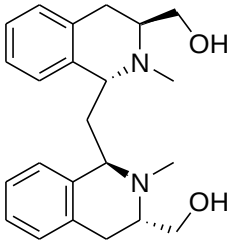

205d

^{1}H NMR	^{13}C NMR
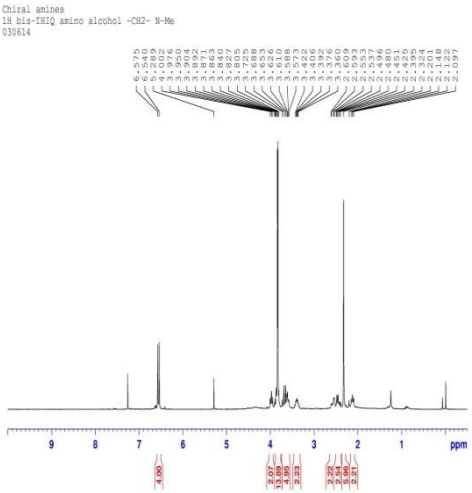	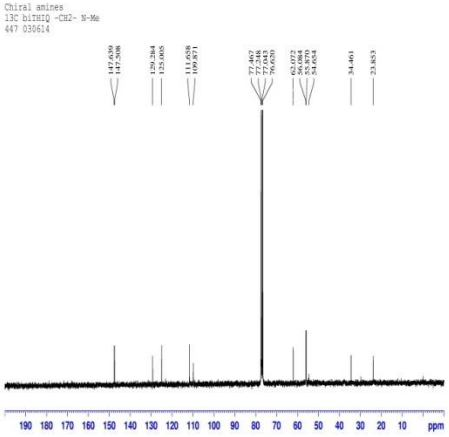
Mass	**FTIR**
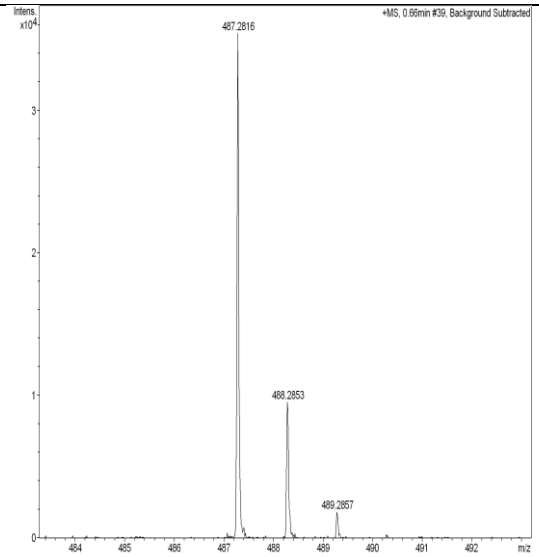	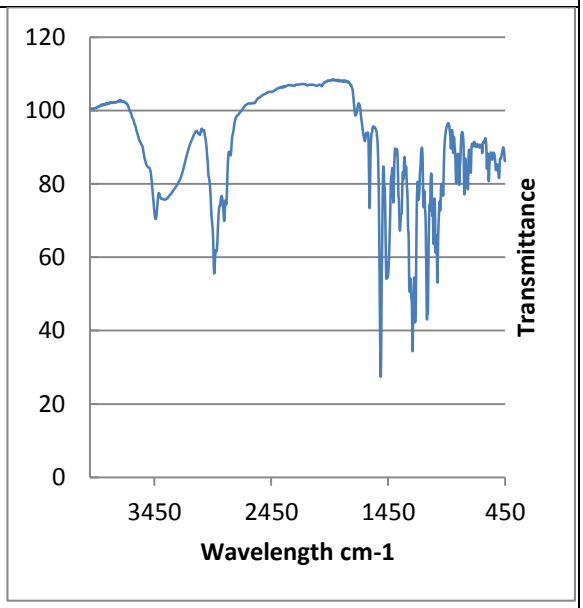

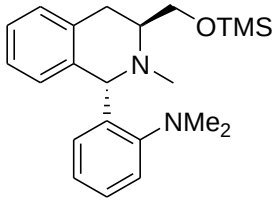

206a

^{1}H NMR	^{13}C NMR
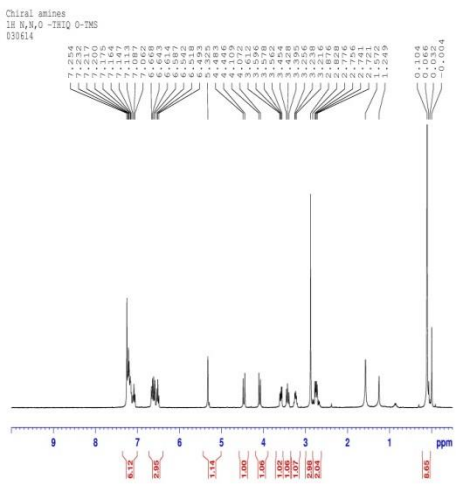	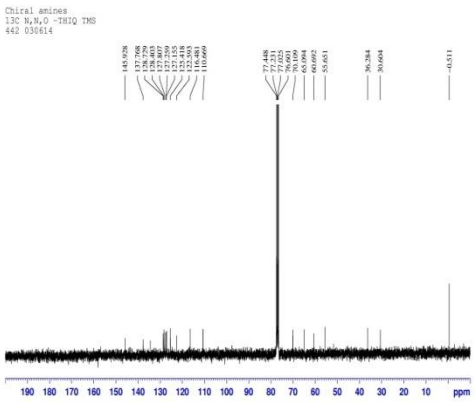
Mass	**FTIR**
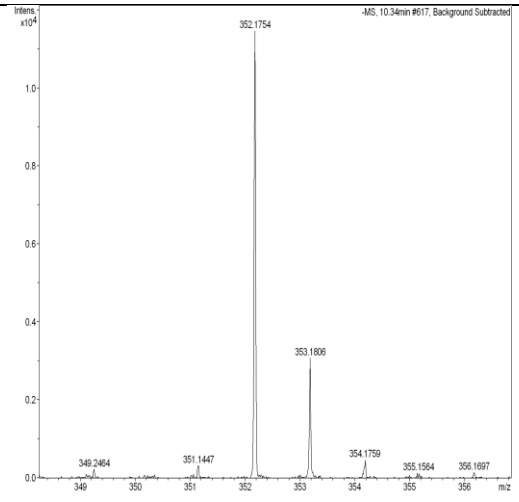	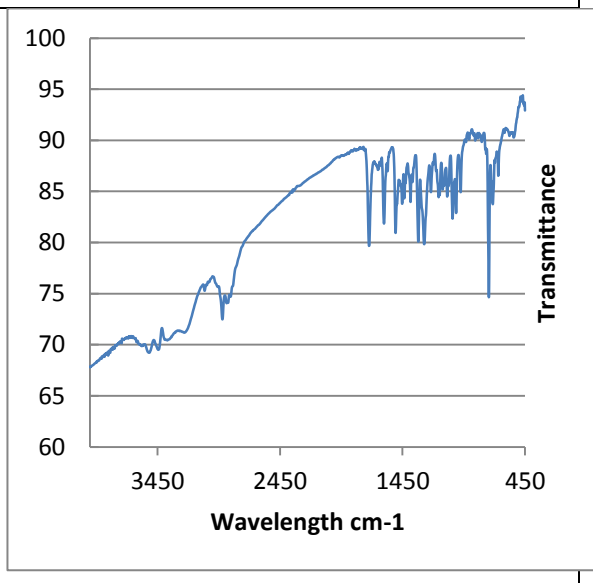

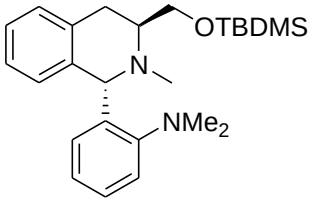

206b

^{1}H NMR	^{13}C NMR
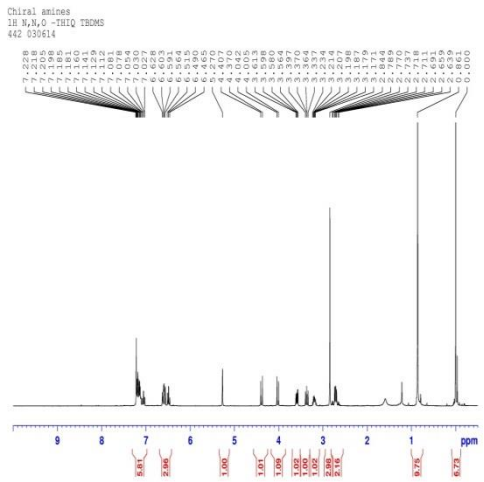	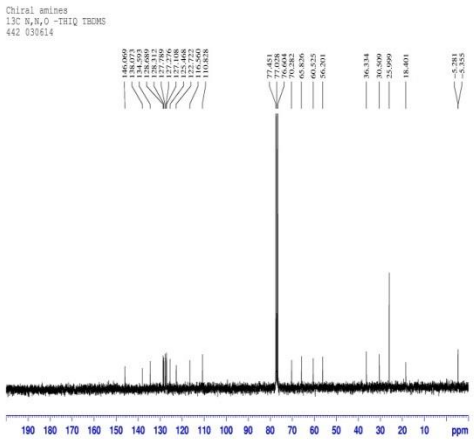
Mass	**FTIR**
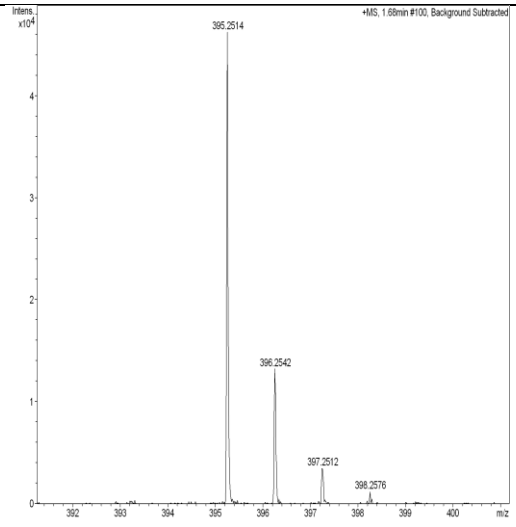	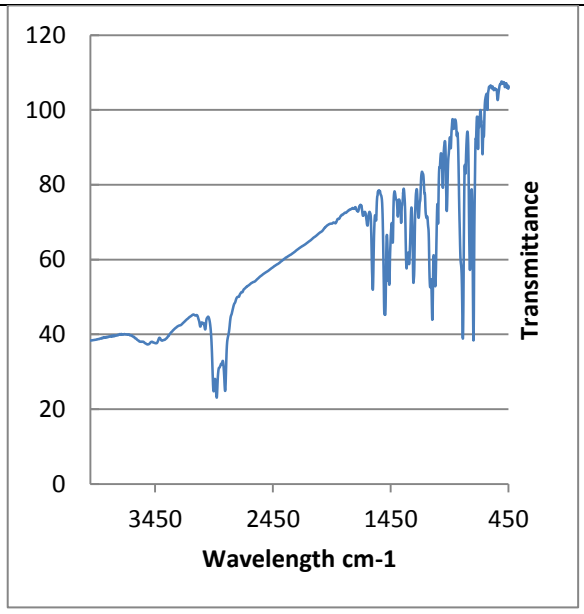

References

[1] *Lancet* **1990**, *336*, 1100-1101.

[2] P. Cintas, *Angew. Chem. Int. Ed.* **2002**, *41*, 1139-1145.

[3] a) J. McConathy and M. J. Owens, *Prim. Care Companion J. Clin. Psychiatry.* **2003**, *5*, 70–73; b) L. A. Nguyen, C. He H Fau - Pham-Huy and C. Pham-Huy, *Int. J. Biomed. Sci.* **2006**, *2*, 85-100.

[4] S. Tseng, G. Pak, K. Washenik, M. Keltz Pomeranz and J. L. Shupack, *J. Am. Acad. Dermatol.* **1996**, *35*, 969-979.

[5] H. AJ, *CNS Spectr.* **2002**, *7*, 14-22.

[6] a) K. C. Nicolaou, D. Vourloumis, N. Winssinger and P. S. Baran, *Angew. Chem. Int. Ed.* **2000**, *39*, 44-122; b) K. C. Nicolaou, E. J. Sorensen and N. Winssinger, *J. Chem. Educ.* **1998**, *75*, 1225.

[7] J. Jacques, A. Collet and S. H. Wilen, *Enantiomers, racemates, and resolutions*, New York : Wiley, **1981**, p.

[8] W. H. Porter, *Pure Appl. Chem.* **1991**, *63*, 1119-1122.

[9] Y. Fujima, M. Ikunaka, T. Inoue and J. Matsumoto, *Org. Process Res. Dev.* **2006**, *10*, 905-913.

[10] M. Kitamura, S. Okada, S. Suga and R. Noyori, *J. Am. Chem. Soc.* **1989**, *111*, 4028-4036.

[11] G. Procter, *Asymmetric Synthesis*, Oxford University Press, **1999**, p.

[12] a) P. D. Bailey, P. A. Millwood and P. D. Smith, *Chem. Commun.* **1998**, 633-640; b) H.-P. Husson and J. Royer, *Chem. Soc. Rev.* **1999**, *28*, 383-394; c) S. Laschat and T. Dickner, *Synthesis* **2000**, 1781-1813; d) P. M. Weintraub, J. S. Sabol, J. M. Kane and D. R. Borcherding, *Tetrahedron* **2003**, *59*, 2953-2989; e) B. Maxime G.P, *Tetrahedron* **2004**, *60*, 1701-1729; f) M. S. M. Pearson, M.

Mathé-Allainmat, V. Fargeas and J. Lebreton, *Eur. J. Org. Chem.* **2005**, *2005*, 2159-2191.

[13] C. Botuha, C. M. S. Galley and T. Gallagher, *Org. Biomol. Chem.* **2004**, *2*, 1825-1826.

[14] a) S. Pasikanti, D. Srinivasa Reddy, B. Venkatesham, P. K. Dubey, J. Iqbal and P. Das, *Tetrahedron Letters* **2010**, *51*, 151-152; b) C. Hirschhäuser, C. A. Haseler and T. Gallagher, *Angew. Chem. Int. Ed.* **2011**, *50*, 5162-5165.

[15] K. Takasu, N. Nishida, A. Tomimura and M. Ihara, *J. Org. Chem.* **2005**, *70*, 3957-3962.

[16] A. Samarat, J. Ben Kraïem, T. Ben Ayed and H. Amri, *Tetrahedron* **2008**, *64*, 9540-9543.

[17] A. Lerchner and E. M. Carreira, *Chem. Eur. J.* **2006**, *12*, 8208-8219.

[18] D. Gray and T. Gallagher, *Angew. Chem. Int. Ed.* **2006**, *45*, 2419-2423.

[19] G. R. Cook, L. G. Beholz and J. R. Stille, *J. Org. Chem.* **1994**, *59*, 3575-3584.

[20] F. Felluga, G. Pitacco, M. Prodan, S. Pricl, M. Visintin and E. Valentin, *Tetrahedron: Asymmetry* **2001**, *12*, 3241-3249.

[21] M.-h. Kim, Y. Park, B.-S. Jeong, H.-g. Park and S.-s. Jew, *Org. Lett.* **2010**, *12*, 2826-2829.

[22] M.-h. Kim, S.-h. Choi, Y.-J. Lee, J. Lee, K. Nahm, B.-S. Jeong, H.-g. Park and S.-s. Jew, *Chem. Commun.* **2009**, 782-784.

[23] T. Kano, F. Shirozu, K. Tatsumi, Y. Kubota and K. Maruoka, *Chem. Sci.* **2011**, *2*, 2311-2313.

[24] S. Hu, S. Kelly, S. Lee, J. Tao and E. Flahive, *Org. Lett.* **2006**, *8*, 1653-1655.

[25] a) A. Partheil, *Arch. Pharm.* **1894**, *232*, 161; b) M. Freund, *Ber.* **1904**, *37*, 22; c) H. R. Ing, *J. Chem. Soc.* **1932**, 2778-2780; d) H. R. Ing, *J. Chem. Soc.* **1932**, 2778; e) E. Spath and F. Galinovsky, *Ber.* **1932**, *65*, 1932.

[26] T. A. Henry, *Plants Alkaloids*, The Blakinston Co., Philadelphia, **1949**, p.

[27] a) M. W. Holladay, M. J. Dart and J. K. Lynch, *J. Med. Chem.* **1997**, *40*, 4169-4194; b) J. P. Michael, *Nat. Prod. Rep.* **1999**, *16*, 675-696; c) D. Paterson and A. Nordberg, *Prog. Neurobiol.* **2000**, *61*, 75-111; d) J. Daly, *Cell Mol. Neurobiol.* **2005**, *25*, 513-552; e) J. Rouden, M.-C. Lasne, J. Blanchet and J. Baudoux, *Chem. Rev.* **2013**, *114*, 712-778.

[28] a) C. Luetje and J. Patrick, *J. Neurosci. 1991, 11, 837-845.* **1991**, *11*, 837-845; b) R. L. Papke and S. F. Heinemann, *Mol. Pharmacol.* **1994**, *45*, 142-149; c) H. K. Happe, J. L. Peters, D. A. Bergman and L. C. Murrin, *J. Neurosci.* **1994**, *62*, 929-944; d) R. L. Papke and S. F. Heinemann, *Mol. Pharmacol.* **1994**, *45*, 142-149.

[29] a) D. Paterson and A. Nordberg, *Prog. Neurobiol.* **2000**, *61*, 75-111; b) A. A. Jensen, B. Frølund, T. Liljefors and P. Krogsgaard-Larsen, *J. Med. Chem.* **2005**, *48*, 4705-4745.

[30] J. W. Coe, H. Rollema and B. T. O'Neill, *Annu. Rep. Med. Chem.* **2009**, *44*, 71-101.

[31] G. K. Lloyd and M. Williams, *J. Pharmacol. Exp. Ther.* **2000**, *292*, 461-467.

[32] J. A. Abin-Carriquiry, G. Costa, J. Urbanavicius, B. K. Cassels, M. Rebolledo-Fuentes, S. Wonnacott and F. Dajas, *Eur. J. Pharmacol.* **2008**, *589*, 80-84.

[33] W. Sihver, P. G. Gillberg, A. L. Svensson and A. Nordberg, *J. Neurosci.* **1999**, *94*, 685-696.

[34] a) E. Giacobini, *J. Neurosci. Res.* **1990**, *27*, 548-560; b) *J. Alzheimers Dis.* **1999**, *1*, 207; c) J. Court, C. Martin-Ruiz, M. Piggott, D. Spurden, M. Griffiths and E. Perry, *Biol. Psychiatry* **2001**, *49*, 175-184.

[35] J. Kawamata and S. Shimohama, *J. Alzheimers Dis.* **2011**, *24 Suppl 2*, 95-109.

[36] a) P. C. Moser, J. M. Hitchcock, S. Lister and P. M. Moran, *Brain Res. Rev.* **2000**, *33*, 275-307; b) N. Ripoll, M. Bronnec and M. Bourin, *Curr. Med. Res. Opin.* **2004**, *20*, 1057-1074.

[37] M. W. Decker, L. E. Rueter and R. S. Bitner, *Curr. Top. Med. Chem.* **2004**, *4*, 369-384.

[38] a) S. R. Breining, *Curr. Top. Med. Chem.* **2004**, *4*, 609-629; b) D. Stead and P. O'Brien, *Tetrahedron* **2007**, *63*, 1885-1897.

[39] J. W. Coe, *Org. Lett.* **2000**, *2*, 4205-4208.

[40] T. R. Govindachari, S. Rajadurai, M. Subramanian and B. S. Thyagarajan, *J. Chem. Soc.* **1957**, 3839-3844.

[41] a) E. E. van Tamelen and J. S. Baran, *J. Am. Chem. Soc.* **1955**, *77*, 4944-4945; b) E. E. van Tamelen and J. S. Baran, *J. Am. Chem. Soc.* **1958**, *80*, 4659-4670.

[42] T. Honda, R. Takahashi and H. Namiki, *J. Org. Chem.* **2004**, *70*, 499-504.

[43] B. Danieli, G. Lesma, D. Passarella, A. Sacchetti, A. Silvani and A. Virdis, *Org. Lett.* **2004**, *6*, 493-496.

[44] C. Botuha, C. M. S. Galley and T. Gallagher, *Organic & Biomolecular Chemistry* **2004**, *2*.

[45] J. D. Schmitt and M. Bencherif in *Chapter 5. Targeting nicotinic acetylcholine receptors: Advances in molecular design and therapies*, *Vol. Volume 35* Academic Press, **2000**, pp. 41-51.

[46] C. Herdeis, C. Kaschinski, R. Karla and H. Lotter, *Tetrahedron: Asymmetry* **1996**, *7*, 867-884.

[47] a) G. P. Moss, *Pure. Appl. Chem.* **1996**, *68*, 2193-2222; b) M. C. Willis, *J. Chem. Soc., Perkin Trans. 1* **1999**, 1765-1784.

[48] E. García-Urdiales, I. Alfonso and V. Gotor, *Chem. Rev.* **2004**, *105*, 313-354.

[49] a) J. L. Vicario, D. Badia, L. Carrillo, E. Reyes and J. Etxebarria, *Curr. Org. Chem.* **2005**, *9*, 219-235; b) Y. Gnas and F. Glorius, *Synthesis* **2006**, *2006*, 1899-1930.

[50] D. A. Evans, G. Helmchen and M. Ruping in *Chiral Auxiliaries in Asymmetric Synthesis*, *Vol.* Eds.: M. Christmann and S. Brase), WILEY-VCH Verlag GmbH & Co. KGaA, Weinheim, **2007**.

[51] A. Studer, *Synthesis* **1996**, *1996*, 793-815.

[52] M. R. Morales, K. T. Mellem and A. G. Myers, *Angew. Chem.* **2012**, *124*, 4646-4649.

[53] W. Oppolzer, *Tetrahedron* **1987**, *43*, 1969-2004.

[54] H.-U. Reissig, *Angew. Chem. Int. Ed.* **1992**, *31*, 288-290.

[55] J. K. Whitesell, H. H. Chen and R. M. Lawrence, *J. Org. Chem.* **1985**, *50*, 4663-4664.

[56] a) M. M. Heravi and V. Zadsirjan, *Tetrahedron: Asymmetry* **2013**, *24*, 1149-1188; b) D. A. Evans, J. Bartroli and T. L. Shih, *J. Am. Chem. Soc.* **1981**,

103, 2127-2129; c) D. A. Evans, M. D. Ennis and D. J. Mathre, *J. Am. Chem. Soc.* **1982**, *104*, 1737-1739.

[57] D. A. Evans and J. Bartroli, *Tetrahedron Lett.* **1982**, *23*, 807-810.

[58] D. A. Evans, J. S. Clark, R. Metternich, V. J. Novack and G. S. Sheppard, *J. Am. Chem. Soc.* **1990**, *112*, 866-868.

[59] a) D. A. Evans, F. Urpi, T. C. Somers, J. S. Clark and M. T. Bilodeau, *J. Am. Chem. Soc.* **1990**, *112*, 8215-8216; b) D. A. Evans, M. T. Bilodeau, T. C. Somers, J. Clardy, D. Cherry and Y. Kato, *J. Org. Chem.* **1991**, *56*, 5750-5752.

[60] a) D. A. Evans, J. S. Tedrow, J. T. Shaw and C. W. Downey, *J. Am. Chem. Soc.* **2001**, *124*, 392-393; b) D. A. Evans, C. W. Downey, J. T. Shaw and J. S. Tedrow, *Org. Lett.* **2002**, *4*, 1127-1130.

[61] D. A. Evans, D. L. Rieger, M. T. Bilodeau and F. Urpi, *J. Am. Chem. Soc.* **1991**, *113*, 1047-1049.

[62] L. T. Liu, P.-C. Hong, H.-L. Huang, S.-F. Chen, C.-L. J. Wang and Y.-S. Wen, *Tetrahedron: Asymmetry* **2001**, *12*, 419-426.

[63] D. A. Evans, K. T. Chapman and J. Bisaha, *J. Am. Chem. Soc.* **1984**, *106*, 4261-4263.

[64] F. M. McRobb, I. T. Crosby, E. Yuriev, J. R. Lane and B. Capuano, *J. med. Chem.* **2012**, *55*, 1622-1634.

[65] A. Sakakura, T. Ohkubo, R. Yamashita, M. Akakura and K. Ishihara, *Org. Lett.* **2011**, *13*, 892-895.

[66] a) N. T. Burdzhiev and E. R. Stanoeva, *Tetrahedron* **2006**, *62*, 8318-8326; b) P. Y. Reddy, S. Kondo, T. Toru and Y. Ueno, *J. Org. Chem.* **1997**, *62*, 2652-2654.

[67] H.-S. Chong, H. A. Song, M. Dadwal, X. Sun, I. Sin and Y. Chen, *J. Org. Chem.* **2009**, *75*, 219-221.

[68] Y. Fu, B. Xu, X. Zou, C. Ma, X. Yang, K. Mou, G. Fu, Y. Lü and P. Xu, *Bioorg. Med. Chem. Lett.* **2007**, *17*, 1102-1106.

[69] J. Dai, K. Krohn, S. Draeger and B. Schulz, *Eur. J. Org. Chem.* **2009**, *2009*, 1564-1569.

[70] C. K. Z. Andrade, R. O. Rocha, O. E. Vercillo, W. A. Silva and R. A. F. Matos, *Synlett* **2003**, *2003*, 2351-2352.

[71] H.-S. Zhang, D.-Z. Feng, L. Chen and Y.-Q. Long, *Bioorg. Med. Chem. Lett.* **2010**, *20*, 2219-2223.

[72] I. Suárez del Villar, A. Gradillas and J. Pérez-Castells, *Eur. J. Org. Chem.* **2010**, *2010*, 5850-5862.

[73] D. Takano, T. Nagamitsu, H. Ui, K. Shiomi, Y. Yamaguchi, R. Masuma, I. Kuwajima and S. Ōmura, *Org. Lett.* **2001**, *3*, 2289-2291.

[74] a) O. Koepler, S. Laschat, A. Baro, P. Fischer, B. Miehlich, M. Hotfilder and C. le Viseur, *Eur. J. Org. Chem.* **2004**, *2004*, 3611-3622; b) J. Stöckigt, A. P. Antonchick, F. Wu and H. Waldmann, *Angew. Chem. Int. Ed.* **2011**, *50*, 8538-8564.

[75] W. N. Speckamp and H. Hiemstra, *Tetrahedron* **1985**, *41*, 4367-4416.

[76] E. L. Larghi, M. Amongero, A. B. J. Bracca and T. S. Kaufman, *Arkivoc* **2005**, *2005*, 98-153.

[77] a) S. K. Chakka, B. K. Peters, P. G. Andersson, G. E. M. Maguire, H. G. Kruger and T. Govender, *Tetrahedron: Asymmetry* **2010**, *21*, 2295-2301; b) T. Naicker, P. I. Arvidsson, H. G. Kruger, G. E. M. Maguire and T. Govender, *Eur. J. Org. Chem.* **2012**, *2012*, 3331-3337; c) T. Naicker, K. Petzold, T. Singh,

P. I. Arvidsson, H. G. Kruger, G. E. M. Maguire and T. Govender, *Tetrahedron: Asymmetry* **2010**, *21*, 2859-2867; d) S. K. Chakka, P. G. Andersson, G. E. M. Maguire, H. G. Kruger and T. Govender, *Eur. J. Org. Chem.* **2010**, *2010*, 972-980; e) R. B. Kawthekar, S. K. Chakka, V. Francis, P. G. Andersson, H. G. Kruger, G. E. M. Maguire and T. Govender, *Tetrahedron: Asymmetry* **2010**, *21*, 846-852; f) B. K. Peters, S. K. Chakka, T. Naicker, G. E. M. Maguire, H. G. Kruger, P. G. Andersson and T. Govender, *Tetrahedron: Asymmetry* **2010**, *21*, 679-687; g) C. Blanc, J. Hannedouche and F. Agbossou-Niedercorn, *Tetrahedron Lett.* **2003**, *44*, 6469-6473; h) K. Stingl, J. Martens and S. Wallbaum, *Tetrahedron: Asymmetry* **1992**, *3*, 223-226.

[78] a) D. A. Evans, T. C. Britton, R. L. Dorow and J. F. Dellaria Jr, *Tetrahedron* **1988**, *44*, 5525-5540; b) D. A. Evans and W. C. Black, *J. Am. Chem. Soc.* **1993**, *115*, 4497-4513.

[79] a) R. E. Taylor and M. Jin, *Org. Lett.* **2003**, *5*, 4959-4961; b) S. Sahli, B. Frank, W. B. Schweizer, F. Diederich, D. Blum-Kaelin, J. D. Aebi, H.-J. Böhm, C. Oefner and G. E. Dale, *Helv. Chim. Acta* **2005**, *88*, 731-750.

[80] a) X. Hu, K. T. Nguyen, C. L. M. J. Verlinde, W. G. J. Hol and D. Pei, *J. Med. Chem.* **2003**, *46*, 3771-3774; b) M. Gersch, F. Gut, V. S. Korotkov, J. Lehmann, T. Böttcher, M. Rusch, C. Hedberg, H. Waldmann, G. Klebe and S. A. Sieber, *Angew. Chem. Int. Ed.* **2013**, *52*, 3009-3014.

[81] H. Sashida, A. Nakayama and M. Kaname, *Synthesis* **2008**, *2008*, 3229-3236.

[82] J. Kimura, Y. Takada, T. Inayoshi, Y. Nakao, G. Goetz, W. Y. Yoshida and P. J. Scheuer, *J. Org. Chem.* **2002**, *67*, 1760-1767.

[83] N. Choy, Y. Shin, P. Q. Nguyen, D. P. Curran, R. Balachandran, C. Madiraju and B. W. Day, *J. Med. Chem.* **2003**, *46*, 2846-2864.

[84] K. Harada, H. Horiuchi, K. Tanabe, R. G. Carter, T. Esumi, M. Kubo, H. Hioki and Y. Fukuyama, *Tetrahedron Lett.* **2011**, *52*, 3005-3008.

[85] T. Kano, F. Shirozu, M. Akakura and K. Maruoka, *J. Am. Chem. Soc.* **2012**, *134*, 16068-16073.

[86] M. Santelli and J.-M. Pons, *Lewis Acids and Selectivity in Organic Synthesis*, CRC Press, New York, **1995**, p.

[87] J. F. Norris and G. W. Rigby, *J. Am. Chem. Soc.* **1932**, *54*, 2088-2100.

[88] J. L. Marshall, K. C. Erickson and T. K. Folsom, *Tetrahedron Lett.* **1970**, *11*, 4011-4012.

[89] J. Iqbal and R. R. Srivastava, *J. Org. Chem.* **1992**, *57*, 2001-2007.

[90] E. C. Blossey, L. M. Turner and D. C. Neckers, *Tetrahedron Lett.* **1973**, *14*, 1823-1826.

[91] B. Ganem and V. R. Small, *J. Org. Chem.* **1974**, *39*, 3728-3730.

[92] a) I. Shiina, S. Miyoshi, M. Miyashita and T. Mukaiyama, *Chem. Lett.* **1994**, *23*, 515-518; b) I. Shiina and T. Mukaiyama, *Chem. Lett.* **1994**, *23*, 677-680.

[93] a) E. Vedejs and O. Daugulis, *J. Org. Chem.* **1996**, *61*, 5702-5703; b) S. V. Pansare, M. G. Malusare and A. N. Rai, *Synth. Commun.* **2000**, *30*, 2587-2592.

[94] S. Kanta De, *Tetrahedron Lett.* **2004**, *45*, 2919-2922.

[95] A. K. Chakraborti and R. Gulhane, *Tetrahedron Lett.* **2003**, *44*, 6749-6753.

[96] P. Saravanan and V. K. Singh, *Tetrahedron Lett.* **1999**, *40*, 2611-2614.

[97] K. K. Chauhan, C. G. Frost, I. Love and D. Waite, *Synlett* **1999**, 1743-1744.

[98] a) A. Orita, C. Tanahashi, A. Kakuda and J. Otera, *Angew. Chem. Int. Ed.* **2000**, *39*, 2877-2879; b) I. Mohammadpoor-Baltork, H. Aliyan and A. Reza Khosropour, *Tetrahedron* **2001**, *57*, 5851-5854; c) A. Orita, C. Tanahashi, A. Kakuda and J. Otera, *J. Org. Chem.* **2001**, *66*, 8926-8934.

[99] M. Miyashita, I. Shiina, S. Miyoshi and T. Mukaiyama, *Bull. Chem. Soc. Jpn.* **1993**, *66*, 1516-1527.

[100] a) N. U. Kumar, B. S. Reddy, V. P. Reddy and R. Bandichhor, *Tetrahedron Lett.* **2013**; b) N. Mamidi and D. Manna, *J. Org. Chem.* **2013**, *78*, 2386-2396.

[101] a) K. Ishihara, M. Kubota, H. Kurihara and H. Yamamoto, *J. Am. Chem. Soc.* **1995**, *117*, 4413-4414; b) K. Ishihara, M. Kubota, H. Kurihara and H. Yamamoto, *J. Org. Chem.* **1996**, *61*, 4560-4567.

[102] H. Zhao, A. Pendri and R. B. Greenwald, *J. Org. Chem.* **1998**, *63*, 7559-7562.

[103] a) A. G. M. Barrett and D. Christopher Braddock, *Chem. Commun.* **1997**, 351-352; b) E. W. P. Damen, L. Braamer and H. W. Scheeren, *Tetrahedron Lett.* **1998**, *39*, 6081-6082; c) P. A. Clarke, N. E. Kayaleh, M. A. Smith, J. R. Baker, S. J. Bird and C. Chan, *J. Org. Chem.* **2002**, *67*, 5226-5231.

[104] P. A. Clarke, R. A. Holton and N. E. Kayaleh, *Tetrahedron Lett.* **2000**, *41*, 2687-2690.

[105] P. A. Clarke, *Tetrahedron Lett.* **2002**, *43*, 4761-4763.

[106] K. Narasaka, *Synthesis* **1991**, 1-11.

[107] A. C. Spivey, A. Maddaford and A. J. Redgrave, *Org. Prep. Proc. Int.* **2000**, *32*, 331-365.

[108] K. Narasaka, F. Kanai, M. Okudo and N. Miyoshi, *Chem. Lett.* **1989**, *18*, 1187-1190.

[109] S. Chandrasekhar, T. Ramachander and M. Takhi, *Tetrahedron Lett.* **1998**, *39*, 3263-3266.

[110] a) D. Seebach, G. Jaeschke and Y. M. Wang, *Angew. Chem. Int. Ed.* **1995**, *34*, 2395-2396; b) D. Seebach, R. E. Marti and T. Hintermann, *Helv. Chim. Acta.* **1996**, *79*, 1710-1740.

[111] B. M. Trost and T. Mino, *J. Am. Chem. Soc.* **2003**, *125*, 2410-2411.

[112] B. M. Trost and H. Ito, *J. Am. Chem. Soc.* **2000**, *122*, 12003-12004.

[113] B. M. Trost, S. Malhotra, T. Mino and N. S. Rajapaksa, *Chem. Eur. J.* **2008**, *14*, 7648-7657.

[114] T. Honjo, M. Nakao, S. Sano, M. Shiro, K. Yamaguchi, Y. Sei and Y. Nagao, *Org. Lett.* **2007**, *9*, 509-512.

[115] F. Iwasaki, T. Maki, O. Onomura, W. Nakashima and Y. Matsumura, *J. Org. Chem.* **2000**, *65*, 996-1002.

[116] Y. Matsumura, T. Maki, S. Murakami and O. Onomura, *J. Am. Chem. Soc.* **2003**, *125*, 2052-2053.

[117] a) J. Y. Lee, Y. S. You and S. H. Kang, *J. Am. Chem. Soc.* **2011**, *133*, 1772-1774; b) M. S. Hong, T. W. Kim, B. Jung and S. H. Kang, *Chem. Eur. J.* **2008**, *14*, 3290-3296; c) B. Jung, M. S. Hong and S. H. Kang, *Angew. Chem. Int. Ed.* **2007**, *46*, 2616-2618.

[118] H. Quast and R. Janiak, *Liebigs Ann. Chem.* **1991**, *1991*, 1305-1308.

[119] a) K. R. Prabhu, N. Pillarsetty, H. Gali and K. V. Katti, *J. Am. Chem. Soc.* **2000**, *122*, 1554-1555; b) L. Palombi, M. Feroci, M. Orsini and A. Inesi, *Chem. Commun.* **2004**, 1846-1847.

[120] K. V. Katti, K. R. Prabhu, H. Gali, N. K. Pillarsetty and W. A. Volkert in *Bifunctional chelating agent for the design and development of site specific radiopharmaceuticals and biomolecule conjugation strategy*, *Vol. US 6635235* The Curators of the University of Missouri, USA, US, **2003**.

[121] M. J. Palframan, K. Tchabanenko and J. Robertson, *Tetrahedron Lett.* **2006**, *47*, 8423-8425.

[122] T. Laïb and J. Zhu, *Synlett* **2000**, *2000*, 1363-1365.

[123] N. Arnaud, C. Picard, L. Cazaux and P. Tisnès, *Tetrahedron* **1997**, *53*, 13757-13768.

[124] M. E. van der Boom, S.-Y. Liou, Y. Ben-David, L. J. W. Shimon and D. Milstein, *J. Am. Chem. Soc.* **1998**, *120*, 6531-6541.

[125] a) J. Mao, B. Wan, F. Wu, R. Wang and S. Lu, *J. Mol. Cat. A: Chem.* **2005**, *232*, 9-12; b) F.-M. Gautier, S. Jones and S. J. Martin, *Org. Biomol. Chem.* **2009**, *7*, 229-231.

[126] a) B. M. Trost, V. S. C. Yeh, H. Ito and N. Bremeyer, *Org. Lett.* **2002**, *4*, 2621-2623; b) E.-M. Tanzer, L. E. Zimmer, W. B. Schweizer and R. Gilmour, *Chem. Eur. J.* **2012**, *18*, 11334-11342.

[127] a) E. J. Corey and J. O. Link, *Tetrahedron Lett.* **1989**, *30*, 6275-6278; b) D. J. Mathre, T. K. Jones, L. C. Xavier, T. J. Blacklock, R. A. Reamer, J. J. Mohan, E. T. T. Jones, K. Hoogsteen, M. W. Baum and E. J. J. Grabowski, *J. Org. Chem.* **1991**, *56*, 751-762.

[128] K. Nakano, K. Nozaki and T. Hiyama, *J. Am. Chem. Soc.* **2003**, *125*, 5501-5510.

[129] C.-Y. Ho, Y.-C. Chen, M.-K. Wong and D. Yang, *J. Org. Chem.* **2005**, *70*, 898-906.

[130] J. V. Bhaskar Kanth and M. Periasamy, *Tetrahedron* **1993**, *49*, 5127-5132.

[131] Y. Xiao, Z. Wang and K. Ding, *Chem. Eur. J.* **2005**, *11*, 3668-3678.

[132] a) M. V. Baker, M. J. Bosnich, D. H. Brown, L. T. Byrne, V. J. Hesler, B. W. Skelton, A. H. White and C. C. Williams, *J. Org. Chem.* **2004**, *69*, 7640-7652; b) S. Kumar, G. Hundal, D. Paul, M. S. Hundal and H. Singh, *J. Org. Chem.* **1999**, *64*, 7717-7726.

[133] a) Z. Zhang, T.-X. Liu, Q. Liu, Z. Zhang and G. Zhang, *Tetrahedron: Asymmetry* **2013**, *24*, 1591-1597; b) S. Gosiewska, M. Lutz, A. L. Spek and R. J. M. Klein Gebbink, *Inorg. Chim. Acta.* **2007**, *360*, 405-417.

[134] a) H. C. Aspinall, *Chem. Rev.* **2002**, *102*, 1807-1850; b) J. Inanaga, H. Furuno and T. Hayano, *Chem. Rev.* **2002**, *102*, 2211-2226; c) M. Shibasaki and N. Yoshikawa, *Chem. Rev.* **2002**, *102*, 2187-2210.

[135] a) S. Kobayashi, I. Hachiya, T. Takahori, M. Araki and H. Ishitani, *Tetrahedron Lett.* **1992**, *33*, 6815-6818; b) S. Kobayashi, I. Hachiya, H. Ishitani and M. Araki, *Tetrahedron Lett.* **1993**, *34*, 4535-4538; c) S. Kobayashi, H. Ishitani, M. Araki and I. Hachiya, *Tetrahedron Lett.* **1994**, *35*, 6325-6328.

[136] a) I. E. Markó and G. R. Evans, *Tetrahedron Lett.* **1994**, *35*, 2771-2774; b) I. E. Markó, G. R. Evans and J.-P. Declercq, *Tetrahedron* **1994**, *50*, 4557-4574; c) I. E. Markó, I. Chellé-Regnaut, B. Leroy and S. L. Warriner, *Tetrahedron Lett.* **1997**, *38*, 4269-4272.

[137] X.-L. Hou, J. Wu, L.-X. Dai, L.-J. Xia and M.-H. Tang, *Tetrahedron: Asymmetry* **1998**, *9*, 1747-1752.

[138] a) S. Kobayashi and M. Kawamura, *Journal of the American Chemical Society* **1998**, *120*, 5840-5841; b) M. Kawamura and S. Kobayashi, *Tetrahedron Lett.* **1999**, *40*, 3213-3216.

[139] A. I. Sanchez-Blanco, K. V. Gothelf and K. A. Jørgensen, *Tetrahedron Lett.* **1997**, *38*, 7923-7926.

[140] C. Qian and L. Wang, *Tetrahedron Lett.* **2000**, *41*, 2203-2206.

[141] C. Qian and L. Wang, *Tetrahedron: Asymmetry* **2000**, *11*, 2347-2357.

[142] K. Mikami, M. Terada and H. Matsuzawa, *Angew. Chem. Int. Ed.* **2002**, *41*, 3554–3572.

[143] a) C. L. Roux and J. Dubac, *Synlett* **2002**, *2002*, 0181-0200; b) R. Dumeunier and I. E. Markó, *Tetrahedron Lett.* **2004**, *45*, 825-829.

[144] R. C. Flanagan, S. Xie and A. Millar, *Org. Process Res. Dev.* **2008**, *12*, 1307-1312.

[145] a) E. García-Urdiales, I. Alfonso and V. Gotor, *Chem. Rev.* **2011**, *111*, PR110-PR180; b) J. M. Palomo and Z. Cabrera, *Curr. Org. Synth.* **2012**, *9*, 791-805.

[146] Ramesh N. Patel, *Adv. Synth. Catal.* **2001**, *343*, 527-546.

[147] J. Tyler, Z. Huimin and R. S. Michael in *Biocatalysis*, *Vol. null* Taylor & Francis, **2007**, pp. 101-110.

[148] A. M. Klibanov, *Nature* **2001**, *409*, 241-246.

[149] K. Griebenow and A. M. Klibanov, *J. Am. Chem. Soc.* **1996**, *118*, 11695-11700.

[150] K. M. Koeller and C.-H. Wong, *Nature* **2001**, *409*, 232-240.

[151] B. Morgan, D. R. Dodds, A. Zaks, D. R. Andrews and R. Klesse, *J. Org. Chem.* **1997**, *62*, 7736-7743.

[152] K. Takabe, Y. Iida, H. Hiyoshi, M. Ono, Y. Hirose, Y. Fukui, H. Yoda and N. Mase, **2000**, *11*, 4825.

[153] L. Banfi, A. Basso, G. Guanti and M. T. Zannetti, *Tetrahedron: Asymmetry* **1997**, *8*, 4079-4088.

[154] A. M. Klibanov, *Trends. Biotechnol.* **1997**, *15*, 97-101.

[155] in *Lipase AK "Amano", Vol.* **2008**.

[156] a) J. García, S. Fernández, M. Ferrero, Y. S. Sanghvi and V. Gotor, *Tetrahedron Lett.* **2004**, *45*, 1709-1712; b) T. Zi-Yang, W. Hong and Z. Min-Hua, *Biocatal. Biotransform.* **2007**, *25*, 408-413; c) X.-F. Li, M.-H. Zong, G.-L. Zhao, Y.-G. Yu and H. Wu, *Biotechnol. Bioprocess Eng.* **2010**, *15*, 608-613; d) T. Rodríguez-Pérez, S. Fernández, S. Martínez-Montero, T. González-García, Y. S. Sanghvi, V. Gotor and M. Ferrero, *Eur. J. Org. Chem.* **2010**, *2010*, 1736-1744; e) S. Casati, E. Santaniello and P. Ciuffreda, *Tetrahedron: Asymmetry* **2012**, *23*, 395-400.

[157] a) A. Miyashita, A. Yasuda, H. Takaya, K. Toriumi, T. Ito, T. Souchi and R. Noyori, *J. Am. Chem. Soc.* **1980**, *102*, 7932-7934; b) S. Akutagawa, *Appl. Catal., A* **1995**, *128*, 171-207.

[158] a) J. Brussee and A. C. A. Jansen, *Tetrahedron Lett.* **1983**, *24*, 3261-3262; b) J. M. Brunel, *Chem. Rev.* **2005**, *105*, 857-898; c) M. Shibasaki and S. Matsunaga, *Chem. Soc. Rev.* **2006**, *35*, 269-279.

[159] a) T. Saito, T. Yokozawa, T. Ishizaki, T. Moroi, N. Sayo, T. Miura and H. Kumobayashi, *Adv. Synth. Catal.* **2001**, *343*, 264-267; b) H. Shimizu, I. Nagasaki, K. Matsumura, N. Sayo and T. Saito, *Acc. Chem. Res.* **2007**, *40*, 1385-1393.

[160] a) M. J. Burk, *Acc. Chem. Res.* **2000**, *33*, 363-372; b) T. Clark and C. Landis, *Tetrahedron: Asymmetry* **2004**, *15*, 2123-2137.

[161] a) D. Müller, G. Umbricht, B. Weber and A. Pfaltz, *Helv. Chim. Acta* **1991**, *74*, 232-240; b) G. Desimoni, G. Faita and K. A. Jørgensen, *Chem. Rev.* **2006**, *106*, 3561-3651.

[162] a) H.-J. Drexler, J. You, S. Zhang, C. Fischer, W. Baumann, A. Spannenberg and D. Heller, *Org. Process Res. Dev.* **2003**, *7*, 355-361; b) J.-P. Genet, *Acc. Chem. Res.* **2003**, *36*, 908-918; c) T. Vilaivan, W. Bhanthumnavin and Y. Sritana-Anant, *Curr. Org. Chem.* **2005**, *9*, 1315-1392; d) S. Gladiali and E. Alberico, *Chem. Soc. Rev.* **2006**, *35*, 226-236; e) K. H. Hopmann and A. Bayer, *Coord. Chem. Rev.* **2014**, *268*, 59-82.

[163] a) D. Carmona, M. Pilar Lamata and L. A. Oro, *Coord. Chem. Rev.* **2000**, *200–202*, 717-772; b) K. A. Jørgensen, *Angew. Chem. Int. Ed.* **2000**, *39*, 3558-3588; c) H. Pellissier, *Tetrahedron* **2008**, *64*, 10279-10317; d) M. Terada, *Chem. Commun.* **2008**, 4097-4112; e) P. Merino, E. Marqués-López, T. Tejero and R. P. Herrera, *Synthesis* **2010**, *2010*, 1-26.

[164] a) T. Bach, *Angew. Chem. Int. Ed.* **1994**, *33*, 417-419; b) S. E. Denmark, J. R. Heemstra and G. L. Beutner, *Angew. Chem. Int. Ed.* **2005**, *44*, 4682-4698; c) M. Shibasaki and S. Matsunaga, *J. Organomet. Chem.* **2006**, *691*, 2089-2100; d) J. M. M. Verkade, L. J. C. v. Hemert, P. J. L. M. Quaedflieg and F. P. J. T. Rutjes, *Chem. Soc. Rev.* **2008**, *37*, 29-41; e) B. M. Trost and C. S. Brindle, *Chem. Soc. Rev.* **2010**, *39*, 1600-1632.

[165] H. Pellissier, *Tetrahedron* **2010**, *66*, 1509-1555.

[166] a) M. Yus, J. C. González-Gómez and F. Foubelo, *Chem. Rev.* **2011**, *111*, 7774-7854; b) M. Bandini, G. Cera and M. Chiarucci, *Synthesis* **2012**, *2012*, 504-512; c) S. Pan and T. Shibata, *ACS Catal.* **2013**, *3*, 704-712.

[167] J. A. Byers in *Synthetic and Mechanistic Studies into the Kinetic Resolution of N-olefins using C1- and C2- Symmetric Zirconocene Polymerization Catalysts, Vol.* California Institute of Technology, **2007**.

[168] a) S. Busato, D. C. Craig, Z. M. A. Judeh and R. W. Read, *Tetrahedron* **2003**, *59*, 461-472; b) G. Qi, Y. Q. Ji and Z. M. A. Judeh, *Tetrahedron* **2010**, *66*, 4195-4205; c) G. Qi and Z. M. A. Judeh, *Tetrahedron: Asymmetry* **2010**, *21*, 429-436; d) G. Qi and Z. M. A. Judeh, *Synth. Commun.* **2011**, *42*, 1585-1592; e) Y. Qiong Ji, G. Qi and Z. M. A. Judeh, *Tetrahedron: Asymmetry* **2011**, *22*, 2065-2070; f) Y. Qiong ji, G. Qi and Z. M. A. Judeh, *Eur. J. Org. Chem.* **2011**, *2011*, 4892-4898; g) Y. Qiong Ji, G. Qi and Z. M. A. Judeh, *Tetrahedron: Asymmetry* **2011**, *22*, 929-935; h) Q. J. Yao and Z. M. A. Judeh, *Tetrahedron* **2011**, *67*, 4086-4092.

[169] J.-C. Kizirian, *Chem. Rev.* **2007**, *108*, 140-205.

[170] a) S. Arai, S. Takita and A. Nishida, *Eur. J. Org. Chem.* **2005**, *2005*, 5262-5267; b) M. C. Elliott and E. Williams, *Org. Biomol. Chem.* **2003**, *1*, 3038-3047.

[171] a) S. Deshpande, A. Kelkar, R. Gonnade, S. Shingote and R. Chaudhari, *Catal. Lett.* **2010**, *138*, 231-238; b) D. G. I. Petra, P. C. J. Kamer, P. W. N. M. van Leeuwen, K. Goubitz, A. M. Van Loon, J. G. de Vries and H. E. Schoemaker, *Eur. J. Inorg. Chem.* **1999**, *1999*, 2335-2341; c) J. S. M. Samec, J.-E. Backvall, P. G. Andersson and P. Brandt, *Chem. Soc. Rev.* **2006**, *35*, 237-248.

[172] P. Daverio and M. Zanda, *Tetrahedron: Asymmetry* **2001**, *12*, 2225-2259.

[173] a) B. Jiang, Z. Chen and W. Xiong, *Chem. Commun.* **2002**, 1524-1525; b) Z. Xu, J. Mao and Y. Zhang, *Catal. Commun.* **2008**, *10*, 113-117.

[174] a) Y.-W. Zhong, P. Tian and G.-Q. Lin, *Tetrahedron: Asymmetry* **2004**, *15*, 771-776; b) C. Palomo, M. Oiarbide and A. Laso, *Angew. Chem. Int. Ed.* **2005**, *44*, 3881-3884; c) H. Y. Kim and K. Oh, *Org. Lett.* **2009**, *11*, 5682-5685; d) V. J. Mayani, S. H. R. Abdi, R. I. Kureshy, N.-u. H. Khan, A. Das and H. C. Bajaj, *J. Org. Chem.* **2010**, *75*, 6191-6195.

[175] a) K. Tomioka, Y. Kubota and K. Koga, *Tetrahedron* **1993**, *49*, 1891-1900; b) A. Iida, M. Kano, Y. Kubota, K. Koga and K. Tomioka, *Chem. Pharm. Bull.* **2000**, *48*, 486-489.

[176] A. R. Katritzky, J. Cobo-Domingo, B. Yang and P. J. Steel, *Tetrahedron: Asymmetry* **1999**, *10*, 255-263.

[177] T. Mecozzi, M. Petrini and R. Profeta, *Tetrahedron: Asymmetry* **2003**, *14*, 1171-1178.

[178] S. Aubry, S. Pellet-Rostaing and M. Lemaire, *Eur. J. Org. Chem.* **2007**, *2007*, 5212-5225.

[179] a) G. Rosini in *1.10 - The Henry (Nitroaldol) Reaction*, *Vol.* Eds.: B. M. Trost and I. Fleming), Pergamon, Oxford, **1991**, pp. 321-340; b) F. A. Luzzio, *Tetrahedron* **2001**, *57*, 915-945; c) N. Ono, *The Nitro Group in Organic Synthesis*, VCH: New York, **2001**, p.

[180] N. Ono in *The Nitro-Aldol (Henry) Reaction*, *Vol.* John Wiley & Sons, Inc., **2002**, pp. 30-69.

[181] Otto M. Berner, L. Tedeschi and D. Enders, *Eur. J. Org. Chem.* **2002**, *2002*, 1877-1894.

[182] R. Ballini, D. Fiorini, M. V. Gil and A. Palmieri, *Tetrahedron* **2004**, *60*, 2799-2804.

[183] H. Sasai, T. Suzuki, S. Arai, T. Arai and M. Shibasaki, *J. Am. Chem. Soc.* **1992**, *114*, 4418-4420.

[184] a) J. Boruwa, N. Gogoi, P. P. Saikia and N. C. Barua, *Tetrahedron: Asymmetry* **2006**, *17*, 3315-3326; b) C. Palomo, M. Oiarbide and A. Laso, *Eur. J. Org. Chem.* **2007**, *2007*, 2561-2574.

[185] a) C. Christensen, K. Juhl, R. G. Hazell and K. A. Jørgensen, *J. Org. Chem.* **2002**, *67*, 4875-4881; b) D. A. Evans, D. Seidel, M. Rueping, H. W. Lam, J. T. Shaw and C. W. Downey, *J. Am. Chem. Soc.* **2003**, *125*, 12692-12693; c) T. Risgaard, K. V. Gothelf and K. A. Jorgensen, *Org. Biomol. Chem.* **2003**, *1*, 153-156; d) S.-F. Lu, D.-M. Du, S.-W. Zhang and J. Xu, *Tetrahedron: Asymmetry* **2004**, *15*, 3433-3441; e) D.-M. Du, S.-F. Lu, T. Fang and J. Xu, *J. Org. Chem.* **2005**, *70*, 3712-3715; f) S. K. Ginotra and V. K. Singh, *Org. Biomol. Chem.* **2007**, *5*, 3932-3937; g) K. Lang, J. Park and S. Hong, *J. Org. Chem.* **2010**, *75*, 6424-6435.

[186] a) S. Liu and C. Wolf, *Org. Lett.* **2008**, *10*, 1831-1834; b) K. Y. Spangler and C. Wolf, *Org. Lett.* **2009**, *11*, 4724-4727.

[187] a) T. Arai, M. Watanabe, A. Fujiwara, N. Yokoyama and A. Yanagisawa, *Angew. Chem. Int. Ed.* **2006**, *45*, 5978-5981; b) H. Maheswaran, K. L. Prasanth, G. G. Krishna, K. Ravikumar, B. Sridhar and M. L. Kantam, *Chem. Commun.* **2006**, 4066-4068; c) T. Arai, M. Watanabe and A. Yanagisawa, *Org. Lett.* **2007**, *9*, 3595-3597; d) M. Bandini, M. Benaglia, R. Sinisi, S. Tommasi and A. Umani-Ronchi, *Org. Lett.* **2007**, *9*, 2151-2153; e) R. Kowalczyk, Ł. Sidorowicz and J. Skarżewski, *Tetrahedron: Asymmetry* **2008**, *19*, 2310-2315; f) S.

Selvakumar, D. Sivasankaran and V. K. Singh, *Org. Biomol. Chem.* **2009**, *7*, 3156-3162; g) W. Jin, X. Li, Y. Huang, F. Wu and B. Wan, *Chem. Eur. J.* **2010**, *16*, 8259-8261; h) A. Noole, K. Lippur, A. Metsala, M. Lopp and T. Kanger, *J. Org. Chem.* **2010**, *75*, 1313-1316.

[188] a) B. M. Choudary, K. V. S. Ranganath, U. Pal, M. L. Kantam and B. Sreedhar, *J. Am. Chem. Soc.* **2005**, *127*, 13167-13171; b) G. Blay, E. Climent, I. Fernández, V. Hernández-Olmos and J. R. Pedro, *Tetrahedron: Asymmetry* **2007**, *18*, 1603-1612; c) G. Blay, V. Hernandez-Olmos and J. R. Pedro, *Org. Biomol. Chem.* **2008**, *6*, 468-476.

[189] Y. Xiong, F. Wang, X. Huang, Y. Wen and X. Feng, *Chem. Eur. J.* **2007**, *13*, 829-833.

[190] K. D. Thinh and Z. M. A. Judeh, *Synthesis*.

[191] E. L. Eliel, S. H. Wilen and L. N. Mander, *Stereochemistry of Organic Compounds*, Wiley: New York **1994**, p.

[192] I. D. Blackburne, A. R. Katritzky and Y. Takeuchi, *Acc. Chem. Res.* **1975**, *8*, 300-306.

[193] P. S. Charifson, J. P. Bowen, S. D. Wyrick, A. J. Hoffman, M. Cory, A. T. McPhail and R. B. Mailman, *J. Med. Chem.* **1989**, *32*, 2050-2058.

[194] A. F. Ibañez, G. Y. Moltrasio Iglesias and J. M. Delfino, *J. Heterocycl. Chem.* **1996**, *33*, 265-270.

[195] O. Irie, T. Kosaka, M. Kishida, J. Sakaki, K. Masuya, K. Konishi, F. Yokokawa, T. Ehara, A. Iwasaki, Y. Iwaki, Y. Hitomi, A. Toyao, H. Gunji, N. Teno, G. Iwasaki, H. Hirao, T. Kanazawa, K. Tanabe, P. C. Hiestand, M. Malcangio, A. J. Fox, S. J. Bevan, M. Yaqoob, A. J. Culshaw, T. W. Hart and A. Hallett, *Bioorg. Med. Chem. Lett.* **2008**, *18*, 5280-5284.

[196] T. A. Crabb and R. F. Newton, *Tetrahedron* **1970**, *26*, 701-713.

[197] T. Naicker, T. Govender, H. G. Kruger and G. E. M. Maguirea, *Acta Crystallogr. Sect. E Struct. Rep. Online.* **2010**, *66 (Pt3)*, o638.

[198] M. Kurosu, M.-H. Lin and Y. Kishi, *J. Am. Chem. Soc.* **2004**, *126*, 12248-12249.

[199] a) C. W. Lim and I. S. Lee, *Nano Today* **2010**, *5*, 412-434; b) S. A. Ansari and Q. Husain, *Biotechnol. Adv.* **2012**, *30*, 512-523.

[200] A. Johnson, A. Zawadzka, L. Deobald, R. Crawford and A. Paszczynski, *J. Nanopart. Res.* **2008**, *10*, 1009-1025.

[201] E.-n. Xun, X.-l. Lv, W. Kang, J.-x. Wang, H. Zhang, L. Wang and Z. Wang, *Appl. Biochem. Biotechnol.* **2012**, *168*, 697-707.

[202] a) M. L. Foresti and M. L. Ferreira, *Enzyme Microb. Technol.* **2007**, *40*, 769-777; b) J. C. Santos, A. V. Paula, G. F. M. Nunes and H. F. de Castro, *J. Mol. Cat. B: Enzym.* **2008**, *52–53*, 49-57; c) A. A. Mendes, R. C. Giordano, R. d. L. C. Giordano and H. F. de Castro, *J. Mol. Cat. B: Enzym.* **2011**, *68*, 109-115; d) J. Brem, M. C. Turcu, C. Paizs, K. Lundell, M.-I. Toşa, F.-D. Irimie and L. T. Kanerva, *Process Biochem.* **2012**, *47*, 119-126; e) L. N. de Lima, C. C. Aragon, C. Mateo, J. M. Palomo, R. L. C. Giordano, P. W. Tardioli, J. M. Guisan and G. Fernandez-Lorente, *Process Biochem.* **2013**, *48*, 118-123; f) S. Kanimozhi and K. Perinbam, *Mater. Res. Bull.* **2013**, *48*, 1830-1836.

[203] a) A. Salis, M. S. Bhattacharyya, M. Monduzzi and V. Solinas, *J. Mol. Cat. B: Enzym.* **2009**, *57*, 262-269; b) A. A. Mendes, P. C. Oliveira, A. M. Vélez, R. C. Giordano, R. d. L. C. Giordano and H. F. de Castro, *Int. J. Biol. Macromol.* **2012**, *50*, 503-511.

[204] A. Erkkilä, I. Majander and P. M. Pihko, *Chem. Rev.* **2007**, *107*, 5416-5470.

[205] G. Bégis, D. E. Cladingboel, L. Jerome, W. B. Motherwell and T. D. Sheppard, *Eur. J. Org. Chem.* **2009**, *2009*, 1532-1548.

[206] M. Ito, A. Sakaguchi, C. Kobayashi and T. Ikariya, *J. Am. Chem. Soc.* **2006**, *129*, 290-291.

[207] H. Quast and R. Janiak, *Liebigs Ann. Chem.* **1991**, *1991*, 1305-1308.

[208] Y.-X. Zhang, D.-M. Du, X. Chen, S.-F. Lü and W.-T. Hua, *Tetrahedron: Asymmetry* **2004**, *15*, 177-182.

[209] T. Honjo, S. Sano, M. Shiro and Y. Nagao, *Angew. Chem. Int. Ed.* **2005**, *44*, 5838-5841.